INTEGRATING MICRO-FLOOD IRRIGATION WITH IN-FIELD RAINWATER HARVESTING

By

SABELO SICELO WESLEY MAVIMBELA

A thesis submitted in accordance with the requirements for the Philosophia Doctor Degree in the Fuculty of Natural and Agricultural Sciences, Center of Sustainable Agriculture, Rural Development and Extension at the University of the Free State, Bloemfontein, South Africa.

February 2012

Promoter: Prof. L. D. van Rensburg

Declaration

I declare that the thesis hereby submitted by me for the Phoilosophiae Doctor in Sustainable Agriculture at the University of the Free State is my own independent work and has not been previously submitted by me to another University/Faculty. I further cede copyright of the thesis in favor of the University of the Free State.

Signature.....

Date: February 2012

Place: UFS, Bloemfontein, South Africa

Acknowledgements

Giving thanks and acknoweldgements to the many individuals and institutions that supported this work is a humbling exercise. I owe gratitude to the following:

- Study leader, pioneer and promoter Professor L. D. van Ransburg for his academic assistance, and invaluable contributions from conception of the problem to the final work of the thesis. His unreserved, timely and academic devotions towards this study.

- Professor A. H. Cloot from the Department of Mathematics in the University of the Free State for his guidance and unreserved contributions that resulted to the publications of two articles from this work.

- Management and technical staff of Parady's Experimental Farm, of the University of the Free State for offering accommodation, support and assistance during the time of field experiments.
- Strategic Academic Cluster: Water Management in Water Scarce Areas of the University of the Free State. Bloemfontein, South Africa.
- Technical team at Kenilworth Experimental Farm for their assistance in oven-drying maize samples from the field experiments.
- Department of Soil Crop and Climate Sciences of the University of the Free State that made it possible for the laboratory experiments to be carried out successfully.
- Strategic Academic Cluster; Water Management in Water Scarce Areas for their financial support during the period of study.
- Ms Liesl van der Westhuizen for her editorial assistance and constructive suggestions during the writing of publications form this study.
- Family back home for their unreserved support and encouragement.
- To the church for their prayers and spiritual inspirations.

Abstract

The main aim of the study was to integrate micro-flood irrigation (MFI) with in-field rainwater harvesting (IRWH). The MFI is a short furrow irrigation system that relies on small inflow rates to mitigate the effect of dry spells in crop fields. The IRWH is an *in situ* based rainwater harvesting technique that harvests rainfall in the form of runoff between crop rows and then concentrates it in the basin area. Given the increased rainfall variability and evaporation (Ev) in the semi arid areas of the central Free State Province of South Africa, the merging of these two technologies is hypothesized to be able to stabilize soil water storage during rainfall and dry spell periods in areas with access to limited irrigation water.

The developments in the study were divided into three phases. The first phase dealt with characterization of pedological and hydraulic properties of the soils earmarked for IRWH at the University of the Free State, 20 Km, south of Bloemfontein. These soils were represented by the Tukulu, Sepane and Swartland soil types with the first two forms also referred as Cutanic Luvisols and the latter as Cutanic Cambisols of the Reference Soil Group. These soils were similar only in the orthic A- horizon. The Tukulu had developed structure only in the prismatic C-horizon and for the Sepane it was in the pedocutanic B- and prismatic C-horizons. The Swartland had a cambic structure in the pedocutanic B-horizon. Corresponding hydraulic properties, soil water characteristic curve (SWCC) and hydraulic conductivity for saturated (Ks) and unsaturated conditions (K-θ) were determined using *in situ* and laboratory procedures for internal drainage (ID) and evaporation (Ev) conditions. Parametric models were used to describe SWCC and to predict K-θ relationships. Model descriptions of SWCC were satisfactory. Predictions of K-θ were only accurate at near saturation, but HYDRUS-1D optimization program had better predictions. Matric suction gradients corresponding to the draining soil profile were found to fall within the matric suction range of 0 to -10 kPa. Drainage rate of 0.001 mm $hour^{-1}$ corresponded to drainage upper limit (DUL) and deep drainage (DD) losses proportional to 1 % of annual rainfall over the fallow period. The Tukulu, Sepane and Swartland soil types had respectively total DD losses of 21, 20 and 52 mm and evaporation losses of 43, 51 and 70 mm. The Ks corresponding to the C-horizons of these soils was 9.6, 1 and 77 mm $hour^{-1}$. During ID and Ev the K-θ functions especially for horizons with a clay content range of 26 to 48 % dropped by several orders of magnitudes, while SWC changed with a narrow margin. At the evaporating surface matric suction of magnitude greater than -1500 kPa were approximated.

The second phase compared four inflow rates (20, 40, 80 and 160 L min^{-1}) based on surface and subsurface irrigation characteristics carried out on the Tukulu soil due its low DD and Ev losses. A single irrigation on a 90 m closed ended furrow and measurements taken at every 10 m furrow distance for advance and opportunity times, stream flow depth, and SWC before and after the irrigation. Infiltrated depths predictions from HYDRUS-2D software were satisfactory from all inflow rates. Distribution uniformity (DU) was higher (≥ 0.89) at 30 m furrow distance from all inflow rates and the smaller inflow rate much easier to handle. Vertical redistribution was characterized at each of the 10 m furrow distance covered with a 2 m x 2 m polythene sheet to prevent Ev. Over the 455 hours of redistribution agreement between measured and predicted SWC from HYDRUS-2D software varied with depth and furrow length. Low vertical redistribution (Vz) from all inflow rates was attributed to the restrictive prismatic C-horizon. Higher rates of Vz were observed within the 0-600 mm profile domain for the small inflow rates and at 0-850 mm for the large inflow rates.

The last phase dealt with the integration of MFI with IRWH, carried out on a 3 x 3 split plot factorial with four blocks in a complete randomized design experiment. Each plot had five 30 m long furrows and a pair of neutron access tubes installed in each plot at the centre of the basin and runoff area. The main treatments were runoff strip width (RSW; 1 m, 2 m and 3 m) and water regime (WR): dryland (DL), supplemental (SPI) and full irrigation (FI). No till and basin tillage was used to prepare the RSW and the 1 m standard basin area (BA). The BA was further smoothed with a ridger for uniform distribution of the advance stream flow. A 120 day maturing maize variety was used. A record of rainfall and SWC was kept. The 40 L min^{-1} inflow rate for 15 minutes irrigation times on a fixed schedule for full and supplemental irrigation, provided by the BEWAB+ irrigation software was used. A soil water balance (SWB) procedure was developed to evaluate the effect of the RSW and WR treatments on the gains and losses in soil water storage. Evapo-transpiration (ET) was partitioned into Ev and transpiration (T) by a β-parameter based on plant canopy area. Findings showed that SWB components were affected by the main effect from the RSW and WR. The 1 m RSW had the total biomass and grain yields that were respectively 21 % and 45 % higher than the 2 m RSW, and 35 % and 89 % higher than the 3 m RSW. Total biomass and grain yields from full and supplemental irrigation were 200 % and 76 % higher than the DL. Though tested for a single season the combination of 1 m RSW and full irrigation produced optimum crop yields and WUE for the newly merged MFI-IRWH water management system and is ready to be used by small scale farmers who have access to irrigation water.

Contents

List of Tables

List of figures

List of Appendices

CHAPTER 1

INTRODUCTION

1.1 Motivation

The traditional role of agriculture as a major source of food and income among developing nations especially South Africa is threatened by growing climatic and soil related challenges. South Africa is generally a water stress country with about 82 % of its land area classified as arid to semi-arid. In average the country receives rainfall of 495 mm, well below the global average of 860 per year (ARC-ISCW, 2005). Arable land constitutes of 16.7 million hectare of which about 1.5 million is under irrigation mainly on areas with insufficient rainfall to sustain economic crop yields. Under this circumstance, dryland crop production is critical in improving food security and is widely practiced in the semi-arid areas with an aridity index of 0.2 to 0.5 (UNESCO, 1977). However, increased rainfall variability and sensitivity of the soils to degradation hazards, typical of drier regions of the world, has increased the risk of dryland food production, especially among small scale farmers.

Food production under the difficult climate and soil conditions existing in the semi-arid areas has been unsustainable. The majority of rainfall events occur in amounts of less than 20 mm which are insufficient to recharge the soil profile water storage. It is estimated that most of this rainfall (40 to 75 % of the annual rainfall) is lost to evaporation mainly from the summer rainfall areas where 85 % of the dryland food production is practised (Bennie and Hensley, 2001). Rainfalls that significantly contribute to the total seasonal rainfall are few and occur as outburst of heavy rainstorms that result in high runoff and evaporation losses. The former is estimated to constitute about 6 to 30 % of annual rainfall (Bennie, Strydom and Vrey, 1998). These unproductive losses are severe under conventional tillage systems from soils susceptible to compaction and surface crusting, especially under the impact of rainstorms (du Plessis and Mostert, 1965). Water induced soil erosion; dry soil water regime and deterioration of organic matter are some of the major factors that undermine the productive potential of semi-arid dryland food production systems.

Current and future predictions have indicated that this situation could be worse given that rainfalls shall decline with greater inter-annual variability (Rockstrom et al., 2007). Globally, loss of productive land under different climatic change and rainfall scenarios was estimated at 10 to 20 % with 1 to 3 billion people of the world population affected by 2080 (Fischer et al.,

2002). The Sub Saharan Africa was estimated to lose about 12 % of its productive area with the majority happening in the Sudan-Sahelian zone, which is already subject to high climate variability and adverse crop conditions. Consistent with these predictions is the growing lack of interest in farming especially among small scale farmers in the past decades because of extreme climatic conditions and loss of the land's productive potential (FAO, 2009; Rockstrom et al., 2007).

However, renewed interest on water management practices that improve rainfall capture and water productivity has remarkably changed the situation. Popular among this management practices is rainwater harvesting sometimes referred as runoff farming involving the harvesting of rainfall in the form of runoff from a larger area and concentrating it to a smaller area for immediate or later productive use (Oweis et al., 1999; Hensley et al., 2000, Prinz and Malik, 2002; Anschütz et al., 2003). More attractive for small scale farmers is the *in situ* rainwater harvesting techniques that maximise rainfall infiltration and soil water conservation by using various forms of conservation tillage and cultural practices (Rockstrom et al., 2007).

Reinventing of small-scale water harvesting in South Africa has resulted to the development of in-field rainwater harvesting technique (IRWH) to address the low productive potential of layered soils predominant in the semi-arid areas of the Free State Province. Through the use of basin and no till IRWH is reported to have reduced ex-field runoff to almost zero. Crop yields increased from 30 to 50 % while rainfall use efficiency increased from 50 to 106 %, respectively compared to conventional tillage system (Hensley et al., 2000). Similar results were also reported on homogeneous soils from the Limpopo Province (Mzezewa et al., 2011). However, concerns of high evaporation losses from the IRWH resulted to the testing of different mulching materials by Botha (2006). Although the suppression of evaporation under organic mulches was beneficial to crop growth but this benefit was dissipated by dry spells that were 14 to 21 days long. Recently, the effect of intercrop on IRWH conservational and water productive potential was investigated and the results on water use efficiently that is dependent on evaporation was inconclusive (Mzezewa and van Rensburg, 2011).

Integrating of *in situ* rainwater harvesting with some form of supplemental irrigation to mitigate the effect of persistent dry spells on crop growth and yields is encouraged in literature (Oweis et al., 1999; Walker, 2003; Rodríguez et al., 2004; World bank, 2005; Rockstrom, 2000; Moult et al., 2009). Increased restriction on available water for irrigation requires that any access be efficiently used through the choice of efficient method and

application regime. Considering the poor resource base of small scale farmers, Austin (2003) developed micro-flood irrigation (MFI) to enhance water productivity and efficiency from soils with an inherent dry water regime. Micro-flood irrigation is mainly driven by gravity and use small inflow rates on short furrows to obtain distribution uniformity as high as 95%, suggesting its competitiveness to other piped irrigation system. Integration of *in situ* rainwater harvesting with some form of micro-flood irrigation has been carried with great success in East African and South Asian countries (Awulachew et al., 2005; World Bank, 2005; Rockstrom et al., 2007). Given that IRWH and MFI involves runoff management but of different forms to improve soil water storage and productivity, their integrating could be very instrumental in advancing food security.

1.2 Objectives of the study

In the light of this background the main objective of the study's overall hypothesis was that the integration of MFI with IRWH would enhance water productivity. To test this hypothesis a series of studies were carried with each having its own set of specific objectives as outlined below.

Study 1 (Chapter 2): This study was titled: "Literature report". The primary objective was to study the body of knowledge pertaining to the development and application of runoff farming technologies with specific attention given to *in situ* rainwater harvesting and flood irrigation methods.

Study 2 (Chapter 3): This study was titled: "*In-situ* evaluation of internal drainage in layered soils (Tukulu, Sepane and Swartland)". The specific objectives were:

(i) to describe the pedological properties that relate to the presence of layering on the three soil types, and

(ii) to determine the soil water release, unsaturated hydraulic conductivity and drainage-time functions that characterised the internal drainage outcomes of layered soils.

Study 3 (Chapter 4): This study was titled: "Evaluating models for predicting hydraulic characteristics of layered soils". The specific objectives were:

(i) to characterise the soil water characteristic curve of the respective horizons of the three soil profiles,

(ii) to validate the conductivity functions based on the soil water characteristic parameters for the estimation of *in situ* unsaturated hydraulic conductivity, and

(iii) to estimate *in situ* unsaturated hydraulic conductivity from optimised soil water characteristic curve based parameters.

Study 4 (Chapter 5): This study was titled: "*In situ* evaluation of evaporation in layered soils". The specific objectives were:

(i) to describe the amount of soil water available to evaporation by the soil water release curve;

(ii) to describe the delivery rate of soil water to the evaporating site by the unsaturated hydraulic conductivity function of soil profile layers; and

(iii) to describe the evaporation flux and accumulative evaporation of the three soils with respect to their hydraulic characteristics.

Study 5 (Chapter 6): This study was titled: "Determining the optimum inflow rates for micro-flood irrigation on the Tukulu soil". The specific objectives were:

(i) to characterise the surface water distribution during the advance-supply phase. Secondly,

(ii) to describe the subsurface water distribution during irrigation with the aid of the HYDRUS-2D software, and

(iii) to evaluate the efficiencies from the irrigation outcomes.

Study 6 (Chapter 7): This study was titled: "Characterising vertical redistribution on irrigated short furrows in the Tukulu soil". The specific objectives were:

(i) to estimate the soil hydraulic parameters of the Tukulu soil that describes soil water movement during redistribution using the Levenberg-Marquardt parameter optimization algorithm,

(ii) to compare the HYDRUS-2D models predictions with field measured soil water content and calculated effective K-coefficient, and

(iii) to estimate the relationship between the rate of redistribution and infiltrated depth from furrows under different soil water regimes.

Study 7 (Chapter 8): This study was titled: "Integrating micro-flood with in-field rainwater harvesting: (i) Soil water balance procedure and application". The specific objectives were:

(i) to develop a procedure for quantifying SWB components for the integrated MFI-IRWH management practice, and

(ii) to determine the effect of runoff strip width (RSW) and water regime (WR) on the SWB components over the production season.

Study 8 (Chapter 9):"This study was titled: Integrating micro-flood with in-field rainwater harvesting: (ii) maize yields and water efficiency".The specific objective was to determine the effect of runoff strip width (RSW) and water regime (WR) on maize production.

1.3 Layout of the thesis

This thesis consists of 10 chapters. Chapter one deals with the motivation and objectives of the study while literature review is reported in chapter 2. Individual chapters (3, 4, 5, 6, 7, 8, and 9) consist of abstracts, introduction, material and methods, results, discussions and references. Chapters 3 to 9 were prepared in article format with four chapters already sent to different Journals for publications. These chapters also include acknowledgements. Chapter 10 provide a perspective on the thesis major findings, contributions and conclusions.

1.4 References

Anschutz, J., Kome A., Nederlof, M., de Neef, R., van de Van, T., 2003. Water harvesting and Soil water retention. Sec ed. *Agromisa Foundation*. Wageningen, Netherlands.

ARC-ASCW, 2005.Overview of agricultural natural resources of South Africa. ARC-ASCW. Report No. GW/A/2004/13. (CD-ROM) ARC-Institute for Soil, Climate and Water, Pretoria, South Africa.

Austin, C., 2003. Micro flood, a new way of applying waters. http://waterright.com. 22/09/2011, 10.00 a.m (LT).

Awulachew, S. B., Merrey, D.J., Kamara, A. B., Koppen Van B., de Vries P. Boelee E., 2005. Experiences and opportunities for promoting small scale/micro irrigation and rainwater harvesting for food security in Ethiopia.

Bennie, A. T. P. and Hensley, M., 2001. Maximising precipitation utilization in dryland agriculture in South Africa- a review. *J. Hydrol.* 241: 124-139.

Bennie, A. T. P., Strydom, M. G. and Vrey, H. S., 1998. The use of computermodels or agricultural water management on ecotope level. Water Research Commission report, TT 102/98, Pretoria, South Africa.

Botha, J. J., 2006. Evaluation of maize and sunflower production in a semi-arid area using In-field rainwater harvesting. Ph.D. (Agric) Dissertation, University of the Free State, Bloemfontein, South Africa.

du Plessis, M. C. F. and Mostert, J.W.C., 1965. Runoff and soil loss at the Agricultural Research Centre at Glen.*S. Afr. J. Agric. Sci.,* 8: 1051-1060.

FAO, 2009. How to feed the world in 2050.www.fao.org., 28/01/2012, 10.30 am (LT). Fischer, G., M. Shah, and van Velthuizen, H., 2002.Climate Change and Agricultural Vulnerability. Special report forthe UN World Summit on Sustainable Development, 26 August–4 September, Johannesburg. Laxenburg, Austria: International Institute for Applied Systems Analysis.

Fischer G., van Velthuizen H, Shah, M and Nachtergaele, F., 2002. Global Agro-ecological Assessment for Agriculture in the 21 Century. IIASA Research Report. IIASA, Laxenburg, Austria.

Hensley, M., Botha, J. J., Anderson, J. J., van Staden, P. P. and Du Toit, A., 2000. Optimising rainfall use efficiency for developing farmers with limited access to irrigation water. Water Research Commission Report no. 878/1/00, Pretoria, South Africa.

Moult N. C., Lecler N. I., and Smithers J. C., (2009). A catchment-scale irrigation systems model for sugarcane; Model application. *WaterSA,* 35: 29-36.

Mzezewa, J. and van Rensburg, L. D., 2011. Effects of tillage on runoff from a bare clayey soil on a semi-arid ecotope in the Limpopo Province of South Africa. *Water SA,* 37; 1-8.

Mzezewa, J., Gwata, E.T. and van Rensburg, L. D., 2011. Yield and seasonal water productivity of sunflower as affected by tillage and cropping systems under dryland conditions in the Limpopo Province of South Africa. *Agricultural water Management,* 98: 1641-1648.

Oweis, T., Hachum, A. and Kijne, J., 1999. Water harvesting and supplementary irrigation for improved water use efficiency in dry areas. IWMI Contribution No. 7, System Wide Initiative on Water Management (SWIM).

Prinz, D., and Malik A. H., 2002.Runoff farming. Institute of Water Resources Management, Hydraulic and Rural Engineering.Department of Rural Engineering, University of Karlsruhe. Germany.

Rockstrom, J., Hatibu, N., Oweis, T. Y. and Wani, S., 2007. Managing water in rain-fed and Designs. Guide and technical document. Department of Biological and irrigation Engineering, Utah State University agriculture, Part 4 In: Unlocking the potential of rain-fed agriculture, IWMI, Colombo, Sri Lanka.

Rockstrom, J., (2000). Water resources management in smallholder farms in Eastern and Southern Africa: An overview. *Phys. Chem. Earth,* 25: 275- 283.

Rodriguez, J. A, Diaz, A., Reyes J. A. and Pujols R., 2004. Comparison between surge irrigation and conventional furrow irrigation for covered black tobacco cultivation in a Ferralsol soil. *Span J. Agric. Res.,* 2: 445-458.

TheWorld Bank, 2005. Shaping the future of water for agriculture; A source book for investment in agricultural water management. Rural and Agricultural Development, Washington D. C. USA.

UNESCO, 1977. World map of desertification. United Nations Conference and Desertification Report 74/2. United Nations, New York, USA.

Walker W. R., 2003. SIRMOD III; Surface Irrigation Simulation, EvaluationWosten, J.H.M. and van Genuchten, T. H. M.,1988. Using texture and other soil properties to predict the unsaturated soil hydraulic functions. Division S-6, Soil water management and conservation. Soil Sci. Soc. Am. J., 52:1762-1770.

CHAPTER 2

LITERATURE REPORT

2.1 Introduction

Development and application of soil water management practices and soil physical principles for crop production in semi-arid and arid areas are the two aspects of literature study covered in this study. The aim was to acknowledge available literature and to develop a framework of body of knowledge upon which the subsequent research studies reported in this thesis shall be developed upon. In this regard the literature study is presented in three sections. The first section reviews the water management practices pertaining to runoff farming practices; the section pays attention to the soil physics theories and concepts applicable in rainwater harvesting water management systems, and the third section acknowledging gab in knowledge in the different areas pertinent to this research.

2.2 Review on runoff farming management practices

2.2.1 Background

Runoff farming embraces water management practices that aims at harvesting rainwater in the form of runoff from a relatively larger area and concentrated it to a smaller area for immediate or later productive use (Owes et al., 1999, Prinz and Malik, 2002, Anschutz et al., 2003). The aspect of later productive use mainly refers to the provision of irrigation to supplement rainfall during times when it is insufficient or persistent dry spells. Evidence of rainwater harvesting that supported ancient farming communities and desert dwellers could still be traced across Australia, south western United States, Middle East and Africa (Rockstrom et al., 2007).

Runoff farming also to be referred as rainwater harvesting in this study is traditionally practiced in water scarce areas. It is widely practiced over 110 countries that roughly contain about 40 % of the world population found across the arid and semi arid regions of the world (Critchley and Siegert, 1991; Rockstrom et al., 2007) where rainfall is low, unevenly distributed and highly random. Annual rainfall is concentrated to few but heavy intensity rainstorms that results to high runoff and evaporation losses. About 6 to 30 % and 60 to 75 % of annual rainfall is reported to be lost as runoff and evaporation, respectively (Bennie et al., 1994). Consequently, soil water induced erosion; compaction and dry soil water regime are

some of the common factors that reduce semi-arid soils productive potential. However, rainwater harvesting has provided management practices that control runoff and substitute a significant portion of evaporation for transpiration. This is achieved by supplementing the water shortages in the cultivated area by runoff harvested from the catchment area.

Rainfall characteristics, topography and soil hydraulic properties determine the effectiveness of rainwater harvesting. A wide range of rainwater harvesting technologies is suitable for areas with annual rainfalls falling within the range 300-700 mm. Some specialized technologies are adapted to very low rainfall areas as low as 100 mm per annum. Small catchments are recommended in areas with uneven slopes of greater than 5 %, increased rainfall seasonality and high runoff coefficient as is the case with clay soils (Owes et al., 1999, Prinz and Malik, 2002; Anschütz et al., 2003; Hillel, 2004; Ali et al., 2007). However, in years when rainfalls are low and erratic small catchments could not be able to store adequate water to sustain the crop (Rockstrom et al., 2007). Catchments with low runoff turnover could either be physically treated by surface clearance and compaction or chemically treated with sodium salts, latex, silicone and asphalt paraffin wax as well as oil emulsions. In certain cases plastic sheets could be used to optimize harvested runoff per unit area (Hillel, 2004).

The benefits of rainwater harvesting are many and multifaceted. Crop responses to improved soil water storage and availability has been remarkable (Hensley et al., 2000; World Bank, 2005; Rockstrom, 2000; Rockstrom et al., 2007). Average grain yields under dryland conditions are about 1500kg ha^{-1} but yields up to 1800 kg ha^{-1} (Botha 2006) and 3100 kg ha^{-1} (Rosegrant et al., 2002) has been reported from *in situ* and supplemental irrigation rainwater management practices. Each 1 % growth in agricultural yields brings about an estimated 0.5 to 0.7 % reduction in number of poor people (World Bank, 2005). Evidence has been shown that costs-benefit ratio for investing in rainwater harvesting techniques has been high (Kundhlande et al., 2004; Joshi et al., 2005). In many instances soils rendered unproductive because of surface desiccation and high salt accumulation as been reclaimed and restored through rainwater harvesting strategies (Hensley et al., 2000; Awulachew et al., 2005).

However, the expansion of rainwater harvesting for food production should be carried out judiciously. Runoff also plays a role in partitioning of rainwater in the landscape. It is responsible for recharging seasonal flows in the major drainage river basins, natural wetlands and underground waters. Current records indicate that over 75 % of major river basins are already utilized for human needs with only 25 % available for ecological functions (FAO,

2009). Underground water resources are also reported to be approaching depletion in a couple of decades if abstraction is to be continued at current rates (FAO, 2009). Under these circumstances, investment in rainwater harvesting should assume a more integrated approach if food production is to be improved or maintained under the growing climate and soil limitations.

2.2.2 Classification of runoff farming systems

Different approaches are mainly used to classify runoff farming systems. These approaches mainly consider the designation of catchment, storage method and nature of harvested runoff. Generally runoff could be harvested from external and *in situ* or infield catchments as well as from roof tops (Pacey and Cullis, 1986). Nasr (1999) classified rainwater harvesting technologies according to their ability to harvest and store runoff in the soil profile of cultivated fields or one that harvest and store runoff offsite the cropped area in the form of surface reservoirs and dams mainly for supplemental irrigation. A different classification is that provided by Critchely and Siegert (1991) that distinguish rainwater harvesting from flood water harvesting. The latter depicts the capture of surface runoff within or diverted from the seasonal streambed towards the cropped area to be stored in the soil profile. Percolation dams, earth bunds and liman terraces are used in flood water harvesting in areas with annual rainfalls ranging from 100 to 600 mm on catchment: cropped area ratio of 100:1 to 10000:1 depending rainfall seasonality (Prinz, 1996). Rockstrom et al., (2007) used the water management aspect to improve water availability and conservation to classify runoff farming practices as shown in Table 2.1. This approach also considered evaporation suppressing and integrated soil, crop and water management practices as components of rainwater harvesting strategies. A simple approach, adopted for discussion purposes in this study, is the one proposed by Prinz, (1996) that classify rainwater harvesting technologies according to the size of the catchments; micro and macro-catchment systems being the main categories (Prinz, 1996). Oweis et al., (1999) modified this approach by including a mini-catchment.

2.2.2.1 Micro-catchment rainwater harvesting technologies

The cultivated area could range from 0.08 m^2 to 250 m^2 for micro-catchments with catchment: cropped area ratio ranging from 1:1 to 20:1. Mini-catchments are adaptable to a wide range of cultivation methods including row, contour and basin cropping systems such as those used in tree and agro-forestry plantations. In cultivated fields this class of rainwater harvesting rely on in-situ soil water management practices to capture and store runoff in the

soil profile. Runoff produced between cropped rows is not allowed to develop to ex-field runoff through the use of contour farming surface structures that maximise infiltration. Example of free standing in-field runoff harvesting surface structures includes among others: bunds or terraces, pitting, furrows, ridges and basins of which most are effective when developed along the contour (Prinz, 1996 and Oweis et al., 1999). Common micro-catchment systems include the semi circular bunds and the eye brow terraces practiced in the Israel and Negev desert, and the Meskat and Negarin types which rely on earth contour bands to hold and distribute runoff along cultivated slopes. Generally regarded as labour intensive preparations of micro-catchments varies from the use of hand tools to highly specialized mechanical ploughs such as the 'wavy' dolphin plough used to prepare the vallerani micro trenches to common basin and ridging implements. Reduction in runoff and soil erosion is reported to have ranged from 50 % to almost negligible levels (Hensley et al., 2000; Anschütz et al., 2003; Joseph, 2007). Because of their small catchment size they could be easily integrated with other cultural practices that reduce evaporation losses similar to those suggested in Table 2.1. Also the use of no-till in the catchment area to enhance in-field runoff (Hensley et al., 2000) and ripping or sub-soiling in the cultivated area (Rockstrom et al., 2007) to encourage deep soil profile storage does improve the effectiveness of micro-catchment water management systems.

A classical example of an *in situ* water management strategy is the in-field rainfall harvesting technique (IRWH) developed by Hensley et al. (2000). The developers preferred to use the term mini-catchment as equivalent to IRWH even though the catchment: cropped area ratio falls within the micro-catchments. No-till was used between the 2 m crop rows to encourage in-field runoff production, while basin tillage along rows retained and facilitated deep infiltration. The IRWH integrated the basin till with mulch as an evaporation management strategy according to Rockstrom et al. (2007) classification. To minimise deep drainage losses the IRWH was developed for the layered and duplex soils predominant in the semi-arid areas of the Free State Province of South Africa. These soils have a clay rich layer of not less 40 % either in the B or C horizons. Runoff coefficient from a typical clay soil was found to be about 0.47 (Botha et al., 2003). A linear function representing the relationship between runoff efficiency (IR) and rainfall (P) from data for over a 3 year period on clay soils was expressed (Botha et al., 2003) as:

$$IR = -0.879 + (0.474) \times P \qquad (r^2 = 0.64) \qquad (2.1)$$

Table 2.1 Rainwater harvesting practices and their management options (Rockstrom et al., 2007).

Aim	Rainwater harvesting strategy	Purpose	Management option
Increase plant water availability	External water Harvesting systems	Mitigate dry spells, protect springs, recharge groundwater, enable off-season irrigation, permit multiple uses of water	Surface micro-dams, subsurface tanks farm ponds, percolation of dams and tanks, diversion and recharging structures
	In situ water harvesting systems, soil and water conservation	Conserve rainwater through runoff to cropped area or other use	Bunds, ridges, broad-beds and furrows, micro-basins, runoff strips,
		Maximise rainfall infiltration	Terracing, contour cultivation, Conservation agriculture dead furrows staggered trenches
	Evaporation management	Reduce non-productive evaporative	Dry planting, mulching, conservation agriculture, intercropping, wind breaks Agro-forestry, early plant vigour and vegetative bunds.
Increase plant water uptake	Integrated soil, crop and water management	Increase proportion of water balance flowing as productive transpiration	Conservation agriculture, dry planting (early), improved crop varieties, optimum crop geometry, soil fertility management, optimum crop rotation, intercropping, pest control and organic matter management

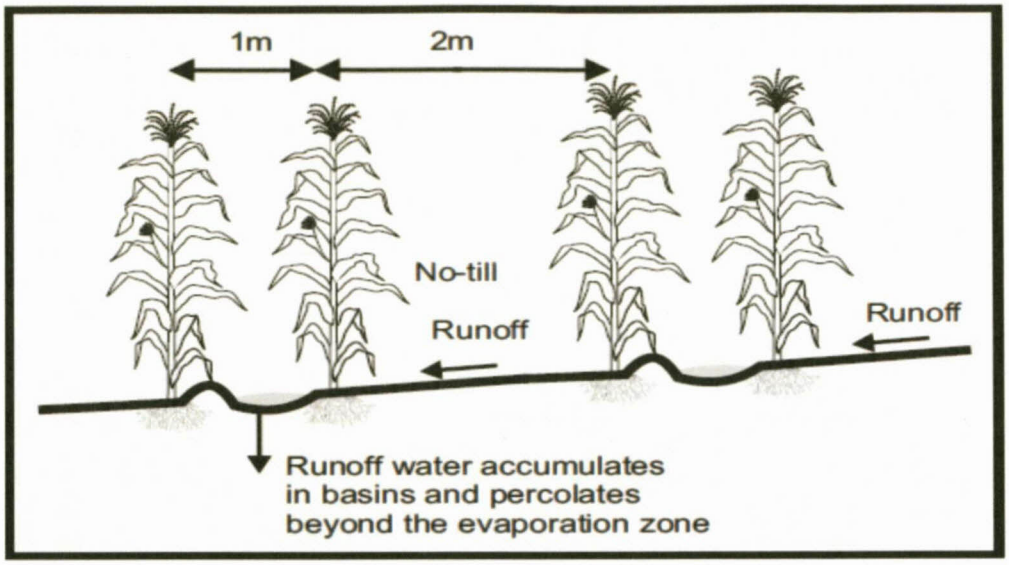

Figure 2.1 A diagrammatic representation of the in-field rainwater harvesting technique (Hensley et al., 2000)

Where -0.879 could be inferred to depict the combined effect of the soil-water system interaction on clays attributed to cracking and swelling tendencies, which reduced IR to about 0.47. This value is relatively high compared to the 0.2 to 0.3 recorded from other studies on micro-catchments with slopes of less than 10 % (Oweis et al., 1999). However higher runoff coefficients of 0.5 in rocky or stony soils were achievable (Anschutz, et al., 2003). Oweis et al. (1999) articulated the effect of cropped area (CA) and runoff area (C) , runoff coefficient (Rc) and rainfall (P) on runoff efficiency or depth (IR) to have the function;

$$IR = \frac{C \times P \times R_c}{CA} \qquad (2.2)$$

The above analogy depicts the inverse relationship of cropped area on runoff efficiency and storage. Although increasing the runoff area (C) in drier areas improves accumulative runoff but issues of prolonged surface ponding along the drainage cropped area could exacerbate evaporation and risk of overtopping. Inconsistencies on slope along large runoff catchments also contribute to lower runoff coefficient (Bruggerman and Oweis, 2001, Anschutz et al., 2003). Similar conclusions were made when 20 m length runoff catchments yielded to erratic and inconclusive runoff efficiency compared to 2 m length catchments (Hensley et al., 2000). It may be tedious to measure runoff coefficients on narrow runoff catchments, but higher flexibility, effective erosion control and runoff turnover per unit area as well as the benefit of

crop canopy cover on the basin area adds to the comparative advantage of micro-catchments systems (Prinz, 1996; Anschutz et al., 2003).

Regardless of any C: CA area ratio crop yields per unit hectare in most cases offsets the loss in productive land as a result of interspacing the cultivated field with catchment runoff area (Oweis et al., 1999; Hensley et al., 2000: Rockstroom, 2000). For the traditional 2:1 C:CA area ratio for the IRWH crop yields and water use efficiency compared to conventional tillage system was consistently higher than conventional tillage systems (Hensley et al., 2000; Botha et al., 2006; Joseph, 2007; Mzezewa et al., 2011; Mzezewa and van Rensburg, 2011). However, the major concern from all these studies was the negative impact long dry spells of about 14 to 21 days had on soil water storage even when the basin area is covered with mulch (Botha, 2006). Figure 2.2 illustrates the severity of water stress on maize plants at tasseling under IRWH on a 10 hectare field following a more than 3 weeks dry spell. Other researchers have reported that different row spacing, does influence soil water storage and crop growth (Sangoi et al., 2001; Eberbatch and Pala, 2005; Acciaresi and Zulunga, 2006; Onyango, 2009). It would be therefore reasonable to determine how different RSW compared with the traditional 2 RSW with respect to soil water storage and crop yields. In addition, the most effective way to break yield reducing dry spells is through supplemental irrigation (Zhang et al., 1998; World Bank, 2005; Rockstrom et al., 2007).

2.2.2.2 Macro-catchment rainwater harvesting technologies

Macro-catchment rainwater harvesting is often simplified as the general collection of runoff from external catchments for immediate or later crop water use. Runoff from grazing lands and long hill slopes draining into secondary water ways is harnessed for macro-catchment rainwater harvesting. Traditionally, runoff from drainage lines is diverted towards and distributed in pastures or cropped fields on low lying lands using wadi structures, stone or earth contour bunds. Water harvesting practices found in macro-catchments systems include among others staggered liman terraces, trapezoidal bunds and semicircular hoops as well as the stone dams, deep trenches and hillside conduit systems. Catchments of area size ranging from 1000 m^2 to 200 ha with inclination of 5 to 60 % are appropriate for macro-catchments runoff harvesting. Cultivated areas with C: CA area ratio ranging from 10:1 to 100 could well be supported by macro-catchment rainwater harvesting designs (Prinz, 1996). Capacity of this system largely depends on rainfall seasonality which could vary between 100 to 1000 mm (Prinz, 1996).

Figure 2.2 A severely water stressed maize crop at tasseling following a dry spell that persisted more than 3 weeks at Parady's experimental farm under in-field rainwater harvesting.

Macro-catchments runoff harvesting is usually elevated into flood water harvesting in areas receiving seasonal rainfalls concentrated into one or two rainstorms. Ephemeral floods from stream beds and wetlands are harnessed either by damming streambed to encourage subsurface flow or diverting surface floods by wadis towards neighbouring cultivated fields (Prinz, 1996). Size of external catchments ranges from 200 ha to 50 km^2 with the runoff to cropped area ratio varying from 100:1 to 10000:1 (Prinz, 1996; Rockstrom, 2000).Spate irrigation practiced in Eritrea and Ethiopia is a typical example of flood water harvesting where runoff from the highland slopes is diverted by earth embankments into low lying fields with levelled basins. Provision of storage structures for seasonal floods provide a much more controlled water supply to crop plants for greater part of the growing season. Earth and concrete dams are widely used to store floods from external catchments depending on capital investment and scale of crop production (Prinz. 1996; Oweis et al., 1999; Rockstrom, 2000). For example, a much smaller pond with carrying capacity of 180-185 m^3 could support supplemental irrigation on fields ranging from 500-1000 m^2, while dams with maximum storage of 50 million m^3 could support supplemental irrigation for an area of about 3000 ha.

Worldwide, the water harvested from main river streams made available to agriculture supports about 28 % of the croplands under irrigation (Rockstrom et al., 2007). This

contributes about 46 % of the global agricultural economic output (FAO, 2009, 2007). In South Africa, about 1.5 million hectare is irrigated and the agriculture sector is by far the biggest consumer of runoff water (Annandale et al., 2011). The agriculture sector used about 7900 million m^3 water compared to the 12900 m^3 shared by the rest of the sector in the year 2000. Greater variability on seasonal flows from the major river basins, because of climatic change and growing pressure for the sector to relinquish more water to others sectors, has increased the need for supplemental or deficit irrigation and efficient irrigation methods.

2.2.2.3 Supplemental irrigation

Supplemental irrigation is a function of rainwater harvested mainly from macro-catchments and stored outside the cultivated area to bridge dry spells. It seeks not to alleviate crops from water stress, but to provide sufficient water for the crop to survive the dry period. Supplementing seasonal rainfall with about 50 to 200 mm of water by irrigation has shown to be sufficient to prevent severe yield losses from drier years (Oweis, 1997; World Bank, 2005). The primary goal for supplemental irrigation is to manage a deficit soil water regime that is sufficient to sustain the crop, but low enough to maximise rainfall capture. This brings into light the concept of profile available water (PAW) that was further defined in South Africa to be the difference between the drained upper limit (DUL) and the lower limit (LL). The DUL is directly correlated to the water content of the root zone where the drainage rate reaches very low values after saturation of the profile (Ratliff et al., 1983). Bennie et al. (1991) defined the LL as a function of (i) evaporative demand (ii) crop factors (canopy and roots) (iii) profile water supply rate (PWSR). Since the PWSR is dependent on soil water content and evaporative demand, plant water stress index is proportional to the gradient of PWSR to atmospheric evaporative demand. In this regard the soil profile hydraulic properties, soil water retention and hydraulic conductivity, become important parameters in the management of supplemental irrigation at different crop growth stages. Higher crop water requirements at silking and fruiting stage could trigger severe crop yields losses if dry spells are not properly supplemented by irrigation (Anrade et al., 1999; Schneekloth and Andeles, 2009).

2.2.2.3.1 Irrigation methods for supplemental irrigation

Advances in technology have resulted to the development of more sophisticated and efficient irrigation methods, but technological transfer to small scale farmers has been slow. Therefore, flood systems especially furrow irrigation is still popular among developing

communities who mainly grow stable foods in row cropping systems (Walker and Skorgeboe, 1987; Crosby et al., 2000). Furrow irrigation efficiencies are estimated to be 25 to 60 % compared to the sprinkler (60 to 95 %) and drip (80 to 95 %) irrigation systems (Waskom, 1994). However, the adoption of blocked ended short furrows with smaller inflow rates has minimized deep drainage and tail end runoff losses (Walker, 2003).

A classical example of a short furrow irrigation is the micro-flood irrigation (MFI) developed by Austin (2003). The MFI (Figure 2.3) uses small inflow rates as low as 20 L min^{-1} driven by gravity from light plastic pipes to irrigate short furrow runs. Distribution uniformity of up to 95% is competitive to sprinkler or drip irrigation was reported by the developer.

Figure 2.3 Micro-flood irrigation technologies as presented to agriculture experts in Kouebokkeveld, South Africa (2003).

A nearly uniform opportunity time between the furrow inlet and end was the justification. Under conventionally long furrows, the same level of performance is attempted through the use of very large inflow rates controlled by some automated valves (Maskom, 1994, Mailhol et al., 1999; Walker, 2003). Short furrow irrigation has been successfully integrated with in-situ rainwater harvesting systems such as those that use basins, furrows and contour ridges. Figure 2.4 shows the usefulness and compatibility of supplemental furrow irrigation when integrated with *in situ* rainwater harvesting techniques.

Based on the evidence picked up in this study the water storage of *in situ* based rainwater harvesting strategies including IRWH do not have the capacity to withstand the drying effect of persistent dry spells. Application of supplemental water during dry spells or when access is

very restricted during the critical crop growth stages could stabilise water availability and crop yields. Since its inception the IRWH has never been integrated with supplementalirrigation. Increased rainfall variability and severe evaporation occurring in the mid summer months, November to January (Botha et al., 2003), when crop water requirement is critical for optimum yields could be suggesting the need for integrating supplemental irrigation with IRWH. However, the irrigation method should have a high application efficiency and compatible with the basin area runoff management structures.

(a) (b)

Figure 2.4 Application of supplemental furrow irrigation along crop row basins (a) and plants supported by supplemental irrigation among crops damaged by insufficient rainfall (b) (Adapted from Rocktrom et al., 2007).

2.3 Review on soil physical principles

2.3.1 Background

Efficient use of soil water resources shall be expected to be improved if the world food production levels are to be improved or sustained. In the light of increased climatic variability and declining productive potential of cultivated soils, water remains the most limiting resource in crop production among the arid and semi arid zones. Therefore the adoption of innovative water management practices based on scientific concepts carries the prospects of enhancing water use efficiency, especially among the small scale farmers of developing nations.

The soil-plant-atmosphere continuum (SPAC) reflects the hydrological processes that characterize the inflow and outflow of water from the soil, plants and atmosphere environment. Given that the soil serve as an immediate reservoir for water, its ability to store

and release water is of critical importance to crop production. In this regard the conservation of mass in the SPAC could be defined with respect to the soil water balance (SWB). Hydrological processes affecting the changes in soil water content (SWC) could also be mathematically described as

$$\Delta SWC = (P + I) \pm R \pm DD - (Ev + T) \quad (3.1)$$

Where ΔSWC is the change in soil water content of the soil profile (mm), P is precipitation or rainfall amount (mm), I being irrigation amount (mm), R is runoff as a loss from the field (ex-field) (-) or harvested as in-field (+), DD is Deed drainage below the soil profile (-) or capillary rise from a water table and Ev and T being water evaporated from the soil surface (mm) and water transpired by crop plants (mm) respectively. Transpiration is regarded as a productive loss since it relates to crop growth and photosynthesis.

The primary goal for any food production system is to minimize the unproductive soil water losses from DD, ex-field runoff and Ev while maximizing T for optimum plant growth and yields. This is a challenge especially in arid and semi-arid areas where Ev exceeds P by flow. Various soil water management strategies including rainwater harvesting and conservation practices have been developed to improve water availability and to suppress Ev. However because of differences in soil physical properties and climatic conditions there is no one water management practice that is suitable to all soils. To make an informed choice reasonable knowledge on soil physical concepts affecting water movement within the SPAC is necessary. Soil physics is defined as that branch of soil science that is concerned with the application of physical principles to characterize soil properties and to understand the variety of dynamic processes occurring in soils (Dani and Wraith, 2002).

2.3.2 Soil physical properties

Soil could be defined as an unconsolidated mineral or organic material on the immediate surface of the earth and serve as a natural medium for plant growth (Hillel, 2004). As a product of weathered rock material the unconsolidated mineral formation assumes a particulate, porous and disperse system that readily mix with air, water and organic matter. An average soil is accepted to have a composition of 45 % mineral matter, 5 % organic matter, air and water having an equal relative proportion of 25 % of the 50 % pore space (Hillel, 2004). However, the reality is that soils differ widely from this idealistic form, especially in arid and semi-arid climates.

Mineral matter of varying particle shape and size distribution or texture forms the bulk of the soil matrix and is a permanent property soils. Soil texture constitutes of the sand, silt and clay fractions that are generally classified to fall within the respective size range of 0.05 to 2 mm, 0.002 to 0.05 mm and less than 0.002 mm (Hillel, 2004). Particle geometry and texture is recognized for determining the solid interfacial surface area, pore volume and pore size distribution that are of significant importance in soil water studies. Through the pore space water and air is drawn and transmitted (Hillel, 2004).Since all pores are connected with one another and with the atmosphere, the air phase usually does not affect flow within the soil matrix. The pore space or porosity is generally classified into micro-, meso- and macro-pores classes with respective pore diameter ranging from less than 0.001 mm, to 1 mm and greater than 1 mm (Luxmoore, 1981) Other porosity classes were given by Clothier and White (1981), Wilson and Luxmoore (1988) and Anderson et al. (1990). Clay has the largest specific surface area and constitutes primarily of the micro-pores appreciated for their high ionic adsorption and capillary activity (Dane and Hopmans, 2002). Soils with high clay content have been found to have a higher adsorption and capillarity; a physical relationship that has widely been used to estimate the soil pore size distribution and other soil water related functions (Bennie, 1991; Simunek et al., 2008; Vereecken et al., 2010; Bouma, 2010). Soils could assume various textural classes depending on the composition of the different mineral size particles (Hillel, 2004).

Under *in situ* conditions the different soil textures in a vertical soil profile could be expressed in the form horizons or layers parallel to the soil surface. Sequence and composition of the horizons is mainly a product of pedological evolution. In this regard soil structure, referring to the way the mineral particles are packed aggregated in the bulk of soil, is of vital importance in determining the relative proportion of water and air filled pores in the soil profile. The pore spaces or macro-pores between the soil aggregates or peds are usually referred to as structural pores (Kutilek, 2004) or drainable pores (Chimungu, 2009). Since these pores are the first to drain when all pores are filled with water they contribute to the proportion of air filled pores. According to Hillel (2004) soil structure could be of single grain; referring to loose and unattached particles typical of windblown sands (Hensley et al., 2007); massive structure referring to heavy or tightly packed structures as in the case of clay soils; and aggregated referring to structure associated with small clods or peds typical of loamy soils. Increasing organic matter and earth worm activity is reported to have improved aggregation and structural pores (VandenBygaart et al., 2000). Loose structure is

acknowledged for its large volume of macro-pores that readily draws and release water, hence assuming a drier soil water regime (Rhoads, and Sukhodolo 1991). However, the proportion of macro-pores could be reduced through compaction and surface sealing by tillage or raindrop impact on course and fine grained soils in particular (Moolman, 1981; Ahuja et al., 1998). On the other hand heavy soils of massive structure have low volume of macro-pores and thus resist water movement although it could open cracks when dry that promote rapid initial water intake or preferential flow (Lin et al., 1998). In layered soils the change in structure and texture between horizons could be of smooth or abrupt transition (Hensley et al., 2007). The layering phenomenon depending on sequence could impair vertical distribution if the underlying horizon is more restrictive (Hensley et al., 2000) or promote unstable flow if the bottom layer is courser than the overlying layer (Jury et al., 2002).

2.3.3 Soil hydraulic properties

Soil hydraulic properties could be simplified to mean the characteristics that describe soil water systems. Characteristics of importance in cultivated soils include soil water content (SWC), flux rates, the relationship between SWC and matric potential and the hydraulic conductivity. These properties could be studied using either the single or non-single porosity models. The single porosity model considers the soil system on at microscopic scale not affected by the bulk of soil water movement including the activity of macro-pores, root channels and fractures (Schroder et al., 2008). In contrast is the non single-porosity media approach that considers the bulk soil water movement as a collective product of textural and structural porosity along with its spatial variability (Simunek et al., 2003). It also considers the representative elementary volume (REV) more meaningful to describe soil physical properties than a single void flow path.

2.3.3.1 Soil water content

Soil water content in the pore space is highly variable and the most limiting factor in food production in drier areas. It could be expressed on mass basis as gravimetric water content; in volume basis as volumetric water content; in depth of equivalent as soil water storage; and in degree of saturation as the ratio of volume of water to the volume of porosity. Soil mechanical properties including strength, compatibility and penetrability (Dane and Klute, 1977) as well as bulk density, the ratio of mass of oven dry soil to its bulk volume, and swelling clays may change as a result of changes in SWC (Dane and Hopmans, 2002). Soil

water content is primarily recharged by rainfall and in very limited cases by irrigation. In drier areas SWC is subject to depletion by either evaporation or transpiration to below the accessible levels to crop plants referred by Bennie (1991) as the lower limit (LL) of plant available water (PAW_{LL}). Following saturation SWC immediately drains away through the macro-pores, but stabilizes once the drainable pores have approached a near equilibrium state usually referred as field capacity (Hillel, 2004) or the drained upper limit (Bennie et al., 1991). Work by Hensley and Jager (1982) successfully estimated LL from plant parameters while DUL was estimated from silt plus clay content (Bennie et al., 1988). The difference between DUL and LL represents the plant available water (PAW) (Bennie, 1995). Pedological features provide evidence of the soils water regime (Hensley et al., 2007) and the relationship between these pedological features with DUL are yet to be defined especially in layered soils.

2.3.3.1.1 Soil water content measurement

Soil water content measurement has rapidly evolved in recent times from the destructive techniques to the modern non invasive soil water sensor technologies. The gravimetric SWC measurement is one of the traditional methods that express gravimetric water content as the mass of water relative to the mass of oven-dry soil. This method is still the most relied upon and widely used to calibrate newer techniques. The neutron scattering method (NSM) is widely applied for field measurement and is non destructive once access tubes are installed. It relies on a radioactive source of high energy-epithermal neutrons to indirectly measure water content from the concentration of hydrogen atoms in the soil (Fare and Polyakov, 2006). Although with effective site calibration the NSM offers accurate results the margin of error often increases near the soil surface (Leib et al., 2003; Hillel, 2004). Dielectric sensors are also becoming popular for laboratory and field soil water studies. Common are the time domain reflectometry (TDR), capacitance (TDR) and the Doppler Flow Meter (DFM) sensors. Evidence from various studies has shown that all these sensors are automated, easy to operate and provide accurate measurements when properly calibrated (Nhlabatsi, 2010; Chimungu, 2009). However, the DFM capacitance sensors occur in various lengths up to 1.8 m making them more appropriate for measuring the soil profile at varying depths. Other methods include the gamma ray attenuation method that could measure in addition to SWC, bulk density and X-ray computed tomography, ground penetrating radar, and nuclear magnetic resonance (Leib et al., 2003).

2.3.3.2 Soil water characteristic curve

Given that water in soils loses its pure and free status, the relationship between SWC (θ) and matric potential (h) is a very important soil hydraulic property. This relationship could be expressed as the soil water characterize curve (SWCC) sometimes refers as the soil water retention curve (SWRC) (Dane and Hopmans, 2002). The matric suction relates to the joint effect of capillarity and adsorptive potential affecting water in the pore space that makes SWCC a physical property that is a function of pore size distribution (Bohne, 2003; Hillel, 2004). This could be explained by the fact that large pores get filled with water at near saturation and because of their large pore radius there is minimum resistance offered by the matric suction; hence they readily release water under gravitational influence. However, the remaining water in the pore space with relatively smaller radius experiences an increase in matric suction that subsequently reduces the outflow rate from the soil matrix. It is therefore not surprising that the SWCC is non linear and the most studied physical property (Gardner, 1956; van Genuchten, 1980; Dane and Hopmans, 2002; Haverkamp et al., 2005). In cultivated soils the matric suction of importance ranges from 0 kPa to near oven dry at -1500 kPa. Most crop plants approach wilting point when soil water content becomes tightly held at matric suction near -1500 kPa.

2.3.3.2.1 Measurement of the soil water characteristic curve

Although there is not yet a universal theory to describe or predict θ-h relationship from soil properties, various methods have been developed and a comprehensive review was done by Dane and Hopmans, (2002). The SWCC could be measured using direct and indirect methods.

Direct methods: These are among the widely used techniques including the hanging water column (Haines, 1930), the pressure plate (Richards, 1941) techniques for laboratory procedures and transducer tensiometers for *in situ* conditions. The hanging water column (HWC) also referred as the Haines apparatus. It constitute of initially saturated undisturbed soil core samples exposed to various lengths of hanging water column capable of inducing soil water release by pores at matric suctions less than -10 kPa. Limitations on the length of hanging column and possible cavitations (Jury et al., 1991) have confined the HWC to near saturation matric suctions. Evidence has shown that structural or drainable pores of diameter larger than 1 mm (Luxmoore, 1981) drains at matric suction range of less than -30 kPa (Jury, 1991). Nhlabatsi (2010) and Chimungu (2009) recorded drainage curves that approached

DUL at matric suctions less than -10 kPa from different clay layered soils for all horizons. In this regard the use of the HWC to describe the matric suction range within which DUL is attained would provide a more practical approach as an entry point for small scale farmers in applying scientific concepts in soil water management practices.

However, to cover a wider matric suction range for the SWCC the pressure plate is appropriate for a suction range of up to -1500 kPa (Klute, 1986; Jury et al., 1991; Bohne, 2005). In this method volumetric water content is monitored as pressure head is increased in a step wise manner until the desired matric suction range is realized. An accuracy of this procedure was observed within a coefficient of variation of 1 to 2% (Reeve and Carter, 1991). However Bittelli and Flury (2009) highlighted some errors associated with the pressure plate technique including the loss of accuracy at lower matric suction due to the clogging of pressure plates by soils particles or algae growth. To this effect the use of the dew point method is recommended for use in collaboration with the pressure plate technique. A much faster method was the controlled outflow method (Lorentz et al., 1993) but due to its hysteresis challenges it was replaced by the flow pump method that was first used by Znidarcic et al. (1991). The SWCC was completed in 3 to 4 days something impossible with the traditional methods, with reproducible results and least hysteresis. However when retention curves were compared with the traditional methods a good agreement was observed (Wildenschild, 1996) suggesting that the investment cost implicated on the new methods were not justifiable with respect to the accuracy of the SWCC.

Tensiometes equipped with electric transducers is the most appropriate method to determine the SWCC under *in situ* conditions. Installed at every horizon it effectively works alongside with SWC measuring sensors such as the TDR or capacitance probes. Apart of the heavy tensiometry instrumentation required the challenges that come along with controlling weather elements and achieving effective soil contact with the porous ceramic cups are limiting the use of this method (Hillel, 2004).

Indirect methods: Alternative to the direct methods is the pedo-transfer and inverse methods. The pedo-transfer approach involves estimation of retention characteristics from physical soil properties such as texture, bulk density, organic matter and clay mineral formation using regression equations (Rawls et al., 1992). Particle size and pore size distribution (Wosten and van Genuchten, 1988) have been successfully used to estimate retention characteristics. Apart

from the promising results of these methods, strong empiricism and secondary information required for the soil in question may limit their application.

On the other hand, the inverse numerical method of estimating retention characteristics from the Richard's flow equation is solved by traditional finite element routine (Kool et al., 1987). Flow controlled variables from an experiment with known initial estimates is fitted on a flow equation and numerically solved using a parameterized hydraulic function. Through inversion the unknown parameters of the retention curve are estimated and optimized using an objective function. Although this procedure relies on mathematical computations and parameters assumptions there is evidence that the estimated retention curves are reasonable (Eching and Hopmans, 1993).

2.3.3.2.2 Mathematical functions of the soil water characteristic curve

To develop the few discrete points measured during the desorption experiment into a complete SWCC a mathematical expression is usually required for smoothening and interpolation (Bohne, 2005). Governed by the Poiseuille's and Darcian flow theory, a number of these expressions were developed. Earlier models are those of Burdine (1953), Brooks-Corey (1964) and Mualem (1976). The latter was then transformed to closed form van Genuchten (1980) that has become the widely used function assuming the following expression:

$$\theta(h) = \theta r + \frac{\theta_{s-}\theta_r}{\{1 + |\alpha h|^n\}^m} \qquad (3.2)$$

Where θ_s and θ_r are the respective saturated and residual values of the volumetric water content, θ (mm mm^{-1}), h is the matric suction (mm), while α and n are the respective shape and pore size distribution parameters, and the condition m=1-1/n should be satisfied. Although the van Genuchten (1980) model is popular the goodness of the interpolation is determined by the ability of the model to fit the measured data. Given that different models assumes a different air entry point it would be therefore appropriate to compare how best the available models fit the measured data before selecting a model for any other reason.

2.3.3.3 Soil hydraulic conductivity

Nevertheless estimation of either saturated or unsaturated hydraulic conductivity is regarded as one of the time consuming and yet sensitive exercises that requires both expertise and specialized equipment. Different approaches using direct and indirect methods including field and laboratory scale measurements have been developed

2.3.3.3.1 Determining soil hydraulic conductivity

Soil hydraulic conductivity could be viewed according to the Darcian law principle (Narasimhan, 2004) and refer to as the ratio of flux rate to the hydraulic gradient operating across the flow domain. While saturated flows are limited to large draining pores, flow under transient conditions continues following de-saturation and may persist much longer on finely textured or compacted soils.

2.3.3.3.2 Saturated hydraulic conductivity

Saturated hydraulic conductivity (Ks) reflects the permeability constant of the soil when all pores are filled with water, a situation that occurs directly after rainfall or irrigation. In the absence of significant matric suctions at near saturation, Ks is representative of the maximum flux rate the soil could assume under steady state conditions. Its dependence to pore size distribution, suggest that each soil shall bear a different Ks value and this could also vary under different tillage management practices. To this effect in situ methods for determining Ks provide meaningful estimates. The sprinkler method or infiltrometer is one common method, but due to kinetic energy of dropslets causing compaction (Hillel, 2004) of the surface, it is more suitable for rainfall simulation than for Ks determination. The double ring method (Haise et al., 1956) was developed for field conditions and is adapted to measure saturated and unsaturated hydraulic conductivity on both homogenous and layered soils. To accommodate spatial variability the selected size and number of plots is of importance (Wildenschild, 1996). Described in details by Haise et al. (1956) the double ring method is an inverse technique that with the necessary instruments and apparatus the entire set of hydraulic parameters could be measured simultaneously.

2.3.3.3.3 Unsaturated soils hydraulic conductivity

Hydraulic conductivity (K) under unsaturated conditions loses its constant status it assumed under saturated flows and become a functional coefficient expressed with respect to either

matric suction (h) or volumetric soil water content (θ). For either case K estimates are largely based on laboratory experiments given the difficulty to control field experiments from environmental elements such as relative humidity. A total of up to 14 different techniques are available to measure K and were summarized by Benson and Gribb (1997). Common among this group are the dried monoliths evaporation method (Wind, 1955), Outflow Methods (Gardner, 1961), Bruce-Klute Method (Klute, 1972), and the Sorptivity Method (Dirksen, 1979). However, difficulties to attain equilibration and need for independent retention data make these procedures cumbersome. More so, laboratory soil columns fail to represent field conditions especially for layer soils with abrupt transitions. The instantaneous profile method (IPM) was traditionally developed for laboratory conditions (Sławinski et al., 2004) but has become a reliable *in situ* procedure especially if the experiment is insulated from weather elements and water content and tensiometry simultaneous measurements are feasible (Hillel et al., 1972). Alternative to the IPM is the inverse method that relies on mathematical models related to those established to characterise the SWCC to predict the K-coefficient. Given that SWCC is the much easier hydraulic property to measure, the early models used the Burdine theory (Millington-Quirk, 1961) based on SWCC to predict the K-coefficient. Follow up work by Brooks and Corey (1964), Mualem, (1976) and van Genuchten (1980) as well as the Kosugi (1996) contributed remarkably to the predicting of K from SWCC parameters. Despite their popularity overseas they have not been fully exploited under local soil conditions especially their ability to predict K under *in situ* conditions.

2.3.4 General flow equation

The knowledge of SWC, SWCC and K functions needs to be known before any physical quantification of soil water movement and storage could be determined. Soil as a multi-porosity system requires hydraulic functions that captures mass and momentum balance in a dimensionless field for steady and transient state conditions. Based on the conceptual representation of soil pores as equivalent capillaries, the first mathematical expression of soil water movement was that of Darcy (1856) which for a three dimensional space (∇) vector under saturated soils was able to conserved mass by the differential expression:

$$q = -K\nabla H \qquad (3.3)$$

Where q is volume flux (cm s^{-1}), K is hydraulic conductivity coefficient (cm s^{-1}). ∇ is the three-dimensional space vector that embraces ∂x, ∂y and ∂z, ∇H is the hydraulic head

gradient in three dimensional space. This equation was extended for unsaturated conditions by Richard (1931) with the provision that K becomes a function of matric suction, K= K (h), assuming the expression:

$$q = -K(h)\nabla H \tag{3.4}$$

Where ∇H is the hydraulic head gradient with reference to matric suction (h) and gravitational potential (z). The Eq. 3.4 can also express K in terms of volumetric water content, K(θ). Richard (1931) also integrated the dynamic aspect of flow on the Darcian mass balance equation that resulted in the general flow equation where saturated and unsaturated conditions could be respectively expressed as:

$$\frac{\partial\theta}{\partial t} = \nabla.\,\mathrm{K}\nabla\mathrm{H} \tag{3.5}$$

$$\frac{\partial\theta}{\partial t} = \nabla.\,(\mathrm{K(h)}\nabla\mathrm{H}) \tag{3.6}$$

The Richard's equations (RE) constitutes two independent variables time (t) and spatial vector (x,y,z) and two dependent variables; volumetric water content (θ) and hydraulic head (∂H), which may include both matrix suction head (h) and gravitational head (z) components as defined in Eq. (3.4). Various forms of the RE are available and could be solved by analytical or numerically schemes once their hydraulic constitutive relations and boundary conditions are defined (Barari et al., 2009). Because of the nonlinearity of the hydraulic functions used as inputs to the RE various physical models have been developed with efficient numerical schemes to solve the RE for diverse flow problems involving the components of SPAC.

One of the attractive physical models is the HYDRUS-1D and HYDRUS-2D computer codes that is equipped with inverse optimization algorithm that allow inversion of the RE for various flow boundary conditions such as those involving deep drainage, redistribution and evaporation (Simunek et al., 2009). Development of optimized physical parameters for some of the local soils earmarked for rainwater harvesting could be a more convenient approach to accelerate the up scalling of water harvesting tillage practices. Although HYDRUS codes is yet to be equipped to simulate surface runoff and to partition total crop water use according evaporation and transpiration; its application in soil water balance studies including drip and surface irrigation has been very attractive (Abbasi et al., 2003; Kandelous and Simunek, 2010). However, evidence shows that simple approaches to characterise surface runoff either

from rainfall (Morin and Benyamini, 1977) or during surface irrigation (Mateos and Oyonarte, 2005) and soil water balance including the partitioning of evapo-transpiration into separate constitutes (Stroosnijder, 1987; Zhang et al., 1998) produce reasonable estimates.

2.4 Gap in knowledge

Evidence from the previous review sections (2.2 to 2.2.2.3.1) points out that rainwater harvesting water management system in practice do improve rainfall water productivity and that a number of alternative strategies that are cost effective and easy to manage were available. In-field rainwater harvesting (IRWH) is one of the attractive strategies that have been developed to improved water productivity in the dryland crop production areas in the semi-arid areas of the Free State Province of South Africa. To improve the productive scope of IRWH in the light of increased concerns on rainfall variability and severe evaporation in the area a series of studies with IRWH being the focus point have been investigated. Some of these works are summarized in Table 2.2. The soil water balance components, physical and pedological features, hydraulic processes and soil physical technologies were illustrated in almost all these studies the concept of IRWH was well developed and substantiated. Soil water balance components studied were comprehensively addressed. However the aspect of redistribution on unsaturated soil profiles was not addressed by all these studies. This component predominant in semi-arid areas where evaporation is severe and rainfalls are erratic and too low to wet the deeper profile layers (Hillel, 2004). In addition, although evaporation has been extensively studied by Hensley et al. (2000); Botha (2006) and Nhlabatsi (2010), the relationship between the soil hydraulic properties and the progression of the drying front into deeper layers of the soil profile on different soil types has not been compared. Evidence shows that soils from semi-arid areas are predominately unsaturated and that most evaporation occurring under these conditions is controlled by the soil hydraulic properties (Wilson et al., 1997; Peters and Durner, 2008). Reliance on the arithmetic mean (Yeh et al., 2005) to determine the soil water balance for the plot is another concern that needs to be addressed given the proportional differences in the surface area demarcated for the runoff and basin area. Computer based technologies are fairly used among these studies including those that predicted runoff and yields such as Putu Run (Walker et al., 2003) and CYP-SA models. Given the increasing difficulties to measure soil hydraulic properties under in-situ conditions the introduction of the HYDRUS-1D and -2D codes (Simunek et al., 2009) to predict these properties from soil physical properties that are easy to measure would be beneficial to IRWH water management systems.

According to the design of IRWH all these studies used the 2 m RSW as a standard catchment size and questions on how this RSW affected soil water storage with respect to crop suppression evaporation through their canopies has never been brought into perspective. The importance of crop canopy cover on suppressing evaporation is well acknowledged in literature (Grena and Hess, 1994; Eberbatch and Pala, 2005; Magbool et al., 2006).

Irrigation according to the developers of IRWH has been out of question given the predominance of rain-fed agriculture in the Province. It is not surprising that that none of the listed studies included irrigation. However, where limited accessible irrigation water is available it could make a significant different in stabilising yields (World Bank, 2005) in the face of persistent dry spells common in the area (Bennie and Hensley, 2001). Applying water where the plant grows and at low cost as possible are the important factors of selecting the irrigation method. The micro-flood irrigation appears to satisfy these criteria but its compatibility with IRWH is yet to be tested.

Water use efficiency is one of the criteria for evaluating the productivity of water management practices. Among the few that applied this criteria only one used the transpiration based water use efficiency. This was more meaningful than the ET based efficiency since it provides a measure of the crop performance under a given set of management practices (Stroosnijder, 1987). The procedure used to partition ET into E and T used by Hensley et al. (2000) relied on the Tanner and Sinclair (1983) that used a crop specific transpiration efficiency that was inherently insensitive to the climatic variability and water stress (Morgan et al., 2003). Therefore, an alternative procedure of practical relevance needs to be proposed mainly within the framework of integrating micro-flood irrigation with IRWH.

Table 2.2 A summary of reviewed local water management studies related to IRWH showing work done (+) and not done (-) on selected water balance, texture, soil hydraulic properties (SHP), special tools or models and nature of water use efficiency (WUE).

			Soil balance components (mm)								Soil texture (%)			SHP		Special tools/	WUE	
Author (s)	Crop	RSW	I	R	DD	RED	RFF	ET	T	E	Clay	Silt	clay	SWCC	K(θ)	models	ET	T or Ev
Hensley et al. (2000)	Maize	2	-	+	+	-	+	+	+	+	+	+	+	-	-	CYP-SA	+	+
Botha, (2006)	Maize	2	-	+	+	-	+	+	+	+	+	+	+	-	-	CYP-SA, PUTU-RUN	+	+
Mandiringana et al. (2003)	Maize	2	-	+	-	-	-	-	-	-	-	-	-	-	-	-	-	-
Joseph, (2007)	Maize	2	-	+	+	-	+	+	+	+	+	+	+	+	+	Tanner and Sinclair (1983	+	+
Fraenkel, (2008)	-	-	-	-	+	-	-	-	-	-	+	+	+	+	+	Pedo-transfer	-	-
Bothma, (2009)	Maize	2	-	+	+	-	+	-	-	-	+	+	+	+	+	Ridger plough	-	-
Chimungu, (2009)	-		-		+	-	-	-	-	-	+	+	+	+	+	RECT	-	-
Nhabatsi, (2010)	-		-	+	+	-	-	-	-	+	+	+	+	+	+	Lysimeters, Sensors	-	-
Mzezewa et al. (2010)	Sunflower cowpeas	2	-	+	-	-	+	+	-	-	+	+	+	-	-	-	-	-
Mzezewa and van Rensbaurg (2010)	-	2	-	+	-	-	+	-	-	-	+	+	+	-	-	Hofrey rainfall simulator	-	-

2.4 References

Abbasi, F., Jacques, D. Simunek, J. and van Genuchten, M.Th., 2003. Inverse estimation of soil hydraulic and solute transport parameters from transient field experiments: Heterogeneous soil. *Am. Soc. Of Agric. Eng.*, 46: 1097-1111.

Acciaresi, H. A, and Zuluaga, M. S., 2006. Effect of plant row spacing and herbicide use on weed above ground biomass and corn grain yield. Planta Daninha, 24: 287-293.

Ahuja L. R, Fiedler F, Dunn GH, Benjamin JG., 1998. Changes in soil water retention curves due to tillage and natural reconsolidation. *Soil Science Society of America Journal,* 62: 1228-1233.

Ali, A., Oweis T., Rashid, M., EI-Nagger, S., Abdul-Ail, A., 2007. Water harvesting options in the drylands at spatial scales. *Land Use and Water Research*, 7: 1-13.

Anderson, S. H., Gantzer, C. J., Brown, J. R., 1990. Soil physical properties after 100 years of continuous cultivation. *J. of Soil Water Conserv.*, 45: 117–121.

Andrade, E.T., de Correa, P. C., Martins, J. H., Alvarenga, E.M., 1999. Avaliacao de dano mecânico em sementes de feijao por meio de condutividade eletrica. *Revista Brasileira de Engenharia Agrícola e Ambiental,* 3:54–60.

Anschutz, J., Kome, A., Nederlof, M., de Neef, R. and van de Van, T., 2003. Water harvesting and Soil water retention.Sec ed. Agromisa Foundation. Wageningen, Netherlands.

Annandale, J. G., Stirzaker, R. J., Singles, A., van der Laan, M. and Laker, M. C., 2011. Irrigation scheduling research: South African experiences and future prospects. *Water SA*, 37: 751-762.

Austin, C., 2003. Micro flood, a new way of applying waters. http://waterright.com.a. 22/ 09/2011, 10.00 a.m (LT).

Awulachew, S. B., Merrey, D. J., Kamara, A. B., Koppen Van, B., de Vries, P. and Boelee, E., 2005. Experiences and opportunities for promoting small scale/micro irrigation and rainwater harvesting for food security in Ethiopia. International Water Management Institute, Working Paper 98, Addis Ababa, Ethiopia.

Barari, A., Janalizadeh, A., Farrokhzad, F. and Ganji, D.D., 2009. Application of homotopy perturbation method and variational iteration method to anonlinear diffusion equation with a reaction term. *J. Appl. FunctionalAnal.*, 4: 300-311.

Bennie, A. T. P, Coetzee, M. J. and van Antewerpen, R., 1988. A water balance model for irrigation based on the water suppy rate from the soil profile and crop water demand. WRC Report No. 144/1/88. Water Research Commision, Pretoria, South Africa.

Bennie A. T. P., 1990. Sound water management concepts and their applications at farm level. Department of Soil Science, University of the Free State, Bloemfontein. South Africa.

Bennie, A. T. P., 1991. Managing the profile available water capacity of soils for irrigation of annual crops in arid regions. Department of Soil Crop Climate Science, University of the Free State, Bloemfontein, South Africa.

Bennie A. T. P., 1994. Managing the profile available water capacity for irrigation of annual crops in arid regions. Department of Soil Crop Climate Science, University of the Free State. Bloemfontein, South Africa.

Bennie, A.T. P., Hoffman, J. E., Coetzee, M. J. and Vrey, H. S., 1994. Storage and utilization of rainwater in soils for stabilizing crop production in semi arid areas (Afr.). Report No. 227/1/94. Water Research Commission, Pretoria. South Africa.

Bennie, A. T. P. and Hensley, M., 2001. Maximising precipitation utilization in dryland agriculture in South Africa- a review. *J. Hydrol.*, 241: 124-139.

Benson, C. H. and Gribb, M. M., 1997, Measuring unsaturated hydraulic conductivity in the laboratory and field, *ASCE GSP*, 68: 113-168.

Bello, W. B., 2008. The effect of rain-fed and supplemetal irrigation on the yield and yield components of maize in Mekelle, Ethopia. *Ethopian J. of Env.Studies and management,* 2: 1- 7.

Bittelli, M. and Flury, M., 2009. Errors in water retention curves determined with pressure plates. *SSAJ,* 73:1453-1460.

Botha, J. J., 2006. Evaluation of maize and sunflower production in a semi-arid area using In-field rainwater harvesting. Ph.D. (Agric) Dissertation, University of the Free State, Bloemfontein, South Africa.

Bohne, K., 2005. An introduction into applied soil hydrology. Lecture notes. Catena Verlag GMBH, Reiskirchen, Germany.

Bouma, J., 2010. Functional characterization of soil structure field descriptions.19th World Congress of Soil Science, Soil Solutions for a Changing World. University of The Netherlands, Wageningen, Netherlands.

Brooks, R. H., and Corey, A. T., 1964. Hydraulic properties of porous media. Hydrology paper no.3. Civil Engineering Dep. Colarado State University, Fort Collins, USA.

Bruggerman, A. and Oweis T., 2001. Water Resource Conservation and Management for agricultural production in dry areas. Project 3.1. www.icarda.org. 24/01/2012, 11.00 a.m (LT).

Burdine, N. T., 1953. Relative permeability calculation from pore size distribution data. *Trans. Am. Inst. Min. Eng.*, 198: 71-78.

Chimungu, J. G., 2009. Comparison of field and laboratory measured hydraulic properties of selected diagnostic soil horizons. M.sc. (Agric) Dissertation, University of the Free State Bloemfontein, South Africa

Clothier, B. E., and White, I., 1981.Measurement of sorptivity and soilwater diffusivity in the field. *Soil Sci. Soc. Am. J.*, 4: 241-245.

Critchley, W. and Siegert, K., 1991. Water harvesting: a manual for the design and construction of water harvesting schemes for plant production. AGL Misc. Pap. 17. FAO, Rome.

Crosby, C. T., de Lange, M., Stimie, C. M. and Stoep, I., 2000. A review of planning and design procedures applicable to small scale farmer irrigation projects. WRC No 578: 2.Darcy, H., 1856. Les Fontaines Publiques de la Ville de Dijon (Fr), Dalmont, Paris.

Dane, J. H., and Klute, A., 1977. Salt effects on the hydraulic properties of a swelling soil. *Soil Sci. Soc. Am. J.*, 41:1043–1049.

Dane, J. H. and Hopmans, J. W., 2002. Soil water retention and storage - Introduction. In: Methods of Soil Analysis. Part 4. Physical Methods (J.H. Dane and G.C. Topp, Eds.). *Soil Science Society of America* Book Series No. 5: 671-674

Darcy, H., 1856. Les Fontaines Publiques dela Ville de Dijon, Dalmont, Paris France (*Fr*).

Eberbatch, P. and Pala, M., 2005. Crop row spacing and its influence on the partitioning of evapo-transpiration by winter- grown wheat in Northern Syria. *Plant and soil*, 268; 195-208.

Eching, S.O. and Hopmans, J.W., 1993. Inverse solution of unsaturated soil hydraulic functions from transient outflow and soil water pressure data. Land, Air and Water Resources Paper No.100021. University of California, Davis, USA.

Eching, S.O., Hopmans, J.W. and Wendroth, O., 1994. Unsaturated hydraulic conductivity from transient multistep outflow and soil water pressure data. *Soil Sci. Soc. Am. J.* 58:687-695.

FAO, 2009. How to feed the world in 2050.www.fao.org., 28/01/2012, 10.30 am (LT). Fischer, G., M. Shah, and van Velthuizen, H., 2002. Climate Change and Agricultural

Vulnerability. Special report for the UN World Summit on Sustainable Development, 26 August–4 September, Johannesburg. Laxenburg, Austria

Fares, A. and Polyakov, V. O., 2006. Advances in Crop Water Management Using Capacitive Water Sensors. In D. Sparks (ed.), *Advances in Agronomy.*Vol.90, Academic Press.

Gardner, W. R., 1956. Calculation of capillary conductivity from pressure plate outflow data. *Soil Sci. Soc. Amer. Proc.*, 20: 317-320.

Grena, A. K. and Hess, T. M., 1994. Water balance and water use of pearl millet-cow pea intercrops in north east Nigeria. *Agricultural Water Management*, 26: 169-185.

Haise, H. R., Donnan, J.T., Phelan, L.F. and Shockley, D.G., 1956. The use of cylinder infiltrometers to determined the intake characteristics of irrigated soil. USDA-ARS and USDA-SCS, ARS 41-7. Gov. Print. Office, Washington, DC.

Hanks, R. J., 1974. Model for predicting plant yield as influenced by water use. *Agron. J.*, 66: 660-665.

Haise, H. R., Donnan, J.T., Phelan, L.F. and Shockley, D.G., 1956. The use of cylinder infiltrometers to determined the intake characteristics of irrigated soil.USDA-ARS and USDA-SCS, ARS 41-7. Gov. Print. Office, Washington, D.C., USA.

Haines, W. B., 1930. The hysteresis effect in capillary properties and the modes of moisture distribution associated therewith. *J. Agric. Sci.*, 20:96–105.

Haverkamp, R., Debionne, D., Viallet, P., Angulo-Jaramillo, R. and de Condapa D., 2005. Soil properties and moisture movement in the unsaturatedzone, in The Handbook of Groundwater Engineering, CRC Press, Boca Raton, Fla.

Hensley, M. and de Jager, J. M., 1982. The determination of the profile available water capacities of soils. Department of Soil Science. University of Fort Hare, Alice, South Africa.

Hensley, M., Botha, J. J., Anderson, J. J., van Staden, P. P. and Du Toit, A., 2000. Optimising rainfall use efficiency for developing farmers with limited access to irrigation water. Water Research Commission Report no. 878/1/00, Pretoria, South Africa

Hensley, M., Le Roux, P., Gutter, J. and Zerizghy, M.G., 2007. A procedure for an improved soil survey technique for delineating land suitable for rainwater harvesting. WRC Report No. TT 311/07, Water Research Commission, Pretoria, South Africa.

Hillel, D., Krentos, V. D., and Stylianou, Y., 1972. Procedure and test of an internal drainage method for measuring soil hydraulic characteristics *in situ. Soil Sci.,* 114:395-400.

Hillel, D. H., 2004. Environmental soil physics. Academic Press, New York, USA.

Joseph, F., 2007. Maize response to in-field rainwater harvesting on the Fort Hare/Oakleaf Ecotope. MSc (Agric) Dissertation, University of the Free State, Bloemfontein, South Africa.

Joshi, P. K., Jha, A. K., Wani, S. P, Joshi, L. and Shiyani. R. L., 2005. Meta-analysis to assess impact of watershed program and people's participation. Comprehensive Assessment of Water Management in Agriculture Research Report 8. IWMI, Colombo, Sri lanka.

Jury, W., Gardener, W. R., and Gardner, W. H., 1991. Soil Physics (5th Ed.). John Wiley and Sons, New York, 1991.

Kool, J. B., Parker, J. C. and van Genuchten, M. Th., 1987. Parameter estimation for unsaturated flow and transport models, a review. *J. Hydrol.*, 91:255–293.

Klute, A., 1986. Water retention: Laboratory methods. *In* A. Klute (ed.). Methods of soil analysis. Part 1, 2nd ed. *Agron. Monogr.* 9. ASA and SSSA, Madison, WI.

Kutilek, M., 2004. Soil water in the system of hydropedology. Nad Patankou 34, 160 00 Prague 6, Czech Republic.

Kandelous, M.M. and Simunek, J., 2010. Numerical simulations of water movement in a subsurface drip irrigation system under field and laboratory conditions using HYDRUS 2-D. *Agricultural Water Management,* 97:1070–1076.

Leib, B.G., Jay, J., Matthews, D. and Gary, R., 2003. Field evaluation and performance comparison of soil moisture sensors. *J. Soil Sci.*, 168: 396-408.

Lin, H.S., McInnes, K. J., Wilding, L.P., Hallmark, C.T., 1998. Macroporosityand initial moisture effects on infiltration rates in vertisols and verticintergrades. *Soil Science,* 163: 2-8.

Lorentz, S. A., DurnFord, D. S. and Corey, A., 1993. Liquid Retention Measurement on Porous Media Using a Controlled Outflow Cell.Proceedings of American Society of Agronomy-Crop Science Society of America-Soil Science Society of America 1991 Annual meeting, Denver, Colorado, USA.

Luxmoore, R., 1981. Micro-, Meso- and macroporosity of soil.*Soil Sci. Sc. Am. J.*, 45: 241-285.

Mailhol, J. C., Priol, M., Benali, M., 1999. A furrow irrigation model to improve irrigation practices in the Gharb valley of Morocco. *Agricultural Water Management*, 42: 65-80.

Maqbool, M. M., Tanveer, A., Ata, Z. and Ahmad, R., 2006. Growth and yield of maize (*Zea Mays L.*) as affected by row spacing and weed competition durations. *Pak. J. Bot.,* 38; 1227-1236.

Mateos, L. and Oyonarte, N.A., 2005. A spreadsheet model to evaluate sloping furrow irrigation accounting for infiltration variability. *Agricultural Water Management*, 76: 62-75.

Millington, R. J. and Quirk, J. P., 1961. Permeability of porous solids.Trans. *Faraday Society*, 57: 1200-1207.

Morgan, C.L.S., Norman, J. M. and Lowery, B., 2003. Estimating plant available water across a field with an inverse yield model. Division S-6; Soil and Water Management and Conservation. *Soil Sci. Soc. Am. J.,* 67: 620-629.

Moult, N. G., Lecler N. L. and Smithers J. C., 2009. A catchment-scale irrigation systems model for sugarcane; Model application. *Water SA,* 35: 29-36.

Morin, J. and Benyamini, Y., 1977. Rainfall infiltration into bare soils. *Water Resour. Res.*, 13: 813–817.

Mualem, Y., 1976. A new model for predicting the hydraulic conductivity of unsaturated porous media. *Water Resour. Res.*, 12: 513-522, 1976.

Mzezewa, J. and van Rensburg, L.D., 2011. Effects of tillage on runoff from a bare clayey soil on a semi-arid ecotope in the Limpopo Province of South Africa. *Water S A.,* 37; 1-8.

Mzezewa, J., Gwata, E.T. and van Rensburg, L. D., 2011. Yield and seasonal water productivity of sunflower as affected by tillage and cropping systems under dryland conditions in the Limpopo Province of South Africa. *Agricultural water Management*, 98; 1641-1648.

Narasimhan, T. N., 2004. Darcy's law and unsaturated flow.*Vadose Zone J.*, 3: 2059.

Nasr, 1999. Assessing desertification and water harvesting in the Middle East and North Africa: No.10, Policy Implications ZET- Discussions.Papers on Development Policy. Bonn, ZEF Bonn, Zentrum fur Entwicklungsforschung, Center for Development Research, Univestat Bonn. Balkema. Rotterdam.

Nhlabatsi, N. N., 2010. Soil water evaporation studies on the Glen/Boheim ecotope. Ph D. Thesis, University of the Free State, Bloemfontein, South Africa.

Onyango, O. C., 2009. Decreased row spacing as an option for decreasing maize (Zea may L.) yield in Trans Nzoi district, Kenya. *J. of Plant Breeding and Crop Science*, 1: 281-283.

Oweis, T., Hachum, A. and Kijne. J., 1999. Water harvesting and supplementary irrigation for improved water use efficiency in dry areas. IWMI Contribution (No. 7), System Wide Initiative on Water Management (SWIM). Colombo, Sri Lanka.

Pacey, A., and Cullis A., 1986. Rainwater harvesting: the collection of rainfall and runoff in rural areas. Intermediate Technology Publ, London. England.

Peters, A. and Durner, W., 2008. Simplified Evaporation Method for Determining Soil Hydraulic Properties. *Journal of Hydrology*, 356: 147– 162.

Prinz, D., 1996. Water harvesting: Past and Future. In Pereira, L.S., (ed), Sustainability of Irrigated Agriculture. Proceedings, NATO Advanced Research Workshop. Vimeiro.

Prinz, D., and Malik A. H., 2002. Runoff farming. Institute of Water Resources Management, Hydraulic and Rural Engineering.Department of Rural Engineering, University of Karlsruhe. Germany.

Ratliff, L. F., Ritchie, J. T. and Cassel, D. K., 1983. Field-measured limits of soil water availability as related to laboratory-measured properties. *Soil Sci. Soc. Am. J.*, 47:770-775.

Rawls, W. J., Ahuja, L. R. and Brakensiek, D. L., 1992. Estimating soil hydraulic properties from soils data. In M.Th. Van Genuchten et al. (ed.). Indirect methods for estimating the hydraulic properties of unsaturated soils. Univ. of California, Riverside, USA.

Reeve, M. J. and Carter A. D., 1991. Water release characteristic. *In* K.A. Smith and C.E.Mullins (ed.) Soil analysis: Physical methods. Marcel Dekker, New York. USA.

Rhoads, B. L. and Sukhodolo, A. N., 1991. Field investigation of three-dimensional flow structure at confluences: 1. Thermal mixing and time-averaged velocities. *Water resources research,* 37:2393-2410.

Richards, L. A., 1941. A pressure-membrane extraction apparatus for soil solution. *Soil Science,* 51: 377-386.

Richards, L. A., 1931. Capillary conduction of liquids through porous mediums. *Physics,* 1: 318–333.

Rockstrom, J., 2000. Water resources management in smallholder farms in Eastern and Southern Africa: An overview. *Phys. Chem. Earth*, 25: 275- 283.

Rockstrom, J., Hatibu, N., Oweis, T. Y. and Wani, S., 2007. Managing water in rain-fed agriculture, Part 4 In: Unlocking the potential of rain-fed agriculture, IWMI, Colombo, Sri Lanka.

Rodriguez, J. A, Díaz, A., Reyes J. A. and Pujols, R., 2004. Comparison between surge irrigation and conventional furrow irrigation for covered black tobacco cultivation in a Ferralsol soil. *Span J. Agric. Res.,* 2: 445-458.

Rosegrant, M., Ximing, C. Cline, S. and Nakagawa, N., 2002. The role of rainfed agriculture in the future of global food production. EPTD Discussion Paper 90. International Food Policy Research Institute, Environment and Production Technology Division, Washington DC,USA.

Sangoi, L., Ender, M., Guidolin, A. F., de Almeida, M. L. and Heberle, P. C., 2001. Influence of row spacing reduction on maize grain yield in regions with a short summer. *Pesq.agropes bras*, 36:861-869.

Schroder, T., Javaux, M., Vanderborgh, J., Körfgen, B., Vereecken, H., 2008. Three dimensional modelling of soil-plant interactions: consistent coupling of soil and plant root systems. *Vadose Zone Journal,* 7: 1089-1098.

Schneekloth, J. and Andales, A., 2009. Irrigation: seasonal water needs and opportunities for limited irrigation for Colorado crops. Department of Agriculture, Colorado State University, Colorado, USA.

Simunek, J., Jarvis, N. J., van Genuchten, M.Th. and Cardenas, A., 2003. Review and comparison of modelsfor describing non-equilibrium and preferential flow and transport in the vadose zone. *J. Hydrol., 272*:14-35.

Simunek, J., van Genuchten, M. Th., and Miroslav, S., 2008. Development andapplications of the HYDRUS and STANMOD software packages andrelated codes. *Soil Sci. Soc. Am. J.*, 7: 587-600.

Simunek, J, Sejna, M., and van Genuchten, M.Th., 2009. The HYDRUS-2D software package for simulating two-dimensional movement of water, heat and multiple solutes in variably saturated media, Version 2.0. Rep. IGCWMC-TPS-53, p 251, Int. Ground Water Model.Cent., Colo. Sch. of Mines, Golden, CO.

Slawinski, C., Witkowska-Walczak, B., and Walczak, R.T., 2004. Determination of water conductivity coefficient of soil porous media. Centre of Excellence for Applied Physics in Sustainable Agriculture. Lublin, Poland.

Stroosnijder, L., 1987. Soil evaporation: test of a practical approach under semi arid conditions. *Neth. J. of Agric. Sci.*, 35:417-426.

The World Bank, 2005. Shaping the future of water for agriculture; A source book for investment in agricultural water management. Rural and Agricultural Development, Washington DC, USA.

Tabuada, M. A., Rego, Z. J. C., Vachuad, G., Pereira, L. S., 1995. Modeling of furrow irrigation. Advance with two diomsnional infiltration. *Agricultural water management*, 28:201-221.

van Rensburg, L. D. and Zerizghy, M. G., 2008. The BEWAB+ computer program for irrigation scheduling. Department of Soil, Crop and Climate Science, University of the Free State, Bloemfontein, South Africa.

Vereecken, H., Weynants, M., Javaux, M., Pachepsky, Y., Schaap, M. G. and van Genuchten, M.Th., 2010. Using pedotrasnfer functions to estimate the van Genuchten-Mualem soil hydraulic properties: A review. *Vadose Zone J.*, 9:795-820.

Walker, W. R. and Skorgeboe, G. V., 1987. Surface irrigation. Theory and Practice. Prentice-Hall, New Jersey. Engineering, Utah State University, Logan, Utah.

Walker S. and Tsubo, M., 2003. PUTURUN: A simulator of rainfall-runoff yield processes with in-field water harvesting. WRC Report No.KV142/03. Pretoria, South Africa.

Walker W. R., 2003. SIRMOD III; Surface Irrigation Simulation, Evaluation and Designs. Guide and technical document. Department of Biological and irrigation Engineering, Utah State University, Logan, Utah.

Waskom, R. M., 1994. Best management practices for irrigation and management Department of Agriculture. Colorado State University.Cooperative Extension Bulletin # XCM-173. Colorado, USA.

Wildenschild, D., 1996. Characterization of unsaturated hydraulic parameters forhomogeneous and heterogeneous soils.Department of Hydrodynamics and Water Resources. Technical University of Denmark, Denmark.

Wilson, G. V., and Luxmoore, R. J., 1988. Infiltration, macroporosity, andmesoporosity distribution on two forested watersheds. *Soil Sci.Soc.* Am. *J.*, 52: 329-335.

Wilson, G. V., Periketi, R. K., Fox, G. A., Dabney, S. M., Shields, F.D., Cullum, R.F., 2007. Soil properties controlling seepage erosion contributions to streambank failure. *Earth Surface Processes and Landforms,* 32: 447–459.

Wind, G.P., 1955. Field experiment concerning capillary rise of moisture in heavyclay soil. *Neth. J Agric Sci.*, 3: 60-69.

Wosten, J. H. M. and van Genuchten, T. H. M., 1988. Using texture and other soil properties to predict the unsaturated soil hydraulic functions. Division S-6, Soil water management and conservation. *Soil Sci. Soc. Am. J.*, 52:1762-1770.

Yeh, M., Khaleel, R. and Yeh, T. C. J. 2005. Stochastic analysis of moisture plume dynamics of field injection experiment. *Water Resource. Res.*, 41: W03013.

Zhang, H., Oweis, T. Y., Garabet, S. and Pala, M., 1998. Water use efficiency and transpiration efficiency of wheat under rain-fed conditions and supplemental irrigation in a Mediterranean-type environment. *Plant and Soil*, 201: 295-305

Znidarcic, D, Illangasekare, T. and Manna, M., 1991. Laboratory Testing and Parameter Estimation for Two-Phase Flow Problems. GeotechnicalEngineering Congress 1991, Vol. II, E G. McLean, D. A. Campbell,and D. W. Harris, Eds., ASCE Geotechnical Special Publication No.27, New York, USA.

CHAPTER 3

IN SITU EVALUATION OF INTERNAL DRAINAGE IN LAYERED SOILS (TUKULU, SEPANE AND SWARTLAND)

Abstract

The soil water characteristic curve (SWCC) and permeability properties of layered soils following deep infiltration depends on the structural and layering composition of the profiles diagnostic horizons. Three South African soils, the Tukulu and Sepane referred to Cutanic Luvisols, and Swartland to Cutanic Cambisols in other countries were selected for internal drainage evaluation. The soil water release curves as a function of suction (h) and unsaturated hydraulic conductivity (K-coefficient) as a function of soil water content, SWC (θ), were characterised alongside the pedological properties of the profiles. The hanging water column nd *in situ* instantaneous profile methods (IPM) were used for this were. Independently, the saturated hydraulic conductivity (Ks) was measured using double ring infiltrometers. The three soils had a generic orthic A- horizon but differed remarkable with depth. A clay rich layer was found in the Tukulu and Sepane at depths of 600 to 850 mm and 300 to 900 mm, respectively. The Swartland was weakly developed with a saprolite rock at a depth of 400-700 mm. During the 50 days drainage period, soil water loss amounted to 21 mm, 20 mm and 51 mm from the respective Tukulu, Sepane and Swartland profiles. An abrupt drop in Ks in conjunction with a steep K-coefficient gradient with depth was supported by the hydromorphic colours on the clay-rich layers of the Tukulu and Sepane indicating that drainage was restricted. These characteristics presented the Tukulu and Sepane as suitable for optimum soil water storage under in-field rainwater harvesting production technique compared to the Swartland with a much drier soil water regime.

Key words: internal drainage, layered soils, pedological properties, hydraulic conductivity

3.1 Introduction

Internal drainage has become a critical factor in soil water conservation especially on layered soils. Since the large soil pores are the first to drain following deep infiltration, their soil water release (SWR) and permeability is dependent on the structural and layering composition of the profile's diagnostic horizons. The SWR and permeability functions could be described by the SWR curve or soil water characteristic curve (SWCC) and unsaturated hydraulic conductivity (K-coefficient), respectively. While the former is expressed as a function of matrix suction (h) and SWC (θ) (Dane and Hopmans, 2002) the latter is expressed as a function of either h or θ (Eching and Hopmans, 1993).

In practice internal drainage depicts the emptying of water filled pores under the influence of gravity. In time and space, drainage rate diminishes with SWC and approaches negligible rates at drainage upper limit (DUL) approximated by Ratliff et al. (1983) to be 0.1 to 0.2 % per day. The DUL could further be reduced to approach the drainage lower limit (DLL), equivalent to the permanent wilting point (Hillel, 2004), by evaporation or transpiration (Bennie et al., 1994). In soils experiencing downward drainage DUL could be achieved between 2 to 12 days for fine-textured soils and up to 20 days in soils with a restrictive layer (Ratliff et al., 1983). The difference between DUL and DLL represents the plant available water (PAW) that is important for estimating crop water requirements (Bennie et al., 1994; Bittelli and Flury, 2006). Therefore accurate measurement of the soil hydraulic functions that determines the extent at which soil water drains away from the profile is crucial for effective soil water management.

In situ internal drainage methods of determining soil hydraulic functions are considered to be more realistic than laboratory methods. Continuum of soil horizons represents the actual boundary conditions under which water flows in a composite profile. Internal drainage under *in situ* conditions was first studied by Richard et al. (1956). Difficulties in measurement of K-coefficient under in situ conditions because of variations in air humidity and the need for simultaneous measurement of many parameters, transient experiments were preferred from the beginning. Early contributions included work by of Nielsen et al. (1964), Rose et al. (1965) and Watson (1966) that culminated to the launching of the instantaneous profile method (IPM) (Hopmans et al. 2002). Inversion of the Richard flow equation provided means to estimate the K-coefficient (Vachaud and Dane, 2002) indirectly from the ratio of drainage flux and effective hydraulic gradient. Other in-situ methods are the internal drainage and zero

flux plane methods described by Vachaud et al. (1978) and tension disk infiltrometers (Hopmans et al., 2002; Simunek et al., 1999). The IPM was consolidated when the in situ procedure to calculate the K-coefficient was published by Hillel et al. (1972). Among earlier studies the unity gradient become popular but was later disputed by Richardts, (1993); Bacchi and Richardts, (1993). To keep pace with the advances in the laboratory methods such as the one step (Kool et al., 1985) and multi-step (van Dam et al. 1994; Eching et al., 1994) outflow experiments, the IPM went through a series of modernization. This included the computational contributions by Libardi et al. (1980) and Bacchi, (1988), and the parameterization of the Richard inversion by Richardts et al. (2004). The first to use parameters based models to inversely estimate soil hydraulic functions from *in situ* experimental data was Dane and Hruska (1983), even though lack of uniqueness of their solution was a concern. Hurtado et al. (2005) used the IPM to estimate hydraulic functions below the DUL while Neto et al. (2007) introduced computer based software to calculate the K-coefficient in internal drainage experiments.

Despite the remarkable works done to improve in situ internal drainage methods, laboratory transient experiments are still by far dominant. Better control of conditions and parameters influencing soil hydraulic functions as well as access to dynamic instrumentation and powerful computers has made laboratory experiments attractive. Transferring some of these technologies to developing farming communities has not been successful in many occasions. Nevertheless, approaches such as the pedo-transfer (Leij et al., 1996; Acutis and Donatelli, 2003) and hanging water column technique (Vomicil, 1965; Dane and Hopmans, 2002) if used in collaboration with the IPM could serve as relatively cheap and yet powerful alternatives.

In the Free State province of South Africa, most of the rural farmers are concentrated on the low agricultural potential areas predominated by layered soils. This group of soils belong to the Duplex land type (Soil Classification Working Group, 1991) and occupy more than 10% of the provincial landscape (Hensley et al., 2007). Erratic soil water regimes common among this soil has led to the development of infield rainwater harvesting (IRWH) production technique (Hensley, 2000; FAO, 2009). This technique seeks to turnaround the high surface runoff and evaporation losses from the 550 mm annual rainfall associated with these soils into deep infiltration and soil water storage. However, the occurrence of clay rich layer either in the B or C-horizon among this group of soils suggests that their conservational prospects for IRWH is dependent on the horizons physical characteristics and layering formation. On

this account, the South African Tukulu and Sepane soil types also referred as Cutanic Luvisols and the Swarland also referred as Cutanic Cambisols of World Reference Base for Soil Resources (1998) were studied. The following objectives were pursuit: Firstly, to describe the pedological properties that relate to the presence of layering on the three soil types. Secondly, to determine the soil water release, unsaturated hydraulic conductivity and drainage-time functions that characterised the internal drainage outcomes of layered soils.

3.2 Material and methods

3.2.1 Site location and soil classification

The field experiments were carried out at Parady's Experimental Farm (29°13'24.69"S, 26°12'40.93"E, altitude 1422 m) of the University of the Free State. Three sites were selected with different soil types to include a typical Swartland (Sw), Sepane (Se), and Tukulu (Tu) soil form, according to the Soil Classification Working Group (1991). Three soil profile pits were prepared in each site at distance intervals of 50 m. Each profile pit was excavated in a step-wise downward fashion to allow double ring infiltrometers for the determination of steady state or saturated hydraulic conductivity for individual horizons. Soil samples from each horizon from these pits were taken for textural analysis and dry bulk density determination. Samples were oven dried at 105°C for 24 hours and particle size distribution was established using the pipette procedures proposed by the Non Affiliated Soil Analysis Work Committee (1990).

3.2.2 *In situ* experimental set up and measurements

3.2.2.1 Saturated hydraulic conductivity

Saturated hydraulic conductivity (Ks) for the individual profile layers of the three soil types was measured using double ring infiltrometers as described by Scotter et al. (1982). On each excavated soil profile horizon both rings with diameters of 400 and 600 mm were fitted into the surface to a depth of 20 mm. A floater with 10 mm calibrated depths was inserted in the central position of the inner ring. The outside ring was first wetted and kept ponded through the experiment to prevent lateral flows. Then the inner ring was ponded immediately over some plastic material to prevent erosion of the surface until the depth of water settled to a calibrated mark on the floater. The clock timer was set and further changes in depths along the calibrated floater were recorded until a steady time was clocked by the falling water head.

The saturated hydraulic conductivity (Ks, mm hour^{-1}) was obtained by the falling head method described of Jury et al. (1991);

$$K_s = \frac{L}{t_1} ln \frac{b_o + L}{b_1 + L} \quad (3.1)$$

Where L is the depth of the soil layer in question (mm), b_0 is the initial depth of total head above the soil column, b_1 is the lowest depth the falling is allowed to reach (mm) (mm), t_1 is the time taken for b_0 to fall to b_1 (in hours). Once the steady state condition was established it was assumed that the soil matrix suction was negligible and did not affect macro-pore domain (Zavattaro and Grignani, 2001).

3.2.2.2 Instantaneous soil water measurement

A field representative site from each soil type was selected for the setting up of the *in situ* instantaneous profile method (IPM). The IPM provides a more realistic approach in capturing the flow dynamics in a heterogeneous soil profile subjected to variable hydraulic processes such as internal drainage and evaporation (Hopmans et al., 2002). In the Sepane and Tukulu a more central position was selected and monoliths of (4 m x 4 m) x 1 m depth were prepared with three connected replications. Monoliths were centrally fitted with three neutron access tubes in a V shape to a depth of 1.1 m. On the Swartland, the monoliths were detached and setup at 30 m distance apart with dimensions of (1.2 m x 1.2 m) x 0.5 m depth. Shallow depths on the Swartland allowed the use of DFM probe loggers at depths of 0.6 m. All monoliths were laterally isolated with plastic sheet to prevent lateral water movement. An earth bund was made to form a ridge around the monoliths to isolate them from surface runoff and to support ponding.

Before soil water content (SWC) measurements commenced the monoliths were ponded with water for three days until it was presumed to have reached saturation. At the end of the 3rd day the monoliths were covered and sealed at the surface with a polythene plastic upon depletion of ponded water. Measurements of SWC were taken using a neutron water probe (NWP) at 200 mm, 500 mm, 850 mm and 1100 mm depth intervals. DFM probe loggers were set to take readings at every hour during the entire drainage period at depths of 100 mm, 300 mm and 550 mm for the Swartland soil profile.Over the first seven days SWC measurements were taken in the morning and afternoon and thereafter once a day for a 50 day period. At the beginning of the field measurements both soil water instruments were calibrated for the respective soil profiles. From each horizon a soil sample was taken using an auger at a 250

mm distance from the NWP and DFM probe. Samples were weighed shortly after packaging in paper bags. They were then oven dried at 105°C for 24 hours to obtain gravimetric water content from their *in situ* bulk densities.

The measured SWC that resulted in a drainage flux of 0.001 mm $hour^{-1}$ was assumed to have reached the drainage upper limit (DUL). In this study the concept of DUL was adopted and slightly extended by relating negligible drainage losses to annual average rainfall of semi arid areas. Given the low and erratic rainfall distribution of semi-arid areas an accumulative deep drainage losses amounting to 1 % of annual rainfall is generally acceptable. Practically a 1 % of the 550 mm annual average rainfall received from the central Free State region would be about 5 mm. This amount could be lost to deep drainage over the seven months (October to April) rainfall period if drainage rate is 0.001 mm $hour^{-1}$. Above this rate deep drainage would be significant and could result to serious implications on the field water balance. Interestingly, various field water studies have found that drainage becomes negligible at flux rates approaching 0.001 mm $hour^{-1}$ (Hensley et al., 2000; Chimungu, 2009; Nhlabatsi, 2011).

3.2.3 Laboratory experimental setup and measurements

Undisturbed soil core samples were taken from the centre of each horizon using a core sampler mounted on a hydraulic jack. Samples were then trimmed, sealed and transported to the laboratory for analysis of the soil water characteristics curve (SWCC). Sampling cores had an inner diameter of 103 mm with a height of 77 mm.

Preparation of samples and desorption experiment was carried out in two phases. Core samples and water used for saturation samples were initially de-aired using a vacuum chamber pump set at -70 kPa for 48 hours under room temperature. Subsequently, de-aired water was introduced on the second chamber with de-aired core samples allowing the inflow to wet samples from below. Ponded water outside the wetted sample was cut-off before water level overtopped the core samples. Core samples were left on the water bath for 24 hours to allow total saturation. Three replications were used for each horizon. Before commencement of the desorption experiment saturated samples were weighed and sealed to control evaporation.

Although the desorption experiment involved three phases from 0-10 kPa, 10-100 kPa and 100-1500 kPa, in this work only the first was illustrated to capture the SWCC during internal drainage. This procedure involved the hanging soil water column tension cup method

described by Dirksen (1999) and Dane and Hopmans (2002). Following saturation the samples were weighted and water that dripped from the sample at weighing time was attributed to the porosity of the samples. Placed on ceramic cups prepared for this purpose hanging 1000 mm from reference point samples, elevation height was gradually reduced at 100 mm intervals for the entire 1000 mm. At every step, interval samples were weighed before and after samples had equilibrated on the ceramic cups. During this experiment samples were covered with a foliar sheath to protect them from radiation. Considering that evaporation was assumed to be negligible under these conditions, change in samples mass was considered to be a true reflection of the amount of water that drained from the samples. The resulting soil water content-matric suction (θ-h) relationship was then regressed to estimate the corresponding θ-h relationship to internal drainage of soil profiles horizons from saturation to drainage upper limit (DUL).

3.2.4. Data analysis

3.2.4.1 Estimation of unsaturated hydraulic conductivity

The unsaturated hydraulic conductivity (K-coefficient) was calculated using the IPM procedure as described by Slawinski et al. (2004) and Neto et al. (2007). One dimensional flux was computed using the mathematical expression:

$$q(z,t) = \int_{z=zo}^{z} \frac{\partial\theta(z,t)}{\partial t} dz \qquad (3.2)$$

Where q is the flux (mm hour^{-1}), θ is volumetric soil water content (mm mm^{-1}), t is the time in hours and z is the reference depth (mm).

The flux expression was then fitted to the extended Darcian law to express the K-coefficient as a function of SWC (θ);

$$K(\theta)(z,t) = \frac{\int_{z=zo}^{z} \frac{\partial\theta(z,t)}{\partial t} dz}{\left(\frac{\partial h(z,t)}{\partial z} + 1\right)} \qquad (3.3)$$

Where K (θ) is the K-coefficient (mm hour^{-1}), h is the matrix suction (mm) and t as defined in equation 3.2. The classical exponential equation proposed by Hillel et al. (1972) was used to obtain a linear regression function on the semi log scale for the plotted K-θ relationships.

3.2.4.2 Statistical analysis

The exponential function describing the K-θ relationships for the three soils were converted into a semi-log scale after which a linear regression coefficient and intercept for each horizon was determined. The coefficient of determination (R^2) provided the accuracy of the fit on the resulting semi-log linearized function. The linearized K-θ relationships were then evaluated for homogeneity using the Bartlett's test or chi-square (χ^2) distribution and pooled regression coefficient F-test as described by Gomez and Gomez (1984). Also the Student's t-test was conducted to compare the regression coefficients between horizons within the same soil profile. Computed values were compared with tabular values, which serve as benchmarks at 95% confidence intervals. If the former was found to be larger than the latter the homogeneity hypothesis was rejected.

3.3 Results

3.3.1 Pedological properties

Table 3.1 summarizes the physical and chemical properties of the Tukulu, Sepane and Swartland soils according to the A-, B- and C-horizon layers. The results are also supported by soil profile photos in Figures 3.1 to 3.3. Further reference is made to the profile descriptions in Appendices A-C. All three soil types occurred within an area of less than 10 hectare, on a straight mid slope of less than 1%. However, both the Tukulu and Swartland occupied the upslope position with the former occurring along the smooth drainage lines. The Sepane soil form occupied most of the down slope areas of the experimental site. Although all the soil types had a generic orthic A-horizon differentiation in the B- and C-horizons gave each soil type unique layering properties.

Tukulu: The soil consisted of an orthic A-, neocutanic B- and prismatic C-horizon. The clay plus silt fraction for the three horizons was 18 %, 31 % and 57 %, respectively with corresponding bulk density of 1670 kg m^{-3}, 1597 kg m^{-3} and 1602 kg m^{-3}. Along with the increase in clay plus silt content with depth, was the transformation in textural classes from fine sandy loam in the A-horizon to a fine sandy clay loam in the B-horizon and to clay in the C-horizon. Corresponding horizons structural representations were massive apedal, weakly sub angular blocky and moderate to strong prismacutanic structure, respectively. A smooth transition between the A- and B-horizons confirmed the common attributes of these horizons including among others colour, texture and youthfulness of structure.

Table 3.1 Summary of the physical and chemical characteristics of the three soil types.

Soil physical properties									
Soil forms	Tukulu			Sepane			Swartland		
Master Horizons	A	B1	C	A	B1	C	A	B1	C
Coarse sand (%)	5.3	9.2	2.1	5.2	3.5	2.3	4.7	3.2	54.3
Medium sand (%)	9.3	8.8	3.8	10	4.1	2.3	7.6	5.3	4.6
Fine sand (%)	41.2	31	28.3	41.9	41	31	42	37.6	17.2
Very fine sand (%)	25.3	21	8.4	21.5	10.5	18	31.7	26.6	2.5
Coarse silt (%)	2.1	2	3	1	3	1	2	3	3
Fine silt (%)	4.6	2.5	6.5	1	3	1	1	2	3
Clay (%)	11.3	26.4	47.9	19	35	45	11.3	21.9	15
Bulk density (kg m^{-3})	1670	1597	1602	1670	1790	1730	1670	1530	1450
Porosity (%)	34.0	33	32.4	34	33.5	33.8	35	39.9	41.6
Ks (mm $hour^{-1}$)	36.1	40	9.6	35.2	18.1	1.9	23.5	42.8	76.5
Chemical properties									
pH (water)	5.8	6.1	6.5	5.9	6.2	6.3	5.5	5.8	6.8
Ca (c $mol_c.kg^{-1}$)	35.3	40.8	62.7	30.53	46	50	23	25.78	45
Mg (c $mol_c.kg^{-1}$)	18.8	20.8	54.7	13.89	21.87	29.76	12.1	13.1	25.4
K (c $mol_c.kg^{-1}$)	12.8	6.8	12.9	4.63	8.21	7.05	5.5	7.45	7.7
Na (c $mol_c.kg^{-1}$)	2.4	2.5	3.4	1.96	3.8	3.91	0.7	1.52	2.3

Ks=saturated hydraulic Conductivity

(a)

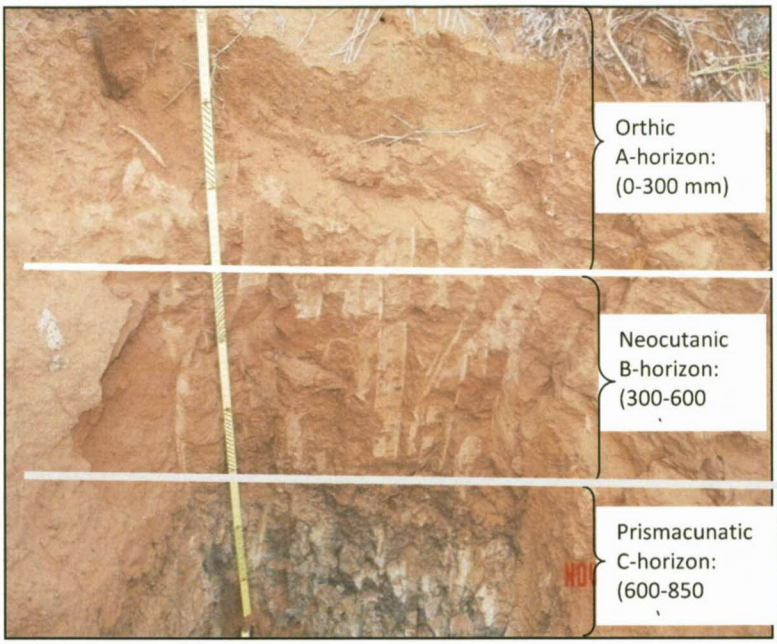

(b)

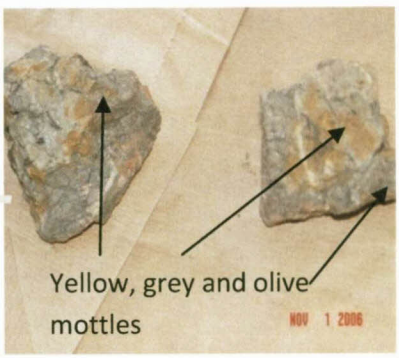

Figure 3.1 (a) Profile of the Tukulu and (b) mottles present in the C-horizon.

(a)

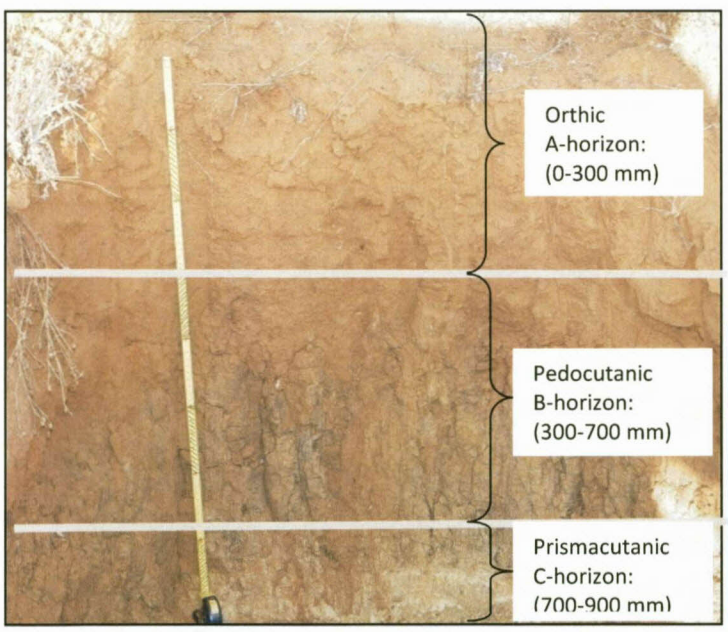

(b)

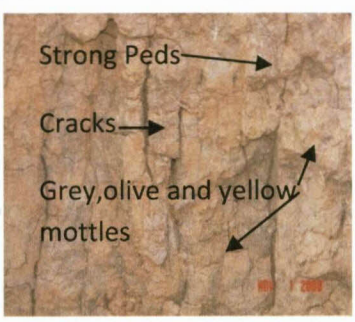

Figure 3.2 (a) Profile of the Sepane and (b) mottles present in the B-horizon.

In contrast, the clear abrupt transition between the B- and C-horizon explained the sudden increase in clay plus silt in the C-horizon, which gave the horizon grey colours compared to the red colours of the upper horizons. The distinct layering on the lower strata also confirmed

the sudden drop in K_s from 40 mm hour^{-1} in the B-horizon to 9.6 mm hour^{-1} in the C-horizon. Yellow, grey and olive mottled colours in the C-horizon shown in Figure 3.1 (b) could also be regarded as indicators, not only of the intensity of layering, but also of the wet soil water regime of this horizon

Sepane: The soil consisted of an orthic A-, pedocutanic B- and prismacutanic C-horizon as shown in Figure 3.2. The clay plus silt fraction of the three horizons was 21%, 41% and 47%, respectively. Corresponding bulk densities to the respective horizons were 1670 kg m^{-3}, 1790 kg m^{-3} and 1730 kg m^{-3}. Accompanying the increase in clay plus silt content with depth, was the transformation in horizon textural classes from fine sandy loam in the A-horizon to a fine sandy clay loam in the B-horizon and to fine sandy clay in the C-horizon. Structural properties unique to these horizon layers were the massive apedal, moderate to course sub angular blocky, and medium to strong prismatic structure, respectively. An abrupt transition between the A- and B-horizons and the smooth transition between the B- and C-horizons explained the concentration of structure between lower horizons of this soil. Changes in red colours from the surface to dull red and darker colours of the interior also pointed to layering that occurred at 300 mm depth splitting this soil into a weakly developed surface and well structured B- and C-horizons. Confirming the contrast in structure between the surface and B-horizon were the well-developed and distinct peds with clay skins shown in Figure 3.2 (b).

Swartland: The soil consisted of an orthic A-, pedocutanic B- and saprolite C-horizon as shown in Figure 3.3. The clay plus silt fraction for the three horizons was 14%, 27% and 21%, respectively. Corresponding bulk densities to the respective horizons were 1670 kg m^{-3}, 1530 kg m^{-3} and 1450 kg m^{-3}, respectively. A smooth transition occurred between the surface A- and B-horizons indicating a gradual build-up in clay content, which resulted from the fine sandy loam in the A-horizon transformed into a fine sandy clay loam in the B-horizon. Between lower horizons there was an abrupt transition from a sub-angular blocky structure in the B-horizon to the saprolite rock of the C-horizon. The presence of dolorite intrusions and many black sesquioxides concretions shown in Figure 3.3 (b) at depths of 200-400 mm explained the general course appearance and lack of abrupt transition in this soil. Although levels of calcium and magnesium showed to increase with depth the predominance of a weakly weathered saprolite at shallow depths of 400 mm also reflected the deficiencies in structure and subsequent dry water regime of this soil.

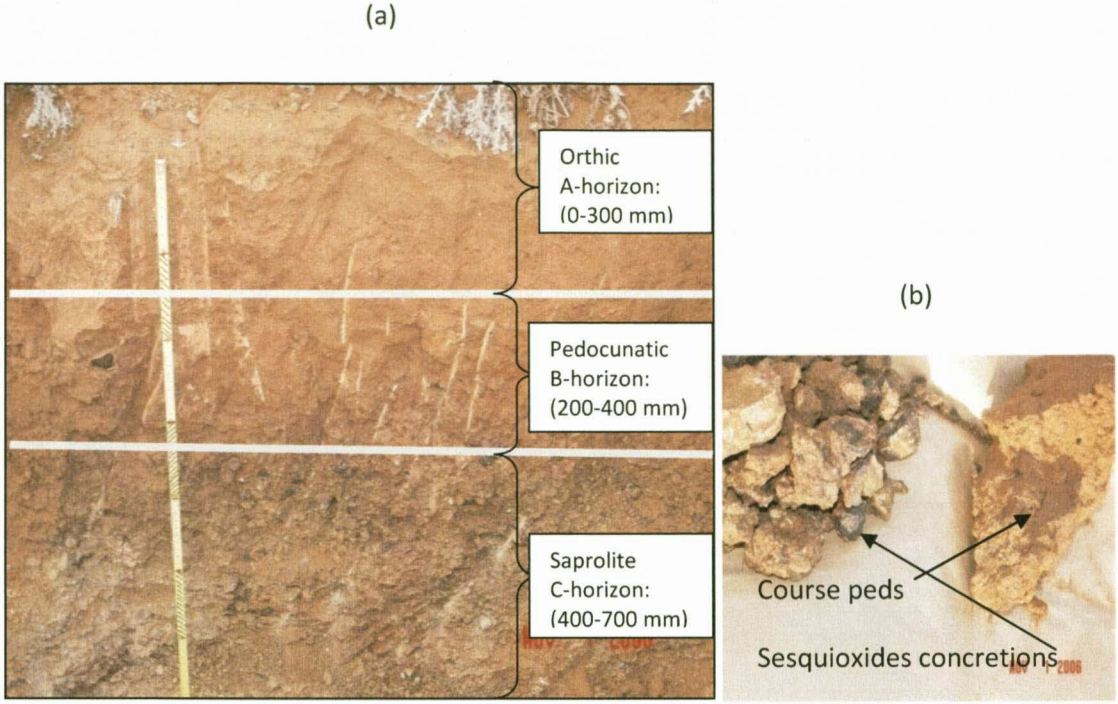

Figure 3.3 (a) Profile of the Swartland and (b) dolorite intrusion present in the B-horizon.

3.3.2 θ-h relationship of soil horizons

Figure 3.4 a, b and c shows the resulting θ-h relationships from the hanging column laboratory desorption of the Tukulu, Sepane and Swartland soil, respectively. Linear regression functions for each of the three soils horizons with the coefficient of determination are shown in Table 3.2. Corresponding Student's t-test analysis for differences between the horizons regressions coefficients are also presented in Table 3.3. Designated to capture the soil water release behaviour under internal drainage conditions, the θ-h relationship was set between the suction ranges of 0 to -1000 mm (10 -kPa). Spatial variations among the three soils appeared to increase with suction, an essential indicator for evaluating the permissibility of water release by the various soil horizons.

Tukulu: The θ-h relationships from the A-, B- and C-horizons appeared to cluster together at near zero matric suctions but after matric suctions < -200 mm their spatiality increased. The A-horizon contained 0.33 to 0.277 mm mm^{-1} of water while the B-horizon contained 0.325 and 0.285 mm mm^{-1} water at matric suctions 0 and -1000 mm. On the other hand, the C-horizon contained 0.324 and 0.321 mm mm^{-1} water at matric suctions, resulting in a θ-h curve with a very small slope (Table 3.2). Effective saturation satisfied porosity only in the C-horizon while the A- and B-horizons were below with 3 % and 1 %, respectively (Table 3.1).

Table 3.2 θ-h regression functions of soils horizons for the 0 -1000 mm suction range.

Soil type	Horizons	Regression	R^2
Tukulu	A	θ = 0.332 - 0.00005 h	0.98
	B	θ = 0.328 - 0.00004 h	0.96
	C	θ = 0.324 - 0.000003 h	0.93
Sepane	A	θ = 0.327 - 0.00007 h	0.99
	B	θ = 0.333 - 0.00004 h	0.99
	C	θ = 0.338 - 0.00004 h	0.99
Swartland	A	θ = 0.339 - 0.00008 h	0.99
	B	θ = 0.347 - 0.00006 h	0.99
	C	θ = 0.345 - 0.00013 h	0.97

Table 3.3 Student's t-test for differences between horizons θ-h regression coefficients.

Soil type	Horizons	Pooled variance	Tabulated variance ($_{\alpha: 0.05}$)
Tukulu	AB	3.002	2.145
	BC	12.295	2.145
	AC	18.688	2.145
Sepane	AB	13.868	2.145
	BC	2.776	2.145
	AC	16.516	2.145
Swartland	AB	5.819	2.145
	BC	8.489	2.145
	AC	5.541	2.145

Corresponding slopes to these θ-h relationships was 0.005%, 0.004% and 0.0003% for the respective A-, B- and C-horizons with the C-horizon having the slowest water release function (Figure 3.4). Although the A- and B-horizon lines could be observed to be close to each other for the given matric suction range, the Student's t-test captured no similarities. Linear regression functions fitted the measured data well with the R^2 of not less than 93%.

Sepane: The θ-h relationships from the A-, B- and C-horizons represented soil columns that exhibited different soil water retention properties for the matric suction range in question. The A-horizon contained 0.328 and 0.257 mm mm^{-1} water while the B-horizon contained 0.332 and 0.289 mm mm^{-1} water at matric suction 0 and -1000 mm. Similar to the B-horizon was the C-horizon that contained 0.338 and 0.299 mm mm^{-1} water. Effective porosity was 3.5% and 1% below porosity on the respective A- and B-horizons while in the C-horizon the effective porosity was fairly satisfied (Table 3.1).

(a)

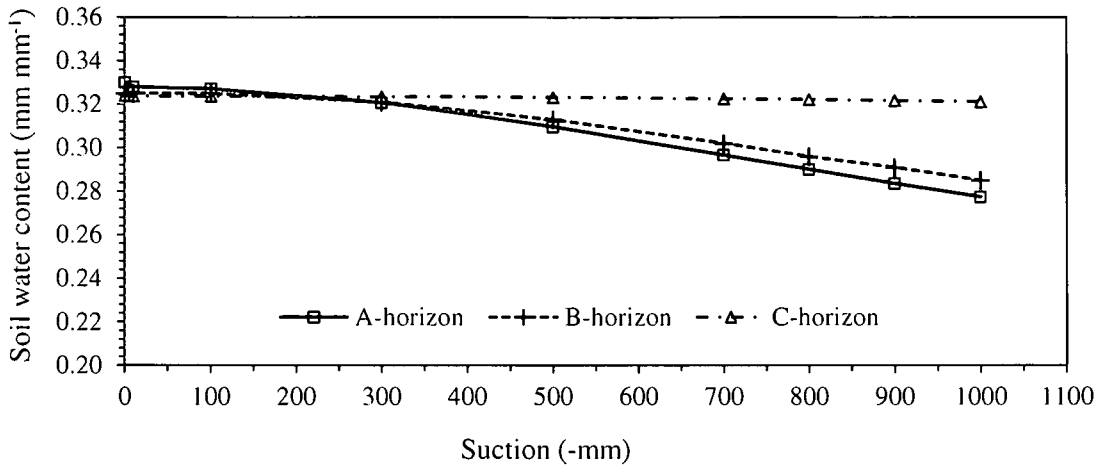

(b)

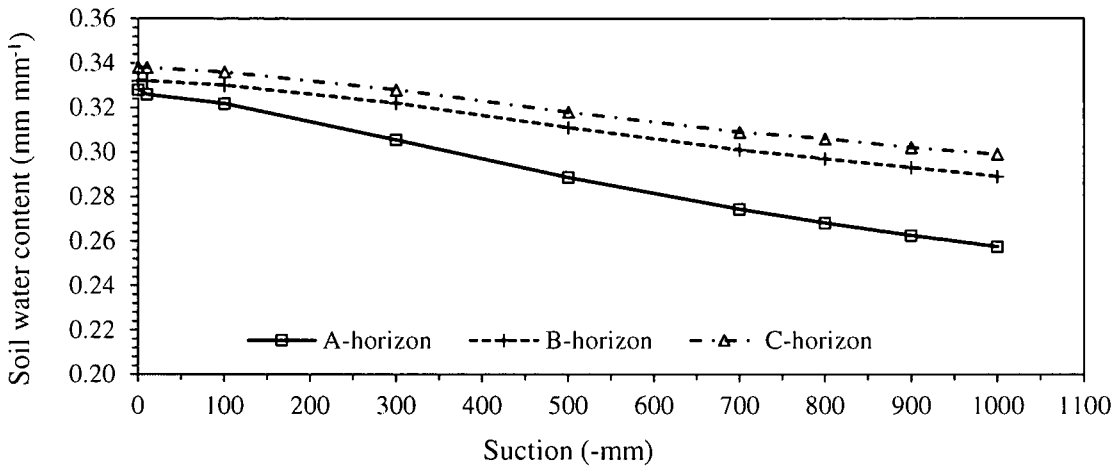

(c)

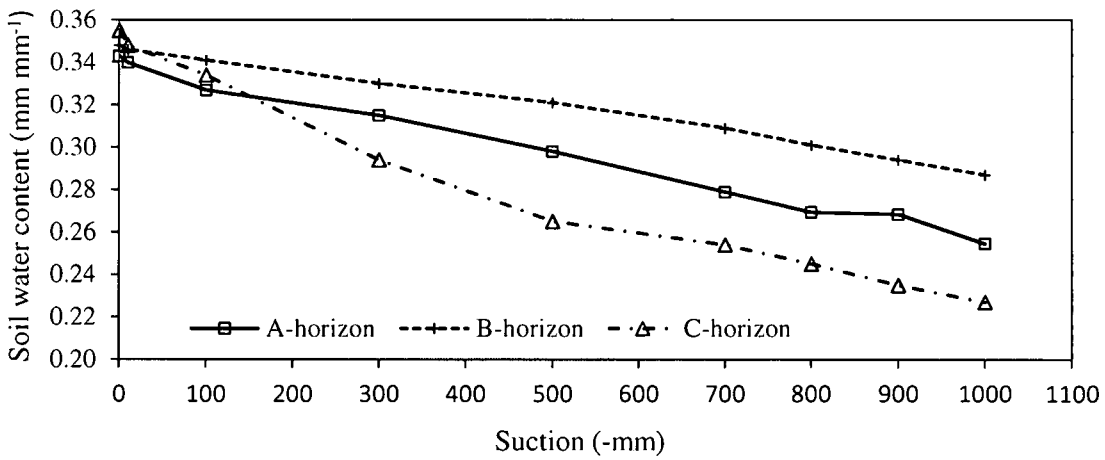

Figure 3.4 θ-h relationships from the (a) Tukulu, (b) Sepane and (c) Swartland soil types.

The resulting slopes from these θ-h relationships (Figure 3.4) were 0.007%, 0.004% and 0.004% for the A-, B- and C-horizons, respectively. Interestingly, all three horizons θ-h functions had R^2 not less than 99%. Student's t-test also captured that the regression coefficients from these horizons were different.

Swartland: Variations in the θ-h relationships of all three soil horizons indicated low water retention for the matric suction in question. For matric suctions 0 and -1000 mm, the A-, B- and C-horizons contained 0.343 and 0.255 mm mm^{-1}, 0.348 and 0.287 mm mm^{-1}, and 0.355 and 0.227 mm mm^{-1}, respectively. Effective saturation was 2%, 12.8% and 14.7% below porosity from the respective A-, B- and C-horizons (Table 3.1). The A-horizon soil water retention curve had a slope of 0.008% while the B-horizon resembled a slope of 0.005%. The greatest slope was found in the saprolite C-horizon of about 0.012%. When compared, regression coefficients from individual horizons θ-h functions were significantly different.

3.3.3 K-θ relationships of soil horizons

Resulting K-θ relationships from the *in situ* desorption of A-, B- and C-horizons of the Tukulu, Sepane and Swartland soils under internal conditions are shown in Figure 3.5 a, b and c, respectively. Corresponding regression exponential K-θ functions are presented in Table 3.4. Statistical homogeneity analysis is also illustrated in Tables 3.5 and 3.6. The differences in K-θ relationships reflected the spatial responses of drainage to the heterogeneity of soil layer permeability.

Tukulu: The resulting K-θ relationships from the A-, B- and C-horizons occupied the SWC range between 0.297 to 0.328 mm mm^{-1} (Figure 3.5a). The K-θ lines of the A- and B-horizons were close to each other close to the origin while that of the C-horizon was close to saturation.The A-horizon had K-θ coefficients ranging from 36.1 to 0.0005 mm $hour^{-1}$ for a SWC ranging of 0.328 to 0.297 mm mm^{-1}. The B-horizon K-θ coefficient ranged from 40 to 0.0009 mm $hour^{-1}$ with a soil water range of 0.325 to 0.299 mm mm^{-1}. For the C-horizon the K-θ coefficient ranged from 9.6 to 0.0005 mm $hour^{-1}$ for a drop in soil water content from 0.324 to 0.309 mm mm^{-1}. The K-θ relationships regression functions had R^2 of not less than 0.94 (Table 3.5) with the horizons significantly different for the Bartlett's test. However, the Student's t-test it was found that K-θ relationships between A- and B-horizons were not comparable (Table 3.6).

(a)

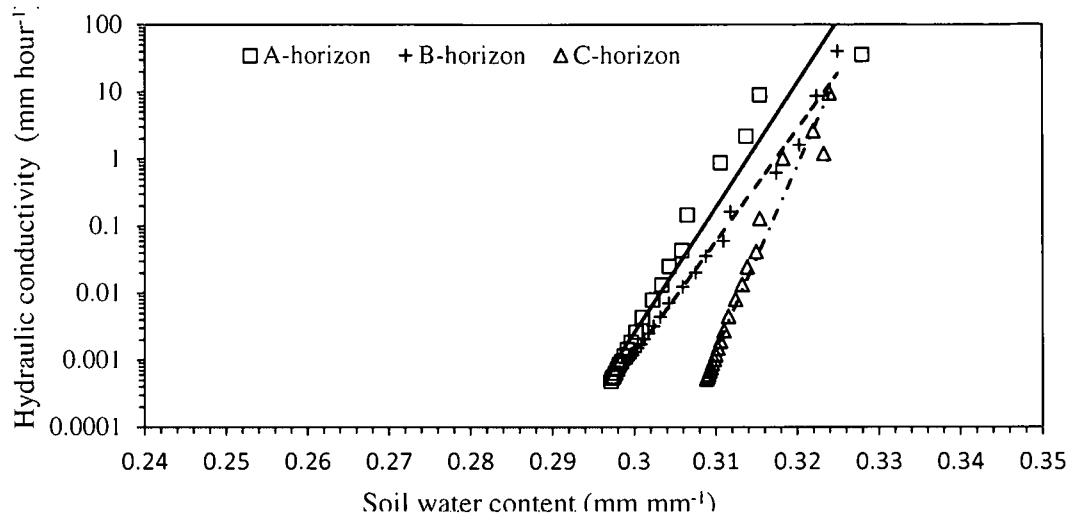

(b)

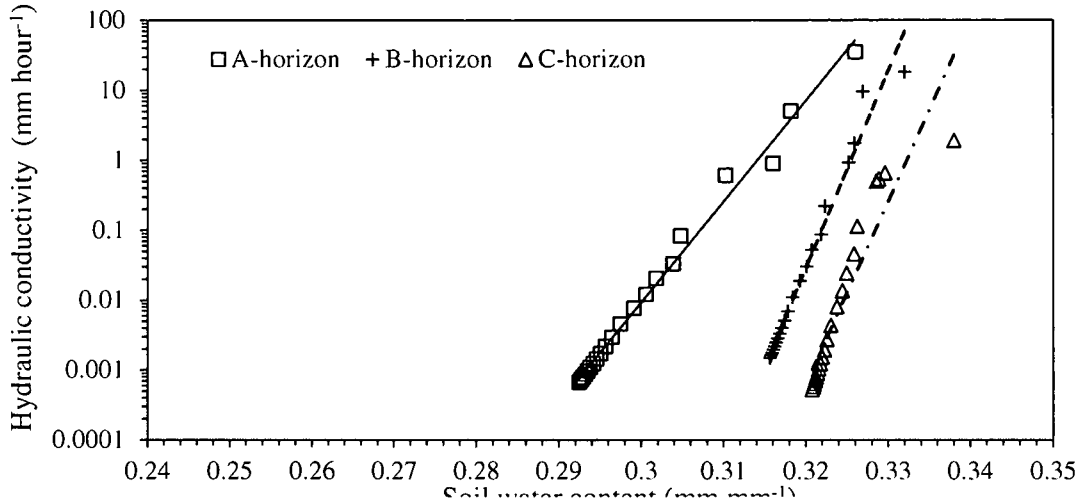

(c)

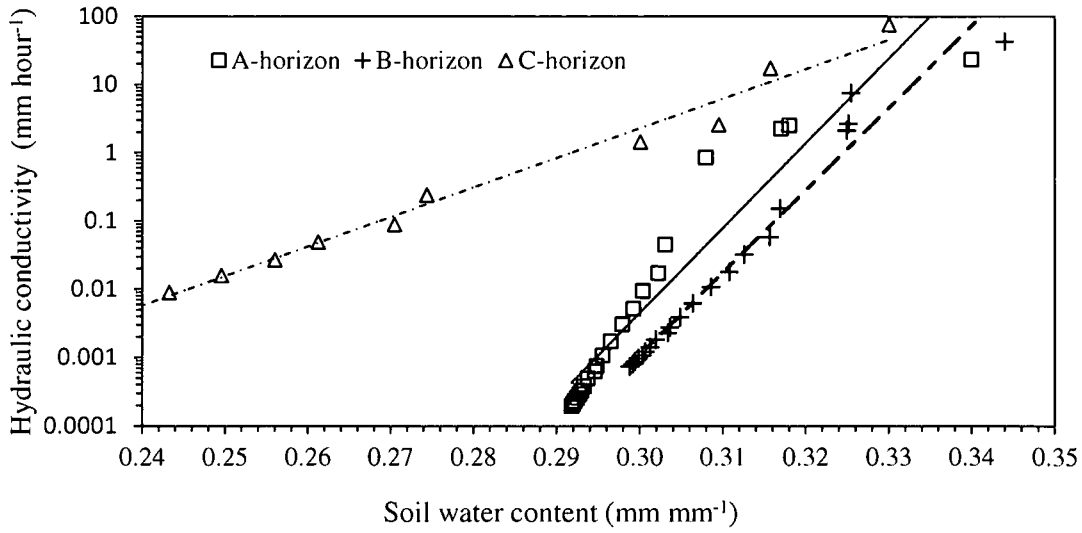

Figure 3.5 K-θ-relationship from the (a) Tukulu, (b) Sepane and (c) Swartland soil types.

Sepane: The resulting K-θ relationships from the A-, B- and C-horizons occupied the SWC range between 0.292 to 0.338 mm mm^{-1} (Figure 3.5b) The K-θ relationship of the A-horizon inclined towards the interior while the B- and C-horizons were closer to each other and to the exterior. The A-horizon had the K-θ coefficient ranging from 35.2 to 0.0007 mm $hour^{-1}$ for a soil water content ranging of 0.326 to 0.292 mm mm^{-1}. The B- and C-horizon K-θ coefficient dropped respectively from 18.1 to 0.0015 mm $hour^{-1}$ and 1.9 mm $hour^{-1}$ to 0.0005 mm $hour^{-1}$ with a corresponding soil water content ranging from 0.332 to 0.316 mm mm^{-1} and 0.338 to 0.321 mm mm^{-1}. Horizons could were significantly different for the Barttle's test and could not be described by one regression coefficient (Table 3.5). However, with the Student's test it was found that K-θ relationships between B- and C- horizons were not compatible (Table 3.6).

Swartland: The resulting K-θ relationships from the A-, B- and C-horizons occupied the SWC range between 0.222 to 0.344 mm mm^{-1} (Figure 3.5c). The K-θ lines of the A- and B-horizons were close to each other and found close to saturation while that of the C-horizon was close to the origin. The A-horizon showed a K-θ coefficient ranging from 23.5 to 0.0002 mm $hour^{-1}$ for a soil water content of 0.332 to 0.292 mm mm^{-1}. The K-θ coefficient for the B-horizon ranged from 42.8 to 0.0007 mm $hour^{-1}$ with a SWC ranging from 0.344 to 0.299 mm mm^{-1}. For the C-horizon the K-θ coefficient ranged from 76.5 to 0.001 mm $hour^{-1}$ with a soil water content ranging from 0.330 to 0.22 mm mm^{-1}. The K-θ relationships from the three horizons attained a coefficient of determination not less than 0.89 (Table 3.4) with horizons significantly different for the Bartletts's test (Table 3.5). However with the Students t-tests it was found that K-θ relationship between A- and B-horizons were not comparable (Table 3.6).

Table 3.4 K-θ relationships linear regression functions for the three soil types.

Soil type	Horizon	Regression	R^2
Tukulu	A	Log K = 186.1(θ) - 58.42	0.94
	B	Log K = 167.4(θ) - 52.24	0.99
	C	Log K = 274.1(θ) - 87.82	0.97
Sepane	A	Log K = 143.9(θ) - 45.21	0.99
	B	Log K = 281.3(θ) - 91.58	0.98
	C	Log K = 260.4(θ) - 86.51	0.87
Swartland	A	Log K = 124.3(θ) -39.64	0.89
	B	Log K = 120.6(θ) 39.15	0.97
	C	Log K = 43.29(θ) - 12.62	0.99

Table 3.5 Homogeneity test for the three soils horizons.

	Bartlett's test		Regression coefficient	
Soil types	Computed $\chi 2$	Tabular $\chi 2$ $(\alpha;\ _{0.05,2})$	Computed F $(\alpha;\ _{0.05,2})$	Tabular F $(\alpha;\ _{0.05,2})$
Tukulu	19.36	5.99	27.71	3.16
Sepane	26.75	5.99	51.99	3.16
Swartland	32.46	5.99	119.29	3.16

Table 3.6 Student's t-test for differences between horizons K-θ regression coefficients.

Soil type	Horizons	Pooled variance	Tabulated variance $(_{\alpha;\ 0.05})$
Tukulu	AB	1.71 ^{ns}	2.03
	BC	9.91	2.03
	AC	5.09	2.03
Sepane	AB	14.56	2.03
	BC	0.84 ^{ns}	2.03
	AC	6.12	2.03
Swartland	AB	0.34 ^{ns}	2.03
	BC	18.58	2.03
	AC	10.73	2.03

ns= not significantly different at 95 % confidence interval

3.3.4 θ-T relationship of soil horizons

The θ-T relationship for the Tukulu, Sepane and Swartland soil types for the first 210 hours of internal drainage are presented in Figure 3.6. The power regression functions for the A-, B- and C-horizons for these soils are presented in Table 3.7 and the Student's t-test for the comparison of regression coefficients between horizons θ-T functions presented in Table 3.8. The presence of restrictive horizon layers influenced the manner in which these soils drained.

Tukulu: The θ-T relationship for this soil indicated an increase in SWC with depth although each layer continued to drain instantaneously. The amount of water that drained away within the first 3 hours was 5.1 mm from the orthic A- and 2.4 mm from the neocutanic B-horizon from an initial field saturation of 0.328 and 0.325 mm mm^{-1}, respectively. At field saturation of 0.324 mm mm^{-1} the C-horizon lost 1.5 mm for the same period. At the end of the 200 hour drainage period the A-, B- and C-horizons drained away water amounting to 8.1 mm, 6.2 mm and 3.1 mm, respectively. The drainage flux of 0.001 mm $hour^{-1}$ equivalent to DUL was realised after 660 hours (28 days) after drainage for the A- and B-horizons while from the C-horizon DUL was realised after 390 hours (16 days).

(a)

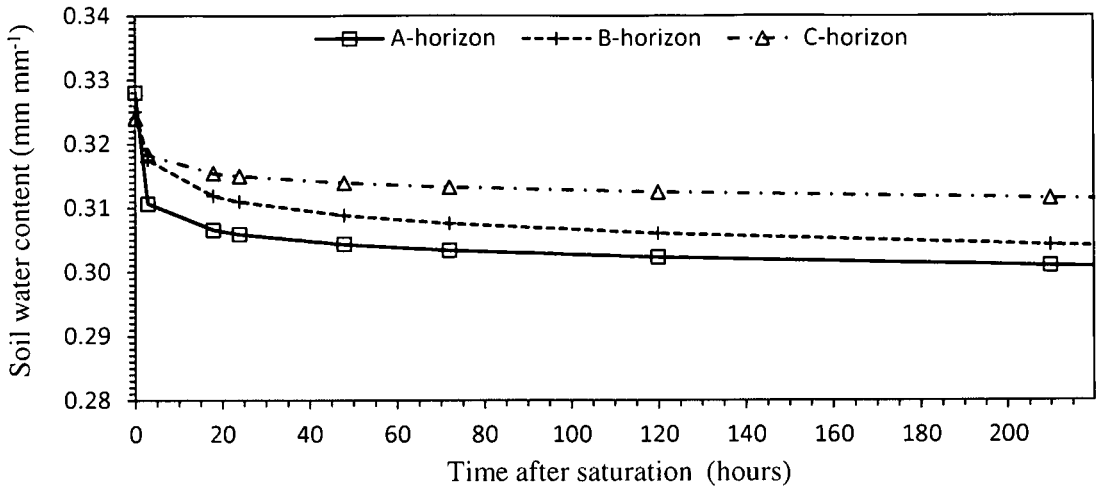

(b)

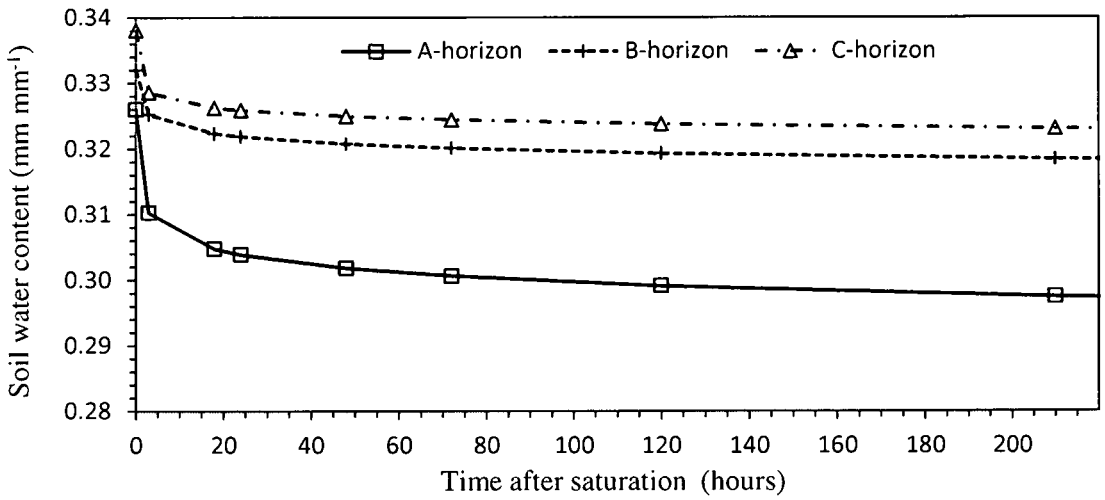

(c)

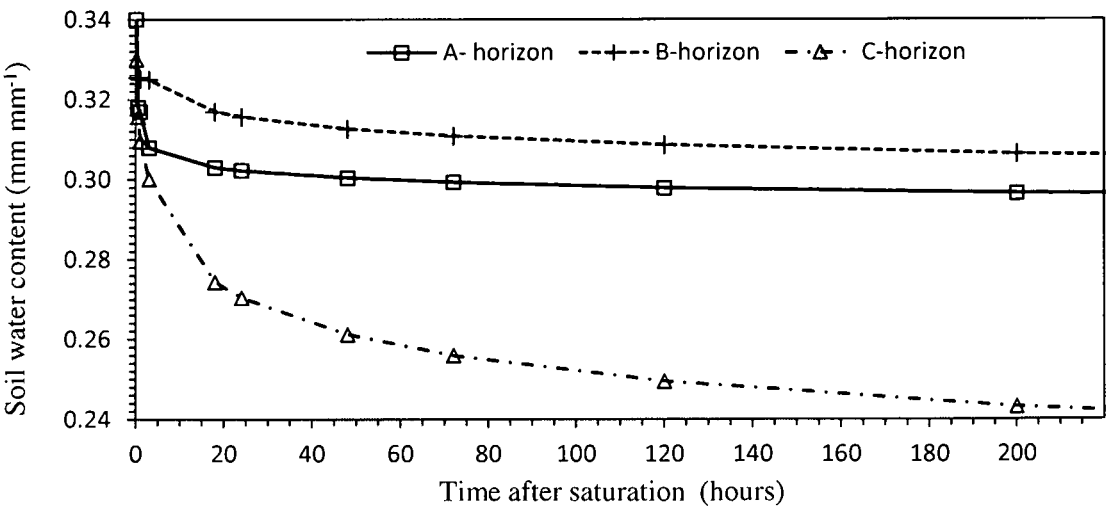

Figure 3.6 θ-T relationships from the (a) Tukulu, (b) Sepane and (c) Swartland soil types.

Corresponding SWC was 0.30 mm mm^{-1} for the A- and B-horizons and 0.31 mm mm^{-1} for the C-horizon. The Student's t-test also confirmed the similarities observed between the upper horizons.

Sepane: From the θ-T relationship of the three horizon layers soil water content increased with depth while drainage rates decreased. The amount of water that drained away from field saturation of 0.326 mm mm^{-1}, 0.332 mm mm^{-1} and 0.338 mm mm^{-1} within the first 3 hours was 4.7 mm, 2.8 mm and 2 mm for the respective A-, B- and C-horizons. At the end of 200 hours the layers drained a respective water content amounting to 8.5 mm, 5.4 mm, and 3 mm. The drainage flux of 0.001 mm $hour^{-1}$ was attained after 660 (27 days), 480 (20 days) and 300 (13 days) hours from saturated SWC of 29.4 mm mm^{-1}, 31.7 mm mm^{-1} and 32.3 mm mm^{-1}, for the A-, B- and C-horizons, respectively. The Student's t-test also confirmed the comparable differences found between these soil horizons.

Table 3.7 θ-T relationships linear regression functions for the three soil types.

Soil form	Horizons	Regression	R^2
Tukulu	A	$y = 0.317x^{-0.009}$	0.96
	B	$y = 0.319x^{-0.009}$	0.99
	C	$y = 0.320x^{-0.005}$	0.99
Sepane	A	$y = 0.316x^{-0.011}$	0.99
	B	$y = 0.328x^{-0.005}$	0.99
	C	$y = 0.332x^{-0.005}$	0.97
Swartland	A	$y = 0.318x^{-0.013}$	0.92
	B	$y = 0.328x^{-0.013}$	0.97
	C	$y = 0.308x^{-0.045}$	0.99

Table 3.8 Student's t-test for the differences between horizons θ-T regression coefficients.

Soil type	Horizons	Pooled variance	Tabulated variance ($_{\alpha: 0.05}$)
Tukulu	AB	1.153 ^{ns}	2.032
	BC	12.977	2.032
	AC	4.145	2.032
Sepane	AB	5.178	2.032
	BC	6.977	2.032
	AC	7.854	2.032
Swartland	AB	3.247	2.032
	BC	44.447	2.032
	AC	13.161	2.032

Swartland: Soil water content was concentrated on the upper soil horizons with the B-horizon assuming a higher water content regime throughout the drainage period. The amount of water that drained away within 3 hours was 4.6 mm from the A-horizon, 3.76 mm from the B-horizon and 6 mm from the C-horizon. After 200 hours of drainage 8.6 mm, 7.5 mm and 26 mm drained from an initial field saturation of 0.332 mm mm^{-1}, 0.344 mm mm^{-1} and 0.33 mm mm^{-1} for the A-, B- and C-horizons, respectively. A drainage flux of 0.001 mm $hour^{-1}$ was achieved after 672 (28 days) hours from the A- and B-horizons with a respective SWC of 0.29 mm mm^{-1} and 0.30 mm mm^{-1}. For the C-horizon flux rates of 0.006 mm $hour^{-1}$ were observed after 672 (28 days) hours of drainage and continued to decline to a rate of 0.003 mm $hour^{-1}$ by the end of the drainage period. Although the Student's t-test found all the horizons to be comparable the pooled variation was smallest between A and B-horizons.

3.3.5 Total drainage and flux rates

Total drainage and flux rates from the internal drainage trial were summarized in Table 3.9 and Figure 3.7, respectively. The respective drainage amounts from the three soil types showed a decrease with depth with the exception in the Swartland. In all the soils the amount that drained away approached negligible levels (DUL) at drainage flux rate of 0.001 mm $hour^{-1}$. At this flux rate the total water loss was equivalent to 0.09% of the 550 mm annual average rainfall of the area.

Table 3.9 Amount of soil water that drained away from horizons.

		Accumulative water depth (mm) at different drainage periods (hrs)								
Soil type	Horizons	18	24	72	210	300	390	660	930	1200
Tukulu	A	6.44	6.63	7.38	8.09	8.33	8.51	8.86	9.08	9.25
	B	3.94	4.21	5.23	6.21	6.54	6.78	7.25	7.56	7.79
	C	2.15	2.26	2.69	3.11	3.25	3.35	3.56	3.69	3.79
Sepane	A	6.38	6.64	7.62	8.56	8.87	9.10	9.55	9.84	10.06
	B	3.88	4.06	4.77	5.45	5.68	5.84	6.18	6.39	6.56
	C	2.36	2.43	2.72	3.00	3.09	3.16	3.29	3.38	3.45
Swartland	A	7.40	7.55	8.15	8.70	8.89	9.04	9.34	9.51	9.65
	B	5.42	5.67	6.64	7.52	7.83	8.08	8.55	8.83	9.04
	C	16.70	17.87	22.21	26.03	27.35	28.37	30.32	31.45	32.29

(a)

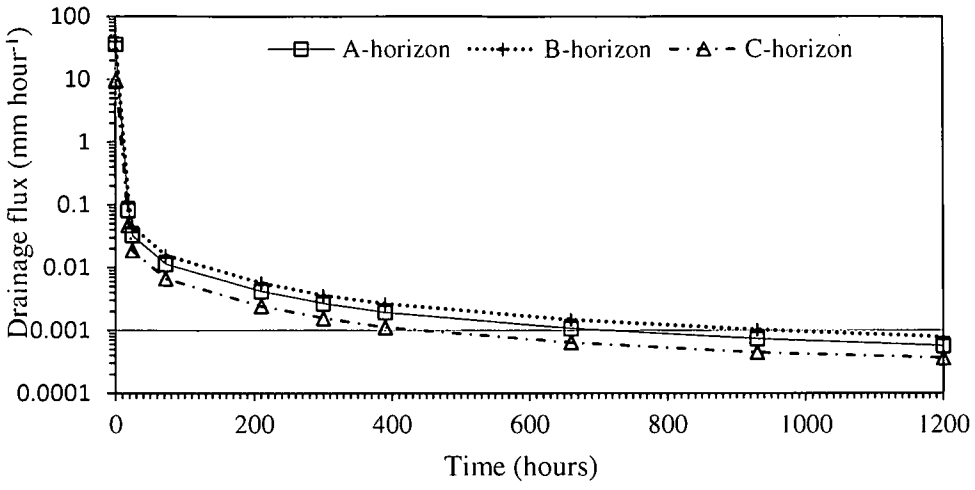

(b)

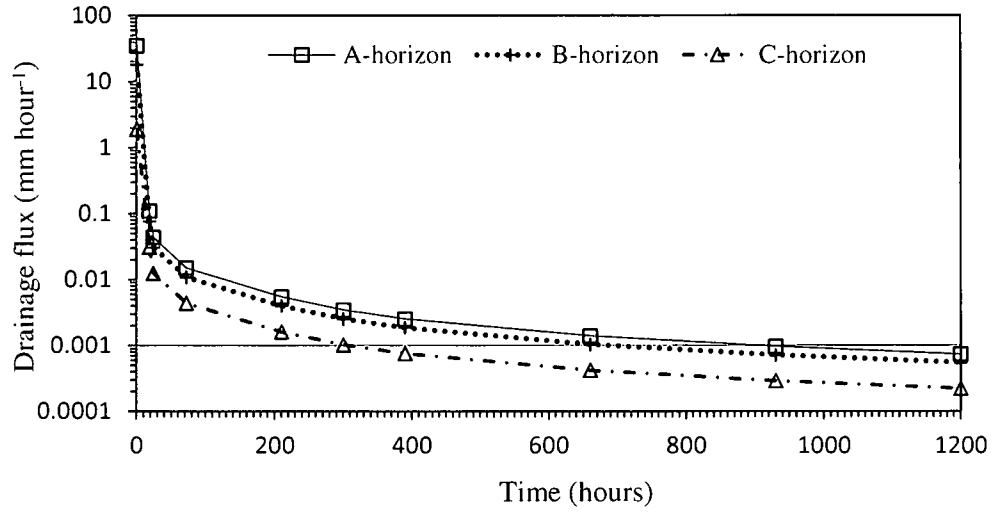

(c)

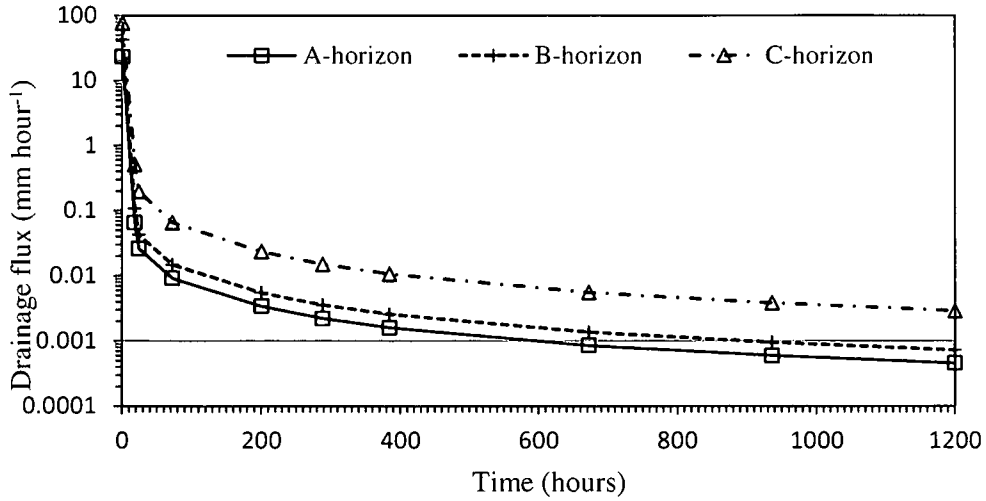

Figure 3.7 Drainage flux from the (a) Tukulu, (b) Sepane and (c) Swartland soil types.

3.4 Discussion

The internal drainage property was consistent with the presence and intensity of layering from the Tukulu, Sepane and Swartland soils. Evidence of slight wind erosion in the absence of flooding or water erosion could suggest that eutrophic conditions of the semi arid environment played a critical role in the development of the layering pattern of these soils. Moderate physical and chemical weathering of underlying material of solid rock of binary origin affirm the *in situ* evolution of the three soil types. Despite the similarities in parent rock material and orthic A-horizons, the differences in subsurface layers could be explained by the geological position each soil occupied in the landscape. The Tukulu and Swartland had a weakly developed A- and B-horizons with a smooth transition at the interface denoting a weak layering between these horizons. Chimungu (2009) treated the Tukulu upper horizons as homogenous in order to describe the internal drainage by the unity gradient approach recommended by Yeh et al. (1985). The clay rich underlying horizons found in the Tukulu and Sepane was indicative of the common drainage line shared by these soils. These clayey horizons are of alluvial origin (Hensley et al., 2007).

Given that internal drainage is accountable to gravitational flow boundary conditions, the hydraulic characteristics of the underlying soil profile layers are key to this process (Blume et al., 2009; Chimungu, 2009; Nhlabatsi, 2010). Consistent with the restrictive clay layer of the prismacutic C-horizons was 21 mm and 20 mm of water that drained away from the respective Tukulu and Sepane soil forms. Corresponding to the weakly developed Swartland was 51 mm drained away from which 32 mm was contributions by the saprolite C- horizon. This was expected given the coarseness of the saprolite rock with Ks values of about 77 mm $hour^{-1}$. Hensley et al. (2000) and Botha et al. (2003) concluded that the saprolite layer was ill-posed for deep soil water storage given its high water release characteristics. This was consistent with the illustrations given by Hillel (2004) about soils with an underlying course texture horizon having a drier soil water regime. However, the pedocutanic B-horizon when fully developed could have clay content exceeding 30 % that was acceptable for soil water conservation under IRWH technique (Hensley et al., 2000; Botha et al., 2007).

Evidence of the slow drainage properties of the clay rich layer(s) in the Tukulu and Sepane was the presence of hydromorphic mottles confirming that soil water was subjected to restricted flow above these layer(s). In the Sepane hydromorphic mottles were also found at depths of 300 to 700 mm reflecting the effect of the pedocunatic clay rich B-horizons on

internal drainage. Nevertheless, the prismacutanic layers were the most restrictive with 9.6 mm hour^{-1} and 1.9 mm hour^{-1} from the Tukulu and Sepane, respectively. The latter realised a flux rate of 0.001 mm hour^{-1} after 13 days of drainage while the former after 16 days. The same flux rate from the Tukulu was recorded after 26 days of drainage by Chimungu (2009). However, the more restriction on internal drainage of the Sepane could be explained by the duality of heavy structured layers in this profile (Fraenkel, 2008). Prospects of having a positive pressure head building up from the restrictive layers (Tartakovsky et al., 2003) does support the high drainage rate observed at the early hours of drainage from the Tukulu and Sepane. Inconsistencies in drainage amounts within each soil profile could reflect poor sealing of the monoliths side walls against lateral leakage, a scenario that was also a concern to Hopmans et al. (2002) and experienced by Chimungu (2009) on the same monoliths. Over and above, the C-horizons from the Tukulu and Swartland controlled the permissible drainage from the upper horizons, a scenario that was confirmed by the fusion of the flux curves from these two soils. Greater spatiality from the Swartland flux curves suggested that the saprolite layer exhibited less control on how the upper horizons drained.

Considering the θ-h and K-θ relationships provided further evaluation of the presence of soil profile layers on the drainage process. Driven by gravitational potential drainage the process involves suction and K-coefficients of permeability near saturation (Schaap and van Genuchten, 2006; Scheffler, 2007). Corresponding drainage pore space are those of diameters ranging from 1000 μm to several mm (Luxmoore, 1981). The variation in these classes of pores was noticeable within the suction range of 300 to 1000 mm from the soil layers of the three soil profiles. However, the small volume of drainable pores (Dane and Hopmans, 2002; Schaap and van Genuchten, 2005) found on clay rich horizons was confirmed by the almost level or gentle slope of the θ-h relationship depicting a slow release. Deficiencies in clay and structure from the Swartland profile layers, especially the saprolite C-horizon resulted to the steep θ-h relationship that was consistent with the high water release during the internal drainage. Intensity of layering among the three soils was also captured by the abrupt changes in Ks downwards the profile within suction ranging from -10 to -100 mm (Zavattaro and Grignani, 2001). Notable was the drop from 40 to 9.6 mm hour^{-1} between the neocutanic B- and prismatic C-horizons for the Tukulu. These discontinuities were consistent with the behaviour of flow and unpredictable nature of hydraulic properties in layered soils (Mathews et al., 2004). Another drop of 18.1 to 2 mm hour $^{-1}$ between the Sepane pedocutanic B- and prismatic C-horizons was recorded alongside the observation that increased clay content with

depth restricted internal drainage (Romano et al., 1996; Bohne, 2005; Gopalakrishnan and Manik, 2007; Jones et al., 2009).

Variation in K-θ relationship was also able to show the decline in available water for drainage irrespective of SWC and depth. Distinguishable were the steep gradients of the K-θ relationships from the pedocutanic and prismatic horizons with corresponding hydraulic gradient fairly above unity. From the orthic and neocutanic horizons this gradient was almost equal to 1 suggesting that the adoption of the unity gradient by Chimungu (2009) in approximating the K-θ relationship of these horizons was reasonable. However, application of the unity gradient is questioned by most researchers especially on clay soils where the K-coefficient could drop by several orders of magnitude within a narrow range of SWC (Reichardt, 1993; Bacchi and Reichardt, 1993). Supporting this sentiment was the observation that the K-coefficient from the Tukulu and Sepane was less than drainage flux at DUL by order of one magnitude. The rapid fall of K-coefficient by several orders of magnitudes while SWC remained within the near saturation range was also acknowledged by Hensley et al. (2000) who related this function to the requirements of IRWH for deep soil water storage. However, the affinity to water shown by soils predominated by micro-pores of diameter less than 30 μm (Luxmoore, 1981), has raised questions on the availability of water tightly held against gravity, to roots of crop plants (Whitmore and Whalley, 2009). Nevertheless, it can be deduced from this work that the presence of soil layers and their respective permeability from the three soils affected drainage differently, and hence soil water storage.

3.5 Conclusions

The evaluation of soil layers on internal drainage from the Tukulu, Sepane and Swartland soil types earmarked for IRWH production technique was the main objective of the study. Integrating *in situ* and laboratory desorption procedures provided the opportunity to reflect on the pedological presence of soil layers and also to relate their morphological features to the hydraulic characteristics that governed the drainage process.

Critical conclusions were drawn from the total and rate of drainage expressed by the three soil profiles. By virtue of their fine size (less than 0.002 mm) the clay fraction determined the extent of layering, both in texture and structure. Consequently, the clay content influenced the soil water release and permeability during drainage. Soil horizons with clay content ranging from 26 to 48 % contributed less than 5 mm to total drainage irrespective of textural and

structural class. This suggests that from an annual rainfall of 550 mm drainage losses from each profile layer with clay content falling in this category should be around 1 % of the total rainfall. Considering drainage flux of 0.001 mm $hour^{-1}$ to correspond to DUL produced realistic estimates that were consistent with the slope of θ-T relationships and could be used to estimate DUL from other layered soils especially those earmarked for IRWH.

Proven by this work was the variation of drainage with the degree of soil layering. The coefficient of both saturation and de-saturation allowed reflection on the extent at which drainage was influenced by the presence of an abrupt or smooth transitional change in clay content and structure. Increased matric suction against gravitational influence on clay rich profile layers had a significant influence in lowering the K-θ coefficient to negligible levels at relatively high soil water contents. This function was transferred to overlying layers irrespective of their textural and structural orientation suggesting the importance of clay soils on the overall permeability of the profile when occurring on the lower horizons in particular. About 1 % of the total annual rainfall was lost from the soil profile layers of the Tukulu and Sepane suggesting their greater potential for soil water conservation, especially for IRWH. Aspects of deep infiltration and runoff could become management issues when clay rich soil layers occur at shallow depths of 300 mm. On the contrary, the deficiency in layers rich in clay and structure from the Swartland proven by the deep drainage and drier soil water regime presented this soil as a lower potential for IRWH development.

Acknowledgements

We acknowledge the technical support rendered by the management and staff of Paradys experiment station. Gratitude's to Prof. Malcom Hensley for his contributions in classifying opened soil profiles and assistance in setting up the hanging soil column method. Special thanks also to Ms. Liesl van der Westhuizen for her constructive suggestions on improving the writing of this manuscript.

3.6 References

Acutis, M. and Donatelli, M., 2003. SOILPAR 2.00; Soft ware to estimate soil hydrological parameters and functions. *Eur. J. Agron.,* 18: 373-377.

Bacchi, O.O.S., 1988. Comparative analysis of soil hydraulic conductivity methods for unsaturated soils. Piracicaba, Escola Superior de Agricultua Luiz de Queiroz, Tese de Doutorado.

Bacchi, O. O. S. and Reichrdt, K., 1993.On simple methods for unsaturated soil hydraulic conductivity determination. *Sci. Agric. Piracicaba*, 50:326-328.

Bennie, A.T. P., 1994. Managing the profile available water capacity for irrigation of annual crops in arid regions. University of the Free State, Bloemfontein, South Africa.

Bittelli, M. and Flury, M., 2009. Errors in water retention curves determined with pressure plates. *SSAJ*, 73:1453-1460.

Bohne, K., 2005. An introduction into applied soil hydrology. Catena Verlag GMBH, Reiskrchen, Germany.

Botha, J. J., van Rensburg, L. D., Anderson, J. J., Hensely, M., Macheli, M. S., van Staden, P. P., Kundhlande, G., Groenewald, D. G. and Baiphethi, M. N., 2003.Water efficiency, food security, and sustainable crop production. Water Research Commission, Report No.,1176/1/03, Pretoria, South Africa.

Botha, J. J., Anderson, J. J., Groenewald, D. C., Mdibe, N., Baiphethi, M. N., Nhlabatsi, N. N. and Zere, T. B., 2007. On-farm application of In-field rainwater harvesting techniques on small plots in the central region of South Africa. Water Research Commission, Report No., TT 313/07, Pretoria, South Africa.

Blume, T., Zehe, E. and Bronstert, A., 2009. Use of soil moisture dynamics and patterns at different spatio-temporal scales for the investigation of subsurface flow processes. *Hydrol. Earth Syst. Sci.,* 13:1215–1234.

Chimungu, J. G., 2009.Comparison of field and laboratory measured hydraulic properties of selected diagnostic soil horizons. M.Sc. (Agric) Dissertation, University of the Free State, Bloemfontein, South Africa.

Dane, J. H. and Hopmans, J. W., 2002. Soil water retention and storage - Introduction. IN: Methods of Soil Analysis. Part 4. Physical Methods. (J.H. Dane and G.C. Topp, Eds.). *Soil Science Society of America* Book Series No. 5: 671-674.

Dane, J. H. and Hruska, S., 1983. *In situ* determination of soil hydraulic properties during drainage. *Soil Sci. Soc. Am. J.*, 47:619–624.

Dirksen, C., 1999. Soil physical measurements. Geo-ecology paperback, Catena verlag GMBH, 35447. Reiskirchen, Germany.

Eching, S. O. and Hopmans, J. W., 1993. Optimization of hydraulic functions from transient outflow and soil water pressure data. Soil Sc. Soc. of America, 57: 1167-1175, 1993.

Eching, S. O., Hopmans, J. W. and Wendroth, O.,1994. Unsaturated hydraulic conductivity from transient multistep outflow and soil water pressure data. *Soil Sci. Soc. Am. J.*, 58: 687- 695.

FAO, 2009. Bio-Physical requirements and socio-economic acceptance of infield rainwater harvesting and conservation in the semi-arid central region of South Africa.http://www.fao.org. 20 /09/ 2009, 10:30 am, LT.

Fraenkel, C. H., 2008. Spatial variability of selected soil properties in and between map units. M.sc. (Agric) Dissertation, University of the Free State, Bloemfontein, South Africa.

Gopalakrishnan, K. and Manik, A., 2007. A mathematical model for predicting isothermal soil moisture profiles using finite different methods. *Inter. Jour. of Computational and Mathematical Sc.* 1:128-134.

Gomez, K. A. and Gomez A.A., 1984. Statistical procedures for agricultural research. 2 ed. John Wiley and Sons, New York, USA.

Hensley, M., Botha, J. J., Anderson, J. J., Van Staden, P. P. and Du Toit, A., 2000. Optimising rainfall use efficiency for developing farmers with limited access to irrigation water. Water Research Commission report 878/1/00, Pretoria, South Africa.

Hensley, M., Le Roux, P. A. L., Du Preez, C. C., Van Huyssteen, C., Kotze, E. and Van Rensburg, L. D., 2007. Soils; the Free State agricultural base. *South African Geographical Journal*, 88: 11-21.

Hillel, D., Krentos, V. D. and Stylianou, Y., 1972. Procedure and test of an internal drainage method for measuring soil hydraulic characteristics in situ. *Soil Sci.*, 114: 395-400.

Hillel, D. H., 2004. Environmental soil physics. Academic Press, New York, USA.

Hurtado, A. L. B., Cichota, R. and Jong van lier, Q., 2005. Parametrização do método do perfil instantâneo para a determinação da condutividade hidráulica do solo em experimentos com evaporação. *R. Bras. Ci.* Solo, 29: 301-307.

Jones, E. W., Koh, Y. H., Tiver, B. J. and Wong, M. A. H., 2009. Modelling the behaviour of unsaturated, saline clay for geotechnical design. School of Civil, Environmental and Mining Engineering, University of Adelaide, Australia.

Jury, W., Gardener, W. R. and Gardner, W. H., 1991. Soil Physics (5th Ed.). John Wiley and Sons, New York, USA.

Kool, J. B., Parker, J. C. and van Genuchten, M. T., 1985. Determining soil hydraulic properties from one step outflow experiments by parameter estimation: Theory and numerical studies. *Soil Sci. Soc. Am. J.*, 49: 1348-1354.

Leij, F. J., Alves, W. J. and van Genuchten, M. T., 1996. UNSODA: The unsaturated soil hydraulic database. U.S. Salinity Lab., Riverside, CA.

Libardi, P. L., Reichardt, K., Nielsen, D. R. and Biggar, J. W., 1980. Simple field methods for estimating soil hydraulic conductivity. *Soil Sci. Soc. Am. J.*, 44: 3-7.

Luxmoore, R., 1981. Micro-, Meso- and macroporosity of soil. *Soil Sci. Sc. Am. J.*, 45: 241-285.

Mathews, C. J., Knight, F. J. and Braddock, R. D., 2004. Using analytic solutions for homogeneous soils to assess numerical solutions for layered soils. ARC Discovery Indigenous Research Development Program. C.mathews@griffith.edu.au, 31/04/ 2011, 17.00 pm, (LT).

Neto, D. D., Reichardt, K., Lúcia da Silva, A., Bacchi, O. O. S., Timm, L.C., Oliveira, J. C. M. and Nielsen, D. R., 2007. A software to calculate soil hydraulic conductivity in internal drainage experiments (SHC, version 2). R. Bras. Ci. Solo, 31: 1219-1222.

Nielsen, D. R., Davison, J. M., Biggar, J. W. and Miller, R. J., 1964. Water movement through Panoche clay loam soil. *Hilgardia*, 35: 491-506.

Non Affiliated Soil Analysis Work Committee, 1990. Handbook of standard soil testing methods for advisory purposes. Soil Science Society of South Africa, Pretoria.

Nhlabatsi, N. N., 2011. Soil water evaporation studies on the Glen/Boheim ecotope. Ph D. Thesis, University of the Free State, Bloemfontein, South Africa.

Ratliff, L. F., Richie, J. T. and Cassel, D. K., 1983. Field measured limits of soil water availability as related to laboratory-measured properties. *Soil Science Society. American J.*, 47:770-775.

Reichardt, K., 1993. Unit gradient in internal drainage experiments for the determination of soil hydraulic conductivity. Sci. Agric. Piracicaba. 50: 151-153.

Reichardt, K., Timm, L. C., Bacchi, O. O. S., Oliveira, J. C. M. and Dourado-neto, D., 2004. A parameterized equation to estimate soil hydraulic conductivity in the field. *Aust. J. Soil Res.*, 42:283-287.

Richards, L. A., Gardener, W. R. and Ogata, G., 1956. Physical processes determining water loss from soil. *Soil Sci. Soc. Am. Proc.*, 20: 310-314.

Romano, N., Brunone, B. and Santini, A., 1996. Numerical analysis of one-dimensional unsaturated flow in layered soils. *Advances in Water Res.*, 21: 315-324.

Rose, C. W., Stern, W. R. and Drummond, J. E., 1965. Determination of hydraulic conductivity as a function of depth and water content for soil in situ. *Aust. J. Soil Res.*, 3: 1-9.

Schaap, M. G. and van Genuchten, M. T., 2006. A modified Mualem–van Genuchten formulation for improved description of the hydraulic conductivity near saturation. *Vadose Zone Journal,* 5:27–34.

Scheffler, G., 2007. Determination of instantaneous moisture content and moisture potential profiles. University of Technology, Dresden, Germany.

Scotter, D. R., Clothier, B. E. and Harper, E. R., 1982. Measuring saturated hydraulic conductivity and sorptivity using twin rings. *Australian Journal of Soil Research*, 20: 295-304.

Simunek, J., Wendroth, O. and van Genuchten, M. T., 1999. Estimating unsaturated soil hydraulic properties from laboratory tension disc infiltrometer experiments. *Water Resour. Res.*, 35: 2965–2979.

Slawinski, C., Witkowska-Walczak, B. and Walczak, R. T., 2004. Determination of water conductivity coefficient of soil porous media. Institute of Agrophysics PAS, Lublin, Poland.

Soil Classification Working Group, 1991. Soil Classification - A taxonomic system for South Africa. Memoirs on the Agricultural Natural Resources of South Africa No.15, Department of Agricultural Development, Pretoria, South Africa.

Tartakovsky, D. M., Lu, Z., Guadagnini, A. and Tartakovsky, A. M., 2003. Unsaturated flow in heterogeneous soils with spatially distributed uncertain hydraulic parameters. *Journal of Hydrology,* 275: 182–193.

The non-affiliated soil analysis work committee, 1990. Handbook of standard soil testing methods for advisory purposes. SSSSA, Pretoria, South Africa.

Vachaud, G. and Dane, J. H., 2002. Instantaneous profile. In: Dane, J.H. and Topp G. C. (ed.) Methods of soil analysis. Part 4. Physical methods. SSSA Book Ser. 5. SSSA, Madison, WI.

Vachaud, G., C. Donko, D. S. and Thony, J. L., 1978. Methodes decaracterisation hydrodynamique in situ dun sol non sature. Aplication a deux types de sol du Senegal en vue de la determination des termes du bilan hydrique. *Ann. Agron.*, 29: 1-36.

van Dam, J. C., Stricker, J. N. M., and Droogers, P., 1994. Inverse method to determine soil hydraulic functions from multistep outflow experiments. *Soil Sci. Soc. Am. J.*, 58:647 652.

Villagra, M. M., Michiels, P., Hartmann, R., Bacchi, O. O. S. and Reichardt, K., 1994. Field determined variation of the unsaturated hydraulic conductivity functions using simplified analysis of internal drainage experiments. Sci. agric., Piracicaba, 51: 113-122.

Vomicil, J. A., 1965. Porosity. In: Black, C. A. (ed), Methods of soil analysis. *Amer. Soc. Agron.,* Madison Wisc, Part 1: 299-314.

Waston, K. K., 1966. An instantaneous profile method for determining the hydraulic conductivity of unsaturated porous materials. *Water Res. Res.*, 2: 709-715.

Whitmore, A. P. and Whalley, W. R., 2009. Physical effects of soil drying on roots and crop growth. *Journal of Experimental Botany*, 60: 2845-2857.

Wildenschild, D., Hopmans, J. W. and Simunek, J., 2001. Flow rate dependence of soil hydraulic characteristics. *Soil Sci. Soc. Am. J.*, 65:35–48.

World Reference Base for Soil Resources (1998). World soil resources report, 84, ISSS / ISRIC FAO, Rome, Italy.

Yeh, T. C. J., Gelhar, L. W. and Gutjahr, A. L., 1985. Stochastic analysis of unsaturated flow in heterogeneous soils, 2, statistically anisotropic media with variable a, *Water Resour. Res.,* 21: 457–464.

Zavattaro, L., and Grignani, C., 2001. Deriving hydrological parameters for modelling water flow under field conditions. *Soil Sci. Soc. Am. J.,* 65:655–667.

CHAPTER 4

EVALUATING MODELS FOR PREDICTING HYDRAULIC CHARECTERISTICS OF LAYERED SOILS

Abstract

Soil water characteristic curve (SWCC) and unsaturated hydraulic conductivity (K-coefficient) are critical hydraulic properties governing soil water activity on layered soils. Several parametric based models have been developed to describe these hydraulic functions under laboratory and *in situ* conditions. Some of these popular models were validated for the South African Tukulu and Sepane soil types similar to Cutanic Luvisols and Swartland soil form also referred to Cutanic Cambisols in other countries. Laboratory measured SWCC was first described using Brooks and Corey (1964), van Genuchten (1980) and Kosugi (1996) parametric models. The conductivity functions of these models were then required to fit *in situ* based K-coefficients derived from instantaneous profile method (IPM) transient experiment. The same K-coefficient was also fitted by HYDRUS-1D using optimised SWCC parameters. Although all parametric models fitted the measured SWCC fairly well their corresponding conductivity functions could not do the same when fitting the *in situ* based K-coefficients. Overestimates of more than two orders of magnitude especially at low soil water content (SWC) were observed. This phenomenon was pronounced among the upper horizons that overlaid a clayey horizon. However, optimized α and n parameters using HYDRUS-1D showed remarkable agreement between fitted and *in situ* K-coefficient with root sum of squares error (RMSE) recording values not exceeding unity. During this exercise the Brooks and Corey was replaced by modified van Genuchten model (Vogel and Cislerova, 1988) since it failed to produce unique inverse solutions. The models performance appeared to be soil specific with van Genuchten (1980) performing fairly well on the orthic and neucutanic horizons while its modified form fitted very well the prismatic and pedo-cutanic horizons. The lognormal distribution model of Kosugi (1996) showed an extraordinary good fit among the Swartland profile horizons especially the saprolite rock layer. It was therefore concluded that *in situ* K-coefficient estimates from SWCC parameters could be acceptable if only rough estimates were required. Optimization of parameters for *in situ* conditions especially for HYDRUS-1D carried much prospects in characterising the hydraulic properties of most of the layered soils earmarked for IRWH in the province.

Key words: hydraulic properties, layered soils, parametric models, HYDRUS-1D

4.1 Introduction

Characterising soil hydraulic properties of layered profiles has become more attractive because of the increased availability of computer based models. These models rely on parameterization of the soil water characteristic curve (SWCC) and unsaturated soil hydraulic conductivity (K-coefficient) that serve as inputs in soil water flow and solute transport simulations. The flexibility of this models to describe hydraulic functions for any given flow domain through parameter optimization implies that most of the inefficiencies from traditional methods could be avoided.

Successes of parameter based models have been based on integrating indirect and inverse techniques. Hopmans et al. (2002) defined inverse modelling as a general mathematical method to determine unknown causes on the basis of observation of their effects. Since SWCC is the much easier function of soil water content (SWC) to measure, early models used the Burdine theory (Millington-Quirk, 1961) based on SWCC to predict the K-coefficient. The convenience of predicting the K-coefficient either as a function of SWC (θ) or suction (h) from SWCC was carried over to subsequent parameters based models with greater accuracies (Brooks and Corey 1964; Mualem, 1976). Under controlled laboratory conditions it later proved that SWCC and K-coefficient could be simultaneously determined from transient outflow experiments (Gardener (1956) by inverse modelling (Valiantzas and Kerkides (1990). Recent models including among others the van Genuchten-Mualem (van Genuchten, 1980), modified van Genuchten (Vogel and Cislerova, 1988) and the Kosugi (1996) have been reported to be more efficient under different conditions (Kosugi et al., 2002). To improve parameters estimation of various soils the pedo-transfer functions were developed that use soil physical properties such as pore-size distribution and bulk density as well as the shape of the SWCC to predict the K-coefficient (Schaap et al., 2001; Hopmans et al., 2002). Although the application of the pedo-transfer functions could be limited to specific soil or horizons (Zavattaro and Grignani, 2001) their rough estimates could facilitate the simulation of water flow and solute transport in the absence of reliable data (Simunek et al., 2008).

Challenges of inverse modelling including parameter uniqueness, selecting of transient flow variables and spatial variations of the porous media have been addressed (Zachman et al., 1982, Kool and Parker, 1988, and Russo et al., 1991; Kosugi and Hopmans, 1998; William and Ahuja, 2003; Simunek et al., 2008; Hunt and Ewing, 2009). Dane and Hruska (1983) was

also among the first to demonstrate that with the correct objective function and parametric model it was possible to improve inverse solutions from *in situ* conditions from the instantaneous profile method (IPM) transient experiment. Essential ingredient of transferring the θ-h relationship from the SWCC to in situ conditions was that the selected model should fit the measured data well for the SWC range in question (van Genuchten, 1980; Kosugi et al., 2002). This was confirmed by Russo (1988) and Chen et al. (1999) who tested various models, respectively for one-step outflow optimization and multistep outflow experimental data and found that only a few fitted the measured data very well. Van Genuchten (1980) model is among the highly rated models and has ability to improve stability of inverse solution supported by other studies (Russo, 1991; Mallants et al., 1996; Chen et al., 1999; Simunek et al., 2008). However, excellent results from other models have been reported (Pachepsky et al., 1996; Tomasella and Hodnett, 1997; Kosugi et al., 2002; Kawamoto et al., 2006; Lamara and Derriche, 2008), but because of the large number of unknown parameters their applications is limited (van Genuchten, 1980).

Critical to *in situ* conditions is taking into account the spatiality of the flow boundary conditions and horizons differentiation especially in layered profiles. To address the sensitivity of the optimised parameters to lower boundary conditions and size of input data, Kool et al. (1987) and Kool and Parker (1988) showed that coupling of the optimization procedure with simultaneous measurements of pressure heads and SWC improves their model's predictions. Increased number of measurements was also found to be able to account better for spatial variations and to improve effect of scaling soil heterogeneity (Abbasi et al., 2003; Sharma et al. 2011). These models have been shown to be more sensitive to the number of optimised parameters than the optimization procedure (Zijlstra and Dane, 1996; Abbasi et al., 2003; Brunone et al., 2003; Simunek et al., 2008).

To address the erratic soil water regime among the cultivated layered soils in the Free State province of South Africa, the in-field rainwater harvesting (IRWH) technique (Hensley et al., 2000) has been developed. This technique is geared to convert surface runoff losses into deep infiltration and soil water storage. However, the success of this initiative and the sustainability there off could not be possible without appropriate knowledge of the soil hydraulic properties. Layered soils earmarked for IRWH developed constitutes about 10% of the provincial landscape (Hensley et al., 2006). Common in this group of soils includes the Tukulu and Sepane that are similar to Cutanic Luvisols and the Swartland also similar to the Cutanic Cambisols of the World Reference Base for Soil Resources (1998). Integrating

laboratory and field based analysis of soil hydraulic properties would be essential to this work. It is therefore within the initiative of this study to attain the following objectives; Firstly, to characterise the SWCC of the respective horizons of the three soil profiles and secondly, to validate the conductivity functions based on the SWCC parameters for the estimation of *in situ* K-coefficient; Thirdly, to estimate *in situ* K-coefficient from optimised SWCC based parameters.

4.2 Material and methods

4.2.1 Experimental site and location

Three soil types cultivated at the Parady's Experimental Farm (29°13'25"S, 26°12'08"E, altitude 1417 m) of University of the Free State were selected. These included Tukulu (Tu), Sepane (Se) and Swartland (Sw) (Soil Classification Working Group, 1991). The SWCC and K-coefficient were determined under laboratory and in situ conditions, respectively.

4.2.2 Theory

Several parametric models are used to describe the measured SWCC using the shape (α) and (n) pore size distribution parameters. Among the common parametric models include the Brooks and Corey (1964), van Genuchten, 1980 and Kosugi (1996). These models constitute of expression that aid in describing the θ-h relationship of the SWCC. Development of these models was informed by the general retention equation (4.1) widely accepted to represent the pore distribution of many of soils.

$$S_e = \frac{\theta_s - \theta_r}{1 + (\alpha h)^n} \tag{4.1}$$

$$S_e = \frac{\theta - \theta_r}{\theta_s - \theta_r} \tag{4.2}$$

Where S_e is effective saturation, θ_s and θ_r are the respective saturated and residual values of the volumetric water content, θ (mm mm^{-1}), h is the matric suction (mm), while α and n are the shape and pore size distribution parameters, respectively.

Brooks and Corey (1964) reduced the expression (1) into the following general equation

$$S_e = |\propto h|^{-n} \tag{4.3}$$

Where α is is the inverse of air entry value and the rest as defined previously. This expression allows a zero slope to be imposed on SWCC as h equals air entry value. S_e equals to unity

when $h \geq -1/\alpha$. This principle gives SWCC a zero slope at relatively higher suctions since measuring SWCC above 85% of saturation was considered impractical and general disconnection of the gas phase (Brooks and Corey 1999). Conductivity function corresponding to this expression is written as:

$$K = K_s S_e^{\frac{2}{n}+1+2} \tag{4.4}$$

Where, 1 is the pore-connectivity parameter approaching 2. Similarly this expression allows K-coefficient to approach Ks at or near air entry matric suctions.

The van Genuchten-Mualem retention model (van Genuchten, 1980) assumes the following expression:

$$\theta(h) = \theta r + \frac{\theta_s - \theta_r}{\{1 + |\alpha h|^n\}^m} \tag{4.5}$$

Where the condition m=1-1/n should be satisfied. According to the mathematical structure of this model θ (h) equals θ_s when at zero or positive matric suction. The square root relationship of θ (h) to n and m parameters gives the SWCC a typical symmetrical shape with zero slope approached both towards θ_s and θ_r. The conductivity function referred to as the van Genuchten- Mualem (1980) equation is given as:

$$(h) = K_s S_e^l \left\{1 - \left\{1 - S_e^{\frac{1}{m}}\right\}^m\right\}^2 \tag{4.6}$$

where the parameters are as defined before with n maintained above unity value. This model has undergone several revisions with the recent modification by Schaap and van Genuchten (2005). However, one modification incorporated in many computer models is that by Vogel and Cislerova, (1988). The modification assumes the same structure the expression except that θ_s and θ_r are replaced by fictitious parameters given as θ_m and θ_a, respectively with θ_m slightly greater than θ_s and θ_a slightly smaller than θ_r. This was done to force the SWCC to be constant between θ_s and some small negative matric suction value. Its corresponding conductivity's expression is complex and was detailed by Schaap and van Genuchten (2005). The introduction of some small capillary height just next to saturation allows the K-coefficient to be more stable than the original version that exhibited a steep slope at suctions very close to saturation with air entry value kept around -0.2 kPa. This modification has made

it to be highly recommended for clay textured soils (Schaap and van Genuchten, 2005; Simunek et al., 2008).

Another parametric model of different form is that of Kosugi (1996) that assumes a lognormal distribution for the retention and conductivity functions. The retention expressions for $S_e(h)$:

$$S_e = \frac{\theta-\theta_r}{\theta_s-\theta_r} = \frac{1}{2} erfc \left\{ \frac{ln(h/\alpha)}{\sqrt{2n}} \right\} \quad (4.7)$$

$$K = K_s S_e^l \left[\frac{1}{2} erfc \left\{ \frac{ln(h/\alpha)}{\sqrt{2n}} + \frac{n}{\sqrt{2}} \right\} \right]^2 \quad (4.8)$$

where symbol α instead of h_o and n instead of σ as used in the original Kosugi (1996) paper are adopted for uniformity reasons by some computer optimization programmes such as RECT and HYDRUS-1D.

4.2.3 Experimental set up and measurements

4.2.3.1 Soil profile classification

Pedological classification of the three soils was carried out on excavated soil profile pits to a depth of 1 m (Appendix A, B and C). Three soil pits were opened on each representative site. Diagnostic horizons were described according to the physical, chemical and biological features used by the SCWG (1991).

4.2.3.2 Soil particle distribution and bulk density

Undisturbed soil core samples from representative profile horizons were taken for the determination of bulk density and soil textural analysis. Sampling cores had an inner diameter of 103 mm and a height of 77 mm. Each core was mounted on a hydraulic jack that was manually operated to extract samples from the various horizons. Particle size distribution was established using the pipette procedures proposed by the Non Affiliated Soil Analysis Work Committee (1990). For the determination of gravimetric soil water content soil samples were oven dried at 105°C for a period of 24 hours.

4.2.3.3 Saturated hydraulic conductivity

Saturated hydraulic conductivity (K_s) for the individual profile layers of the three soils were measured using double ring infiltrometers as described by Scotter et al. (1982). Soil profile pits were excavated in a stepwise manner to allow the fitting of both rings with diameters of 400 and 600 mm to a depth of 20 mm. The falling head over a distance of 10 mm depth was used to determine K_s with every fall recorded by means of a timer and a calibrated floater. After a steady state was recorded for three consecutive times the K_s constant value (mm hour^{-1}) was computed using the Jury et al. (1991) formula given as:

$$K_s = \frac{L}{t_1} ln \frac{b_o + L}{b_1 + L} \quad (4.9)$$

where L is the depth of the soil layer in question (mm), b_o is the initial depth of total head above the soil column, b_1 is the depth the falling head is not allowed to fall below (mm), t_1 is the time taken for b_o to fall to b_1 (in hours).

4.2.3.4 Internal drainage experiment

The instantaneous profile method (IPM) (Hillel et al., 1972, Marion et al., 1994) was used to determine soil water flux and unsaturated hydraulic conductivity from the draining profiles. Monoliths of 4 m x 4 m surface area with 1 m depth from the Tukulu and Sepane were prepared in triplicates. From the Swartland monoliths were of 1.2 m x 1.2 m with a depth of 0.5 m. To minimise spatial variations monoliths were semi-detached but difficulty in excavating the Swartland soil resulted in solitary monoliths at spacing of 30 m interval. Neutron access tubes to a depth of 1.1 m were installed on the central area of each monolith section from the Tukulu and Sepane while DFM probes were installed to a depth 0.6 m. Side walls were isolated with polythene plastics with ridges around sides and a slurry prepared to seal the sides from the surface. Monoliths were pre-ponded for three executive days and then covered to keep weather elements from interfering with the trial. Measurements were taken at the centre of each profile horizon daily for a period of 50 days. Changes in water storage between time intervals were computed into drainage flux (q_{Dr}; mm hour^{-1}) which was then described using the Darcy's Law given as:

$$q_{Dr} = -K(\theta)\left\{\frac{dh}{dz} + 1\right\} \quad (4.10)$$

Where K (θ) is unsaturated hydraulic conductivity (mm $hour^{-1}$), dh is the change in matric suction (mm) between the neighbouring horizons, Z (mm) being the thickness of the horizon layer in question.

4.2.3.5 Measurements of the soil water characteristics curve

Determination of the SWCC for the three soil profile horizons was carried out by a laboratory desorption experiment. Undisturbed soil samples in triplicates were first de-aired with a vacuum chamber pump set at -70 kPa for 48 hours under room temperature. De-aired water was then introduced to saturate samples by capillarity for a 24 hour period. Samples were then desorbed through the following series of pressure heads including a 0 to -10 kPa, -10 to -100 kPa and -100 to -1500 kPa. The first phase of desorption involved the hanging water column method, described by Dirksen (1999). At every step, interval samples were weighted before and after equilibration. At suctions of -100 to -1500 kPa samples were disturbed and packed in 2000 mm^3 PVC tubes at the measured bulk densities. Measured soil water content (θ) at every matric suction (h) level was plotted to produce the θ-h relationship that depicted the SWCC.

4.2.3.5.1 Mathematical description of soil water characteristic curve

Parametric models use hydraulic parameters to describe the SWCC. A parameter optimization computer program RECT (van Genuchten et al., 1991) included some of these such as the Brooks and Corey (1964), van Genutchen (1980) and Kosugi (1996) models. A summary of physical characteristics from the three soil profiles used as inputs into these models are summarized in Table 4.1. Parameters related to pore-size distribution (n) and shape (α) of the SWCC was initially fitted using the Rosetta pedo-transfer (Schaap et al., 2001) and then optimised for the respective models.

4.2.3.5.2 Estimating unsaturated hydraulic properties for field based K-coefficient

Hydraulic parameters pertaining to the shape (α) and pore size distribution (n) of the SWCC were inversely optimised for the description of *in situ* K-coefficient. The software HYDRUS -1D (Simunek et al., 2008) was used for this optimization and also for the fitting of the *in situ* K-coefficient at plot scale derived by the instantaneous profile method (IPM). This model numerically solves the Richard flow equation in one dimension using a Galerkin-type linear finite element scheme.

Table 4.1 Summary of the physical characteristics of the three soil types.

Soil physical properties									
Soil forms	Tukulu			Sepane			Swartland		
Master Horizons	A	B1	C	A	B1	C	A	B1	C
Coarse sand (%)	5.3	9.2	2.1	5.2	3.5	2.3	4.7	3.2	54.3
Medium sand (%)	9.3	8.8	3.8	10	4.1	2.3	7.6	5.3	4.6
Fine sand (%)	41.2	31	28.3	41.9	41	31	42	37.6	17.2
Very fine sand (%)	25.3	21	8.4	21.5	10.5	18	31.7	26.6	2.5
Coarse silt (%)	2.1	2	3	1	3	1	2	3	3
Fine silt (%)	4.6	2.5	6.5	1	3	1	1	2	3
Clay (%)	11.3	26.4	47.9	19	35	45	11.3	21.9	15
Bulk density (kg m^{-3})	1670	1597	1602	1670	1790	1730	1670	1530	1450
Porosity (%)	34.0	33	32.4	34	33.5	33.8	35	39.9	41.6
K_s (mm $hour^{-1}$)	36.1	40	9.6 (1.9)	35.2	18.1 (10.2)	1.9 (1)	23.5	42.8	76.5

K_s = Saturated hydraulic Conductivity

A wide variety of parameter optimization problems could be handled through the minimization accomplished by the Levenberg-Marquardt nonlinear weighted least squares approach (Hopmans and Simunek, 1999; Lazarovitch et al., 2009; Wollschlager, et al., 2009; Kandelous and Simunek, 2010).

In this work the objective function contained pressure head from horizons centre block and K-coefficient's determined by IPM as a function of soil water content (SWC). Preliminary tests on the parametric models showed that the Brooks and Corey (1964) required simultaneous optimisation of several parameters, an exercise that compromised the uniqueness of the inverse solution (Simunek et al., 2008). Therefore, only the van Genuchten-Mualem (van Genuchten, 1980), Modified van Genuchten (Vogel and Cislerova, 1988) and Kosugi (1996) models were selected for the optimization of the conductivity function. To enhance the convergence the l exponent parameter from the Mualem's (1976) equation was optimised as well. Initial conditions were set at saturated soil water content for the respective soil profile horizons. Observation points were fixed at centre block corresponding to field measurements. The constraint of respecting the model assumptions and the code requirements was followed in all data analysis.

4.2.4 Statistical analysis

Measured and optimised drainage and unsaturated hydraulic conductivity as well as the pertinent hydraulic parameters constituted the major findings. The coefficient of determination (R^2), root mean square error (RMSE) and the index of agreement or D-index as proposed by Willmot et al., (1985), were the statistical tools used to quantify the quality of fit and variability between measured and fitted data. A 1:1 line was used to show the degree of scatter of the optimised model fit from the field based K-coefficient.

4.3 Results

4.3.1 Soil water characteristics curve

Figure 4.1 shows the measured and fitted soil water characteristics curves (SWCC) for the A, B and C horizons of the Tukulu, Sepane and Swartland soil forms. The fitted hydraulic parameters from Brooks and Corey (1964), van Genuchten (1980) and Kosugi (1996) models are summarized in Table 4.2 with their corresponding statistical measure of fit.

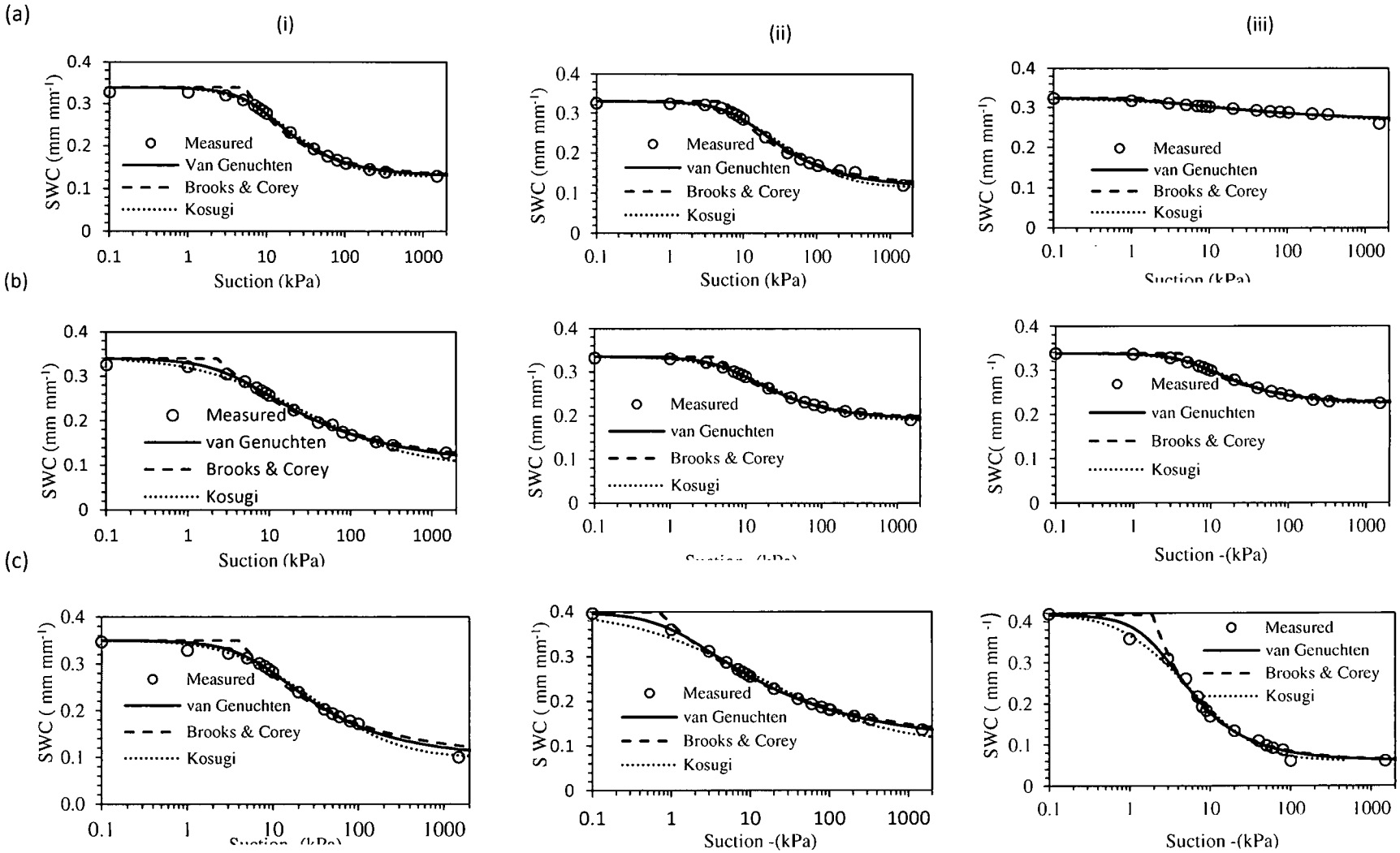

Figure 4.1 Measured and fitted soil water content (SWC) and matric suction relationships for the Tukulu (a), Sepane (b) and Swartland (c) diagnostic horizons A (i), B (ii) and C (iii).

Table 4.2 Fitting models to the hydraulic parameters of the SWCC for the Tukulu, Sepane and Swartland form soils.

Tukulu soil										
RetentionModels	Horizons	θ_s	θ_r	K_s	α	n	m	R^2	RMSE	D-index
Brooks & Corey	A	0.34	0.13	36.10	0.0019	0.62	1.000	0.977	0.0112	0.9945
van Genutchen	A	0.34	0.13	36.10	0.0012	1.77	0.436	0.995	0.0054	0.9987
Kosugi	A	0.34	0.13	36.10	2084.0	1.41	0.359	0.995	0.0054	0.9987
Brooks & Corey	B	0.33	0.116	40.00	0.0018	0.47	1.000	0.991	0.0066	0.9979
van Genutchen	B	0.33	0.116	40.00	0.0009	1.62	0.381	0.990	0.0046	0.9990
Kosugi	B	0.33	0.116	40.00	3378.9	1.59	0.359	0.987	0.0083	0.9967
Brooks & Corey	C	0.32	0.26	1.90	0.0079	0.21	1.000	0.925	0.0043	0.9806
van Genutchen	C	0.32	0.26	1.90	0.0059	1.22	0.182	0.940	0.0038	0.9841
Kosugi	C	0.32	0.26	1.90	4770.7	3.38	0.359	0.964	0.0029	0.9905
Sepane soil										
Brooks & Corey	A	0.340	0.100	35.19	0.0044	0.31	1.000	0.985	0.0082	0.9963
van Genutchen	A	0.340	0.100	35.19	0.0027	1.37	0.270	0.994	0.0054	0.9983
Kosugi	A	0.340	0.100	35.19	2787.3	2.45	0.359	0.988	0.0063	0.9977
Brooks & Corey	B	0.335	0.190	10.20	0.0025	0.47	1.000	0.988	0.0053	0.9971
van Genutchen	B	0.335	0.190	10.20	0.0015	1.59	0.369	0.990	0.0018	0.9996
Kosugi	B	0.335	0.190	10.20	2343.6	1.73	0.359	0.997	0.0028	0.9992
Brooks & Corey	C	0.338	0.225	1.00	0.0025	0.54	1.000	0.987	0.0045	0.9968
van Genutchen	C	0.338	0.225	1.00	0.0014	1.69	0.408	0.998	0.0016	0.9996
Kosugi	C	0.338	0.225	1.00	1934.8	1.55	0.359	0.999	0.0013	0.9997
Swartland soil										
Brooks & Corey	A	0.350	0.100	23.48	0.0025	0.39	1.000	0.974	0.0053	0.9987
van Genutchen	A	0.350	0.100	23.48	0.0014	1.50	0.333	0.992	0.0055	0.9999
Kosugi	A	0.350	0.100	23.48	3010.0	1.84	0.359	0.990	0.0104	0.9996
Brooks & Corey	B	0.399	0.105	42.80	0.0141	0.26	1.000	0.995	0.0095	0.9996
van Genutchen	B	0.399	0.105	42.80	0.0088	1.30	0.231	0.999	0.0054	0.9999
Kosugi	B	0.399	0.105	42.80	1333.9	3.06	0.359	0.989	0.0040	0.9999
Brooks & Corey	C	0.416	0.061	76.50	0.0052	0.69	1.000	0.980	0.0094	0.9990
van Genutchen	C	0.416	0.061	76.50	0.0041	1.76	0.433	0.992	0.0100	0.9996
Kosugi	C	0.416	0.061	76.50	547.73	1.58	0.359	0.992	0.0162	0.9990

Tukulu: measured and fitted SWCC were fairly similar in all horizons. The measured SWCC assumed the general segmoidale shape especially from the A and B horizons, while the C horizon resembled a near linear and small slope. The A, B and C horizons had a θ-h relationship with saturated (θ_s) soil water content (SWC) to residual water content (θ_r) ranging from 0.34 to 0.13 mm mm^{-1}, 0.33 to 0.12 and 0.324 to 0.26 mm mm^{-1}, respectively. Corresponding Ks for these layers were 36.1, 40 and 1.9 mm $hour^{-1}$. The van Genuchten-Mualem and Kosugi models approached θ_s at matric suctions of about 0.1 kPa with an air

entry of around -1 kPa from the A and B horizons and -1.5 kPa for the C-horizon. On the other hand the Brooks and Corey's model approached θ_s at about -5 kPa for the A and B horizons and -2 kPa from the C horizon. Fitting α parameter from the Brooks and Corey for the A, B and C horizons was 0.0019, 0.0018 and 0.0079 with corresponding n values of 0.62. 0.47 and 0.21. From the van Genuchten-Mualem model the A and B horizons shared the same α value of 0.001 while the C horizon had a value of 0.005. The n constant from this model was 1.77, 1.62 and 1.22 for the respective A, B and C horizons. The Kosugi's model had a lognormal α parameters of 2084, 3379 and 4770.7 for the respective A, B and C horizons with corresponding n values of 1.41, 1.59 and 3.38. The R^2 from the 1:1 linear relationship between the measured and predicted values ranged from 0.99 to 0.93 with lowest coefficient associated with the C horizon from Brooks and Corey model. Similarly, the D-index ranged from 0.999 to 0.981 with the lowest value depicting the least good fit from the C horizon. The RMSE from the A horizon ranged from 0.0115 to 0.005 with both van Genuchten-Mualem and Kosugi models having the lowest values depicting a better fit. From the B and C horizon the RMSE ranged from 0.004 to 0.005 and 0.003 to 0.008, respectively with van Genuchten and Kosugi attaining a better fit with the former.

Sepane: a good fit between the measured and fitted SWCC was observed in all three horizons. The A, B and C horizons had a θ-h relationship with SWC of 0.34 to 0.1, 0.335 to 0.19 and 0.338 to 0.225 mm mm^{-1} with K_s of 35, 10 and 1 mm $hour^{-1}$ from the respective A, B and C horizons. At near saturation the van Genuchten-Mualem and Kosugi models approached θ_s at matric suctions between -0.1 to -0.01 kPa with an air entry value of around -1 kPa from the three horizons. Brooks and Corey model approached θ_s at around -1.1, -2.1 and -2.7 kPa for the A, B and C horizons, respectively. Fitting α parameters from the Brooks and Corey were 0.004 for the A horizon and 0.003 for the B and C horizons with corresponding n values of 0.31, 0.47 and 0.54 for the A, B and C horizons, respectively. The α parameter for the van Genuchten model were 0.003 from the A horizon, 0.002 for the B-horizon and 0.0014 for the C-horizons with corresponding n values of 1.37, 1.59 and 1.69 for the A, B and C horizons. Residual squares were in the range of 0.999 to 0.985 and Brooks and Corey with the lowest coefficients. Similarly the D-index recorded lower agreement from the Brooks and Corey especially from the A horizon. The RMSE ranged from 0.0082 to 0.0054 and 0.053 to 0.0018 from the A and B horizons respectively with the van Genuchten-Mualem model recording the lowest value in both cases indicating a better fit. From the C horizon the RMSE ranged from 0.0045 to 0.0013 with Kosugi attaining the better fit.

Swartland: Greater variability between measured and fitted SWCC were observed in this soil. The A horizon recorded a SWC ranging from 0.35 to 0.1 mm mm^{-1} and B horizon with a range from 0.399 to 0.105 mm mm^{-1}. The C-horizon had a SWC ranging from 0.412 to 0.06 mm mm^{-1}. Saturated hydraulic conductivity was 23.5 mm $hour^{-1}$ for the A horizon with 42.8 and 76.5 mm $hour^{-1}$ for the respective B and C horizons. Brooks and Corey's model had α parameter that increased with depth ranging from 0.0025 to 0.00141. In a similar manner this parameter ranged from 0.0014 to 0.0088 for the van Genuchten model. From the Kosugi model α decreased with depth at a range of 3010 to 547.73. Corresponding n values in the A, B and C horizons ranged from 0.26 to 0.688 from the Brooks and Corey, 1.30 to 1.764 for the van Genuchten-Mualem and 1.58 to 3.06 for the Kosugi models, respectively. Models approached saturation at 0.1 to 0.01 kPa with the exception of Brooks and Corey that recorded 2.6, 2.1 and 1.9 kPa in the A, B and C horizons. The R^2 was in the range of 0.99 to 0.92 with Brooks and Corey recording the least from the A horizon. Similarly the D-index recorded lowest agreement from the Brooks and Corey especially from the A horizon. The RMSE ranged from 0.0104 to 0.0053 and 0.0095 to 0.004 from the respective A and B horizons with better fit obtained from Brooks and Corey in the former and Kosugi in the latter. From the C horizon the RMSE ranged from 0.0162 to 0.0094 with a better fit attributed to Kosugi model.

4.3.2 Predicting K-coefficient from soil water characteristics curve

Figure 4.2 to 4.4 illustrates the variation between *in situ* K-coefficient derived from instantaneous profile method (IPM) and estimated by conductivity based parametric models. Fitting parameters from measured SWCC including K_s were used to predict K-coefficient as a function of SWC. Statistical measure of fit from estimated K-coefficients are summarised in Table 4.3 for the Tukulu, Sepane and Swartland soil horizons.

Tukulu: deviation between *in situ* and estimated K-coefficient could be observed especially at lower SWC. The *in situ* K-coefficient in the A horizon ranged from 0.006 to 36.1 mm $hour^{-1}$, for SWC range from 0.297 to 0.34 mm mm^{-1}. For the same SWC range the estimated K-coefficient ranged from 9.72 to 36.08, 3.36 to 36.1 and 2.18 to 36.1 mm $hour^{-1}$ from the Brooks and Corey, van Genuchten-Mualem, and Kosugi models. In the same order these models for the B horizon estimated K-coefficient within the range of 3.93 to 40, 14.13 to 40 and 2.73 to 40 mm $hour^{-1}$, while the *in situ* ranged from 0.0006 to 0.0006 mm $hour^{-1}$.

(a)

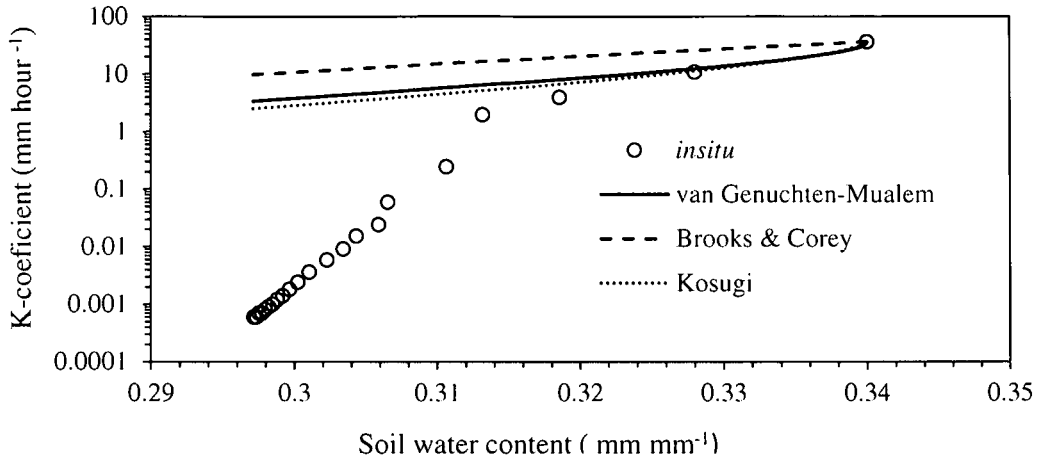

(b)

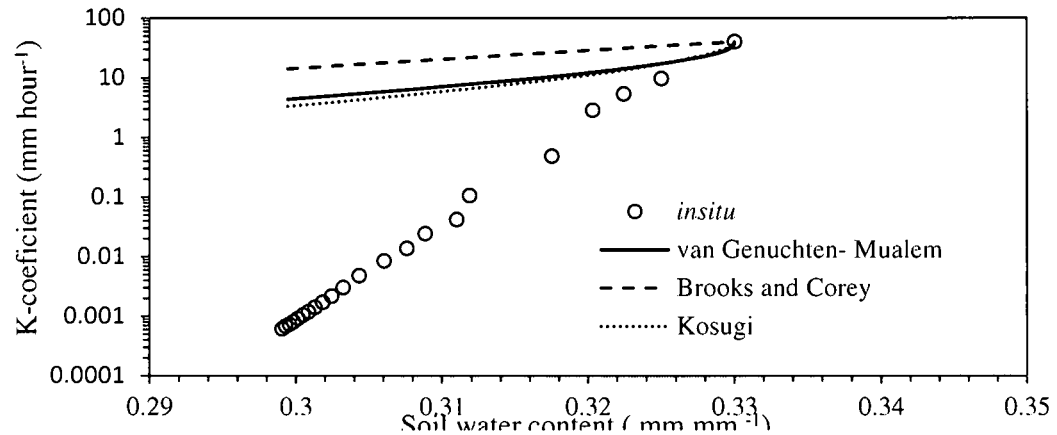

(c)

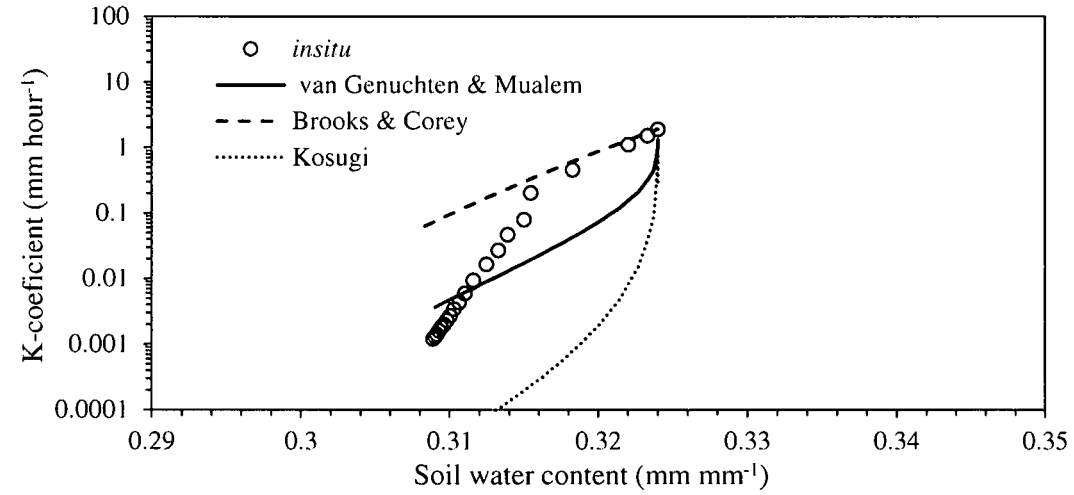

Figure 4.2 Comparison of K-coefficient from *in situ* and fitted by retention models for the Tukulu A (a), B (b) and C (c) diagnostic horizons.

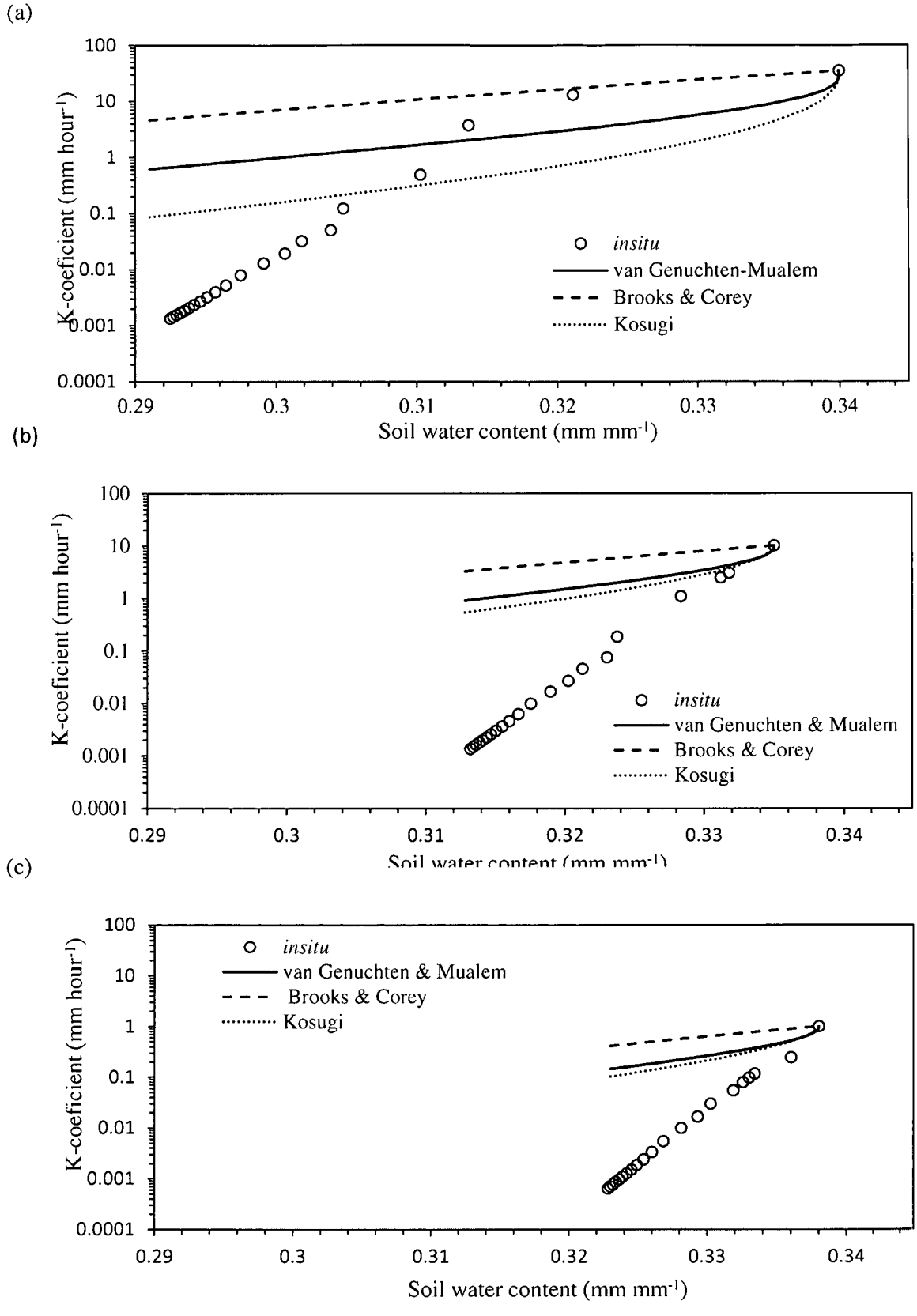

Figure 4.3 Comparison of K-coefficient from *in situ* and fitted by retention models for the Sepane A (a), B (b) and C (c) diagnostic horizons.

(a)

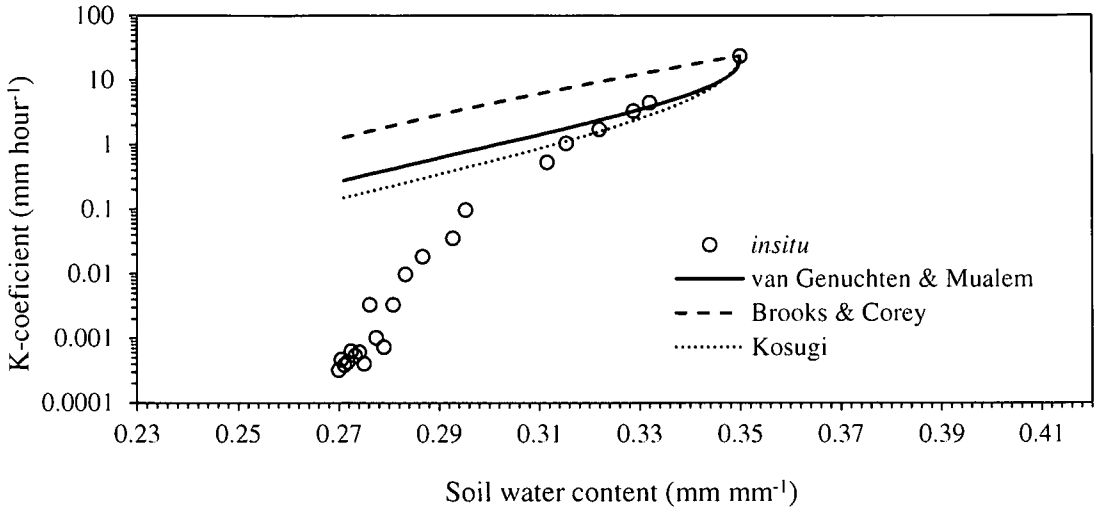

(b)

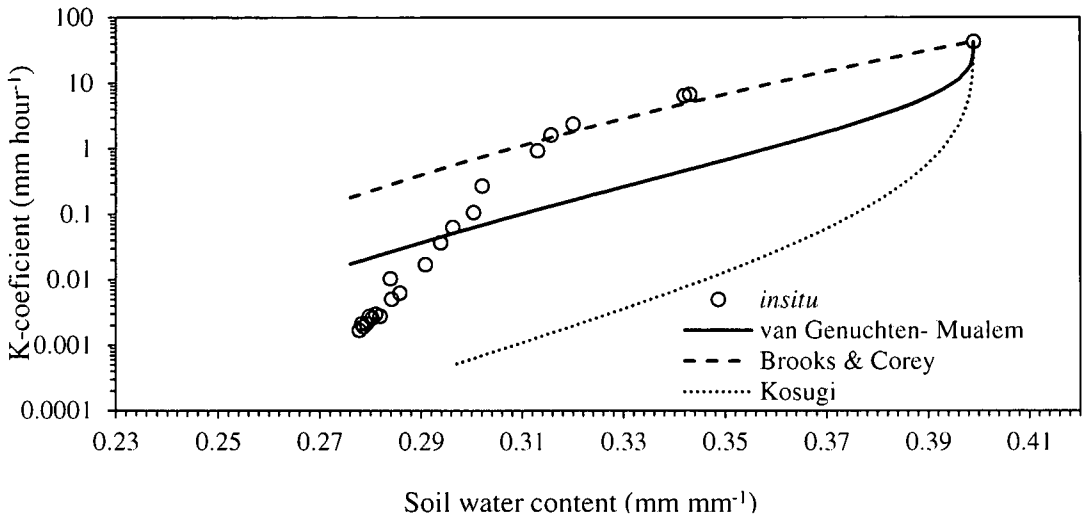

(c)

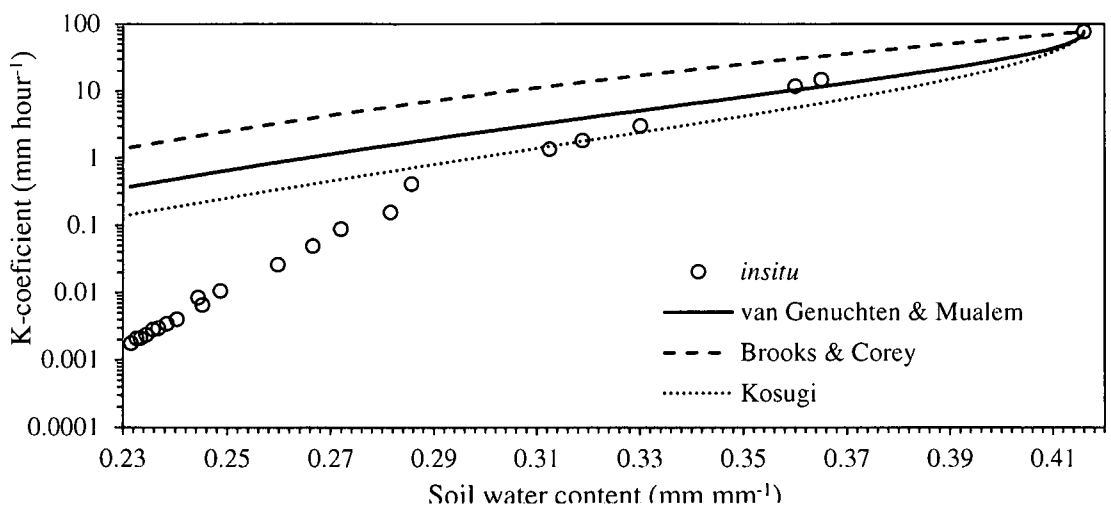

Figure 4.4 Comparison of K-coefficient from *in situ* and fitted by retention models for the Swartland A (a), B (b) and C (c) diagnostic horizons.

In the C horizon the *in situ* K-coefficient ranged from 0.0012 to 1.9 mm hour^{-1} while estimates from Brooks and Corey, van Genuchten-Mualem, and Kosugi models ranged from 0.0689 to 1.9, 0.003 to 1.9 and 0.00002 to 1.9 mm hour^{-1}, respectively. The R^2 from the A and B ranged from 0.64 to 0.95 and 0.53 to 0.89 with the lowest values associated with Brooks and Corey. In the C horizon R^2 ranged from 0.78 to 0.99 with the lowest value.

Table 4.3 Statistical measure of fit for conductivity based parametric models on *in situ* K-Coefficient for the Tukulu, Sepane and Swartland soil horizons.

		Tukulu			Sepane			Swartland		
Models	Horizons	R^2	RMSE	D-index	R^2	RMSE	D-index	R^2	RMSE	D-index
Brooks &Corey	A	0.64	11.467	0.577	0.85	5.337	0.881	0.79	4.558	0.812
van Genutchen-Mualem	A	0.90	4.046	0.928	0.96	2.35	0.974	0.99	0.381	0.998
Kosugi	A	0.95	2.763	0.966	0.94	2.78	0.965	0.99	0.312	0.999
Brooks and Corey	B	0.53	18.218	0.359	0.59	4.461	0.405	0.59	7.531	0.895
van Genutchen- Mualem	B	0.83	6.678	0.851	0.91	1.160	0.932	0.93	4.089	0.95
Kosugi	B	0.89	5.124	0.910	0.97	0.656	0.978	0.96	3.794	0.966
Brooks and Corey	C	0.99	0.105	0.990	0.52	0.532	0.235	0.93	7.471	0.948
van Genutchen-Mualem	C	0.82	0.357	0.852	0.87	0.148	0.884	0.99	1.229	0.999
Kosugi	C	0.78	0.377	0.824	0.83	0.175	0.839	0.99	1.580	0.998

Sepane: considerable variability between *in situ* and estimated K-coefficient was observed especially at lower SWC. The IPM captured SWC ranging from 0.292 to 0.34, 0.313 to 0.335 and 0.323 to 0.338 mm mm^{-1} from the respective A, B and C horizons. Corresponding K-coefficient ranged from 0.0013 to 35.19, 0.0014 to 10.2 and 0.0006 to 1 mm hour^{-1}. For the same SWC range the estimated K-coefficient from the A horizon were 3.95 to 35.19, 0.621 to 35.19, and 0.0953 to 35.19 mm hour^{-1} from Brooks and Corey, van Genuchten-Mualem, and Kosugi models. Corresponding predictions from these models for the B and C horizons were 3.47 to 10.2 and 0.433 to 1, 0.81 to 10.2 and 0.101 to 1, and 0.413 to10.2 and 0.112 to 1 mm hour^{-1}, respectively. *In situ* based K-coefficients from the B horizon ranged from 0.0014 to 10.2 mm hour^{-1}, while from the C horizon ranged from 0.0006 to 1 mm hour^{-1}. The R^2 from the A, B and C horizons ranged from 0.85 to 0.96, 0.59 to 0.97 and 0.52 to 0.87, respectively, with Brooks and Corey scoring the lowest value in all three horizons. Van Genuchten-Mualem model had a better fit from the A and C horizons shown by RMSE of 2.35 and 0.148 and D-index values of 0.97 and 0.88, respectively. The Kosugi model recorded a better fit in the B horizon with RMSE of 0.656 and D-index of 0.98.

Swartland: remarkable spatiality between *in situ* and estimated K-coefficient was also observed. During the drainage period SWC ranged from 0.27 to 0.35, 0.28 to 0.35 and 0.23 to 0.42 mm mm^{-1} from the A, B and C horizons, respectively. Corresponding to these horizons was the *in situ* K-coefficient ranging from 0.0002 to 23.48, 0.0028 to 42.8 and 0.002 to 76.5 mm $hour^{-1}$. Estimated K-coefficient by Brooks and Corey, van Genuchten-Mualem, and Kosugi models from the A horizons were 1.4 to 23.48, 0.22 to 23.48, and 0.132 to 23.48, respective. From the B and C horizons these models in their respective order estimated K-coefficient within the range of 1.18 to 42 and 0.37 to 76.5, 4.63 to 42.8 and 1.42 to 76, and 0.52 to 42.8 and 0.13 to 76.5 mm $hour^{-1}$. Estimates from Brooks and Corey had the lowest R^2 of 0.79, 0.59 and 0.93 from the respective A, B and C horizons. The Kosugi had a better fit in the A reflected by RMSE of 0.312 and D-index of 0.999. In the B-horizon van Genuchten-Mualem and Kosugi model shared similar RMSE and D-index values of 3.7 and 0.97, respectively. Kosugi also had a better fit in the C horizon with RMSE of 0.853 and D-index of 0.999.

4.3.3 Parameter optimisation for HYDRUS -1D application

Table 4.4 shows the optimised α and n parameters for the fitting of the *in situ* based K-coefficient using HYDRUS-1D program. Statistical measure of coefficient of determination from these optimised parameters corresponding to the fixed θ_s, θ_r and K_s values were also shown. Figure 4.5 illustrates how the fitted K-coefficient compared with the field based K-coefficient on a 1:1 line from the Tukulu (a) Sepane (b) and (c) Swartland soils for the A (i) B (ii) and C (iii) horizons.

Tukulu: a general greater degree of accuracy could be observed from the fitting of the field based K-coefficient by optimised parameters using the inverse solution. The van Genuchten-Mualem (van Genuchten, 1980) and modified van Genuchten (Vogel and Cislerova, 1988) models shared the same optimised σ of 0.0015 and n of 2.511 to attain a better fit with a RMSE of 0.324 and D-index of 0.9996 in the A horizon. The Kosugi (1996) models had used the same optimised α value of 1000 and n value of 1 for all three horizons. A better fit was realised in the B horizon with a RMSE of 0.234 and a D-index of 0.9995. The modified van Genuchten model showed a better fit with α value of 0.0055 and n value of 1.656 for the C horizon. The RMSE from this soil ranged from 1.2 to 0.023 and D-index from 0.999 to 0.91. The crowding of the fitted data along the 1:1 line confirms this statistics not only at higher

SWC but also for lower SWC with B and C horizons showing a good agreement for the entire curve.

Table 4.4 Optimised parameters for the fitting of *in situ* K-coefficient from the Tukulu, Sepane and Swartland soil horizons using HYDRUS -1D.

Tukulu soil							
Conductivity models	Horizons	α	n	l	R^2	RMSE	D-index
van Genutchen & Mualem	A	**0.0015**	**2.511**	**0.5**	0.9992	0.324	0.9996
Modified van Genuchten	A	**0.0015**	**2.511**	0.5	0.9992	0.324	0.9996
Kosugi	A	**1000**	**1.000**	0.5	0.9891	1.233	0.9937
van Genutchen & Mualem	B	**0.0019**	**2.000**	**0.5**	0.9999	0.324	0.9997
Modified van Genuchten	B	0.0039	2.000	0.5	0.9932	1.071	0.9888
Kosugi	B	**1000**	**1.000**	0.5	0.9997	0.234	0.9996
van Genutchen & Mualem	C	**0.0026**	1.500	**0.5**	0.9988	0.278	0.9046
Modified van Genuchten	C	**0.0055**	**1.646**	0.5	0.9993	0.023	0.9995
Kosugi	C	**1000**	**1.000**	0.5	0.9502	0.188	0.9638
Sepane soil							
van Genutchen & Mualem	A	**0.0030**	**3.514**	0.5	0.9997	0.200	0.9997
Modified van Genuchten	A	**0.0027**	**3.461**	0.5	0.9997	0.202	0.9998
Kosugi	A	**405.62**	**0.590**	8.9	0.9996	0.224	0.9998
van Genutchen & Mualem	B	**0.0007**	2.368	0.5	0.9989	0.164	0.9978
Modified van Genuchten	B	**0.0023**	**1.915**	0.5	0.9999	0.041	0.9998
Kosugi	B	**1113.70**	**1.228**	8.7	0.9998	0.050	0.9997
van Genutchen & Mualem	C	**0.0004**	1.500	0.5	0.9992	0.013	0.9992
Modified van Genuchten	C	**0.0005**	**1.751**	0.5	0.9999	0.002	0.9998
Kosugi	C	**683.42**	**1.015**	32.7	0.9999	0.002	0.9999
Swartland soil							
van Genutchen & Mualem	A	0.0017	1.85000	0.5	0.9998	0.025	0.9990
Modified van Genuchten	A	0.0018	1.97700	0.5	0.9998	0.025	0.9990
Kosugi	A	877.19	1.010	65.8	0.9999	5.092	0.7280
van Genutchen & Mualem	B	0.0028	2.4300	0.5	0.9998	0.155	0.9980
Modified van Genuchten	B	0.0028	2.4300	0.5	0.9998	0.155	0.9980
Kasugi	B	539.08	0.910	16.0	0.9999	0.119	0.9990
van Genutchen & Mualem	C	0.0019	1.760	0.5	0.8560	3.285	0.9890
Modified van Genuchten	C	0.0015	1.760	0.5	0.8560	3.285	0.9890
Kosugi	C	949.69	1.000	30.6	0.8900	2.877	0.9921

Bold letters = optimised to improve objective function solution

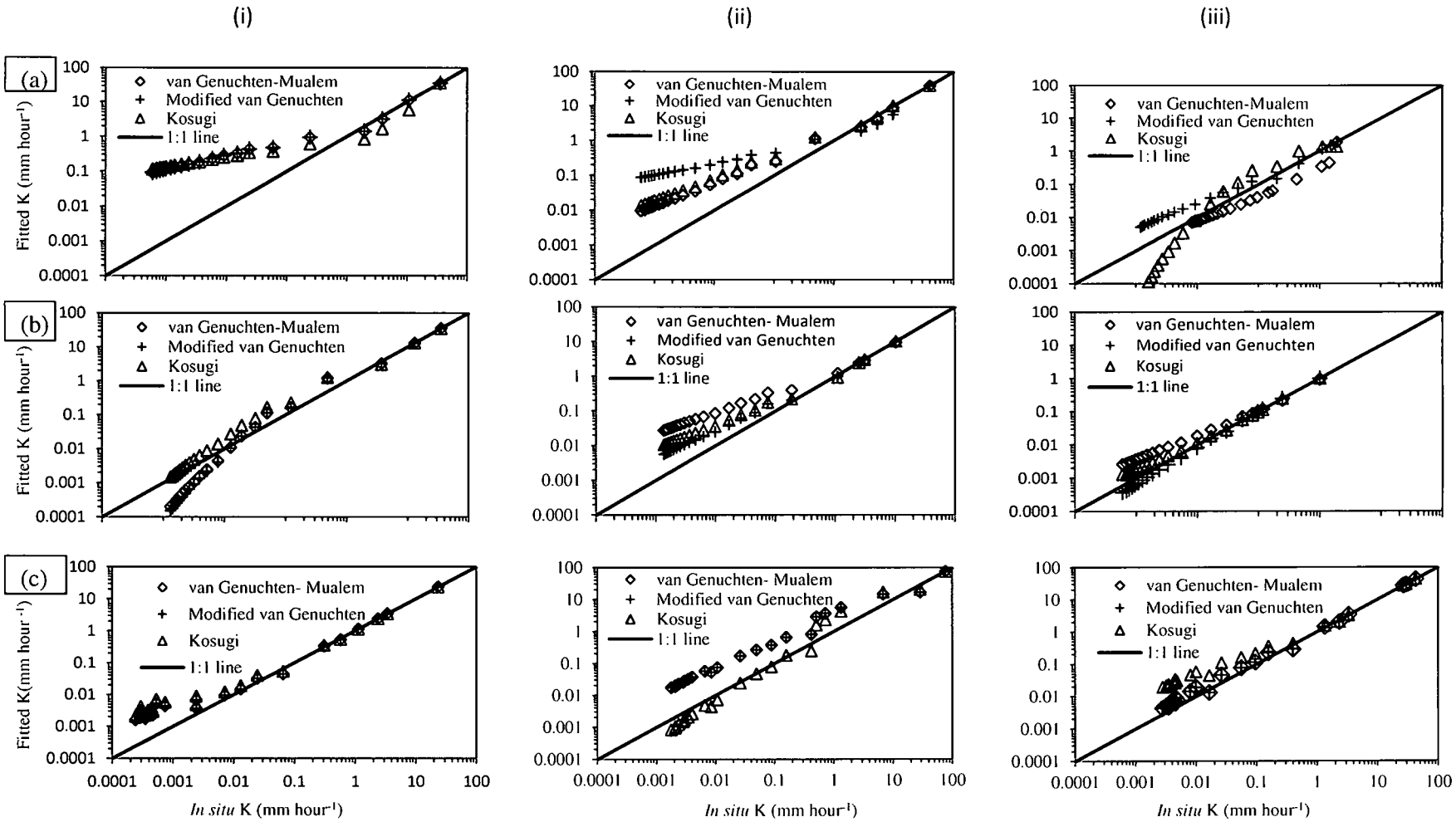

Figure 4.5 Comparison of *in situ* and fitted K-coefficient for the Tukulu (a), Sepane (b) and Swartland (c) diagnostic horizons A(i), B(ii) and C (iii) using HYDRUS-1D optimised parameters.

Sepane: the most accurate fit were recorded from this soil. The R^2 and D-index from fitting models exceeded 0.99 from all the soil horizons. Fitted data clustered closely to the 1:1 line especially from the A and C horizons. The van Genuchten-Mualem model with α of 0.003 and n of 3.514 attained a better fit from the A-horizon with a RMSE of 0.2, followed by the modified form with RMSE of 0.202. The latter also showed a better fit in the B and C horizon alongside Kosugi model with a RMSE as low as 0.04 to 0.002, respectively.

Swartland: improved accuracy and better fit were limited to the upper horizons of this soil profile. The modified van Genuchten model attained better fit from the A horizons with RMSE of 0.02 while the Kosugi model attained better fit from the B and C horizons with RMSE of 0.12 and 2.8. All model had the poorest fit coming from the C horizon given that R^2 ranged from 0.90 to 0.80.

4.4 Discussion

The goodness of fit from characterising SWCC to the estimating of *in situ* K-coefficient was found to vary among models and soil types. Optimised parameters also exhibited the same trend even though consistency with *in situ* K-coefficient showed remarkably improvement. Could these findings therefore, indicate that these hydraulic models were well developed to produce better fit than others or for specific soil types?

Fitting of SWCC was satisfactory from all the parametric models used. Of interest was the manner at which the traditional 'S' shape of the SWCC was modified among the three soils from the models. Among the sandy textured orthic and neocutanic horizons this shape was well defined while from strongly textured prismacutanic and pedocunatic horizons it was diffused to almost a straight line. These findings were similar with those made by Wilson et al. (1997), Wildenchild et al. (2001), Chimungu (2009), and Fraenkel (2008) on sandy and clayey horizons. Narrow pore size distribution from the former could have triggered rapid drainage rates at near saturation due to the small air entry values associated with these soils (Kosugi et al., 2002). Consequently, the remaining SWC could have been subjected to very steep hydraulic gradients as suctions are increased giving the SWCC a symmetrical shape observed by van Genuchten (1980), Simunek et al. (2008) and Lamara and Derriche (2008). Given the diverse pore pathways in clayey horizons a strong matrix activity could have been triggered as suctions were increased resulting to an appreciable but slow release curve consistent with structured soils (Wildnchild et al., 2001; Zavattaro and Grignani, 2001).

Nevertheless, the parametric models were consistent with the shape of the measured SWCC with the exception of Brooks and Corey especially at near air entry value. This was not a strange phenomenon since this model imposes a zero slope on the SWCC at near air entry point given the assumption that measuring saturations above 85 % was impractical, because of the general disconnection of the gas phase at this range of SWC (van Genuchten, 1980; Brooks and Corey, 1999). The Brooks and Corey (1964) was also reported to produce poor fit in soils with an S-shaped SWCC such as fine textured soils and undisturbed field soil (Kosugi et al., 2002).

Application of the conductivity functions based on SWCC parameters to estimate *in situ* K-coefficient derived by the IPM produced very high inconsistencies. Agreements were only limited at and near the saturation domain. *In situ* K-coefficient was generally overestimated by more than 2 to 3 orders of magnitude. This was well pronounced among the upper horizons of the Tukulu and Sepane. Overestimates from Swartland were less than 2 orders of magnitude especially at low SWC. Zavattaro and Grignani (2001) also observed that overestimation of K-coefficient was common among horizons overlying clay rich soils given the effect of abrupt transition on flow rates. Wildenchild et al. (2001) substantiated this by demonstrating that K-coefficient was dependent on flow rates. Sensitivity of the inverse problem to the lower boundary condition as could also be another factor (Dane and Hruska 1983; Hopmans et al. 2002). Given the absence of layering from soil columns used to measure SWCC it was reasonable to consider that estimates of K-coefficient would be generally greater than those derived from IPM under *in situ* environment. Similar results were recorded by Abbasi et al. (2003) when infiltration data, SWC and solute concentrations from layered soil were compared with predicted values.

Differences in suction range under which SWCC and *in situ* coefficient were determined could be another source of inconsistency. This view was also supported by Zavattaro and Grignani (2001). The SWCC was determined using matric suction range of -0.1 to -1500 kPa while from the IPM ranged from -0.01 to about -1 kPa. The latter depicts structural pore domain while the former constitutes all the entire pore size distribution (Nhlabatsi, 2010). Therefore, desorption of pores in the IPM was only represented by a small section on the SWCC. Although the parametric models were able to transfer the θ-h relationship from SWCC to of the field, the accuracy of this function was said to depend on how good these models fitted the SWCC (van Genuchten, 1980; Kosugi et al., 2002). This situation could be

illustrating why inconsistencies from Brooks and Corey model were pronounced irrespective of soil type. Van Genuchten (1980) observed that if θ_r was inaccurately measured among the input parameters, given that it falls outside the IPM flow domain, inconsistencies when *in situ* K-coefficient is estimates may arise. Under these circumstances the shape and pore-size distribution parameters representing θ-h relationship affecting the IPM based K-coefficient would need to be different from SWCC. This view was also shared by Zavattaro and Grignani (2001) who suggested that among others the shape (α) and pore size distribution (n) parameters of SWCC should be optimised for *in situ* applications. It was therefore not surprising that the use of SWCC based conductivity functions generally produced poor estimates of *in situ* K-coefficients especially at low SWC irrespective of soil type. Despite these inconsistencies some estimates from Brooks and Corey in the Tukulu C-horizon and Kosugi in the Swartland horizons were within acceptable range. The coarseness of these horizons could be the reason.

The view of optimising SWCC parameters for *in situ* application was then validated using HYDRUS-1D hydrological model. Inverse solution converged readily when α and n parameters were optimised allowing the rest of the parameters fixed under the constant SWC lower boundary condition for the Tukulu and Sepane while Swartland was allocated free drainage. The resulting matric suction distribution with depth from optimised parameters was shown in Figure 6. Matric suctions ranged from 0 to -700, 0 to -550 and -150 to -650 mm in the the Tukulu, Sepane and Swartland soil profiles consisted with matric suctions corresponding to structural pore domain (Kosugi et al., 2002 ; Wang et al., 2003; Chimungu, 2009; Nhlabatsi, 2010). Evidence of differences in physical properties at interface could be seen by the change of regime in matric suction with depth. This could also be used to illustrate the extent of layering among the three soil profiles and the effect on hydraulic properties. A build up in positive matric suction at depth corresponding to the prismatic C-horizons of the Tukulu and Sepane after 24 hours of drainage indicates the restrictiveness of this horizon an observation that was also made by Chimungu (2009) and Fraenkel (2008) on the respective profiles. Interestingly, optimised α values appeared to increase with depth on profile with restrictive horizons while from free draining Swartland profile the opposite was observed. Could it be that this spatial; response of parameters is indicative of their sensitivity to the soils profile layers boundary conditions. At present any meaningful insight about this observation could not be drawn. Failure to attain saturation from the Swartland after deep

wetting was also indicative of the high permeability of this profile especially the underlying saprolite rock with average Ks of 76.5 mm hour^{-1}.

Improvements in R^2 from optimised parameters were noticeable from the three soils irrespective of model used. However, level of agreement was variable among soils and horizon layers. The van Genuchten-Mualem model produced consistent K-coefficient estimates among the weakly structured horizons of the Tukulu and Sepane soil profiles. The modified van Genuchten model produced better fit on the clay rich horizons while Kosugi model matched fairly well with K-coefficient from the Swartland soil. The use of lognormal distribution to describe pore size distribution among the Swartland layers could have given the Kosugi model a better urge over the van Genuchten expressions. Given the exponential mathematical background of the van Genuchten-Mualem model it is reasonable to associate its better fit in the orthic A and neocutanic B horizons to the well defined pore size distribution of the sandy texture that this horizons have. Soils of the same texture were associated with a typical S-shape SWCC and without a distinct air entry value (Kosugi et al., 2002). However, due its exponential inheritance when n value approaches its lower limit of 1 then K-coefficient drops sharply at near saturation that could result to poor fit on clay soils with an appreciable drainage (Schaap and van Genuchten, 2006). The introduction of an extrapolated parameter that impose a non zero matric suction from saturation to some very small matric suctions could be attributed to the better fit of the modified van Genuchten model among the clay rich horizons (Schaap and van Genuchten, 2006; Simunek et al., 2008).

4.5 Conclusions

The question on to what extent could *in situ* based K-coefficient be estimated from SWCC based parameters was evaluated. Firstly the SWCC were parameterised using the Brooks and Corey (1964), van Genuchten (1980) and Kosugi (1996). The three models fitted fairly well the retention functions from the soil profile horizons. Brooks and Corey model showed some deviation near or at the entry point given its assumption to impose a zero slope at this matric suction from saturation. Secondly, the conductivity based expressions that rely on SWCC parameters from these three models were used to fit the *in situ* K-coefficient derived from IPM. Coefficient of determination from all models showed remarkable overestimated of the *in situ* K-coefficient by more than two orders of magnitude, especially at lower SWC. This finding gives the impression that SWCC parameters were not necessary appropriate to

describe *in situ* based K-coefficient but could be used when rough estimates are required particularly from layered soil. Thirdly, the SWCC based parameters were inversely optimised to serve as input to the HYDRUS-1D hydrological for the fitting of *in situ* K-coefficient from a plot scale simulation. Agreement between fitted and *in situ* K-coefficient improved by more than one order of magnitude from those obtained from SWCC parameters. The van Genuchten-Mualem model by van Genuchten (1980) appeared to be well posed for sandy textured soils while the modified van Genuchten model by Vogel and Cislerova (1988) was well posed for clay rich horizons. On the other hand the lognormal distribution model of Kosugi (1996) was able adapted for the Swartland soil profile layers. Over and above, the optimization procedure as well as the application of HYDRUS-1D carries a lot of prospects in improving the knowledge on the hydraulic properties that characterise layered soils earmarked for IRWH.

Acknowledgements

Thanks to Prof. Malcom Hensley for his assistance during the laboratory desorption measurements and classification of the three soil profiles. Special thanks also to Prof. A. H. Cloot for the constructive comments and suggestions to improve the manuscript.

4.6 References

Abbasi F., Jacques, D., Simunek, J., van Genuchten, M.Th., 2003. Inverse estimation of soil hydraulic and solute transport parameters from transient field experiments: Heterogeneous soil. *Am. Soc. Of Agric. Eng.*, 46: 1097-1111.

Brooks, R. H., and Corey, A.T., 1964. Hydraulic properties of porous media. Hydrology paper no.3.Civil Engineering Dep. Colarado State University, Fort Collins, USA.

Brooks, R. H., and Corey, A. T., 1966. Properties of porous media affecting fluid flow. J. Irrig. Drain Div., *Am. Sc. Civil Eng.*, 92: 61-88.

Brunone, B., Ferrante, M., Romano, N., and Santini, A., 2003. Numerical simulations of one-dimensional infiltration into layered soils with the Richard equation using different estimates of the interlayer conductivity. *Vadose Zone J.*, 2:193-200.

Campbell, G. S., 1974. A simple method for determining unsaturated conductivity from moisture retention data. *Soil Sci.*, 117:311–314.

Chen, J., Hopmans, J. W. and Grismer, M. E., 1999. Parameter estimation of two-fluid capillary pressuresaturationand permeability functions. *Adv. Water Resour.*, 22: 479-493.

Chimungu, J. G., 2009. Comparison of field and laboratory measured hydraulic properties of selected diagnostic soil horizons. M.sc. (Agric) Dissertation, University of the Free State Bloemfontein, South Africa.

Dane, J. H., and Hopmans, J. W., 2002 . Soil Water Retention and Storage - Introduction. IN: Methods of Soil Analysis.Part 4.Physical Methods.(J.H. Dane and G.C. Topp, Eds.).*Soil Science Society of America* Book Series No. 5: 671-674.

Dane, J. H., and Hruska, S., 1983. In-situ determination of soil hydraulic properties during drainage. *Soil Sci. Soc. Am. J.*, 47:619–624.

Dirksen, C., 1999. Soil physics measurements. GeoEcology paperback, Catena Verlag GMBH, 35447 Reiskirchen, Germany.

Fraenkel, C. H., 2008. Spatial variability of selected soil properties in and between map units. M.sc. (Agric) Dissertation, University of the Free State, Bloemfontein, South Africa.

Gardner, W. R., 1956. Calculation of capillary conductivity from pressure plate outflow data. *Soil Sci. Soc. Am. Proc.*, 20:317–320.

Gupta, S.D., Mohanty, B. P., and Kohne, J. M., 2006. Soil hydraulic conductivities and their spatial and temporal variation in a vertisol. *Soil Sci. Soc. Am. J.*, 70: 1872-1881.

Hensley, M., Botha, J. J., Anderson, J. J., Van Staden, P. P., and Du Toit, A., 2000. Optimising rainfall use efficiency for developing farmers with limited access to irrigation water. Water Research Commission report, 878, Pretoria, South Africa.

Hensley, M., le Roux, P.A. L., Du Preez, C. C., van Huyssteen, C.W., Kotze, E.,and van Rensburg, L.D., 2007. Soils: The Free State's agricultural base. South African Geographical Journal, 88: 11- 21.

Hillel, D., Krentos, V. D., and Stylianou. Y., 1972. Procedure and test of an internal drainage method for measuring soil hydraulic characteristics in situ. *Soil Sci.*, 114:395-400.

Hopmans, J. W., and Simunek, J., 1999. Review of inverse estimation of soil hydraulic properties. 643–659.In M.Th. van Genuchten et al. (ed.) Characterization and measurement of hydraulic properties of unsaturated porous media. University of California, Riverside, CA.

Hopmans, J.W.,Simunek, J., Romano, N., and Durner,W., 2002. Simultaneous determination of water transmission and retention properties. Inverse Methods. IN: Methods of Soil Analysis.Part 4.Physical Methods.(J.H. Dane and G.C. Topp, Eds.). *Soil Science Society of America* Book Series No. 5: 963-1008.

Jury, W., Gardener, W.R., and Gardner, W.H., 1991. Soil Physics (5th Ed.). John Wiley and Sons, New York, USA.

Kandelous, M. M., and Simunek, J., 2010. Comparison of numerical, analytical, and empirical models to estimate wetting patterns for surface and subsurface drip irrigation. *Irrig. Sci.*, 28:435–444.

Kawamoto, K., Moldrup, P., Ferre, T. P. A., Tuller, M., Jacobsen, O. Komatsu, T., 2006. Linking the Gardner and Campbell Models for Water Retention and Hydraulic Conductivity in Near-Saturated Soil.*Soil Science*, 171: 573-584.

Kool, J. B., and Parker, J. C., 1988. Analysis of the inverse problem for transient unsaturated flow. *Water Resour. Res.*, 24: 817–830.

Kosugi, K., 1996. Lognormal distribution model for unsaturated soil hydraulic properties, *Water Resour. Res.*, 32: 2697-2703

Kosugi, K., Hopmans, J. W., and Dane, J. H., 2002. Water Retention and Storage - Parametric Models. IN: Methods of Soil Analysis. Part 4.Physical Methods.(J.H. Dane and G.C. Topp, (Eds.). *Soil Science Society of America* Book Series No. 5: 739-758.

Lamara, M., and Derriche, Z., 2008. Predictions of unsaturated hydraulic properties of dune sand on drying and wetting paths. Vol (13) Bund.B, EJGE.

Lazarovitch, N., Warrick, A.W., Furman, A., and Zerihum, D., 2009. Subsurface water distribution from furrows described by moments analyses. *J. of Irrig. and Drain. Eng.*, 135, 7-12.

Mallants, D., Mohanty, B. P., Jacques, D., and Feyen, J., 1996. Spatial Variability of Hydraulic Properties in A Multi-Layered Soil Profile. *Soil Science*, T. A., 161: 167-181.

Marion, J.M., Rolston, D. E., Kavvas M. L., and Biggar, J.W., 1994. Evaluation of methods for determining soil-water retentivity and unsaturated hydraulic conductivity. *Soil Sci.*, 58: 1-13.

Mathews, C. J., Cook, F. J., Knight, J. H., and Braddock, R. D., 2004. Handling the water content discontinuity at the interface between layered soils within a numerical scheme. Super Soil 2004: 3rd Australian New Zealand Soils Conference, 5 -9 December 2004, University of Sydney, Australia.

Mathews, C. J., Knight, F. J., and Braddock, R. D., 2004. Using analytic solutions for homogeneous soils to assess numerical solutions for layered soils. ARC Discovery Indigenous Research Development Program.C.mathews@griffith.edu.au , 31/4/ 2011, 17.00 pm, (LT).

Millington, R. J., and Quirk, J. P., 1961. Permeability of porous solids. *Trans. Faraday Soc.*, 57:1200-1206.

Mualem, Y., 1976. A new model for predicting the hydraulic conductivity of unsaturated porous media. *Water Resour. Res.*, 12:513-522.

Nhlabatsi, N. N., 2010. Soil water evaporation studies on the Glen/Boheim ecotope. Ph D. Thesis, University of the Free State, Bloemfontein, South Africa.

Pachepsky, Y. A., Timlin, D. J., and Ahuja, L. R., 1996. Estimating Saturated Soil Hydraulic Conductivity Using Water Retention Data and Neural Networks. *Soil Science*, 164: 552-560.

Russo, D., 1988. Determining soil hydraulic properties by parameter estimation: On the selection of a model for the hydraulic properties. *Water Resour. Res.*, 24:453-459.

Russo, D., Bresler, E., Shani, U., and Parker, J.C., 1991. Analysis of infiltration events in relation to determining soil hydraulic properties by inverse problem methodology. *Water Resour. Res.*, 27:1361-1373.

Schaap, M.G., and van Genuchten, M.T., 2005. A modified Mualem–van Genuchten formulation for improved description of the hydraulic conductivity near saturation. *Resour. Res.*, 41:1-12.

Schaap, M.G., Leij, F.J., and van Genuchten, M.T., 2001. Rosetta: A computer program for estimating soil hydraulic parameters with hierarchical pedotransfer functions. *J. Hydrol.*, 25:1163–176,

Scotter, D.R., Clothier, B.E., and Harper, E.R., 1982. Measuring saturated hydraulic conductivity and sorptivity using twin rings. *Australian Journal of Soil Research*, 20: 295-304.

Simunek, J., van Genuchten, M.Th., and Sejna M., 2008. Development and applications of the HYDRUS and STANMOD software packages, and related codes. *Vadose Zone J.*, 7: 587-600.

Simunek, J., and Hopmans, J.W., 2009. Modelling compensated root water and nutrient uptake. *Ecological modelling*, 220: 505-521.

Sharma, P., Shukla, M. K., Mexal, J. G., 2011. Spatial variability of soil properties in Agricultural Fields of Southern New Mexico. *Soil Science*, 176: 288-302.

Soil Classification Working Group, 1991. Soil Classification - A taxonomic system for South Africa. Memoirs on the Agricultural Natural Resources of South Africa No. 15. Department of Agricultural Development, Pretoria.

Tomasella, J., and Hodnett, M. G., 1997. Estimating Unsaturated Hydraulic Conductivity of Brazilian Soils Using Soil-Water Retention Data. *Soil Science,* 162: 703-712.

Tuli, A., Denton, M.A., Hopmans, J. W., Harter, T., and MacIntyre, J. L., 2001. Multi-step outflow experiments: from soil preparation to parameter estimation. LAWR Report No.100037.

Valiantzas, J. D., and Kerkides, D. G., 1990. A simple iterative method for the simultaneous determination of soil hydaulic properties from one-step outflow data. *Water Resour. Res.*, 26:143–152.

van Genuchten, M.Th., 1980. A closed-form equation for predicting the hydraulic conductivity of unsaturated soils. *Soil Sci. Soc. Am. J.*, 44: 892-898.

van Genuchten, M. T., Leij, F. J., and Yates, S. R., 1991. The RETC code for quantifying the hydraulic functions of unsaturated soils. Rep. EPA/600/2–91/065. R.S. Kerr Environmental Research Laboratory, USEPA, Ada, OK.

Vogel, T., and Cislerova, M., 1988. On the reliability of unsaturated hydraulic conductivity calculated from the moisture retention curve, *Transport in Porous Media, 3*: 1-15.

Wang, Z., Wu, L., Harter, T., Lu, J. and Jury, W.A., 2003. A field study of unstable preferential flow during soil water redistribution. Water Resour. Res., 39: 1075-1086.

Wilson, G.W., Fredlund, D. G., and Barbour, S. L., 1997. The effect of soil suction on evaporative fluxes from soil surfaces. *Can. Geotech. J.*, 34:145-155.

Wildnschild, D., Hopmans, J. W., and Simunek, J., 2001. Flow rate dependence of soil hydraulic characteristics. *Soil Sci. Soc. Am. J.*, 65: 35-48.

Willmotti, C. J., Ackleson, S. G., Davis, R. E., Feddema, J. J., Klink, K. M., Legates, D. R., O' Dennel, J., and Rowe, C.M., 1985. Statistics for the Evaluation and Comparison of Models. *Jour. of Geophysical Research*, 90: 8995-9005.

Wollschlager, U., Pfaff, T., and Roth, K., 2009. Field-scale apparent hydraulic parameterisation obtained from TDR time series and inverse modelling. *Hydrol. Earth Syst. Sci.*, 13: 1953–1966.

World Reference Base for Soil Resources, 1998. World soil resources report, 84, ISSS / ISRIC FAO, Rome, Italy.

Yeh, T. J., Yeh, M., and Khaleel, R., 2005. Estimation of effective unsaturated hydraulic conductivity tensor using spatial moments of observed moisture plume. *Water Res. Res.*, 41: 1-12.

Zachmann, D. W., Duchateau, P. C. and Klute, A., 1982. Simultaneous approximation of water capacityand soil hydraulic conductivity by parameter identification. Soil Sci., 134: 157–163.

Zavattaro, L., and Grignani, C., 2001. Deriving hydrological parameters for modelling water flow under field conditions. *Soil Sci. Soc. Am. J.*, 65:655-667.

CHAPTER 5

IN SITU EVALUATION OF EVAPORATION IN LAYERED SOILS (TUKULU, SEPANE AND SWARTLAND)

Abstract

Knowledge about the influence of soil layers on evaporation is essential for the optimization of in-field rainwater harvesting (IRWH) in the semi-arid areas of the Free State province of South Africa. Among the soils earmarked for IRWH development includes the Tukulu, Sepane and Swartland with the first two referred as Cutanic Luvisols and the latter as Cutanic Cambisols in other countries. In IRWH these soils are required to capture and store rainwater within the soil profile layers away from the evaporation zone. To determine how the three soils release and deliver soil water at the evaporating site, a 21 day evaporation experiment was conducted on pre-drained monoliths. Instantaneous soil water content (SWC) from *in situ* and soil water characteristic curve (SWCC) from laboratory was measured. Separate soil samples of 15 mm thickness were also evaporated under the same conditions to establish the extent of drying and hydraulic gradient at the soil surface. The Darcian evaporative flux and unsaturated hydraulic conductivity (K-coefficient) were also determined. At the surface suctions of magnitude greater than -1500 kPa were observed from all monoliths. Total contribution to evaporation from the Tukulu, Sepane and Swartland was 43, 51 and 70 mm, respectively. The low contributions were explained by the presence of the prismacutanic C-horizon in the Tukulu and Sepane at respective depths of 600 and 700 mm. This layer was associated with the steepest suction gradient that restrained further upward fluxes by subsequent lowering for the K-coefficient with more than two orders of magnitudes within a narrow range of SWC. However, the presence of the pedocutanic B-horizon at depths of 300 mm undermined this restrictive function through the appreciable capillary activity demonstrated by clays at near evaporating surfaces. The shallowness and deficiency in structure of the Swartland was consistent with the high contribution to evaporation that gave this soil a dry soil water regime. It was therefore concluded that the Tukulu offered soil profile layers that could reasonably satisfy the soil water conservation requirements for IRWH.

Key words: soil water, soil layers, evaporation, soil hydraulic characteristics

5.1 Introduction

Field water storage from infield rainwater harvesting (IRWH) cannot be optimized without evaluating the influence of soil layers on evaporation. In the absence of a crop soil, water captured by IRWH over the growing season is likely to decrease by either deep drainage or evaporation. The presence of clay rich layer at the bottom of most soils earmarked for IRWH restricts deep drainage losses (Hensley et al., 2000, Botha, 2006; Chimungu, 2009). However, information concerning the functional role of soil profile layers on evaporation is yet to be demonstrated. Losses by evaporation could exceed 50 percent of the soil water resources particularly in semi-arid areas. For example, layered soils including the Tukulu, Sepane and Swartland of the central Free State province of South Africa are subject to an annual evaporation potential of 2198 mm (Botha et al., 2007) and yet seasonal rainfall rarely exceeds 550 mm. Under these conditions the fate of the soil water balance is mainly determined by the hydraulic responses of soil profiles against the high evaporative demand (at the soil surface).

A number of variables determine the evaporation process from bare soil surfaces. Direct solar radiation and ambient air temperature provides the energy responsible for transformation of soil water to vapour state. About 590 calories of heat energy is required for every gram of water evaporated at the soil surface in a vapour state at 15°C (Hillel, 2004). The vapour could be carried away by windy conditions from the evaporating site and be replaced by drier air. In this situation a steep vapour pressure gradient could be maintained. To sustain the evaporative stream, water from neighbouring subsurface layers needs to be released and conducted to the evaporating site. In the absence of a water table contribution this capillary flux is dependent on soil water stored by the oil profile layers. Given that soil water is not freely available its release and delivery to the surface is determined by the permeability of the soil profile layers (Hillel, 2004; Wilson et al., 1997; Peters and Durner, 2008).

In drier climates evaporation is mainly characterised by the falling stage. Evaporation declines once actual evaporation falls below evaporation potential since the soil becomes too dry to deliver at the potential rate (Simunek and Hopmans, 2009). Upon de-saturation the soil surface begins to rely on the delivery of water from underlying layers, enhancing the progression of the drying front (Zeng et al., 2009).The lag time and the hysteric effect of soil water release and permeability of subsurface layers towards the advancing drying front triggers the subsequent drop in evaporation (Simunek and Hopmans, 2009). Wilson et al.

(1997) approximated that evaporation falls to constant levels once matrix suction at the soil surface falls to around -1500 kPa. Soil surface crusting in semi-arid and desert soils could limit evaporation to only the few millimetres of the soil profile (Hensley et al., 2000; Sullivan, 2002; Hillel, 2004) Soil water content within the upper 100 mm of a dried sandy loam was as low as 0.09 mm mm^{-1} with a matric suction of -1000 kPa (Leconte and Brissette, 2001). Total suctions including matric and osmotic suctions exceeded -3000 kPa at the surface of various textured soils (Wilson et al. 1997). Despite drier conditions at the surface a considerable amount of soil water remains stored within the profile (Sullivan, 2002).

Literature acknowledges the ability of clay soils to withstand the effect of temporal drying periods. Increasing matric suction attraction upon desorption is one way that clay soils restrict capillary water from being available for evaporation (Wilson et al., 1997; Wildenschild et al., 2001; Jones et al., 2009). Restricting the propagation of the drying front is another. Some clay shrinks upon drying, a phenomenon that increases the bulk density of the matrix and thus retaining much if its water (Whitmore and Whalley, 2009). In either ways the unsaturated hydraulic conductivity (K-coefficient) tends to drop by orders of several magnitudes at relatively high soil water content (SWC) (Hillel, 2004; Bohne, 2006). In a similar fashion clay soils restrict available water for extraction by crop plants roots (Whitmore and Whalley, 2009). However, opening of cracks on swelling clays may advance the drying to deeper soil profile layers (Sullivan, 2002; Grismer, 1992). In many instances the amounts available for evaporation has been modified by means of soil cover and mulching materials (Botha, 2006; Sullivan, 2002; Arlauskien et al., 2010).

Analysis of evaporation from layered soils earmarked for the development of IRWH is limited to only a few studies. Most these studies (Hensley et al., 2000; Botha, 2006; Nhlabatsi, 2010) focused on the climatic and soil surface factors influencing soil water evaporation. Under semi-arid conditions soil water evaporation occurs from unsaturated soils and available water is only controlled by the hydraulic properties of the soil profile layers. The aim of this paper was to test whether soil water evaporation differed for Tukulu, Sepane and Swartland soil profile layers. The South African Tukulu, Sepane and Swartland soil types were studied. The first two soil forms are similar to Cutanic Luvisols and the latter to Cutanic Cambisols of the World Reference Base for Soil Resources (1998). In this regard the specific objectives included; Firstly, to describe the amount of soil water available to evaporation by the soil water release curve; Secondly, to describe the delivery rate of soil water to the evaporating site by the unsaturated hydraulic conductivity function of soil profile layers; and

thirdly, to describe the evaporation flux and accumulative evaporation of the three soils with respect to their hydraulic characteristics.

5.2. Material and methods

5.2.1 Site location and soil classification

The field experiments were carried out at the Paradys Experimental Farm 29°13'24,73"S, 26°12'40,93"E, altitude 1417 m) of the University of the Free State. Three sites were selected with different soil types including a typical Swartland, Sepane, and Tukulu soil form according to the Soil Classification Working Group (Soil Classification Working Group, 1991). The total surface land area for the three soil types was about 10 ha on a straight and gentle slope of 1% with a Southerly aspect.

The three soils share a generic orthic A- horizon of a fine sandy loam with an average depth of 300 mm for the Tukulu and Sepane and 200 mm for the Swartland (Appendix A,B and C). The Tukulu has a neocutanic B-horizon with 26% clay content of sub angular structure that forms a smooth transition with the apedal massive A-horizon with 11% clay content. The prismatic C-horizon occurs at depths of 600 to 850 mm with a clay content of 48%. The Sepane has a well developed pedocutanic B-horizon with a depth of 400 mm and a clay content of 35%, and forms an abrupt transition with the surface horizon with clay content of 19%. Below the latter is the prismatic C horizon with a clay content of 45%. The Swartland constitutes a course and sub-angular blocky pedocunatic B-horizon with 22% clay content that forms a smooth transition with A- horizon with 11% clay content. The saprolite rock appears at a depth of 400 mm and is weakly weathered and has a conspicuous course appearance. The Tukulu and Swartland occupied the upland slope with the former occupying the smooth drainage lines while the Sepane occupied the down slope areas of the experimental site.

5.2.2 Soil water characteristic curve

The plot of SWC versus matric soil is referred as the soil water characteristic curve (SWCC) (Fredlund, 2006) or release curve (Whitmore and Whalley, 2009). The curve provides a measure of soil water available for desorption or the amount of water to be released at a given matric suction i.e. the θ-h relationship. The SWCC was measured from a laboratory desorption experiment involving three phases from 0 to -10 kPa, -10 to -100 kPa and -100 to -1500 kPa. Corresponding to these phases are the regions of saturation that characterise the

SWCC known as the boundary effect, transitional and residual zones (Fredlund, 2006). The θ-h relationship for the first and second phases were determined from undisturbed core soil samples using the hanging soilwater column (Dirksen, 1999) and pressure plate chambers, respectively. Samples for lower matric potentials were disturbed and packed in triplicate at the measured bulk densities using 2000 mm^3 PVC tubes. Disturbance was carried out because desorption at higher suction is not dependent on connective structural pores, but rather on textural pores (Hillel, 2004). Soil samples were weighted after each and every step of desorption until the retention characteristic was completed.

5.2.3 Determination of actual evaporation

The evaporation experiment for Sepane and Tukulu was carried out on 4 m x 4 m monoliths with a depth of 1 m. Monoliths were prepared in triplicate attached to each other and three neutron access tubes centrally installed to a depth 1.1 m. On the Swartland it was more convenient to prepare 1.2 m x 1.2 m monoliths of 0.5 m depth, detached and 30 m apart given the challenges encountered in digging the trenches. Special DFM probe loggers were inserted to a depth of 0.6 m with soil water sensors at corresponding depths of 100, 300 and 550 mm. Lateral sides of monolith trenches were isolated with plastic sheets to prevent lateral water movement. An earth bund around the monoliths was prepared to prevent surface runoff and support ponding during the soaking of the profile with water. After deep wetting the profile surfaces were sealed from evaporation influences with a polythene sheet. The soil profiles were allowed to drain and SWC measured with a Neutron water meter until the change in soil water storage was negligible a stage referred as the drainage upper limit (DUL). Once DUL was realised it was assumed that all macro-pores sensitive to gravitational head were desorbed and the remaining soil water represented capillary and adsorbed water content (Hensley et al., 2000; Nhlabatsi, 2010). Monoliths were then opened to the atmosphere to encourage further drying of the soil profile through the evaporation process. Instantaneous soil water measurement were made using a neutron water probe (NWP) at 200 mm, 500 mm, 850 mm and 1100 mm depth intervals for a period of 21 days. The first week measurements were taken in mornings and evenings and then daily for the rest of the trial. The DFM probes were set to take readings every hour. Drying properties of the soil surface from the three soils was determined using an evaporation test on a thin soil surface section of about 15 mm thickness set under the same in-situ environment. Triplicate samples were weighed daily to determine gravimetric SWC. Measurements were stopped once the thin layer had dried to almost a constant gravimetric soil water measurement.

5.2.4 Data processing and analysis

5.2.4.1 Soil water characteristic curve

The plotted SWCC was subdivided into the three degrees of saturation with more emphasis on the mid-section that denotes the transitional zone. This section was able to describe the soil water release during the evaporation process. A regression function was used to transfer the θ-h relationships from the SWCC to *in situ* SWC measurements.

5.2.4.2 Estimation of evaporative flux

The upward flux per unit depth (Z) towards evaporating surface was depicted by the mathematical expression:

$$q_{ev}(z,t) = \left\{ {}^{\partial\theta}/_{\partial t} \right\} \qquad (5.1)$$

Where q_{ev} is the evaporative flux (mm hour^{-1}), θ is volumetric soil water content (mm mm^{-1}), t is the daylight time (12 hours) and Z is the reference depth (mm) of the soil layer subject to evaporation.

5.2.4.3 Estimation of unsaturated hydraulic conductivity

The unsaturated hydraulic conductivity (K-coefficient) was calculated using the instantaneous profile procedure as described by (Hillel, 2004).

The flux expression (Eq. 5.2) was then fitted to the extended Darcian law to give K-coefficient as function of SWC (θ) for each respective soil profile horizon to be:

$$K(\theta)(Z,t) = \frac{q_{ev}}{\left\{ {}^{dh}/_{dZ} - 1 \right\}} \qquad (5.2)$$

Where K (θ) is K-coefficient (mm hour^{-1}), dh is the change in matrix suction (mm) between the evaporating surface and the soil layer in question of thickness Z (mm). Since flow was in upward direction the negative sign was used, and t as defined in equation 2. Evaporative flux (q_{ev}) was described by a positive hydraulic gradient and when negative or meaningless gradients were observed on particular sections of the flow domain the unity gradient was employed as described by Yeh et al. (1985). The classical exponential equation proposed by Hillel et al. (1972) was used to obtain a linear regression function on a semi-log scale for the plotted K-θ relationships.

5.2.4.4 Statistical analysis

Soil water characteristic curves and K-coefficients pertinent to the evaporation process after DUL was realised were described using regression functions. The quality of fit of the regression was estimated by the coefficient of determination (R^2). Homogeneity between horizon regression coefficients was evaluated using the Bartlett's test or chi-square ($\chi 2$) distribution and pooled regression coefficient F tests as described by Gomez and Gomez (1984). A Student's t-test was also used to identify horizons with comparable regression coefficients. Regression coefficients were regarded to have failed the homogeneity test if computed values were greater than tabular values at 95 % confidence interval.

5.3 Results

5.3.1 Soil water characteristic curves

Figure 5.1 shows the variations of the θ-h relationship on the SWCC from the A, B and C-horizons of the Tukulu, Sepane and Swartland soil types, respectively. The subdivisions of 0 to -3 kPa, -3 to -100 kPa and -100 to -1500 kPa were more applicable in describing the SWCC of these soils. Soil water activities that are of importance to the soil water balance of cultivated fields normally occur within the 0 to -100 kPa suction range. The -100 to -1500 kPa is referred as the residual zone because of the SWC in this range being unproductively low for most economic crops. Consistent with the -3 to -100 kPa matric suction range results coincided with the de-saturation during the evaporation experiment. The relationship established the in-situ suction boundary conditions and Table 5.1 outlines the resulting θ-h regression functions and coefficient of determination for each of the three soil horizons. Table 5.2 presents the corresponding Student t-test analysis for the differences between soil horizons regression coefficients.

Water available for desorption between 0 and 100 kPa varied among soils and horizons. In the Tukulu soil the A and B-horizons had a change in SWC ranging from 0.328 to 0.16 and 0.325 to 0.17 mm mm^{-1}, respectively. The C-horizon desorbed from 0.324 to 0.29 mm mm^{-1}. Under *in situ* conditions the amounts available for desorption corresponded to 50, 47 and 8.5 mm for the A, B and C-horizons respectively. In the Sepane desorption effected a release from 0.33 to 0.17, 0.335 to 0.22 and 0.338 to 0.24 mm mm^{-1} for the respective A-, B- and C-horizons.

(a)

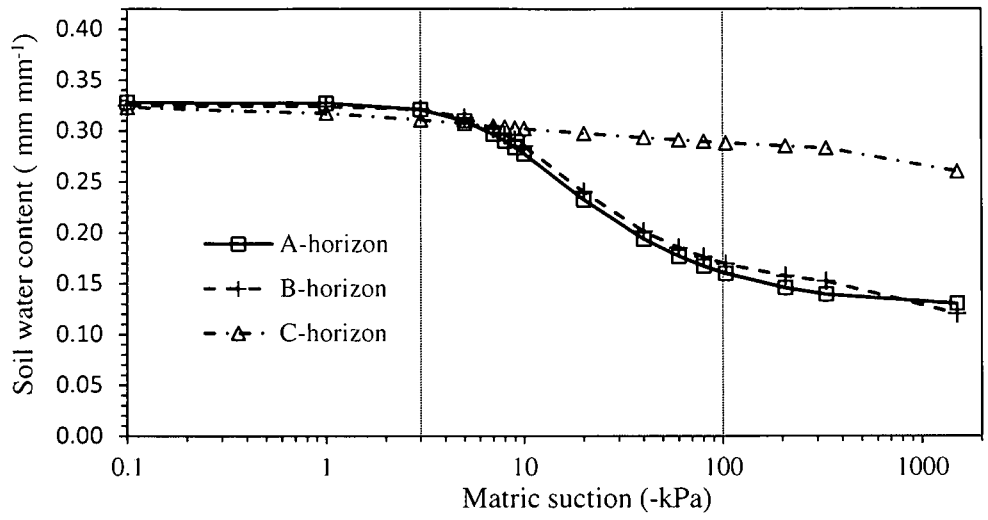

(b)

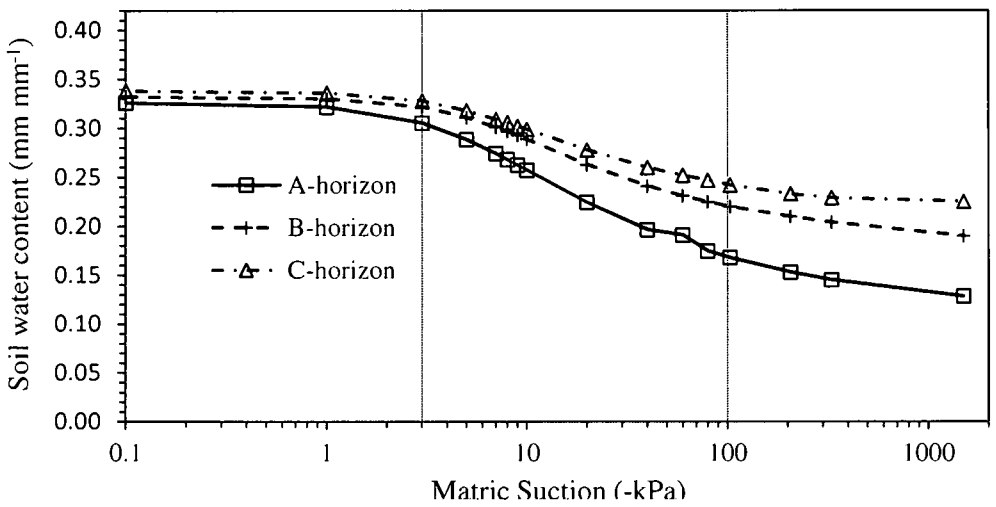

(c)

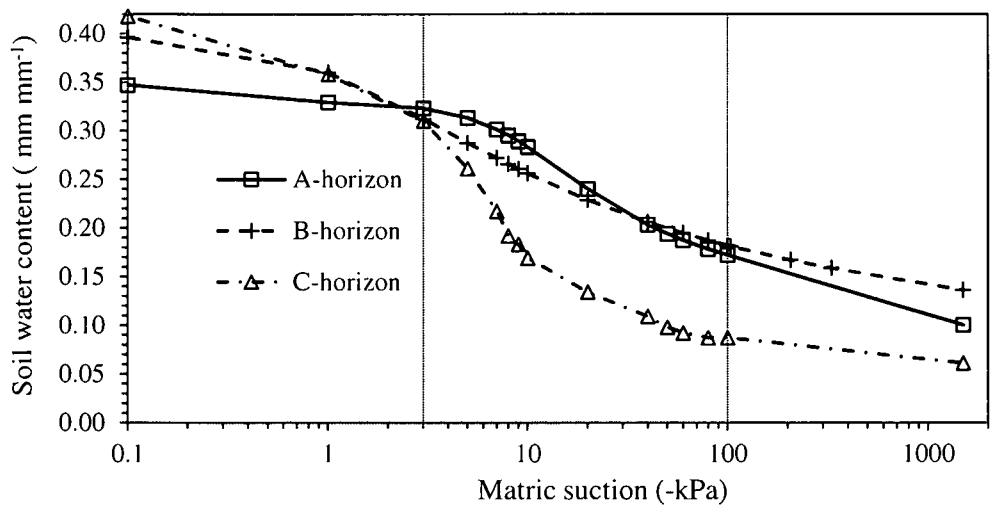

Figure 5.1 θ-h relationship curves for the (a) Tukulu, (b) Sepane and (c) Swartland soil forms.

The amount of water released under *in situ* conditions corresponded to 48, 46 and 20 mm for the A, B and C-horizons, respectively. The Swartland released water from 0.35 to 0.17, 0.39 to 0.18 and 0.42 to 0.087 mm mm^{-1} from the respective A, B and C-horizons. These amounts corresponded to 36, 42, and 100 mm of soil water available for desorption under *in situ* conditions.

The θ-h relationships for the -3 to -100 kPa matric suction range was regressed using a power function that yielded a coefficient of determination that was good for all the soil horizons (> 0.98). Student's t-test captured that the regression coefficients from the A and B-horizons were significantly different from the Tukulu soil C-horizon while all horizons from the Sepane and Swartland were not significantly different.

Table 5.1 θ-h regression functions of soils horizons for the 10 -100 kPa matric suction range.

Soil type	Horizons	Regression	R^2
Tukulu	A	$\theta = 0.466\ h^{-0.23}$	0.99
	B	$\theta = 0.463\ h^{-0.22}$	0.99
	C	$\theta = 0.317\ h^{-0.02}$	0.99
Sepane	A	$\theta = 0.388\ h^{-0.18}$	0.99
	B	$\theta = 0.379\ h^{-0.12}$	0.99
	C	$\theta = 0.369\ h^{-0.09}$	0.99
Swartland	A	$\theta = 0.456\ h^{-0.21}$	0.99
	B	$\theta = 0.364\ h^{-0.15}$	0.99
	C	$\theta = 0.419\ h^{-0.36}$	0.98

Table 5.2 Student's t-test for differences between soil horizons regression coefficients.

Soil type	Horizons	Pooled variance	Tabulated Variance $T_{\alpha:0.05}$
Tukulu	AB	0.13^{ns}	2.26
	BC	6.13	2.26
	AC	6.13	2.26
Sepane	AB	1.25^{ns}	2.26
	BC	0.96^{ns}	2.26
	AC	2.17^{ns}	2.26
Swartland	AB	1.40^{ns}	2.26
	BC	1.60^{ns}	2.26
	AC	0.47^{ns}	2.26

ns= not significant at 0.05 Student t-test

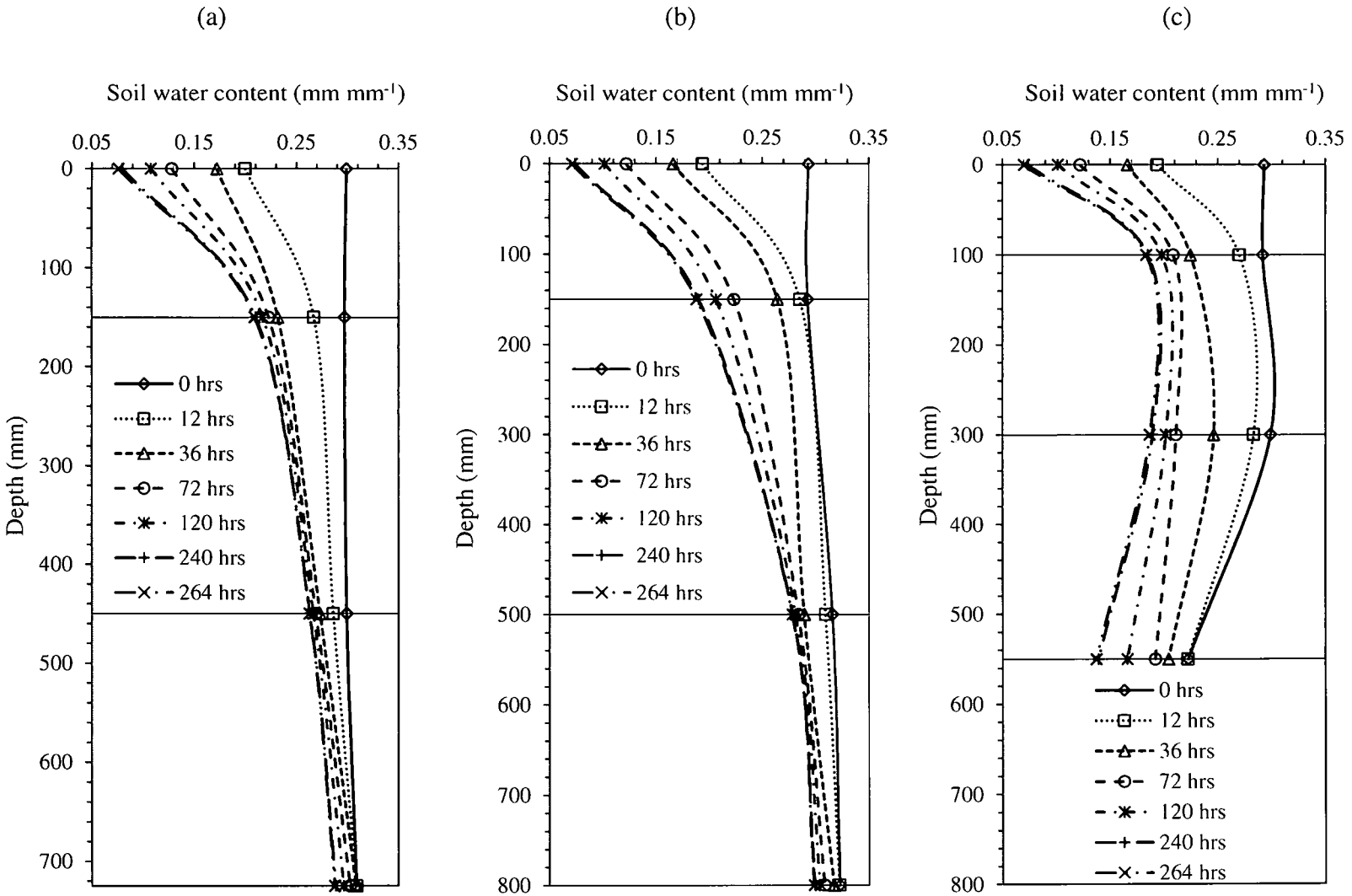

Figure 5.2 Change in soil water content during the evaporation period for the (a) Tukulu, (b) Sepane and (c) Swartland soils.

5.3.2 Change in profile water content during evaporation

Figure 5.2 shows the variation in soil water content from the near surface to deeper profile layers during the 264 hour evaporation period. Allowing the three soils to drain to DUL appeared to have given the profiles a more uniform soil water gradient (SWG) prior to the evaporation experiment. However, this changed as the SWG showed a decline with depth as available water for evaporation became less available.

Inter-block initial SWC from the Tukulu profile was about 0.30 mm mm^{-1} from the surface to a depth 450 mm while at 725 mm it was 0.31 mm mm^{-1}. Within 36 hours of evaporation the SWC at the surface was about 0.17 mm mm^{-1} while at the bottom layer changes were insignificant. At the end of the 264 hours evaporation period SWC had changed from 0.30 to 0.08 mm mm^{-1} at the surface, 0.30 to 0.21 mm mm^{-1}at 150 mm depth, 0.30 to 0.26 mm mm^{-1} at 450 mm and 0.31 to 0.29 mm mm^{-1} at 725 mm.

Soil water content from the Sepane profile had stabilised at 0.29 mm $mm^{-1}$from the surface to 150 mm depth and about 0.32 mm $mm^{-1}$from 500 and 800 mm depths prior to evaporation. Within 36 hours of evaporation the SWC at the surface was 0.17 mm mm^{-1} while consecutive depths recorded 0.26, 0.29 and 0.32 mm mm^{-1}. By the end of the 264 hours the SWC had changed from 0.29 to 0.07 mm mm^{-1} at the soil surface while at depths of 150, 500 and 800 mm recorded changes from 0.29 to 0.19, 0.32 to 0.28 and 0.32 to 0.30 mm mm^{-1}, respectively.

The Swartland profile exhibited greater uniformity within its upper horizons with initial SWC recording 0.29 from the surface to 150 mm depth. At 300 and 450 mm depth a respective 0.30 and 0.22 mm mm^{-1} was recorded. After 36 hours of evaporation the corresponding amounts with respect to depth were 0.17, 0.22, 0.25 and 0.22 mm mm^{-1}. At the end of the evaporation period SWC had changed from 0.29 to 0.07 at the soil surface, 0.29 to 0.18 at 150 mm depth, 0.30 to 0.19 at 300 mm depth and 0.22 to 0.20 at 450 mm depth.

5.3.3 K-θ relationships of soil horizons

Figure 5.3 shows the variation in K-θ relationship from the time the three soil profiles reached DUL and were opened to evaporate until 264 hours. Table 5.3 presents the resulting K-θ relationship linear regression functions from the A, B and C-horizons of the Tukulu, Sepane and Swartland soils.

(a)

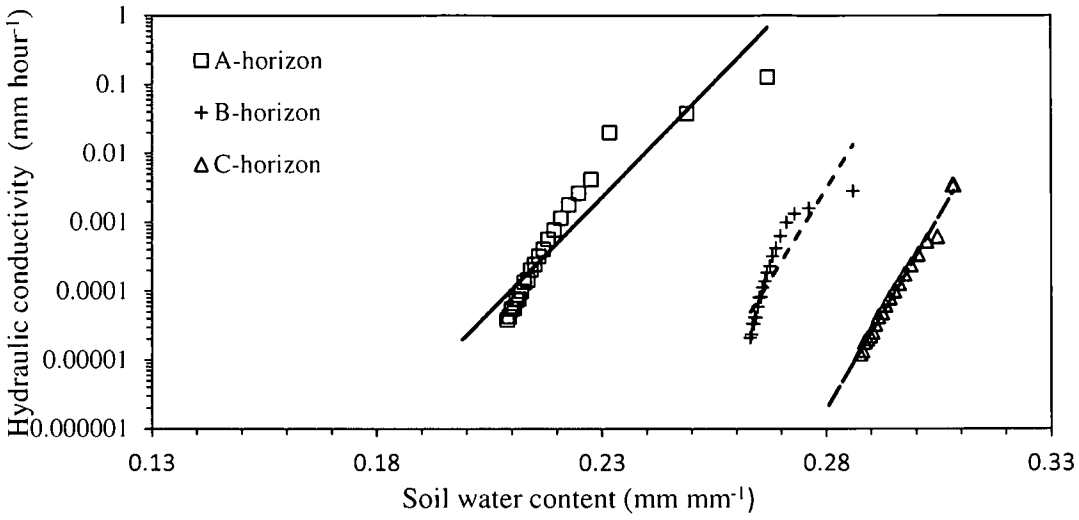

(b)

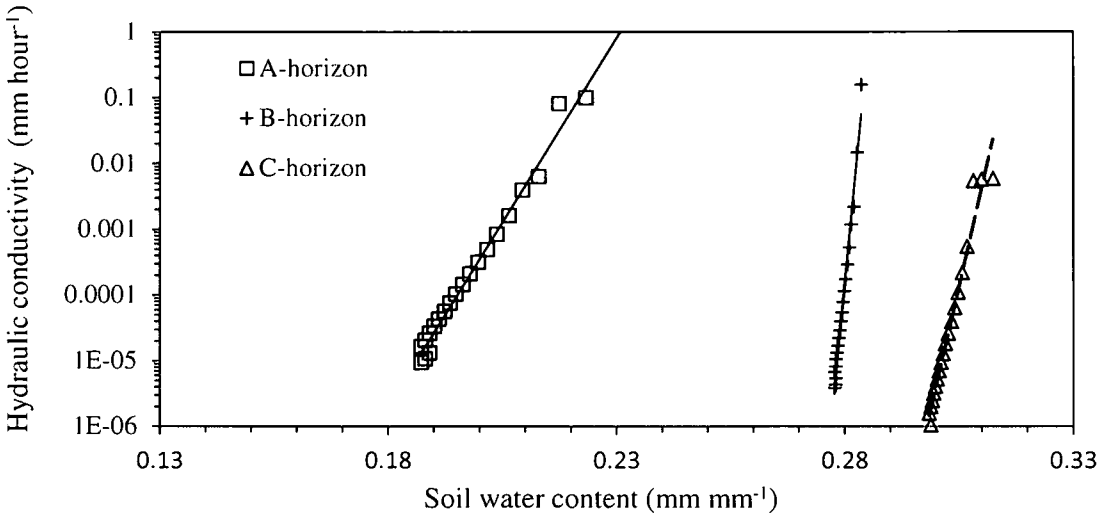

(c)

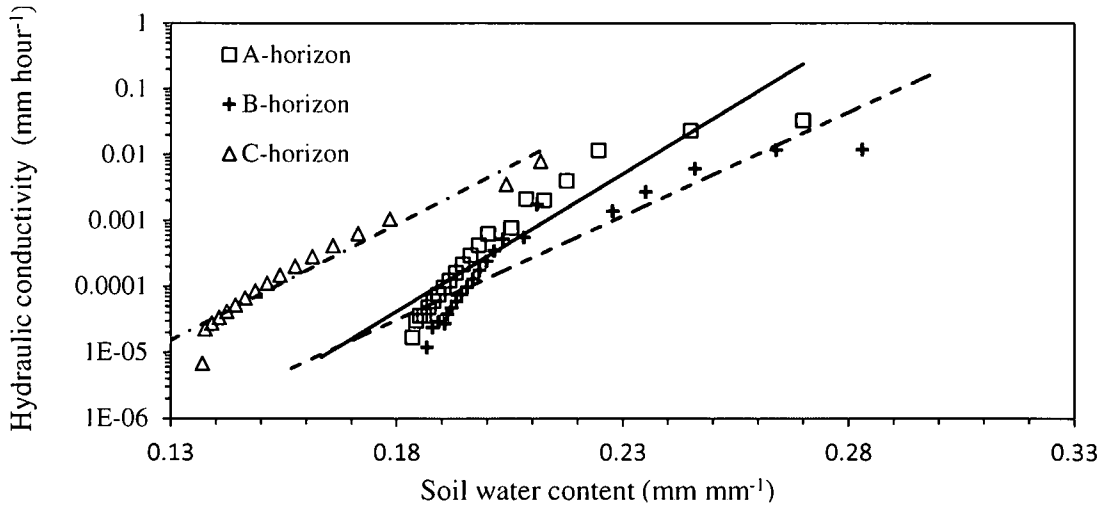

Figure 5.3 K-θ-relationship from the (a) Tukulu, (b) Sepane and (c) Swartland soil.

In all three soils the K-θ relationship from the A-horizon covered a wider range of the SWC than the deeper B and C-horizons indicating steepening K-θ relationship with depth during the evaporation process.The corresponding statistical test of homogeneity and Student t-test for the comparison of regression coefficients between profile layers were shown in Tables 5.4 and 5.5, respectively. The accumulative and flux rate of evaporation shown in Table 5.6 and Figure 5.4 respectively portrays the evaporation process from the Tukulu, Sepane and Swartland soil layers.

The Tukulu had K-coefficients that ranged from 0.1 to 0.00004, 0.003 to 0.00002 and 0.004 to 0.00001 mm hour^{-1}, from the respective A, B and C-horizons. The K-θ relationships were regressed using a semi log linear exponential function that had a coefficient of determination that was good for all horizons (>0.83). Failure of the Bartlett's homogeneous test was consistent with pooled variance regression coefficient analysis.

Table 5.3 K-θ relationships linear regression functions for the three soil types.

Soil type	Horizon	Regression	R^2
Tukulu	A	Log K = 46.52(θ) - 13.67	0.83
	B	Log K = 220.80(θ) - 62.57	0.97
	C	Log K = 111.7(θ) - 37.01	0.99
Sepane	A	Log K = 48.41(θ) - 13.86	0.97
	B	Log K = 320.9(θ) - 94.43	0.98
	C	Log K = 111.2(θ) - 39.08	0.99
Swartland	A	Log K = 41.75(θ) - 11.89	0.87
	B	Log K = 35.67(θ) - 11.03	0.91
	C	Log K = 34.14(θ) – 9.26	0.94

The Sepane had K-coefficients that ranged from 0.1 to 0.00001, 0.2 to 0.000004 and 0.01 to 0.000001mm hour^{-1}, from the respective A, B and C-horizons. The quality of fit of the corresponding regression function was good for all horizons (>0.97). Significant differences were found by both Barttlets and pooled variance analysis among horizons. However, the student's test confirmed similarity in regression coefficients between the B and C-horizons.

The Swartland evaporation process effected a K-coefficient ranging from 0.033 to 0.00002, 0.012 to 0.00001 and 0.008 to 0.00001 mm hour^{-1}, from the respective A, B and C-horizons. On the semi-log scale the exponential regression function had a good fit for all horizons (> 0.87). Bartlett's homogeneity test failed to capture significant differences among the horizon

regression coefficients while the pooled variance showed significant differences. A clearer analysis was provided by the Student's t-test that indicated regression coefficients between B and C horizons were not comparable.

Table 5.4 Homogeneity test for the K-θ relationships of the horizons of the three soils.

	Bartlett's test		Regression coefficient	
Soil types	Computed$\chi 2$	Tabular $\chi 2$; $_{0.05,2}$	Computed F	Tabular F;$\alpha_{0.05,2;57}$
Tukulu	6.92	5.99	328.48	3.15
Sepane	11.168	5.99	33.546	3.15
Swartland	0.348^{ns}	5.99	5.367	3.15

Table 5.5 Student's t-test for the regression coefficient comparison between horizons.

Soil type	Horizons	Pooled variance	Tabulated variance $T_{\alpha;0.05}$
Tukulu	AB	25.63	2.02
	BC	7.03	2.02
	AC	15.54	2.02
Sepane	AB	5.74	2.02
	BC	0.22^{ns}	2.02
	AC	7.67	2.02
Swartland	AB	2.07	2.02
	BC	1.24^{ns}	2.02
	AC	3.38	2.02

5.4 Discussion

Given that the soil profiles were already desorbed to DUL at the onset of evaporation, the drying process represented the emptying of capillary or meso-pores. Soil water release and availability from this group of pores is controlled by matrix suction activity that is dependent on soil texture and structure. Under these conditions available water is limited and its release is dependent on the soil hydraulic characteristics rather than climatic parameters and hence, the falling stage of evaporation.

(a)

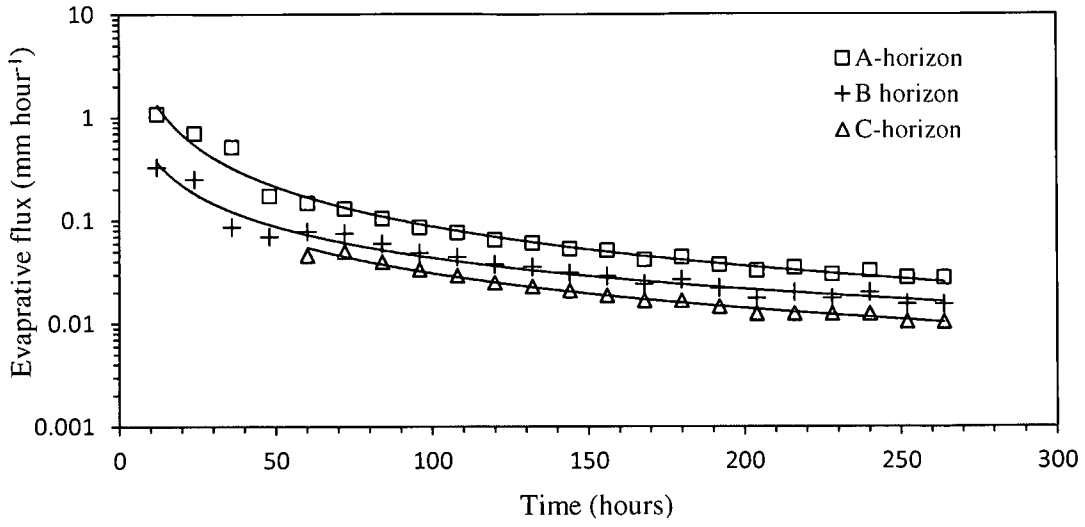

(b)

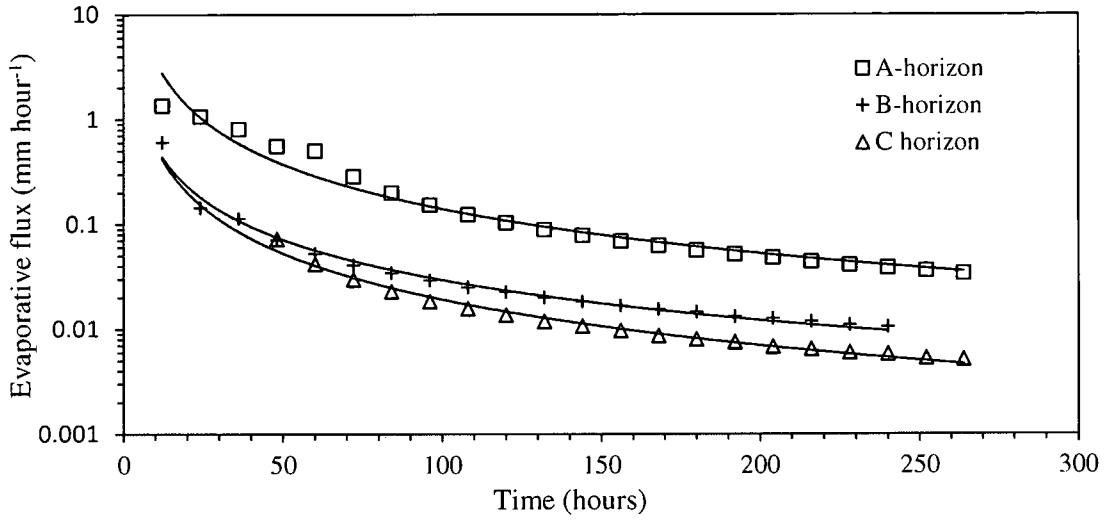

(c)

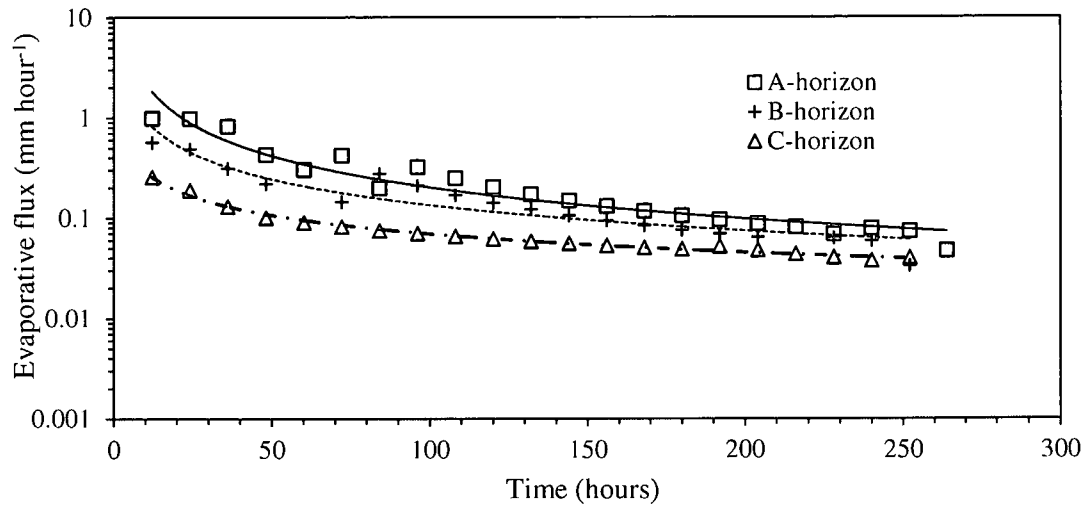

Figure 5.4 Evaporative flux from the (a) Tukulu, (b) Sepane and (c) Swartland soil layers.

Table 5.6 Accumulative evaporation from the soils horizons and profile.

Accumulative depth of water (mm) lost to evaporation at particular time (hrs) intervals								
Soil type	Horizons	12	36	72	120	240	264	Total %
Tukulu	A	9.05	19.61	22.34	24.05	26.15	26.45	61.96
	B	3.91	7.81	9.04	9.79	10.78	10.90	25.53
	C	0.038	0.19	1.64	3.16	5.09	5.34	12.50
	Profile	12.99	27.60	33.01	37.00	42.01	42.68	
Sepane	A	2.24	8.56	20.76	25.83	30.72	31.31	61.18
	B	2.64	10.61	12.82	13.86	14.92	15.06	29.42
	C	0.10	1.13	2.86	3.71	4.69	4.81	9.40
	Profile	4.98	20.30	36.44	43.40	50.33	51.18	
Swartland	A	4.35	13.44	16.65	18.74	21.33	21.66	31.08
	B	3.16	10.56	17.57	19.46	21.92	22.43	32.18
	C	0.11	5.47	9.17	16.95	25.01	25.61	36.75
	Profile	7.63	29.47	43.39	55.15	68.26	69.71	

*Total % = propotional contribution to total soil profile evaporation by horizons.

The amount of soil water made available during the 264 hour evaporation period varied among soils and horizons. An amount of 43, 51 and 70 mm was accounted to accumulative evaporation from the Tukulu, Sepane and Swartland soil profiles. This result reflects the different influences the soil profile horizon layers had on evaporation. The surface orthic A-horizon was generic to all three soils and it was reasonable to assume that it had a common effect on evaporation (Hensley et al., 2000).

Presence of the prismacutanic C-horizon in the Tukulu and Sepane with a clay content of 48 and 45 percent, respectively could explain the low evaporation recorded from these soils. The C-horizon was found at 600 to 850 mm depth in the Tukulu and at 700 to 900 mm depth in the Sepane. The Sepane also had a pedocutanic B-horizon with 35 percent clay at depths of 300 to 700 mm in contrast to the Tukulu that had neocutanic B-horizon of fine sandy clay loam at 300 to 700 mm depth. This contrast in layering within the midsection of the profile explained the greater capillary activity that resulted in a higher evaporation loss from the Sepane compared to the Tukulu. Botha et al. (2006) also observed that soils with a clay rich layer near the soil surface were susceptible to high evaporation losses. However, soil water retained by restrictive clay layer at depths below 300 mm was hardly affected by temporal drying spells (Botha et al., 2007; Hillel, 2004; Whitmore and Whalley, 2009).

One aspect of the heavy structure of clay rich horizons is the ability to restrict the progression of drying front. The steep SWG observed from the Tukulu and Sepane supports this notion. The SWC from the prismacutanic C-horizon of these soils remained unchanged for the first 72 hours of evaporation, pointing to the time equivalent to the propagation of the drying front at this depth. The drying front took approximately 36 hours to reach the saprolite C-horizon at depth of 400 mm indicating the structural deficiency of Swartland. Consistent with the high evaporation was the nearly uniform SWG that stretched to deeper layers of this soil profile. The different drying regimes resulting from the lag time of the drying front from the Tukulu and Sepane soil profiles was illustrated by the 60, 30 and 10 percent contributions to total evaporation from the respective A, B and C-horizons. This skewed distribution of total evaporation with depth was in agreement with the hypothetical shape of the drying front illustrated by Hillel (2004).

Although the distribution of SWG with depth was consistent with the amounts contributed by horizons to evaporation it could not explain the process. Within the first 12 hours of evaporation SWC from the bare soil surfaces dropped from 0.3 to 0.2 mm mm^{-1} from the Tukulu and 0.29 to 0.19 mm from the Sepane and Swartland. Corresponding matric suction increased from -6.59 to -36.76, -4.38 to -43.17 and -7.75 to -52.32 kPa from the respective Tukulu, Sepane and Swartland. By the end of the evaporation period, SWC at the surface was around 0.07 mm mm^{-1} with corresponding matric suctions of -2231.15, -10965.39 and -5708.84 kPa from the Tukulu, Sepane and Swartland, respectively. The greater suctions from the Sepane were attributed to the higher clay content of 19 percent in the A-horizon compared to 11.3 percent from its counterparts. Nevertheless these matric suctions fell in the same category to those recorded by Wilson et al. (1997). The resulting hydraulic gradient was in agreement with the upward evaporative flux. Steep gradients were associated with the prismatic C-horizons and pedocutanic horizons with the steepest recorded for the Sepane. This was not surprising because of the greater affinity of clay soils for water (Whitmore and Whalley, 2009).

This phenomenon was also illustrated by the θ-h relationship from the horizons whereby a within a narrow range of SWC the matric suction increased by more than two orders of magnitude. Similar observations on clay rich horizons were made by Chimungu (2009) and Nhlabatsi (2010). Therefore, the steep gradients of the K-θ relationships shown by subsurface horizons especially from the Tukulu and Sepane were expected. Of interest was that the K-coefficients at the onset of evaporation were greater than the final values attained during the

draining of these profiles (results not shown). This suggests that the orientation of pores towards drainage and evaporation was accountable to different hydraulic gradients. The complexity of this phenomenon could be explained by the non isotropic nature of the K-θ relationships especially in layered soils (Hillel, 2004). Beyond 0.001 mm hour^{-1}, the SWC irrespective of depth showed very little change from the three soils. However, this coefficient was attained at different times and flux rates suggesting that the release and delivery rate of water at the evaporating site varied among the profiles. Noticeable from the three soils was also the failure of the K-θ relationship from upper horizons to follow a straight line on the semi-log coordinate system. This was not strange given the interaction of high evaporative demand of the atmosphere and the soils desorption restrictive responses at the surface. The diurnal and hysteric nature of the movement of liquid and vapour near the evaporating surface have been recognised to be sources of non-linearity in this regard (Hillel, 2004; Gupta et al., 2006). Also the diffusive nature of evaporation near the surface especially on course textured soils (Hillel, 2004) could be responsible for the lower but still acceptable goodness of fit from all surface horizons. Given the coarseness of the Swartland horizons it could therefore be understood why the K-θ relationship exhibited greater non-linearity and a fit that was lower than its counterparts.

5.5 Conclusions

The effect of soil horizon layers on soil water evaporation from pre-drained Tukulu, Sepane and Swartland soil profiles was evaluated. The amount and rate of evaporation was found to differ among the three soil profiles under the same climatic conditions. The Tukulu profile with a distinct prismatic C-horizon contributed 43 mm to evaporation during the 264 hour period. The Sepane with dual clay-rich layers in the pedocutanic B and prismatic C-horizon contributed 51 mm while the Swartland with youthful horizons contributed 70 mm for the same period. Correspondingly the slopes of the θ-h and K-θ relationships from the clay-rich horizon layers had a steeper gradient for a narrow change in SWC. This was consistent with literature about the hydraulic properties of clay soils and based on this finding the Tukulu had the least contribution to soil water evaporation. In this regard the layering of the Tukulu soil profile horizons could be regarded to be appropriate for the development of IRWH and with careful considerations in design, especially those that enhance early ground cover, soil water evaporation could be further be reduced.

Acknowledgements

We acknowledge the technical support rendered by the management and staff of Paradys experiment station. Special thanks also to Ms. Liesl van der Westhuizen for her constructive suggestions on improving the writing of this manuscript.

5.6 References

Arlauskiene, A., Maiksteniene, S. and Slepetiene, A., 2010. Effect of cover crops and straw on the humic substances in the clay loam Cambisol. *Agronomy Research*, 8:397-402.

Bohne, K., 2006. An introduction into applied soil hydrology. Catena Verlag GMBH, Reiskrechen, Germany.

Botha, J. J., 2006. Evaluation of maize and sunflower production in a semi-arid area usingin-field rainwater harvesting. Ph.D. (Agric) Dissertation, University of the Free State, Bloemfontein, South Africa.

Botha, J. J. Anderson, D. C., Groenewald, N., Mdibe N., Baiphethi, M.N., Nhlabatsi, N. N. and Zere, T.B., 2007. On-farm application of In-field rainwater harvesting techniqueson small plots in the central region of South Africa. Water Research Commission, Report, TT 313/07, Pretoria, South Africa.

Chimungu, J. G., 2009. Comparison of field and laboratory measured hydraulic properties of selected diagnostic soil horizons. Master's (Agric) Dissertation, University of the Free State, Bloemfontein, South Africa.

Dirksen, C., 1999. Soil physical measurements. Geo-ecology paperback, Catena verlag GMBH, 35447, Reiskirchen, Germany.

Fredlund, D.G., 2006. Unsaturated soil mechanics in engineering practice. *Journal Geotechnical and Geo environmental Engineering*, 132: 286-321.

Gomez, K.A. and Gomez, A.A., 1984, Statistical procedures for agricultural research, 2nd ed., A Wiley-Inter-science Publication, New York, USA.

Grismer, M. E., 1992. Cracks in irrigated clay soil may allow some drainage. *California Agriculture,* 46: 9-11.

Gupta., S.D. and Mohanty, B. P. and Köhne, J. M., 2006. Soil hydraulic conductivities and their spatial d temporal variations in a vertisol.*Soil Science Society of America Journal*, 70: 1872-1881.

Hensley, M., Botha, J. J., Anderson, J. J., van Staden, P. P. and DuToit, A., 2000. Optimisingrainfall use efficiency for developing farmers with limited access to irrigation water, Water Research Commission report 878/1/00, Pretoria, South Africa.

Hillel, D., 2004. Introduction to environmental soil physics, Academic Press, New York, USA.

Hillel, D., Krentos, V. D. and Stylianou, Y., 1972. Procedure and test of an internal drainage method for measuring soil hydraulic characteristics *in situ*, *Soil Science*, 114: 395-400.

Jones, E.W., Koh, Y. H., Tiver, B. J., Wong, M. A. H., 2009. Modelling the behaviour of unsaturated, saline clay for geotechnical design, School of Civil Environment and Mining Engineering, University of Adelaide, Australia.

Leconte, R. and Brissette, F. P., 2001. Soil moisture profile model for a two-layered soil basedon sharp wetting front approach, ASCE. *Journal of Hydrologic Engineering,* 6:141-149.

Nhlabatsi, N. N., 2011. Soil water evaporation studies on the Glen/Boheim ecotope, Ph.D. (Agric) Dissertation, University of the Free State, South Africa.

Peters, A. and Durner, W., 2009. Simplified evaporation method for determining soil hydraulic properties. *Journal of Hydrology*, 356:147-162.

Simunek, J. and Hopmans, J. W., 2009. Modelling compensated root water and nutrient uptake. *Ecological modelling,* 220: 505-521.

Soil Classification Working Group, 1991. Soil Classification: A taxonomic system for South Africa. Memoirs on the Agricultural Natural Resources of South Africa No. 15, Department of Agricultural Development, Pretoria, South Africa.

Sullivan, P, 2002. Drought resistant soil, Agronomy Technical Note, National Centre for Appropriate Technology.www.attra.ncat.org, 11/06/2011.

Whitmore, A. P. and Whalley,W. R., 2009.Physical effects of soil drying on roots andcrop Growth.*Journal of Experimental Botany*, 60: 2845-2857.

Wildenschild, D., Hopmans, J. W. and Simunek, J., 2001. Flow rate dependence of soil hydraulic characteristics. *Soil Science Society of America Journal*, 65: 35-48.

Wilson, G. W., Fredlund, D.G. and Barbour, S.L., 1997. The effect of soil suction on evaporative fluxes from soil surfaces. *Canada Geotechnical Journal,* 34: 145-155.

World Reference Base for Soil Resources, 1998. World soil resources report, 84, ISSS / ISRIC FAO, Rome, Italy.

Yeh, T. C. J., Gelhar, L.W. and Gutjahr, A. L., 1985. Stochastic analysis of unsaturated flow in heterogeneous soils, 2. Statistically anisotropic media with variable xa. *Water Resources Research*, 21: 457-464.

Zeng, Y., Su, Z., Wan, L., Yang, Z., Zhang, T., Tian, H., Shi, X., Wang, X. and Cao, W., 2009. Diurnal pattern of the drying front in desert and its application for determining the effective infiltration. *Hydrology and Earth System Science,* 13: 703-714.

CHAPTER 6

DETERMINING THE OPTIMUM INFLOW RATES FOR MICRO-FLOOD IRRIGATION ON THE TUKULU SOIL

Abstract

The dependence of micro flood irrigation (MFI) on small inflow rates was evaluated on 90 m closed ended furrows in the South African Tukulu soil also referred as Cutanic Luvisols in other countries. A single irrigation was used to characterise the surface and subsurface soil water distribution from the 20, 40, 80 and 160 L min^{-1} inflow rates treatments at every 10 m distance intervals starting at 5 m from the inlet. Neutron access tubes were installed at these stations to a depth of 1 m. The HYDRUS-2D software was also used to predict the initial and final soil water content. Surface water distribution from the 20 L min^{-1} sustained the advance stream up to 60 m furrow length while from other treatments it reached the end. Agreements between measured and predicted soil water content were fairly good although inconsistencies due to spatial variations were to be expected. Effect of horizons layers was also observed through discontinuities in subsurface water distribution. Distribution uniformity at longer furrow distances was highest from the 80 and 160 L min^{-1} with the 29 and 40 L min^{-1} recorded similar performances at shorter distances. Given the practicality and flexibility of working with small inflow rates, it was suggested that the 40 L min^{-1} inflow rate be adopted for furrow distances of less than 60 m.

Key words: Furrow irrigation, Inflow rates, Infiltrated depth, HYDRUS-2D, Distribution uniformity.

6.1 Introduction

Dependence of micro flood irrigation (MFI) on small inflow rates has made the achievement of high application efficiencies comparable to pressured systems a reality in furrow irrigation. Because furrow irrigation relies on the soil surface to convey and distribute water it has been associated with poor distribution uniformity and inefficient water losses through deep drainage and tail end runoff. Given the growing water scarcity and food insecurity in many developing countries inefficient irrigation practices could no longer be acceptable. Advances in technological breakthroughs have brought remarkable improvement in furrow irrigation but very few of these have been sustainable among the rural farming communities where this method is widely practiced.

In principle furrow irrigation is said to have attained high application efficiencies when the infiltrated depth from the inlet to the furrow end is almost uniform. For this condition to be realised the stream flow and opportunity time during irrigation should be about the same along the furrow length. Practically this is not possible given that the inflow begins to infiltrate at the inlet and if it not large enough it could go to zero before reaching the furrow end. Even when the advance stream is sizeable to reach the end differences in the intake opportunity time become the major source of non-uniformity (Walker, 2003).

Various approaches have been investigated for improving distribution uniformity on furrows. One approach focuses on reducing the roughness and infiltration rate of the furrow surface. This is usually achieved by compacting and smoothening of the furrows (Bargar et al., 1999; Clemmens et al., 2001; Walker, 2003). Other modifications could include grading and levelling the field to ensure that advance stream flows much faster and uniformly. Increasing volumes of stream flows is another way of attaining more uniform irrigation especially on long furrows (Walker, 2003). Difficulties of managing advance stream and runoff in long furrows that could be as long as 1000 m (Wohling and Maihol, 2007) undermines this approach. To improve control of large inflow rates and tail end runoff automatic cutback and cyclical or surge flows are recommended (Walker, 2003 Rodriguez et al., 2004). Another approach is to increase intake opportunity time at the lower quarter of the furrow by encouraging ponding through blocking the furrow end (Walker, 2003).

Transfer of some of these technologies to rural farming communities that have access to irrigation water has been a challenge. Although lack of infrastructural development and access to capital are the common reasons (Awulachew et al., 2005), the unavailability of

alternative furrow irrigation methods is the major setback. Of critical importance is that most of the rural communities' practices farming at a small scale and widely distributed on marginal soils that are susceptible to erratic soil water regimes and fertility degradation. Therefore, access to alternative furrow irrigation technologies that are user friendly and preserve the resource base could not be overemphasised. Having considered these contributing factors to food insecurity Austin (2003) proposed the (MFI) system. This system combines the benefits of soils water intake and subsurface redistribution to optimise irrigation efficiencies using inflow rates as small as 20 L min^{-1}. Distribution efficiencies as high as 95% were recorded along unconventional furrows of 20 m long prepared on sandy loam soils (Austin, 2003).

In the Free State province of South Africa, a similar situation of unavailability of alternative irrigation methods is encountered by rural farming communities. These communities are densely populated on the low productive areas with the majority of the soils belonging to Duplex group (Hensley et al., 2007). Common to this group is the occurrence of a clay rich layer either in the B or C-horizon underlying a weakly developed course textured A- horizon. Sensitivity of these soils to dry soil water regimes and runoff-erosion degradation is well documented (Hensley et al., 2000; Botha, 2006). Therefore, crop failure during prolonged dry spells is common phenomenon among these communities.

Could the higher efficiencies achieved by the MFI be reproduced on any of the layered soils cultivated in the province? In search for answers to this question the Tukulu soil also similar to the Cutanic Luvisols that occupies 500 to 600 million hectares worldwide (World Reference Base for Soil Resources, 1998), was selected in pursuit of the following objectives; Firstly, to characterise the surface water distribution during the advance-supply phase. Secondly, to describe the subsurface water distribution during irrigation with the aid of the HYDRUS-2D software and thirdly: to evaluate the efficiencies from the irrigation outcomes.

6.2 Material and methods

6.2.1 Site location

The field experiments were carried out at Paradys Experimental Farm (29°13'24, 73"S, 26°12'40, 93"E, altitude 1417 m) of the University of the Free State, South Africa. The selected site was of a typical Tukulu (Tu) soil form according to the Soil Classification Working Group (1991). This soil type represents a group of layered soils that covers 12%

land area of the province landscape. The A- and B-horizons are of orthic and neocutanic structure, respectively with the underlying C-horizon with a moderate to strong prismacutanic structure. Physical properties of the Tukulu soil were summarized in Table 6.1 accompanied with a soil profile photo Figure 6.1.

Table 6.1 Summary of the soil physical of the Tukulu soil form.

Physical properties	Master horizons		
	A	B1	C
Coarse sand (%)	5.3	9.2	2.1
Medium sand (%)	9.3	8.8	3.8
Fine sand (%)	41.2	31	28.3
Very fine sand (%)	25.3	21	8.4
Coarse silt (%)	2.1	2	3
Fine silt (%)	4.6	2.5	6.5
Clay (%)	11.3	26.4	47.9
Bulk density (kg m^{-3})	1670	1597	1602
Porosity (%)	34.0	33	32.4
(Ks, mm hour $^{-1}$)	36.1	40	9.6

Ks= saturated hydraulic conductivity

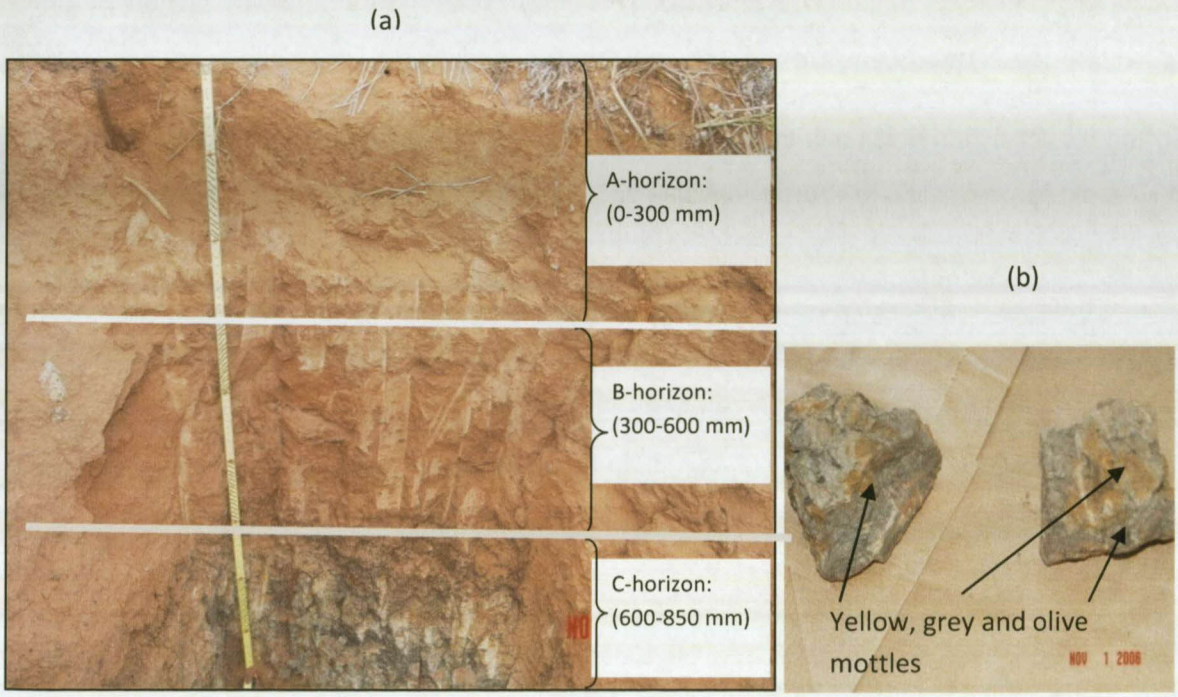

Figure 6.1 (a) Profile of the Tukulu and (b) mottles present in the C-horizon.

6.2.2 Experimental design and measurements

Four plots with three furrow replications were prepared which were 90 m long and had 2 m row spacing. Four inflow rate treatments including 20 L min^{-1}, 40 L min^{-1}, 80 L min^{-1} and 160 L min^{-1} were systematically allocated to the four plots with the largest assigned to the plot nearest to the delivery line and the smallest inflow rate to the last plot. A 40 mm low pressure delivery pipe was fitted to the distributor from the primary reservoir. Each plot had a single delivery pipe with a control valve. A rigder was used to open furrows that assumed a trapezoidal shape with a top width and bottom of 350 mm and 150 mm with a depth of 200 mm. All furrows followed a dead zero slope along the field contour lines and had a blocked furrow end.

Soil water measurements were taken by a neutron probe soil water meter. A set of 10 neutron probe access tubes of 1.2 m height were installed along the furrow shoulders of the central furrow at 10 m distance intervals beginning from the 5 m from the inlet. Readings were taken at depths of 150 mm, 450 mm and 725 mm corresponding to the mid points of the respective horizons layers. A single irrigation event was used for this work and measurements were taken before and after irrigation. Inflow controlling valves were calibrated just before irrigation and one furrow was irrigated at a time. Above ground measurements focused on the advance-supply and recession-depletion phases. During the irrigation period the times of starting and cutting off supply was recorded with the latter initiated when the advancing front was at 80 m distance. Times of the advancing front were also recorded at every neutron probe. Depth of stream flow behind the advancing front was also measured at each station and also during the ponding phase. The resulting arithmetic average was considered as the stream flow wetting depth at that particular station.

6.2.3 Simulations and inverse analyses

Infiltration during furrow irrigation could be assumed to be two-dimensional in the plane of the cross section of the furrow (Tabuada et al., 1995). The installation of one neutron probe at each measurement stations restricted this work to observe vertical soil water distribution. In addition, continuous measurement of soil water content (SWC) during the irrigation process was impractical. Therefore, the HYDRUS-2D software code of Simunek et al., (2009) was employed to simulate the two dimensional infiltration from the different inflow rates. This model numerically solves the two dimensional form of the Richard flow equation and are able to minimize the objective function for parameter optimization by using the Levenberg-

Marquardt non linear- squares approach (Marquardt, 1963). The HYDRUS-2D code has been successfully employed in simulating studies of subsurface soil water distribution during furrow irrigation and redistribution (Abbasi et al., 2003; Wohling and Maihol, 2007; Lazarovitch et al., 2009).

In this work SWC before and after irrigation with corresponding opportunity times constituted the objective function. Model predictions were compared with field-measured SWC and infiltrated depths. The 5 m, 55 m and 85 m furrow distances were selected for model predictions. Selected distances from the furrow that received the 20 L min^{-1} were 5 m, 35 m and 55 m because the advancing stream flow only reached the 60 m mark. Laboratory based soil water characteristic curve (SWCC) for all soil horizons was parameterised using the closed-form equation of van Genuchten (1980):

$$\theta(h) = \theta_r + \frac{\theta_{s-}\theta_r}{\{1 + |\alpha h|^n\}^m} \qquad (6.1)$$

Where θ_s and θ_r are the respective saturated and residual values of the volumetric water content, θ (mm mm^{-1}), h is the matrix suction (mm), while α and n are the shape and pore size distribution parameters, respectively. The condition m=1-1/n should be satisfied and θ (h) equals θ_s when at zero or positive matric suctions. Parameters related to pore-size distribution (n) and shape (α) of the SWCC were estimated from the Rosetta pedo-transfer (Schaap et al., 2001) program included in the HYDRUS-2D hydraulic parameters option. A summary of the fitted hydraulic parameters were summarized in Table 6.2. To be in agreement with the rest of the parameters the field based saturated hydraulic conductivity (Ks, mm $hour^{-1}$) derived from the double ring infiltrometer (Scotter et al., 1982) was optimised during estimation of n and α parameters.

Table 6.2 Soil hydraulic characteristics of the Tukulu soil.

	Soil horizons		
Parameters	A	B	C
θ_r(mm mm^{-1})	0.13	0.12	0.26
θ_s(mm mm^{-1})	0.34	0.33	0.32
α	0.00116	0.00094	0.0052
n	1.773	1.617	1.226
Ks(mm $hour^{-1}$)	36.1	40	9.6 (1.9)

(*) = value from parameter optimisation procedure

The van Genuchten (1980) model with air entry value of -0.2 kPa was used to describe soil hydraulic properties during the infiltration simulation. A soil profile flow domain of 4 000 mm by 850 mm dimensions and a finite element mesh of 50 mm was defined with the furrow at the symmetric position (Figure 6.2). The profile was also discretisized into three layer materials corresponding to the *in situ* soil horizons. The pressure head was selected for initial pressure conditions with the assumption that pressure head was uniform in each horizon. Constant head was appropriate for the furrow boundary condition while along the vertical sides a no flux condition was assigned. At the bottom of the profile a free drainage boundary was selected.

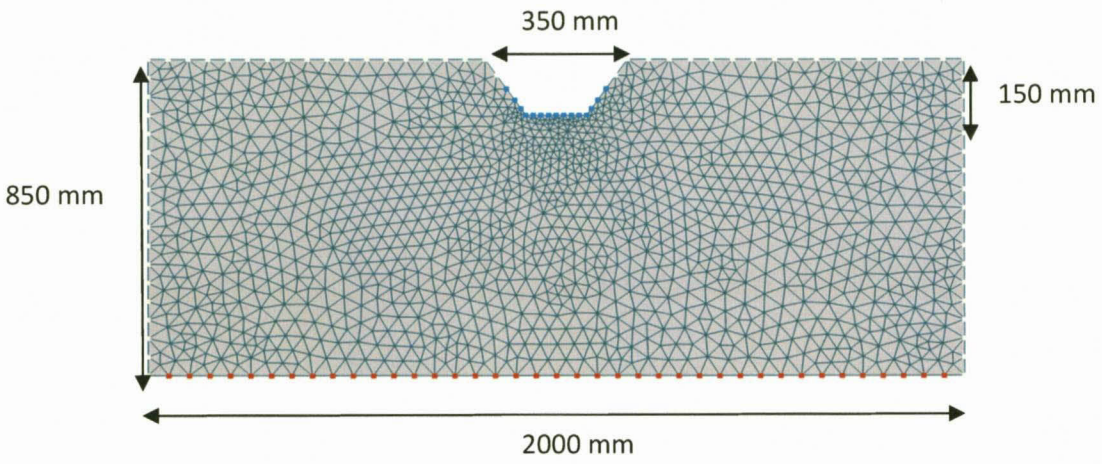

Figure 6.2 Fine element mesh and boundary conditions assigned inside the furrow (constant head), zero flux at the surface and vertical sides and free drainage at the bottom of the profile.

6.2.4 Experimental data analysis

Processing of measured and predicted SWC into infiltrated depth and function was the measure focus of this experiment. The geometric mean was selected for averaging infiltrated depth at different points along the furrow length in consideration of soil spatial variability that could be a source of non linearity (Romano et al., 1996; Abbasi et al., 2004). Infiltration functions were assumed to be directly proportional to the actual opportunity time determined by the advance-recession phase. From the selected three furrow measurement points (5, 55 and 85 m) the infiltrated depth with corresponding opportunity times were averaged to determine the average furrow infiltration function (AFIF). This function was validated by averaging the one point time rate change in SWC simulated by HYDRUS-2D. Since one

point values were used to estimate the AFIF this approach was considered to be representative of the one point method described by Clemmens et al. 2001). The AFIF was also simplified to a simple power function and expressed as (Clemmens et al., 2001);

$$D = k\tau^{a} \tag{6.2}$$

Where D is infiltrated depth (mm), τ is the infiltration opportunity time and k and a are parameters. Best fit curves were used to estimate the parameters with the objective to improve the conservation of mass with the final average infiltrated depth. Where measured and predicted final infiltrated depth varied the parameters were adjusted to agree with final infiltrated depth at the specified opportunity time. The AFIF was then used to approximate infiltrated depths 30 and 60 m furrow distances with respect to the corresponding average opportunity times.

Estimating the irrigation performance of the 20, 40 80 and 80 L min^{-1} inflow rates at different furrow lengths the distribution uniformity (DU), application efficiency (AE) and deep percolation ratio (DPR) (Clemmens et al., 2001; Oyonarte et al., 2002). In the absent of tail end runoff on blocked ended furrows these criterion using average accumulative infiltration could take the following expressions;

$$\text{DU} = \frac{\text{infiltrated depth at the lower quarter of the furrow(mm)}}{\text{furrow infiltrated depth (mm)}} \tag{6.3}$$

$$\text{AE} = \frac{\text{infiltrated depth within the root zone (mm)}}{\text{infiltrated depth of the profile}} \tag{6.4}$$

$$\text{DPR} = \frac{\text{infiltrated depth below the root zone (mm)}}{\text{Total infiltrated depth (mm)}} \tag{6.5}$$

6.2.3 Statistical analysis

Agreement between the measured and predicted SWC content measurement was evaluated using the root mean square error (RMSE) and the index of agreement or D-index as proposed by Willmot et al. (1985). A 1:1 line was further used to assess the quality of fit alongside the coefficient of determination (R^2). The model predictions are considered satisfactory if the values of RMSE approach zero and both the D-index and R^2 approach unity. Subsequent analysis of secondary data was subjected to the Bartletts or chi-square (χ^2) homogeneity test and Student's t-test analysis. The homogeneity hypothesis was accepted if computed values were equal or less than the reference tabulated value.

6.3 Results

6.3.1 Surface flow characteristics

Figure 6.3 shows the time-distance relationships of the advance and recession phase from the 20, 40, 80 and 160 L min^{-1} inflow rates tested on the Tukulu soil 90 m furrow runs. The advance time recorded from the 20 L min^{-1} was 160 minutes at a 60 m distance before the advancing stream approached zero. The 40, 80 and 160 L min^{-1} inflow rates reached the furrow end at different times of 105, 38, and 23 minutes, respectively. Corresponding cut off times were 160 minutes (2.7 hours), 105 minutes (1.08 hours), 35 minutes (0.6 hours) and 23 minutes (0.4 hours) for the 20, 40, 80 and 160 L min^{-1} inflow rates. Recession phase from the 20 and 40 L min^{-1} inflow rates was observed from the 162 to 166 and 106 to 112 minutes, respectively. The 80 and 160 L min^{-1} inflow rates had recession period from the 38 to 100 and 28 to 99 minutes from irrigation.

The average depth of the advancing stream flow and opportunity times along the 10 m interval measuring points were summarized in Table 6.3. The average depth of stream flow ranged from 15 to 60 mm from the 20 L min^{-1} inflow with an opportunity time range of 2 to 162 minutes. In the 40 and 80 L min^{-1} had a respective stream flow depth ranging from 33 to 80 mm mm and 63 to 80 mm with a corresponding opportunity time range of 7 to 105 and 37 to 65 minutes. The 160 L min^{-1} recorded an average stream flow depth ranging from 70 to 125 minutes with opportunity times from 27 to 76 minutes.

6.3.2 Subsurface soil water content

Figure 6.4 presented the measured and predicted SWC before and after irrigation on a 1:1 line. Optimised parameters for the improvement of model's predictions were summarized in Table 6.4 Statistical measure of fit between the measured and predicted SWC are also presented in Table 6.5.

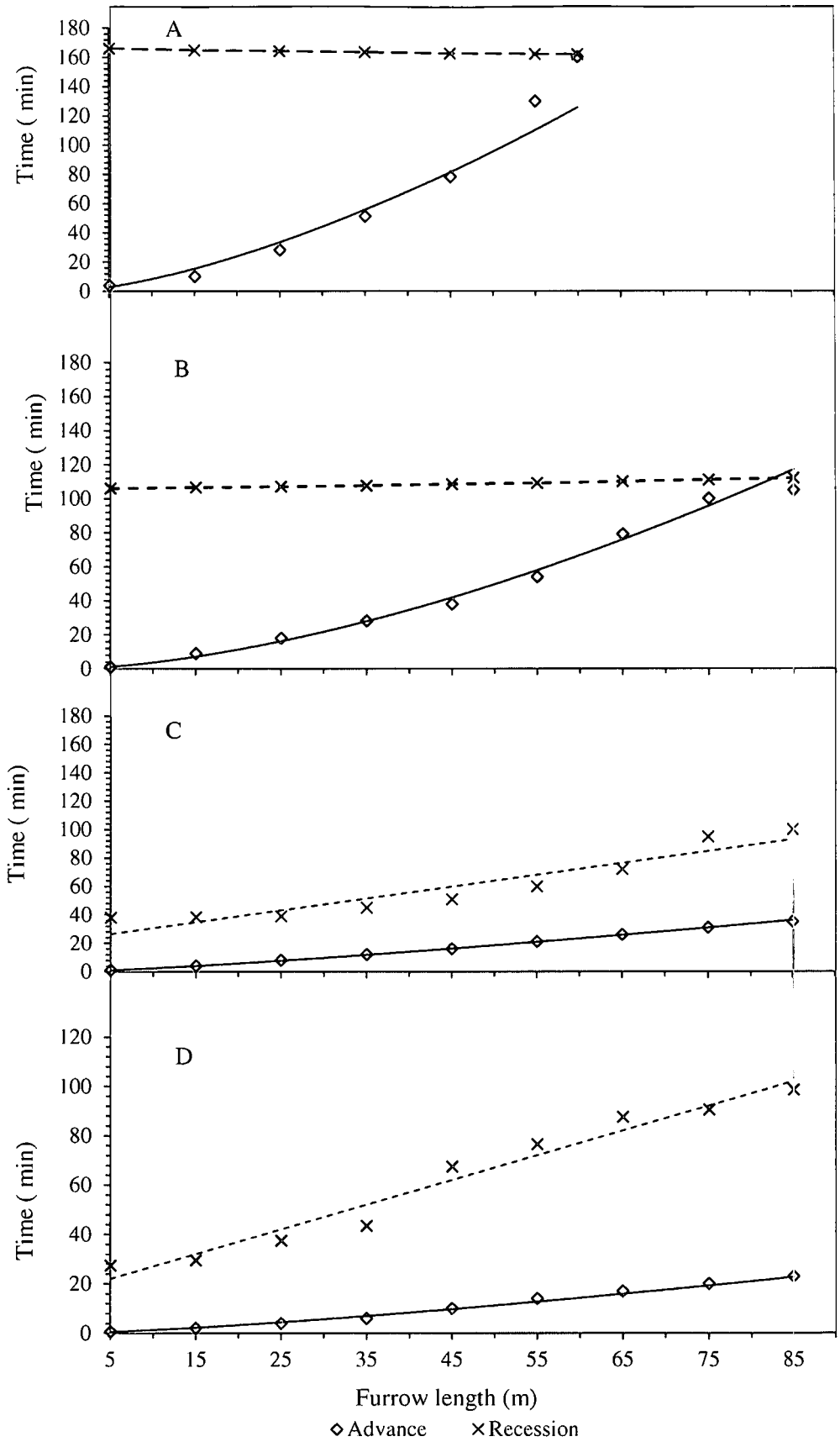

Figure 6.3 Measured advance and recession times for the 20 (A), 40 (B), 80 (C) and 160 (D) L min^{-1}.

Table 6.3 Stream depth and opportunity time of stream-flow along furrows under different inflow rates.

Furrow length	Inflow rates (L min^{-1})							
	20		40		80		160	
	SD (mm)	OT (min)	SD (mm)	OT (min)	SD (mm	OT (min)	SD (mm)	OT (min)
5	60	162	80	105	80	37	90	27
15	60	155	77	98	85	34	125	28
25	60	136	67	89	92	31	110	34
35	50	112	65	80	83	33	105	38
45	50	85	60	71	80	35	100	58
55	20	32	55	55	75	39	90	63
65	15	2	50	31	70	46	85	71
75			38	11	65	64	80	71
85			33	7	63	65	70	76

OT; opportunity time in minutes

SD; stream depth

Table 6.4 Optimised parameters to improve model's predictions.

Distance		Inflow rates (L min^{-1})							
		20		40		80		160	
5 m	Horizons	θr	α	θr	α	θr	α	θr	α
	A	-	0.0006	0.13	-	-	0.0022	-	0.0028
	B	-	0.0005	0.19	-	-	0.0005	-	0.0007
	C	-	0.0457	0.25	-	-	0.0159	-	0.0433
55 (35)	A	0.13	-	-	0.0042	-	0.0070	-	0.0013
	B	0.05	-	-	0.0005	-	0.0006	-	0.0009
	C	0.26	-	-	0.0175	-	0.0056	-	0.0015
85(55)	A	-	0.0023	-	0.0143	0.13	-	-	0.0017
	B	-	0.0005	-	0.0003	0.16	-	-	0.0008
	C	-	0.0467	-	0.0639	0.26	-	-	0.0015

( ) = Furrow distance from the 20 L min^{-1}

There was generally good agreement between measured and predicted SWC at various lengths of the furrow from all inflow rates (Figure 6.4). At depth of 150 mm all furrows had an initial SWC measurement ranging from 0.13 to 0.145 mm mm^{-1} while the predicted ranged from 0.13 to 0.139 mm mm^{-1}. Following irrigation the measured SWC ranged from 0.24 to 0.32 mm mm^{-1} while the predicted ranged from 0.27 to 0.34 mm mm^{-1}.

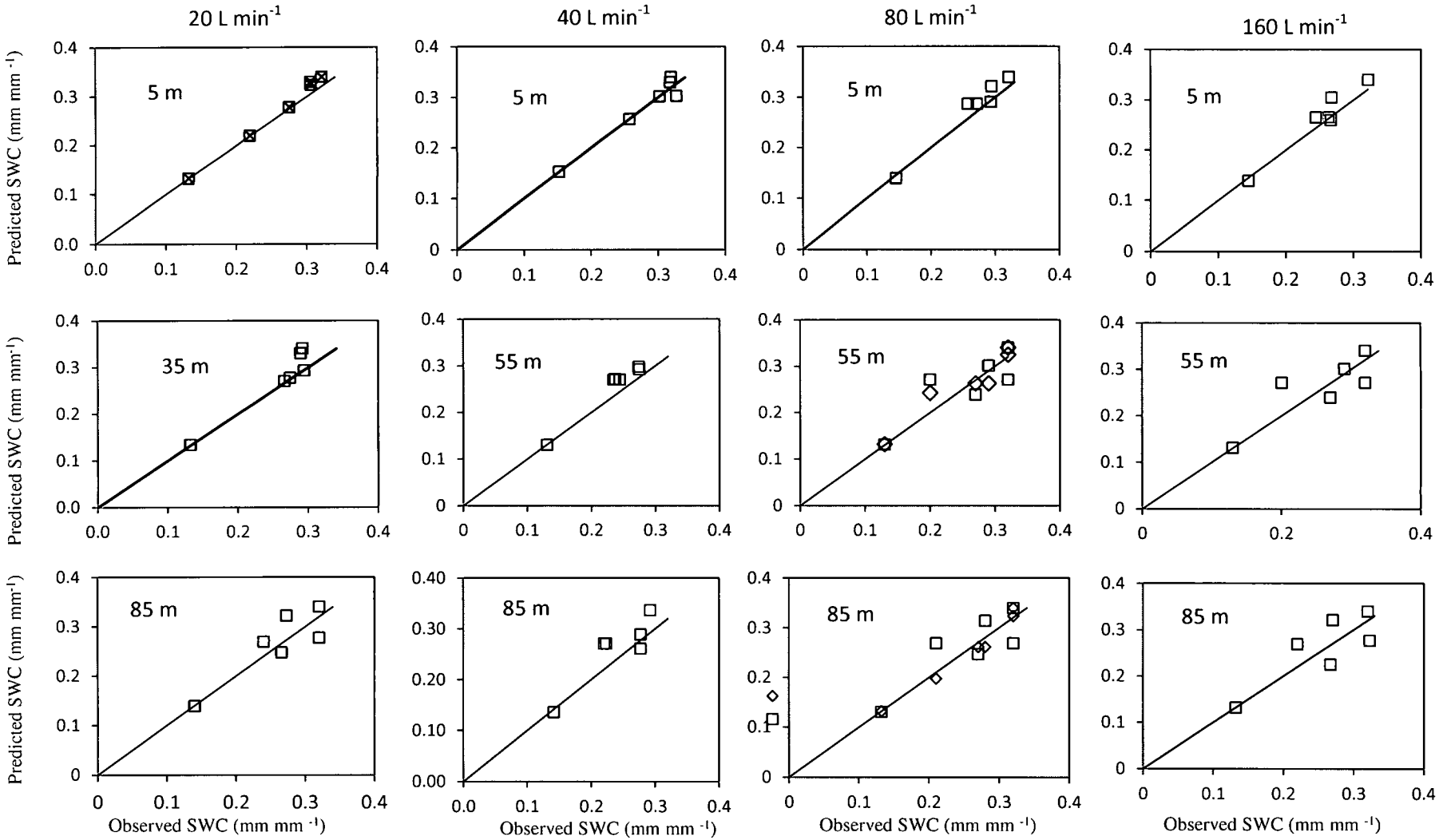

Figure 6.4 Measured and predicted soil water content (SWC) for the profile depth layers (0-300; 300-600, and 600-850 mm) before and after irrigation HYDRUS-2D software from the 20, 40, 80 and 160 L min^{-1} inflow rates at three furrow distances.

At depth of 450 mm the measured initial and final SWC ranged from 0.20 to 0.27 mm mm^{-1} and 0.22 to 0.327 mm mm^{-1}, respectively. Predicted initial SWC ranged from 0.26 to 0.29 mm mm^{-1} and final SWC within the range of 0.265 to 0.30 mm mm^{-1}. At depth of 725 mm the measured initial SWC was from 0.265 to 0.29 and the predicted from 0.23 to 0.30 mm mm^{-1}. After irrigation the measured and predicted values ranged between 0.27 to 0.32 and 0.29 to 0.33 mm mm^{-1}, respectively. The values of R^2 was good (> 0.98) for all inflow rates throughout the furrow lengths. The D-index also indicated a good agreement (> 0.97) between the measured and predicted values especially at the inlet. Further away from the inlet the D-index showed a decrease but still within the acceptable range (> 0.90). Consistent with this result was the RMSE of 0.02 near the inlet and further away the furrow length recording a value of 0.04 in all the furrows.

Table 6.5 Statistical measure of fit from measured and predicted soil water content at three furrow distance measuring points.

Inflow rate (L min^{-1})	Distance (m)	RMSE	D-index	R^2
20	5	0.025	0.966	0.997
	35	0.026	0.957	0.998
	55	0.035	0.902	0.995
40	5	0.022	0.975	0.998
	55	0.039	0.910	0.990
	85	0.025	0.944	0.999
80	5	0.020	0.974	0.999
	55	0.016	0.984	0.999
	85	0.018	0.981	0.998
160	5	0.019	0.973	0.998
	55	0.031	0.935	0.994
	85	0.039	0.906	0.989

6.3.3 Subsurface soil water distribution

Variation in measured and predicted infiltrated depth along the wetted furrow was shown in Figure 6.5 with reference to the three selected distance points. At the 5 m distance from the furrow inlet measured infiltrated depth was 90, 101, and 57 and 59 mm from the 20, 40, 80 and 160 L min^{-1} inflow rates, respectively. In the same order corresponding predicted values were 92, 85, 68 and 72 mm. The 20 L min^{-1} wetted the furrow up to the 60 m with infiltrated depth decreasing monotonously with distance recording an infiltrated depth of 46 mm at 55 m distance with predicted value of 67 mm. Having reached the 90 m distance the 40, 80 and 160

L min^{-1} inflow rates recorded measured infiltrated depths of 35, 80 and 88 mm while the corresponding predicted depths were 41, 80 and 89 mm. Two-dimensional predicted soil water distributions from selected furrow measurement point for the different inflow rates are presented Figures 6.6, 6.7, 6.8 and 6.9. The saturated infiltrated depth (SID) was at different levels of developments with the 20 and 40 L min^{-1} at the inlet 5 m point showing a continuous blocky infiltrated zone reaching the C-horizon. The SID for the wetted furrow end was limited to only the upper layer within the wetted perimeter of the furrow. In the 80 and 160 l/min inflow rates the SID was restricted at the inlet to the upper layer while further away it had progressed towards the C-horizon. On all the snapshots constrictions on the SID, transitional zone and wetting front could be noted at depth of 300 and 600 mm. The R^2 values given by the HYDRUS-2D were good (>0.95) at the 5 m distance from all inflow rates. At the last wetted point of the furrow the R^2 value had decreased sharply, but was still acceptable (> 0.69).

6.3.4 Irrigation infiltration functions

Average furrow infiltration functions derived from one point method were shown in Figure 6.10. Parameters for the simple power based infiltration function and the outcomes of homogeneity tests are summarized in Table 6.6.

Average infiltration function projected infiltrated depths that varied from those from predicted measurements, especially at the early stages of infiltration. In the 20 L min^{-1} the predicted measurements reflected a rapid start, while that of the infiltration function was slow up to the 0.78 hour mark where both curves matched fairly well until the end of the plot. In a similar manner the curves from the 80 and 160 L min^{-1} inflow rate matched at about 0.67 and 0.81 hours. A different trend was observed from the 40 L min^{-1} with predicted depths overestimated by the infiltration function up to the 0.18 hour mark after which the two curves run close to each other. The final average opportunity time was 0.38 hours compared to the 1.1, 0.83 and 1.01 hours for the 20, 80 and 160 L min^{-1} inflow rates.

Table 6.6 Bartlett's homogeneity test between measured and predicted infiltration functions for the different inflow rates

Inflow rates (L min^{-1})	Computed $\chi 2$	Tabular $\chi 2_{(0.05,2)}$
20	0.4221	3.84
40	0.0000012	3.84
80	0.0038	3.84
160	0.0048	3.84

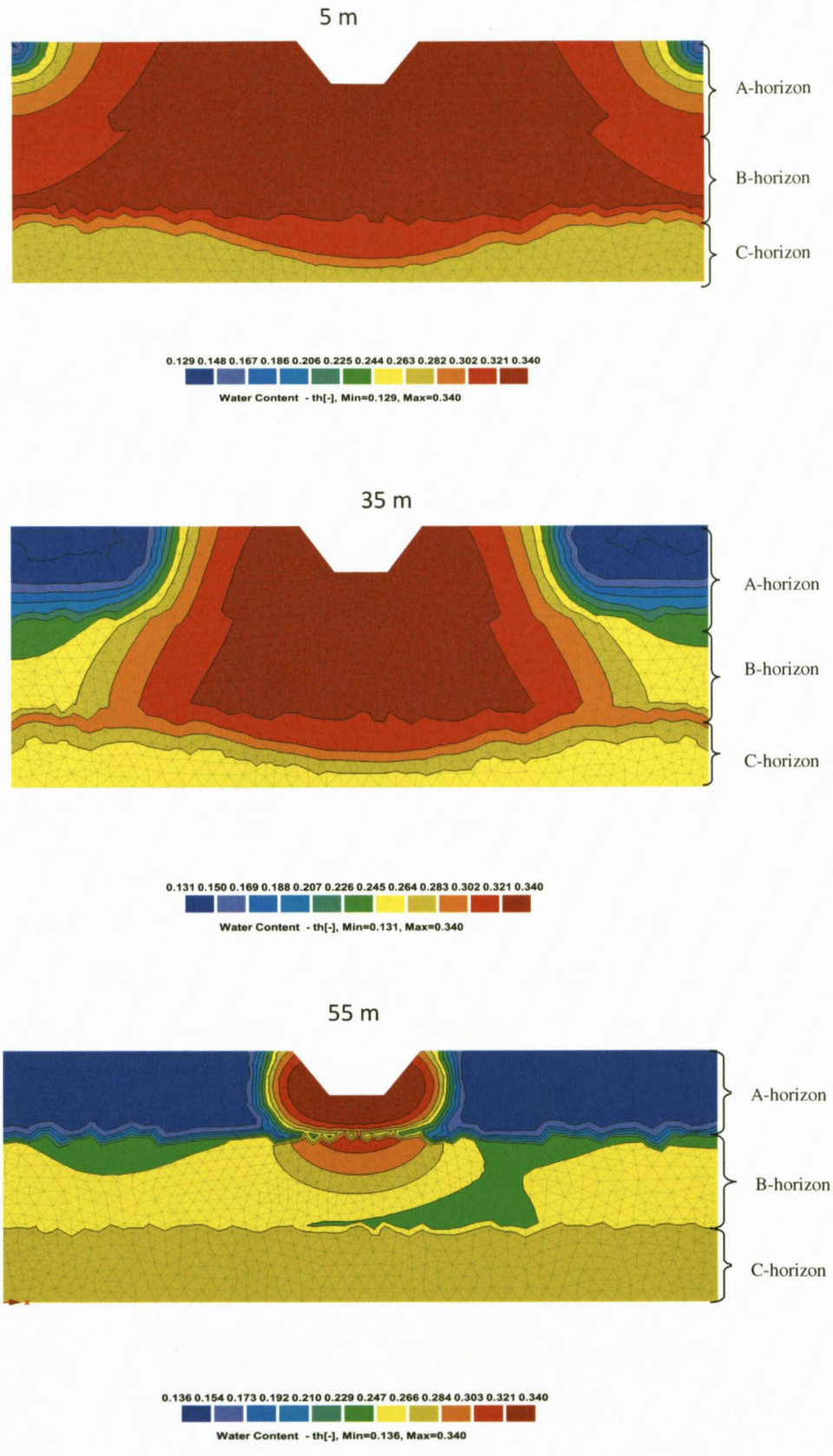

Figure 6.5 Subsurface soil water distribution following irrigation at 5 m, 35 m, and 55 furrowlength for the 20 L mm^{-1} inflow rate.

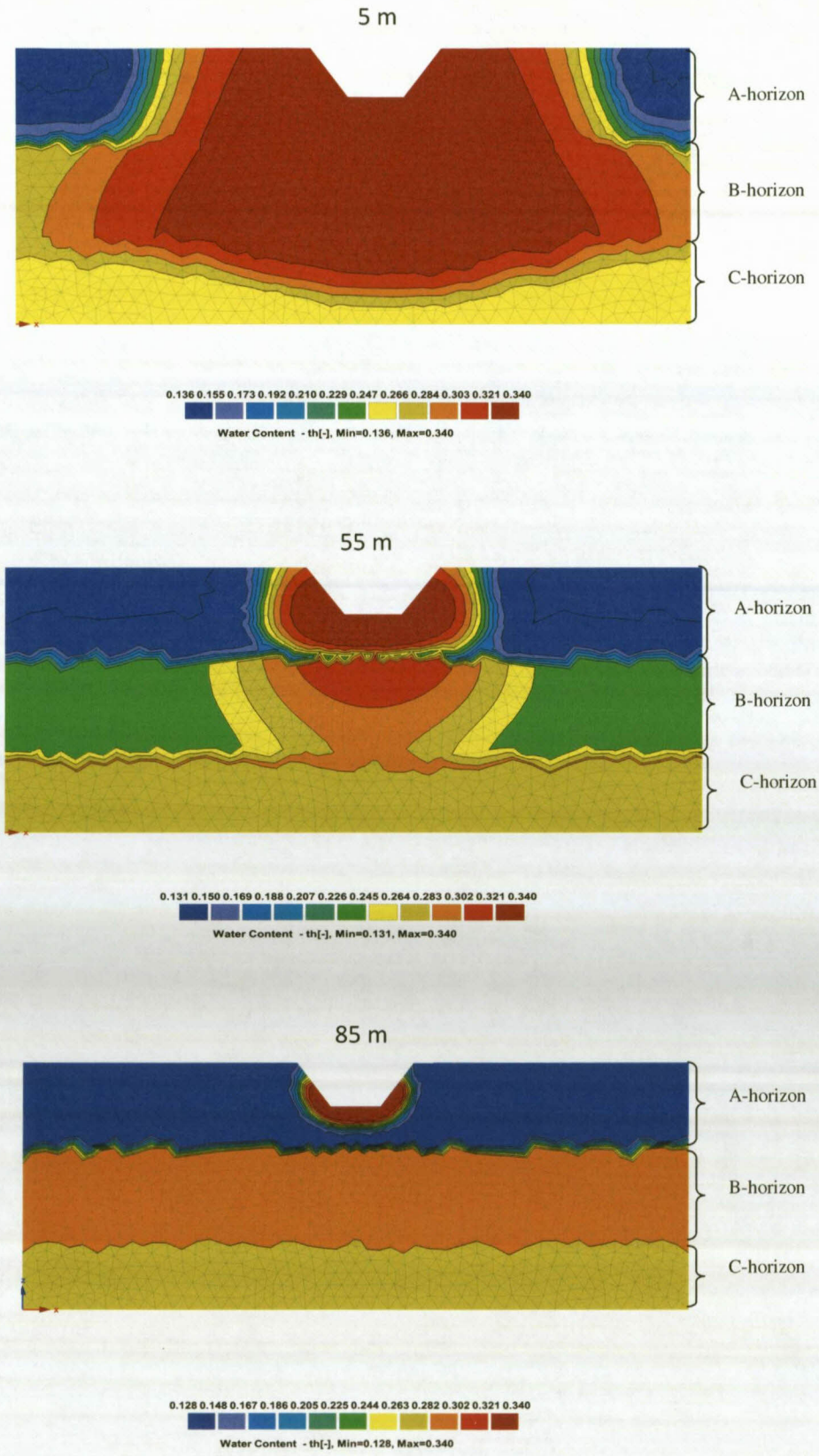

Figure 6.6 Subsurface soil water distribution following irrigation at 5 m, 55 m, and 85 m furrow length for the 40 L mm^{-1} inflow rate.

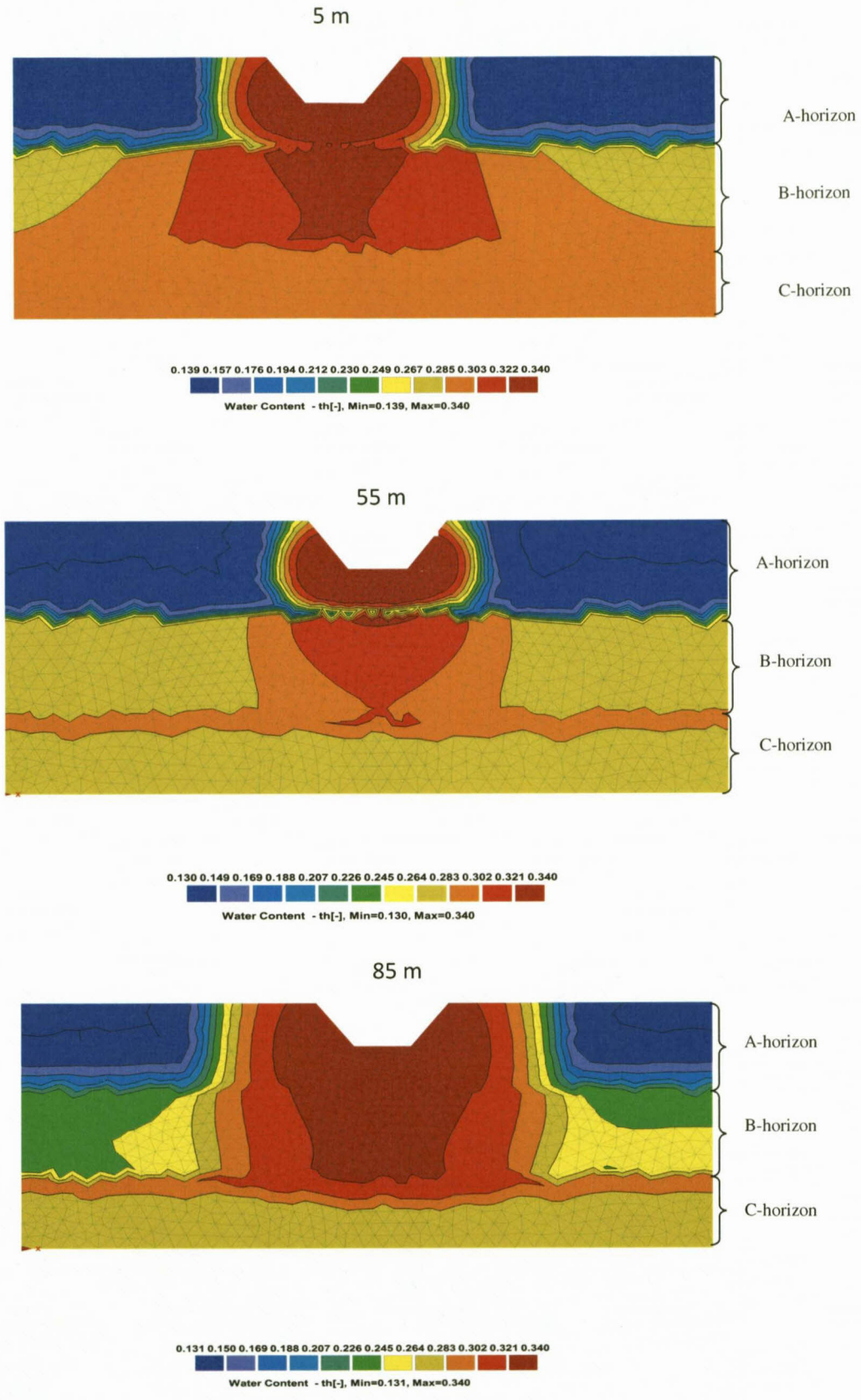

Figure 6.7 Subsurface soil water distribution following irrigation at 5 m, 55 m, and 85 furrow length for the 80 L mm^{-1} inflow rate.

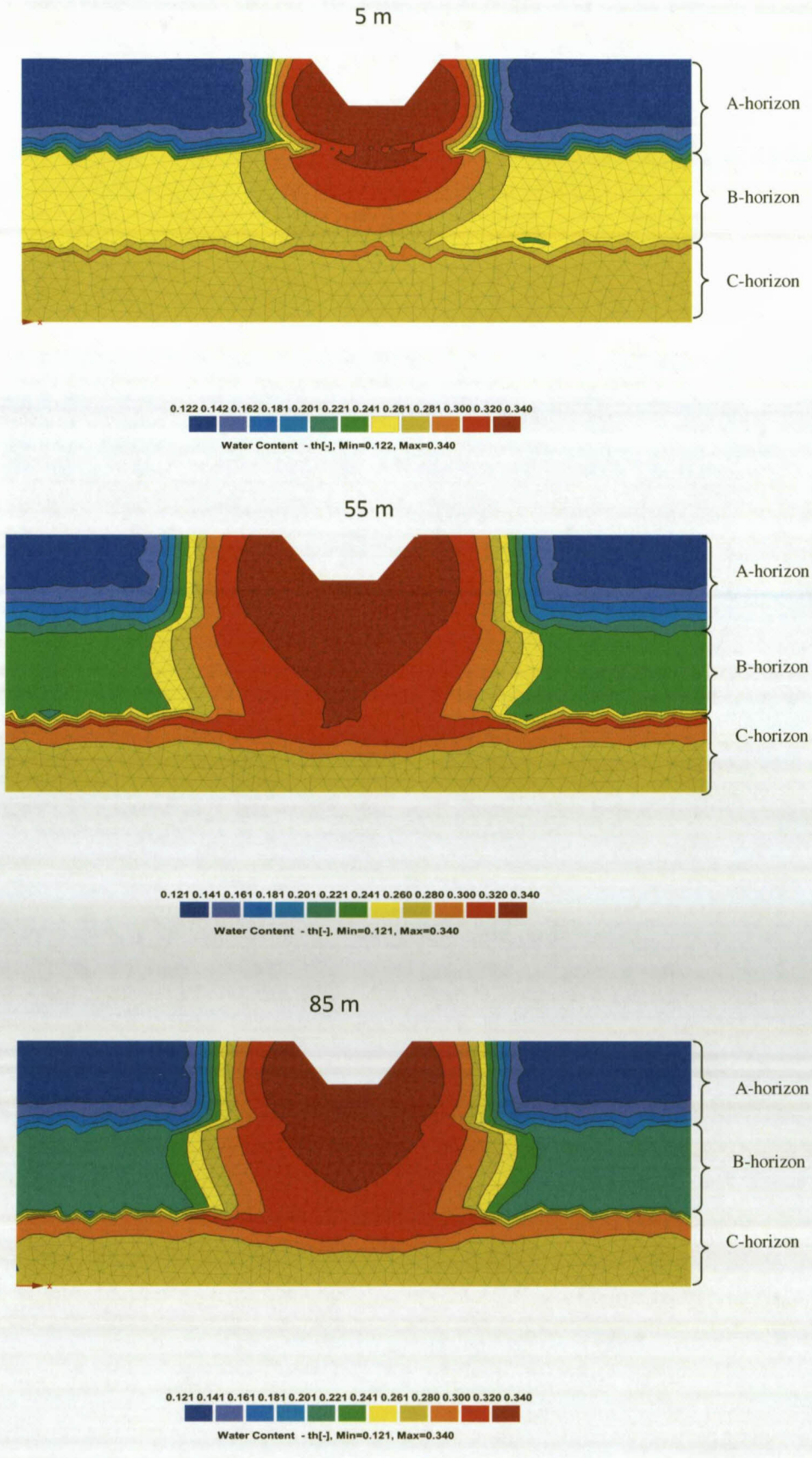

Figure 6.8 Subsurface soil water distribution following irrigation at 5 m, 55 m, and 85m furrow length for the 160 L mm^{-1} inflow rate.

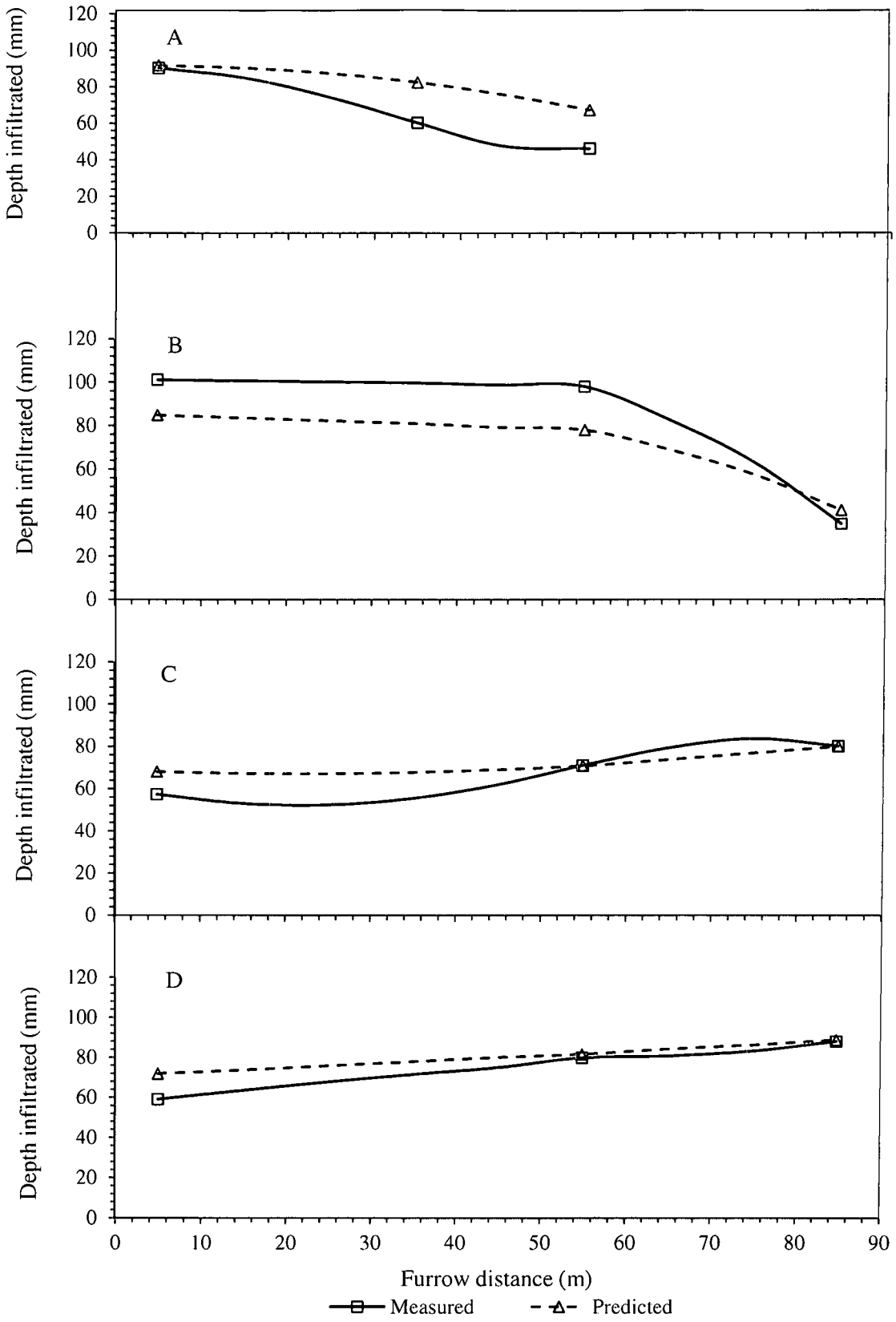

Figure 6.9 Distribution of infiltrated depth along the furrow length for the 20 (A), 40 (B), 80 (C) and 160 L min^{-1} (D) inflow rate.

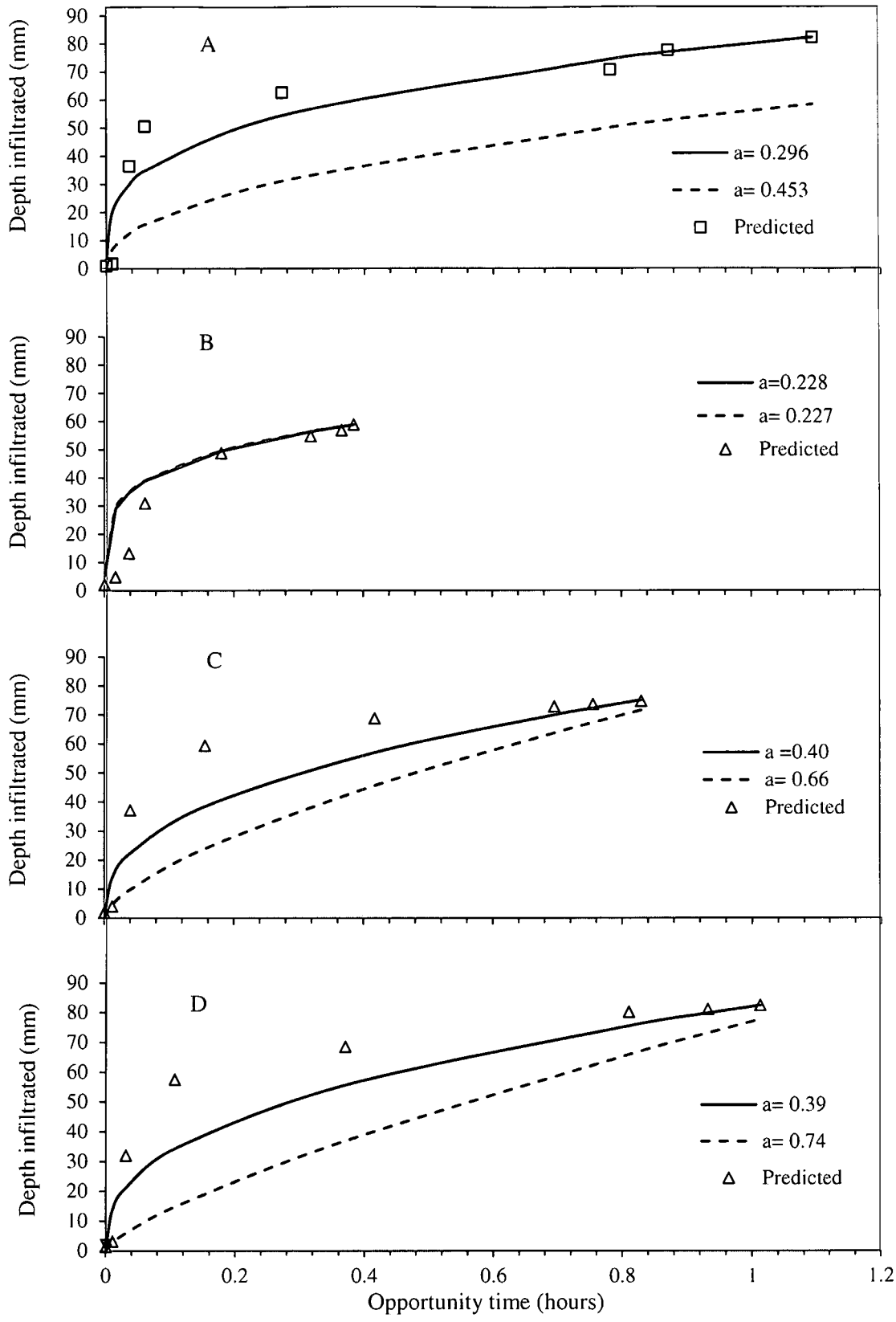

Figure 6.10 Average furrow irrigation functions for predicted (solid line) and for measured (broken line) corresponding to the different constants (a) adjusted to conserve mass for the 20 (A), 40 (B), 80 (C) and 160 (D) L min^{-1} inflow rates.

6.3.5 Average infiltration depth and measures of performance

Average infiltrated depths from measured and predicted SWC measurements from actually wetted furrow distanced are presented in Table 6.7. Average infiltrated depths approximated from the average furrow infiltration function (AFIF) for the 60 and 30 m long furrows are also shown. In addition appropriate measures of irrigation performance including DU, AE and DPR were given.

Average infiltrated depth for the 90 m furrow distance ranged from 66 to 87 mm and 74 to 71 mm from the respective measured and predicted SWC measurements. The highest depth from the measured came from the 40 L min^{-1} inflow rate while from the predicted was from the 160 L min^{-1}. At this furrow distance average infiltrated depths between measured and predicted SWC were found to be homogeneous. At the 60 m distance only the 20 L min^{-1} was able to actually wet this furrow distance with average depths of 67 and 82 mm from the measured and predicted SWC. These two averages were comparable according to the Student t-test analysis. For same 60 m furrow lengths, the average infiltrated depth approximated using the AFIF ranged from 64 to 95 mm and 91 to 64 mm for the measured and predicted SWC. Highest depths were from the 160 L min^{-1} and the least from the 40 L min^{-1} .The Student's t-test analysis found the approximated infiltrated depths from the measured and predicted SWC of the 40, 80 and 160 L min^{-1} not comparable for the 60 m furrow length. Corresponding to the 30 m furrow length, average infiltrated depths ranged from 34 to 58 mm and 58 to 69 mm for the respective measured and predicted SWC. The highest average infiltrated depth was from the 40 L min^{-1} under measured SWC while from the predicted SWC was given by the 160 L min^{-1} inflow rate. Comparable differences between the measured and predicted SWC average infiltrated depths were found from the 80 and 160 L min^{-1} inflow rates.

Measures of performance included the DU, EA and DPR and were found applicable to the actual furrow distances wetted by the selected inflow rates. Where the AFIF infiltrated depth-oppotunity time relationship was employed to intepolate irrigation parameters for the 30m and 60m furrow lengths, only DU was used. In the 90 m long furrows the DU ranged from 0.69 to 0.85 and 0.67 to 0.92 from the respective measured and predicted SWC. Corresponding EA ranged from 0.93 to 0.99 and 0.88 to 0.78 while the DPR ranged from 0.01 to 0.07 and 0.12 to 0.22, respectively.

Table 6.7 Average infiltrated depth and performance indicators for different furrow lengths and inflow rates.

Furrow length (m)	Inflow rates (l/min)	ID (m)		DU		AE		DPR	
		Measured	Predicted	Measured	Predicted	Measured	Predicted	Measured	Predicted
30	20	34.30	57.71	0.89	0.93	-	-	-	-
	40	58.22	58.16	0.96	0.96	-	-	-	-
	80	50.51*	60.65*	0.96	0.97	-	-	-	-
	160	55.29*	68.79*	0.89	0.94	-	-	-	-
60	20	67.15*	82.40*	0.70*	0.87	0.93	0.88	0.06	0.16
	40	63.68	63.64	0.83	0.83	-	-	-	-
	80	81.19	81.05	0.998	0.99	-	-	-	-
	160	94.38	91.14	0.87	0.93	-	-	-	-
90	20	-	-	-	-	-	-	-	-
	40	86.50	72.90	0.69	0.67	0.93	0.88	0.07	0.12
	80	65.99	71.15	0.82	0.95	0.94	0.86	0.06	0.14
	160	74.23	73.74	0.85	0.92	0.99	0.78	0.01	0.22

* significant different at 0.05 T-test
ID = Infiltrated depth
AE = Application efficiency
DPR= Deep percolation ratio
DU = Distribution uniformity

The 20 L min^{-1} was able to actually wet the 60 m furrow distance with a DU and EA values of 0.7 and 0.87 from the measured SWC and 0.93 and 0.88 from the predicted SWC with a corresponding DPR value of 0.06 and 0.16. From the 20, 40, 80 and 160 L min^{-1} inflow rates the DU ranged from 0.9 to 0.7 and 0.99 to 0.83 for the measured and predicted SWC. In the 30 m furrow distance the corresponding DU values were ranging from 0.86 to 0.89 and 0.93 to 0.93.

6.4 Discussion

Selecting an inflow rate that satisfies the claims of soil water infiltration and runoff of the advance stream to the furrow end is one of the many challenges in designing furrow irrigation. Surface and subsurface water distribution from single run irrigation with a 20, 40, 80 and 160 20 L min^{-1} inflow rates on a 90 m long furrows provided insight on the appropriate inflow rate-furrow length combination for the Tukulu soil.

Among the inflow rates it was only the 20 L min^{-1} that could not sustain an advance stream to the furrow end, but approached zero at the 60 m point. Despite the inflow rate being small the high surface roughness of the newly prepared furrow is one reason the advance stream went to zero. According to the Manning Roughness Index a newly prepared furrow has a roughness coefficient of about 0.06 and 0.02 for very smooth furrows (ASAE, 2003). Restrictive effect of furrows with high surface roughness on the advance stream is well acknowledged in literature (Clemmens et al., 2001; Walker, 2003; Hulugalle et al., 2007; Clemmens and Bautista, 2009). Raising the inflow rate to 40 L min^{-1} was able to reach the 90 m, but at the advance time of 105 minutes compared to the 35 and 23 minutes clocked by the 80 and 160 20 L min^{-1} inflow rates. The small advance times were expected given the high runoff potential of large inflow rates (Walker, 2003). The high roughness could have had little effect on the advance times of the larger inflow rates. However the immediate rise in averaged depth at the 25 m point to 92 and 105 mm does suggest that advance at this distance were slowing down and high roughness of the furrow surface being the most appropriate reason. Following cut off the recession periods between the furrow inlet and end from the 20 and 40 L min^{-1} is about 4 and 7 minutes, respectively. Because of the small recession periods irrigation could be implied to have stopped simultaneously at cut off an assumption that is upheld by the kinematic wave model (Walker and Skorgeboe, 1987). In the 80 and 160 L min^{-1} the time difference of recession period between the furrow inlet and end was 62 and 71 minutes, respectively. Occurrence of ponding at the furrow end was the main reason for the

large differences in recession for the 80 and 160 L min^{-1}. The generally high average stream flow depth and the signs of furrow shape deformations as well as potholing near the inlet despite provisions made to prevent erosion could be regarded as indicators of the risk of erosion and overtopping from the 80 and 160 L min^{-1} inflow rates. Walker (2003) shared the same sentiment and suggested emergency facilities to drain excess water especially when large inflow rates are applied. Management of advance on long furrows was also seen to be more challenging compared to short furrows by Wohling and Maihol (2007).

Application of the HYDRUS-2D software in predicting the infiltrated depth from initial and final SWC measurements was satisfactory. Agreement between the measured and predicted initial and final SWC were observed from all inflow rates. Optimised parameters for all horizons was the θ_r from the 20 and 40 20 L min^{-1} and the α from the 80 and 160 L min^{-1} Overestimates of infiltrated depth was common among the predicted SWC measurements especially at the inlet from the larger inflow rates while from the smaller inflow rates it was towards the furrow end. The model assumed θ_s to be equal to the porosity value and yet under field conditions the presence of dead end pores, entrapped air and bulk density variations makes achievement of maximum saturation impractical (Hillel, 2004). Underestimation of infiltrated depth was only pronounced in the 40 and 20 L min^{-1} with a fairly good agreement at the furrow end. These variations were expected given that SWC measurements were one dimensional while the predicted values were computed using a two dimensional model. Much of the erratic variations could be attributed to spatial variability of the soil properties along the 90 m furrow length. Similar situations were also encountered by Raghuwannshi and Wallender (1996), Abbasi et al. (2003), and Wohling and Maihol (2007). However, good agreement at the lower quarter of the furrow especially from the 80 and 160 L min^{-1} could be pointing out to the homogenizing effect of ponding on this soil.

Infiltrated depth from both measured and predicted SWC showed greater consistency to the opportunity time and average depth of stream flow. This was not surprising because surface and subsurface water distribution should conserve mass. Total water volume applied during irrigation according the inflow rate and irrigation-cut off time was equivalent to 3.2, 4.2, 2.8, and 3.7 m^3 from the 20, 40, 80 and 160 L min^{-1} inflow rates. The higher volume of water applied for small inflow rates corresponds to the large irrigation times, 162 and 105 minutes for the respective 20 and 40 L min^{-1}, attributed to the slow advance stream observed from these inflow rates. Of interest was the distribution of the water in the profile since no water escaped at the blocked ended furrow. As expected infiltrated depth was greater at the inlet

from the 20 and 40 L min^{-1} while from the 80 and 160 L min^{-1} was skewed towards the lower quarter of the furrow. This variation could be explained by the fact that most of the delivered water from the smaller inflow rates was infiltrated before making significant advances implying that the inflow rate were very close to the soil water basic intake. On the contrary, the 80 and 160 L min^{-1} inflow rate recorded small advance times indicating that a significant proportion of its streamflow was able to reach the furrow end before making time for infiltration. This observation was supported by the high opportunity times at the furrow end due to ponded water implying the 80 and 160 L min^{-1} were way above the soil water basic intake. The graphical snapshots from HYDRUS-2D did capture clearly the two situations represented by the two groups of inflow rates. At the inlet of the 20 and 40 L min^{-1} the saturated infiltrated depth (SDI) extends uniformily to the C-horizon where it developed sideways. This phenomenon suggests the presence of a restrictive layer at the 600 mm suggesting that deep drainage losses was not a major problem in this soil. Confirming this observation was the abrupt transition of 40 to 1.9 mm $hour^{-1}$ in Ks values from the B to the C-horizon. Hensley et al. (2000) shared the same sentiment about the formation of heavy structured clay rich underlying C-horizon among group of layered soils in the Free State province as key to profile soil water storage. Between the A and B horizon a discontinuity in SID and wetting front could be observed suggesting that the layering between these horizons was not severe and that it had little effect on deep infiltration.

The use of one point method to determine the AFIF was thought to be able to give reasonable estimates of infiltrated depth for any furrow depth since it was based on improving the conservation of mass. The backwater effect from the 80 and 160 L min^{-1} inflow rates as a result of ponding at lower end of the blocked furrow should have made the two point method (Clemmens et al., 2001; Walker, 2003) ill posed for this work. The AFIF was based on infiltrated depth-opportunity time relationship because ponded infiltration is a function of time rather than surface infiltration characteristics (Clemmens et al., 2001). Application of the geometric mean, considered by some to be appropriate for non linear conditions, could not eliminate the inconsistencies caused by spatial variations and the use of a simplified power law infiltration model. Therefore, guarantees for accuracy from the AFIF could not be made. Differences in infiltration parameters between measured and predicted AFIF was the major source of variations. This was expected given the differences in opportunity times between the furrow inlet and end from all inflow rates. A similarity between measured and predicted average infiltration parameters by AFIF for the 40 L min^{-1} was an exception and

can be explained by the spatial distribution of infiltrated depth and opportunity times relationship depicted in Figure 6.9 (B). This observation could be indicating the challenges this inflow rate encountered in sustaining adequate stream flow to wet the furrow end. For the 20 L min^{-1} it was able to attain a higher opportunity time at the 55 m point because the advance stream was given some time to demonstrate if it could progress beyond the 60 m mark or not. Austin (2003) under similar circumstance noted that once the advance stream along the furrow length has been reduced to soil basic water intake, it instantly goes to zero. Further supply of water increases infiltrated depth rather than advance distance. This analogy explains why infiltrated depth was high near the inlet of the 20 and 40 L min^{-1}. Better water distribution along the furrow contributed to the higher average infiltrated depth from the 160 L min^{-1}. The 40 and 20 L min^{-1} had higher distribution at shorter distances. Underestimations from the infiltration function were not uncommon especially at early stages of infiltration; overshooting tendencies of infiltration on initially dry soil is the contributing factor (Hillel, 2004).

A strong agreement between the AFIF with the final infiltrated depth from the three selected measurement point made it feasible to generate infiltrated depth for the entire wetted furrow based on the corresponding opportunity times. The resulting distribution of infiltrated depth was typical of the subsurface distribution from various irrigation regimes. For the 90 m distance the 40 L min^{-1} had the highest average infiltrated depth of 86.5 mm and this was consistent with the 4.2 m^3 volume of water applied in this furrow. Although 80 and 160 L min^{-1} supplied smaller volumes of 2.8 and 3.7 m^3, respectively they had a better corresponding DU and AE. This was consistent with observations of Austin (2003) that higher inflow rate produce better irrigation efficiencies despite difficulties in managing large advance streams. Reduction of furrow length to 60 m produced average infiltrated depths, as determined by AFIF that improved distribution uniformity from all inflow rates. Even from the 20 L min^{-1} was from actual observations produced reasonably high measures of performance. This was in agreement with the view that shortening the furrow length would reduce differences in opportunity time between the furrow inlet and the end (Walker, 2003; Austin, 2003). For the 30 m furrow length the average infiltrated depths were decreasing proportional to opportunity time. Inconsistencies from the 80 and 160 L min^{-1} in the 60 m length could be attributable to overestimation of the opportunity time that included the ponding phase for the lower quarter of the furrow. Improvement of DU was remarkable from the 20 and 40 inflow rates while from the large rates it was stable. Such a phenomenon could

be explained by view upheld by Austin (2003) that small inflow rates on short furrows could achieve efficiencies as good as those from pressured systems. Interestingly, the average infiltrated depths between measured and predicted SWC from all inflow rates that wetted the 90 m point passed the homogeneity test, but the same inflow rates with the exception of the 40 L min^{-1} failed the same test for the 30 m furrow length. Could this mean that the applications of the larger inflow rates were ill posed for the 30 m furrow length?

6.5 Conclusion

The exercise of determining the appropriate inflow rate for micro-flood irrigation on the Tukulu soil was undertaken by a single irrigation with four different inflow rates on a 90 m long furrow. Surface water distribution during irrigation measured during the advance-supply and recession phases varied among the inflow rates. During the irrigation period the advance-supply phase demonstrated its dependence on the size of inflow rate. The 20 L min^{-1} required 2.7 hours to support an advance stream that went to zero at the 60 m point after 2.7 hours of irrigation time. The 40 L min^{-1} reached the 90 m after 1.8 hours while the 80 and 160 L min^{-1} becuase of their large streamflow size required 0.4 and 0.6 hours of irrigation time, respectively. The recession time was directly related to the size of inflow rate with the smaller inflow rates lasting less than 7 minutes while the larger rates lasted more than an hour.

Involvement of the HYDRUS-2D to predict initial and final SWC for the soil profile horizons provided further insight on the subsurface water distribution under the wetted furrows. It also aided to the application of the one point method for determining the AFIF for the respective inflow rates. Model inverse predictions were improved with minimum number of parameters optimised. Variations between the measured and predicted SWC as well as the AFIF were to be expected given soil spatial variations common in layered soils. However, conservation of mass was able to be improved when average infiltrated depth and adjustment of infiltration parameters was carried out.

Consistency of the infiltrated depth to opportunity time made it practical for the AFIF to approximated corresponding depth for the 30 and 60 m distance furrows. Assessment of subsurface water distribution indicated that the prismatic C-horizon of the Tukulu soil restricted deep drainage losses from all inflows rates irrespective of furrow length. Measures of performance reflected higher AE and DU from the 80 and 160 L min^{-1} inflow inflows at 90 m furrow distances. Reducing the furrow length to 60 and 30 m showed a remarkable

improvement in DU among the 20 and 40 L min^{-1} while for the larger inflow rates it remains more stable. Given the practicality of working with small inflow rates and the flexibility to adjust the time and frequency of irrigation it would be recommended that the 40 L min^{-1} inflow rate be adopted for furrow distances of less than 60 m.

Acknowledgements

Special thanks to the staff and management of Paradys experiment station of the technical and hospitality they provided during this experiment. Gratitude's to Ms Liesl van der Westhuizen for constructive suggestions on improving the writing of this manuscript.

6.6 References

Abbasi, F. Fayen, J. and van Genuchten, M. Th., 2004. Two-dimensional simulation of water flow and solute transport below furrows: model calibration and validation. *Journal of Hydrology,* 290: 63–79.

Abbasi, F. Jacques, D. Simunek, J. van Genuchten, M. Th., 2003. Inverse estimation of soil hydraulic and solute transport parameters from transient field experiments: Heterogeneous soil. *Am. Soc. Of Agric. Eng.*, 46: 1097-1111.

ASAE, 2003. Evaluation of Irrigated Furrows, ASAE EP419.1 FEB03, *American Society of Agricultural Engineers.*

Austin, C., 2003. Micro flood, a new way of applying water. http://waterright.com. 22/09/2011, 10.00 am (LT).

Awulachew, S B, Merrey, D J, Kamara, A B, van Koppen B, Penning de Vries F, Boelee E. 2005. Experiences and opportunities for promoting small-scale/micro irrigation and rainwater harvesting for food security in Ethiopia. International Water International Water Management Institute, Working paper 98, Addis Ababa, Ethiopia.

Bargar, B, Swan, J. B. and Jaynes, D., 1999. Soil water recharge under un-cropped ridges and furrows. *Soil Sci. Soc. Am. J.*, 63: 1290–1299.

Botha, J. J., 2006. Evaluation of maize and sunflower production in a semi-arid area using In-field rainwater harvesting. Ph.D. (Agric) Dissertation, University of the Free State, Bloemfontein, South Africa

Clemmens, A. J., Eisenhauer, D. E. and Maheshwari, B. L., 2001. Infiltration and roughness equations for surface irrigation: How form influences estimation. The Society for Engineering in Agricultural, Food and Biological Systems, Paper number 01-2255.

Clemmens, A. J. and Bautista, E., 2009. Toward physically based estimation of surface irrigation. *J. of Irrig.and Drain. Eng.*, 135: 588-596.

Hensley, M. Botha, J. J., Anderson, J. J., Van Staden, P. P., Du Toit, A. 2000. Optimising rainfall use efficiency for developing farmers with limited access to irrigation water. Pretoria, Water Research Commission report 878/1/00, South Africa.

Hensley, M., Le Roux, P., Gutter, J. and Zerizghy, M.G., 2007. A procedure for an improved soil survey technique for delineating land suitable for rainwater harvesting. WRC Report No. TT 311/07.Water Research Commission, Pretoria, South Africa.

Hillel, D. H., 2004. Environmental soil physics. Academic Press, New York, USA.

Hulugalle, N. R., McCorkell, B.E., Weaver, T.B., Finlay, L.A. and Gleeson J., 2007. Soil properties in furrows of an irrigated Vertisol sown with continuous cotton (Gossypium hirsutum L.). *Soil and Tillage Research,* 97: 162–171.

Lazarovitch, N., Warrick, A.W., Furman, A. and Zerihum D. 2009. Subsurface water distribution from furrows described by moments analyses. *J. of Irrig.and Drain. Eng.*, 135: 7-12.

Marquardt, D.W.,1963. An algorithm for least squares estimation of non-linear parameters. *J. Ind. Appl. Math.*, 11: 431-441.

Oyonarte, N. A., Mateos. L. and Palomo, M.J., 2002. Infiltration variability in furrow irrigation. *J. of Irrig.and Drain. Eng.*, 128:26-33.

Raghuwanshi, W.W. and Wallender, W.W. 1996. Modelling seasonal furrow irrigation. *J. of Irrig. and Drain. Eng.,*122: 235-242.

Rodriguez, J. A., Diaz, A., Reyes, J. A., and Pujols R. 2004. Comparison between surge irrigation and conventional furrow irrigation for covered black tobacco cultivation in a Ferralsol soil. *Spanish Journal of Agricultural Research,* 2: 445-458.

Romano, N., Brunone, B. and Santini, A.,1996. Numerical analysis of one-dimensional unsaturated flow in layered soils. *Advances in Water Res.*, 21: 315-324.

Schaap, M.G., Leij, F. J. and van Genuchten, M. Th., 2001. Rosetta: A computer program for estimating soil hydraulic parameters with hierarchical pedotransfer functions. *J. Hydrol.,* 25: 1163-176.

Scotter, D. R., Clothier, B. E. and Harper, E. R., 1982. Measuring saturated hydraulic conductivity and sorptivity using twin rings. *Australian Journal of Soil Research*, 20: 295-304.

Simunek, J. Sejna, M., and van Genuchten, M.Th., 2009. The HYDRUS-2D software package for simulating two-dimensional movement of water, heat and multiple solutes in variably saturated media, Version 2.0. Rep. IGCWMC-TPS-53, p. 251, Int. Ground Water Model.Cent., Colo. Sch. of Mines, Golden, CO.

Soil Classification Working Group, 1991. Soil Classification - A taxonomic system for South Africa. Memoirs on the Agricultural Natural Resources of South Africa No. 15. Department of Agricultural Development. Pretoria, South Africa.

Tabuada, M. A., Rego, Z. J. C., Vachaud, G. and Pereira, L. S., 1995. Two-dimensional infiltration under furrow irrigation, its validation and application. *Agricultural water management,* 27: 105-123.

van Genuchten, M.Th., 1980. A closed-form equation for predicting the hydraulic conductivity of unsaturated soils. *Soil Sci. Soc. Am. J.*, 44: 892-898.

Walker, W.R., 2003. Surface irrigation simulation evaluation and design - User Guide and Technical Documentation.Utah State University, Logan, Utah.

Wohling, T. H., and Maihol, J. C., 2007. A physically based coupled model for simulating 1-D and surface 2-D subsurface flow and plant water uptake in irrigation furrows. II: model test and evaluation. *J. of Irrig.and Drain. Eng.,* 133: 543-553.

World Reference Base for Soil Resources (1998). World soil resources report, 84, ISSS / ISRIC FAO, Rome, Italy.

CHAPTER 7

CHARECTERISING VERTICAL REDISTRIBUTION ON IRRIGATED SHORT FURROWS IN THE TUKULU SOIL

Abstract

Subsurface soil water redistribution in the Tukulu soil of South Africa also referred as the Cutanic Luvisols in other countries was evaluated on a closed ended, 90 m furrow. Following single run irrigation with 20, 40, 80 and 160 L min^{-1} inflow rate treatments, changes in soil water content (SWC) at the three profiles diagnostic horizons were monitored using a neutron water meter. Measurements were made at every 10 m distance starting from 5 m from the furrow inlet for a period of 455 hours from irrigation. The HYDRUS-2D software was used to estimate the soil hydraulic parameters through the inverse optimization algorithms for the redistribution process at the inlet, midpoint and furrow end of the different furrows. Models optimised parameters were comparable with initial estimates and the agreement between measured and predicted SWC was quite satisfactory, despite noticeable spatial variability. Calculated effective K-coefficient (K_{eff}) for the 0-600 and 0-850 mm profile flow domains demonstrated linearity with average SWC although inconsistencies under field conditions were inevitable. The underlying layer restricted gravity and augmented redistribution with K_{eff} assuming a steeper gradient than normal. Converting the linearity between K_{eff} and average SWC into a ratio assisted in quantifying redistribution of the infiltrated depth for the consecutive profile flow domains.

Key words: Soil water redistribution, inflow rates, effective unsaturated hydraulic conductivity, infiltrated depth, HYDRUS-2D.

7.1 Introduction

Subsurface soil water redistribution is one of the important determinants of furrow irrigation efficiencies. In recent times efforts towards improving furrow irrigation techniques has been complimented by advances in mathematical tools to describe the infiltration dynamics and the water flow and solute transport long after irrigation has ceased. The latter is referred as redistribution; a hydrological process depicting the transient flow of infiltrated water from the nearly saturated upper layers to the less infiltrated lower layers of the profile.

Soil water redistribution along furrows is dependent to a number of factors. Design factors include furrow shape, stream flow depth and wetted perimeter (Clemmens et al., 2001) while management factors embraces initial soil water content, crop and climate factors, and infiltrated depth (Lazarovitch et al., 2009). Another important determinant of redistribution is the soil hydraulic properties and their pertinent parameters. The soil water characteristics curve (SWCC) represents the unique relationship between the soil water content (SWC) and matric suction of a particular soil and the unsaturated hydraulic conductivity (K-coefficient) are the primary hydraulic functions widely used as input data into the governing flow equations. Despite the latter being the most difficult hydraulic property to measure, physical based approaches of describing the transient nature of redistribution requires accurate estimates of the K-coefficient (Hillel, 2004). The K-coefficient usually varies with depth as the upper and lower profile layers desorbs and wets monotonically. The effect of textural and structural spatiality on soil water redistribution across the flow domain results to a unique relationship between the infiltrated depth to the matrix suction and K-coefficient (Rubin, 1967; Leconte and Brissette, 2001; Hillel, 2004).

Various numerical methods with varying levels of complexity have become available for the estimation of K-coefficient along partially wetted furrows. One of these techniques is spatial moments (Aris, 1956), that has a strong pedigree with the description of movement and spread of a solute plume (Sudicky, 1986; Barry and Sporto, 1990; Srivastava et al., 2002). Recently, it has become popular in quantifying redistribution of soil water plume especially from drip and furrow irrigation systems (Gee and ward, 2001; Yeh et al., 2005; Lazarovitch, et al., 2007, 2009). This technique relies on SWC measurements to calculate the zeroth moment, first moment and second moments in one or more flow dimensions to describe the change in soil water storage, spatial variance of the centre of the plume and the spread of the plume, respectively. In a layered soil, the spatial heterogeneity of the flow domain is usually

treated as an equivalent homogeneous medium by means of ensemble mean or spatial average of the hydraulic properties. This concept was successfully demonstrated by Yeh et al. (2005) who estimated average or effective K-coefficient from the spatial moments. Previous work on effective hydraulic properties have found this approach acceptable and offering reasonable estimates of the average flow behaviour under spatially variable conditions (Warrick, 1991; Baker et al., 1999; Wildenschild and Jensen, 1999; Gastro et al., 2002).

An alternative method of estimating the hydraulic properties including the K-coefficient during redistribution is the inverse technique. Numerous studies have used this approach with great success (Wohling et al., 2004 and Wohling and Maihol, 2007) also in layered soils (Abbasi et al., 2003). Lazarovitch et al. (2009) used this technique to estimate the soil hydraulic parameters which were processed further to generate spatial moments for soil water plume below furrows. In essence the inverse method estimates the K-coefficient either as a function of SWC or matrix suction (h) from physical properties such as SWC and h that are easier to measure (Kool and Paker, 1988; Hopmans et al., 2002). Having evolved under laboratory conditions several hydraulic models that predict the K-coefficient from the SWCC curve (Brooks and Corey, 1964; van Genuchten, 1980; Kosugi, 1996) have become more available. Development of the physically based models such as the HYDRUS-2D code (Simunek et al., 2009) that includes inverse optimization algorithm has made the inverse method more attractive.

Growing need to improve food production has increased the cultivation of layered soils in the semi-arid areas of the Free State Province of South Africa. Such an initiate has been confronted with the dry soil water regime that is exacerbated by high runoff and evaporation losses from these soils. In response the in-field rainwater harvesting (IRWH) production technique (Hensley et al., 2000) was developed to transform surface runoff between crop rows into deep infiltration. Because of the restrictive layer underlying the profile of this group of soils, deep infiltration contributes to soil water storage. However, the need for supplementary irrigation during the prolonged dry spells has resulted into the adoption of micro-flood irrigation (MFI) from Austin (2003) that is currently being developed to operate alongside the IRWH technique. Given that subsurface water storage is a function of redistribution, it is therefore critical that the redistribution hydraulic properties be characterised before the two techniques are merged.

It was therefore against this background that the Tukulu (Tu), as a representative of the layered group of soils occupying more than 12 % of the provincial landscape, was used to describe how its profile horizon affected redistribution along short furrows under different inflow rates. The South African Tukulu is similar to the Cutanic Luvisols of the Reference Soil Group and covers an estimated 500 to 600 million hectares worldwide (World Reference Base for Soil Resources, 1998). The specific objectives of this study were firstly, to estimate the soil hydraulic parameters of the Tukulu soil that describes soil water movement during redistribution using the Levenberg-Marquardt parameter optimization algorithm. Secondly, to compare the HYDRUS-2D models predictions of field measured soil water content and calculated effective K-coefficient and thirdly to estimate the relationship between the rate of redistribution and infiltrated depth from furrows under different soil water regimes.

7.2 Material and methods

7.2.1 Experimental site

The field experiment was carried out at Parady's Experiment Farm (29°13'24, 69"S, 26°12'40, 93" E, altitude 1422 m) of the University of the Free State, South Africa. The selected site was predominately of the Tukulu soil form according to the Soil Classification Working Group (1991). The soil profile description is summarized in Table 7.1 and illustrated in a photo in Figure 7.1.

Table 7.1 Summary of the soil physical properties of the Tukulu soil form

Physical properties	Master horizons		
	A	B1	C
Coarse sand (%)	5.3	9.2	2.1
Medium sand (%)	9.3	8.8	3.8
Fine sand (%)	41.2	31	28.3
Very fine sand (%)	25.3	21	8.4
Coarse silt (%)	2.1	2	3
Fine silt (%)	4.6	2.5	6.5
Clay (%)	11.3	26.4	47.9
Bulk density (kg m^{-3})	1670	1597	1602
Porosity (%)	34.0	33	32.4
(Ks, mm $hour^{-1}$)	36.1	40	9.6

Ks= saturated hydraulic conductivity

(a)

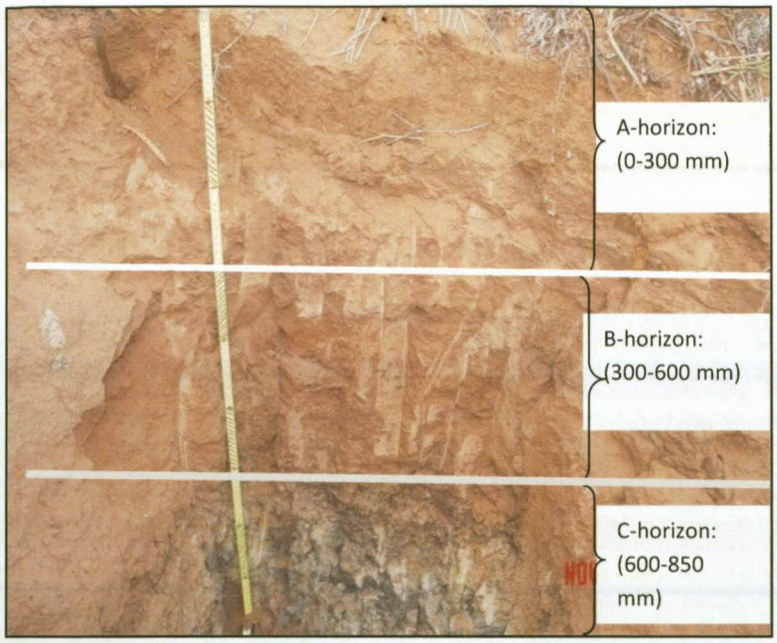

(b)

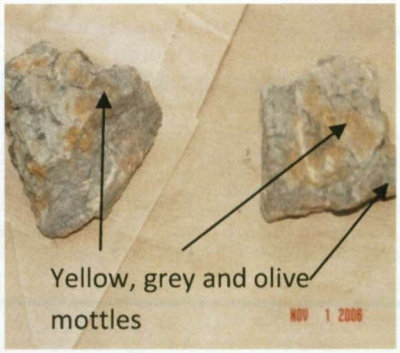

Figure 7.1 (a) Profile of the Tukulu and (b) mottles present in the C-horizon.

7.2.2 Experimental design and measurements

Redistribution of soil water in the Tukulu soil was characterized on 90 m distance furrows that has been irrigated with a single run. Four plots with three furrow replications were systematically assigned to four inflow rates including the 20, 40, 80 and 160 L min^{-1}. Only the central furrow in a plot was installed with neutron access tubes of 1. 2 m long at 10 m distance intervals starting from the 5 m from the furrow inlet. An area of 2 m by 2 m around each access tube was covered with a plastic to minimise the influence of evaporation on subsurface water redistribution as shown in Figure 7.2. A site calibrated neutron soil water meter was used to monitor the change in SWC during the redistribution period that commenced immediately after the depletion-recession phase of irrigation. Measurements were taken two times a day for the first week and then daily for a fortnight taken at depths of 150 mm, 450 mm, and 725 mm.

Figure 7.2 Shading of the furrow section measurement stations at 10 m intervals.

7.2.3 Description of the soil hydraulic properties

Soil water characteristic curve (SWCC) corresponding to the diagnostic A-, B- and C-horizons of the Tukulu soil was determined by using a combination of the hanging water column method and the pressure chamber plate desorption technique. The hanging water column measured the matric suction (h) and soil water (θ) relationship for a range of 0 to -10kPa, while suctions from -10 to -1500 kPa mm were measured using chambers of various pressure sizes. The resulting θ-h relationship was then parameterised using the closed-form equation of van Genuchten (1980) expressed as:

$$\theta(h) = \theta_r + \frac{\theta_{s-}\theta_r}{\{1 + |\alpha h|^n\}^m} \qquad (7.1)$$

Where θ_s and θ_r are the respective saturated and residual values of the volumetric soil water content, θ (mm mm^{-1}), h is the matric suction (kPa), while α and n are the shape and pore size distribution parameters, respectively. The condition m=1-1/n should be satisfied and θ (h) equals θ_s when at zero or positive suctions. Parameters related to pore-size distribution (n) and shape (α) of the SWCC was estimated from the Rosetta pedo-transfer (Schaap et al., 2001) in agreement with the field measured saturated hydraulic conductivity (Ks). Table 7.2 summarizes the initial estimates of soil hydraulic parameters for the Tukulu soil horizons before optimization.

Table 7.2 Initial estimates of soil hydraulic parameters.

Parameters	A	B	C
θ_s (mm mm^{-1})	0.34	0.33	0.32
θ_r (mm mm^{-1})	0.13	0.12	0.26
α	0.00116	0.00094	0.005
n	1.773	1.617	1.226
K_s (mm hour^{-1})	36.1	40	9.6

7.2.4 Prediction of two-dimensional redistribution

A two-dimensional soil water movement during redistribution on irrigated furrows was predicted using the HYDRUS-2D software (Simunek et al. 2009). This model numerically solves the two dimensional form of the Richard flow equation and able to improve parameter optimization by using the Levenberg-Marquardt non linear- squares approach (Marquardt, 1963). The HYDRUS-2D code has been successfully employed in simulating studies of subsurface soil water distribution during furrow irrigation and redistribution (Abbasi et al., 2004; Wohling and Maihol, 2007; Lazarovitch et al., 2009).

In this paper soil water movement during redistribution was inversely predicted using SWC measurement versus time as the objective function. To improve the models predictions the laboratory based SWCC hydraulic parameters had to be optimised (Abbasi et al., 2004). Any of the parameters that were found to improve predictions was selected, but a combination of more than three parameters was discouraged given the instability of the inverse optimization method (Abbasi et al., 2003; Simunek et al., 2009). A soil profile flow domain of 2 000 mm by 850 mm with the trapezoidal furrow shape at the symmetric position were used in this exercise. The flow domain was described by a finite element mesh of 50 mm and discretisized into three layer materials. Final pressure head from the irrigation phase was exported as the initial pressure condition for the redistribution phase. The zero flux boundary condition was assigned at the soil surface, inside the furrow, and along the vertical sides of the flow domain. A free drainage boundary condition was selected for the bottom of the soil profile. Three furrow distant sections were used for model predictions including the 5 m, 35 m and 55 m from the 20 L min^{-1} inflow rate furrow, because the advance stream could not reach the furrow end. In the 40, 80 and 160 L min^{-1} inflow rate furrows the three distant sections used were the 5 m, 55 m, and the 85 m.

7.2.5 Experimental data analysis

The measured and predicted SWC were used to characterise the redistribution process with respect to depth and time. Firstly, the measure of dispersion between the measured (M) and predicted (P) soil water content (θ) from the various soil profile horizons of the three respective furrow distant sections was determined. To this condition the following simple mathematical expression was found to be convenient for this purpose:

$$\left|\frac{\Delta\theta_P}{\Delta\theta_M}\right| \tag{7.2}$$

Wherever, the predicted and measured variations of SWC are similar, this ratio being of the order of one. Soil water content measurements at 150 mm, 450 mm, and 725 mm depths allowed the profile to be discretised into two flow domains, 0-600 mm and 0-850 mm, applicable to describe redistribution under different soil water regimes. The redistribution flux across these flow domains was quantified using the unsaturated hydraulic conductivity (K-coefficient) and the hydraulic gradient that operated between the upper nearly saturated layer and the lower layer that has been less infiltrated. The inter block or effective K-coefficient (K_{eff}) was thought to be appropriate for the Tukulu soil profile. Given the assumption that furrow irrigation usually leaves the upper layer nearly saturated compared to the lower unsaturated layers, the Darcian flux expression for redistribution from Gasto et al., (2002) was simplified to become:

$$q_{eff} = K_{eff}\left[\frac{h_L - h_U}{z_L - z_U} + 1\right] \tag{7.3}$$

Where, q_{eff} is the average flux between the upper (U) and lower (L) horizons, h_L and h_U and Z_L and Z_U representing the corresponding matrix suctions and depths of the horizons in questions. Unity value was assigned to the gravitational gradient ($\Delta z/\Delta z$) with the positive sign for downward water flow. The horizons thickness was also considered to be large enough for the redistribution process to be consistent with the principles of K_{eff}. Before irrigation and at the onset of redistribution it was assumed that profile layers not infiltrated to near saturated are near residual SWC and that redistribution flux was a function of K_{eff} and infiltrated depth. The geometric mean as described by Warrick (1991) was used to estimate the effective SWC and K-coefficient for the 0-600 mm and 0-850 mm selected soil profile flow domains.

The rate of distribution was therefore taken to be represented by the ratio of the derivatives of the estimated K_{eff} and soil water content of the flow domain (0- 600 mm or 0-850 mm) of interest. This analogy is fairly similar to that of Yeh et al. (2005) used to describe the rate of change of the first spatial moments in the z direction (Vz) written as:

$$\frac{dK_z}{d\theta} = Vz(\theta) \tag{7.4}$$

The resulting derivatives from the three furrow distant sections were then plotted against the corresponding measured infiltrated depth to obtain a linear relationship between redistribution and infiltrated depth. This function could be been extended, if adequate data was available, to determine the moisture diffusivity length ($\boldsymbol{\lambda}$) described by Yeh et al., (2005) as follows:

$$\lambda(\theta) = \frac{D(\theta)}{\frac{dK(\theta)}{d\theta}} \tag{7.5}$$

7.2.6 Statistical analysis

The quality fit between the measured and estimated SWC during the redistribution period was evaluated using the 1:1 line. The coefficient of determination (R^2), root mean square error (RMSE) and the index of agreement or D-index as proposed by Willmot et al. (1985) were also used. The Bartlett's test (Gomez and Gomez, 1984) was preferred for evaluating the homogeneity of the error variances between K-coefficients calculated from averages of measured and predicted SWC

7.3 Results

7.3.1 Parameter optimization and HYDRUS-2D inverse solution

Table 7.3 shows a summary of the various parameters optimised at various points of the furrow that received different inflow rates. Statistical measure of quality of fit was also shown. A comparison between the measured and predicted SWC was drawn on a 1:1 line presented in Figure 7.3 along with the coefficient of determination (R^2). The parameter most sensitive to the optimisation procedure was the θ_s followed by the θ_r and n, with the α and Ks being the least.

Table 7.3 Optimised parameters to improve HYDRUS-2D model prediction.

Inflow rate ($L\ mm^{-1}$)	Distance (m)	Horizons	Hydraulic parameters						
			θ_s	θ_r	α	n	K_s	RMSE	D-index
20	5	A	0.331	-	-	1.522	-	0.008	0.905
		B	0.319	-	-	-	-	-	-
		C	0.313	-	-	1.297	-	-	-
	35	A	0.331	-	-	1.522	-	0.014	0.853
		B	0.319	-	-	-	-	-	-
		C	0.313	-	-	1.297	-	-	-
	55	A		0.160	-	-	-	0.013	0.931
		B		0.206	-	-	-	-	-
		C		0.199	-	-	-	-	-
40	5	A	0.327	0.271	-	-	139	0.012	0.57
		B	0.329	0.303	-	-	266	-	-
		C	0.330	0.267	-	-	4	-	-
	55	A	0.346	-	0.001	-	-	0.027	0.565
		B	0.349	-	1.222	-	-	-	-
		C	0.294	-	0.005	-	-	-	-
	85	A	0.275	-	0.001	-	-	0.022	0.844
		B	0.381	-	0.0004	-	-	-	-
		C	0.276	-	0.012	-	-	-	-
80	5	A	0.337	-	-	1.570	-	0.025	0.295
		B	0.333	-	-	1.290	-	-	-
		C	0.306	-	-	1.342	-	-	-
	55	A	0.340	-	-	1.525	-	0.022	0.800
		B	0.343	-	-	1.223	-	-	-
		C	0.274	-	-	1.182	-	-	-
	85	A	0.324	0.241	-	-	-	0.008	0.957
		B	0.286	0.259	-	-	-	-	-
		C	0.323	0.318	-	-	-	-	-
160	5	A	0.328	0.260	-	-	-	0.007	0.925
		B	0.278	0.261	-	-	-	-	-
		C	0.307	0.261	-	-	-	-	-
	55	A	0.326	0.225	-	-	-	0.012	0.922
		B	0.280	0.240	-	-	-	-	-
		C	0.332	0.318	-	-	-	-	-
	85	A	0.340	0.181	-	-	-	0.019	0.788
		B	0.330	0.167	-	-	-	-	-
		C	0.320	0.308	-	-	-	-	-

θ_s = Saturated volumetric water content; θ_r= Residual volumetric water content;α = pore shape or geometry parameter; n = pore size distribution parameter; K_s = Saturated hydraulic conductivity; RMSE = root mean square error; and D-index= index of agreement

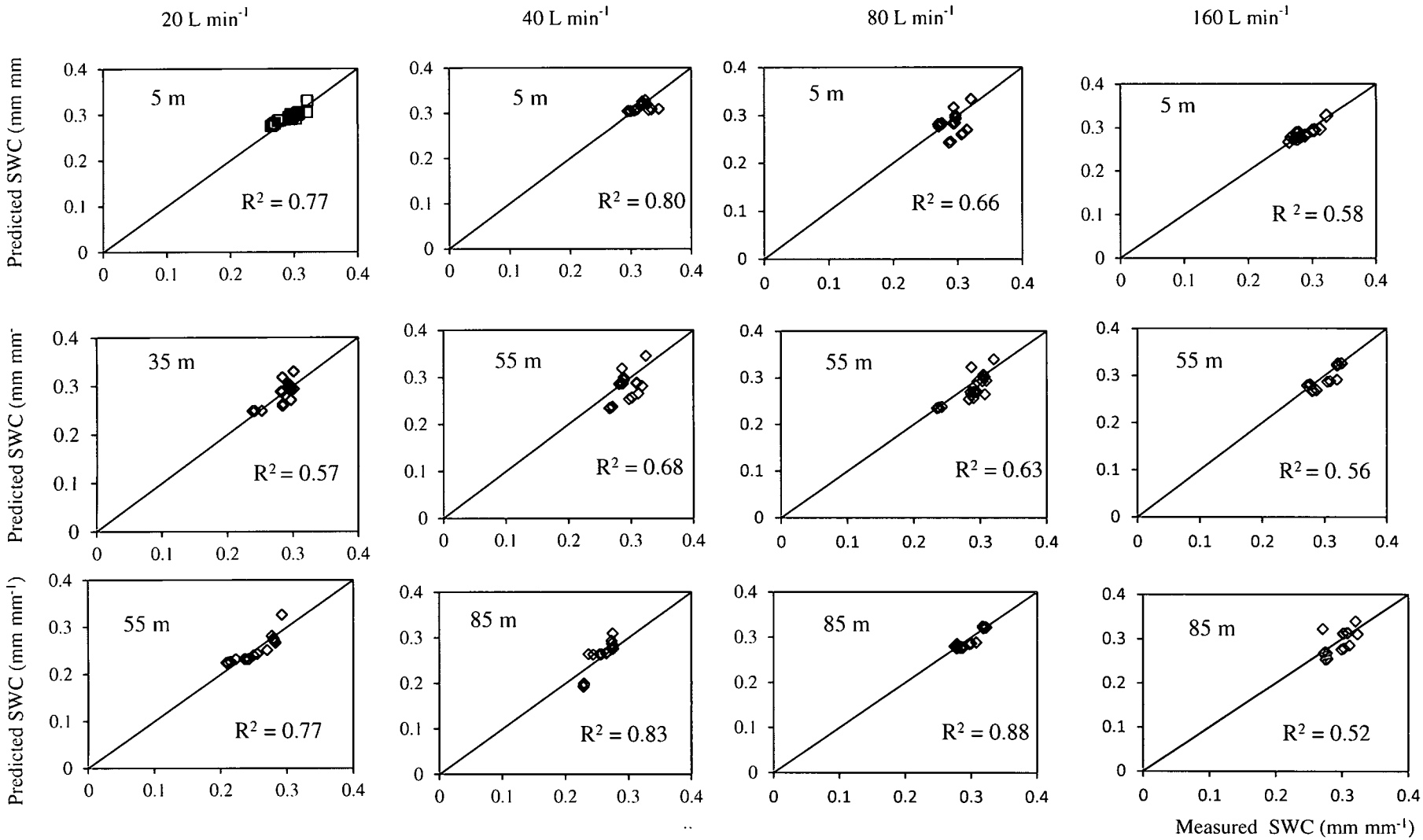

Figure 7.3 Measured and predicted soil water content (SWC) of the soil profile during redistribution from the 20, 40, 80 and 160 L min^{-1} inflow rates at various furrow distances covered by the advance stream.

Optimised θ_s were highly variable among the inlet, midpoint and furrow end with the exception in the 20 L min^{-1} inflow rate furrow where values were similar for both 5 and 35 m distances. Optimised θ_s values that were similar to the initial estimates were only observed in the 160 L min^{-1} inflow rate furrow at the 85 m distance point. Comparable to the initial estimates were noticed among the A- and B-horizons, especially in the 80 L min^{-1} inflow rate furrow. Only in the 160 L min^{-1} inflow rate furrow was the θ_r optimised at all three distance points and all cases showing greater variability with the exception in the 5 m point where almost the same value was assigned to the soil horizons. Similarly, the n assumed different values along the furrow length and in depth that were not comparable with the initial estimates with the exception in the C-horizon of the 55 m point from the 80 L min^{-1} inflow rate furrow. The α and Ks were optimised once and it was in the 40 L min^{-1} inflow rate furrow at the 85 m and 5 m points, respectively. The α value showed similarities with the initial estimates especially in the A and C-horizons while the Ks values were not comparable at all depths.

The quality of fit from the optimised parameters when the HYDRUS-2D was initialized exhibited variability along the furrow distance points from the four inflow rate treatments. The R^2 ranged from 0.57 to 0.77, 0.68 to 83, 0.63 to 0.88 and 0.52 to 0.58 for the 20, 40, 80 and 160 L min^{-1} inflow rate furrows, respectively. Corresponding RMSE and D-index ranged from 0.013 to 0.008 and 0.85 to 0.93, 0.027 to 0.012 and 0.57 to 0.84, 0.25 to 0.008, 0.295 to 0.96, 0.019 to 0.007 and 0.788 to 0.925, respectively.

7.3.2 Changes in soil water content during redistribution

The changes in SWC with depth from the inlet, mid and furrow end from the different inflow rates at different times of redistribution were summarized in Figure 7.4. Results are given by means of a XY one dimensional curves to provide a simply comparison between the measured and predicted SWC. Table 7.4 illustrates the measure of dispersion between the measured and predicted SWC at the different horizon layers from the four inflow rate treatments. For simplicity the time intervals of 0, 45 and 455 hours from the onset of redistribution were assumed to be applicable to all four inflow rate furrow treatments. Changes in SWC were indicated by the prefix (-) if representing a loss in volumetric SWC from the flow domain while the prefix (+) represented a gain.

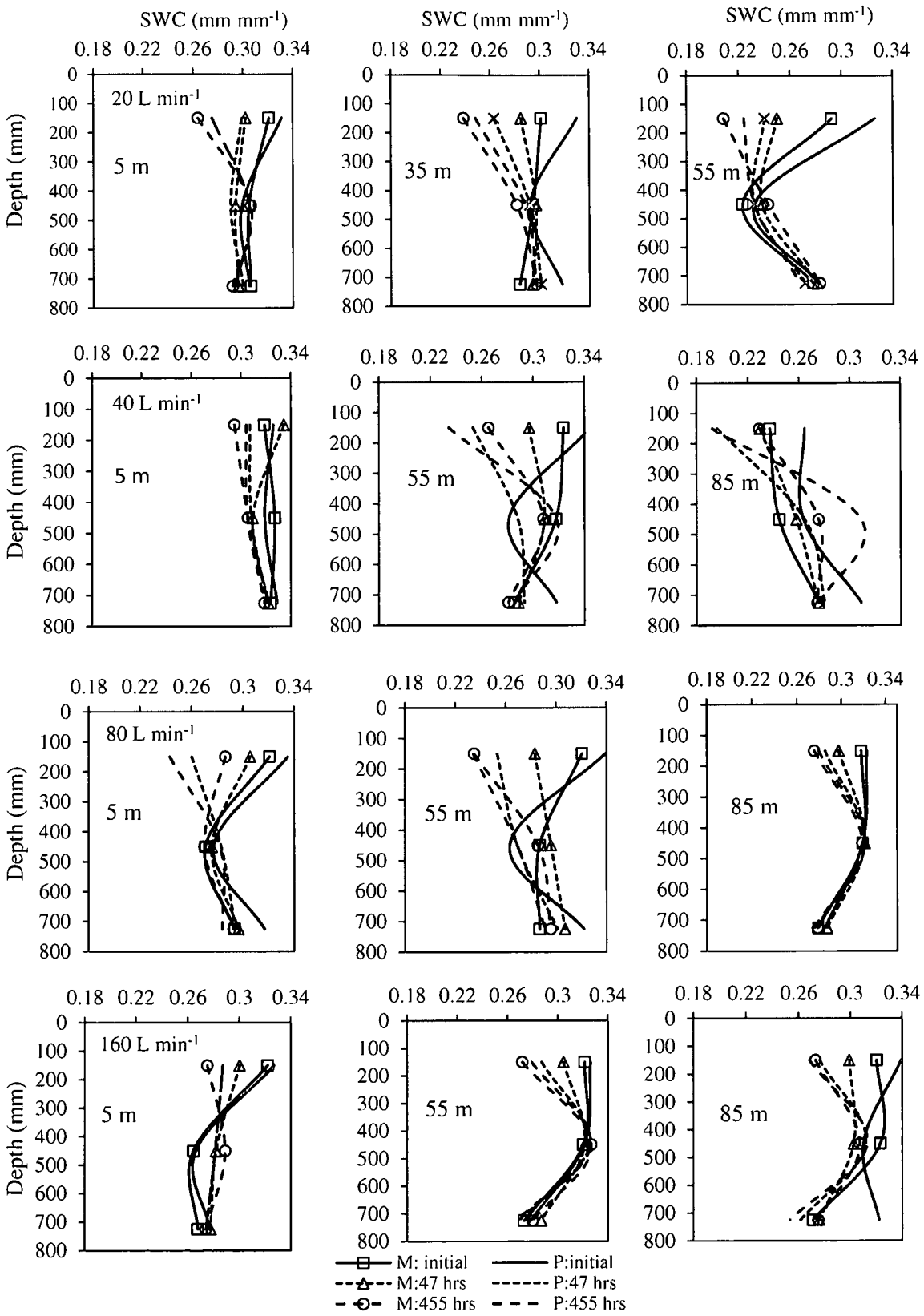

Figure 7.4 Measured and predicted soil water content (SWC) for the initial and selected time intervals during redistribution at different furrow distances and soil profile depths for the 20, 40, 80 and 160 L min^{-1} inflow rates.

Along the 20 L min^{-1} inflow rate furrow, changes between the measured and predicted SWC during the 455 hour redistribution period were variable in space and time. Changes in volumetric SWC, with respect to layers thickness of 300 mm for the A and B-horizons and 250 mm for the C-horizons, were -17, -9 and -4 mm for the respective A, B and C-horizons at the 5 m furrow section. Predicted volumetric SWC for the corresponding horizons was -16, +2 and -3 mm. Dispersion between the measured and predicted SWC was 1.0, 3.9 and 0.8 from the respective A, B and C-horizons. At the 35 m furrow section changes in measured volumetric SWC were -19,-4 and +3 mm while from the predicted was -24, -1 and -5 mm, from the respective A, B and C-horizons. At the 55 m furrow section, measured volumetric SWC changed by -25, +6, and +1 while the predicted changed by -31, 0 and -4 mm, from the respective A, B and C-horizons. Corresponding dispersion between measured and predicted SWC at 35 and 55 m furrow sections for the profile horizons ranged from 0.3 to 1.6 and 0 to 2.6, respectively.

In the 40 L min^{-1} inflow rate furrow, after the 455 hour of redistribution measured volumetric SWC at the 5 m furrow section had changed by -7 mm from the A and B-horizons and -1 mm from the C-horizon. The predicted volumetric SWC recorded changes of -7, -4 and -3 mm from the respective A, B and C-horizon. Corresponding changes from the measured and predicted volumetric SWC at the 35 furrow section were -18, -3 and -1 mm and -33, +11 and -8 mm, respectively. At the 85 m furrow section changes from the measured and predicted volumetric SWC amounting to -2.5, +9, and -8 mm and -22, +14 and -8.3 mm, respectively were observed corresponding to the A, B and C-horizons. Measure of dispersion between the measured and predicted SWC ranged from 0.6 to 2.0, 1.9 to 7.1, and 1.5 to 25.2 from the 5, 55 and 85 m soil profile horizons, respectively.

From the 80 L min^{-1} inflow rate furrow, noticeable changes in volumetric SWC after the 455 hour redistribution at the 5 m furrow section were amounting to -10, -0.24 and -0.23 from the measured while from the predicted were -28, +1.5 and -8.3 mm from the respective A, B and C-horizons. After 47 hours gains of 1.5 and 1 mm from the measured SWC were noticed from the B and C-horizons, respectively. At the 55 m furrow section at the of the redistribution period the volumetric SWC has changed by -26, -0.4 and +2.2 mm from the measured while the predicted by -32, +2 and 8 mm, from the respective A, B and C-horizons. After 47 hours of redistributions the measured volumetric SWC had recorded changes of -11, +3 and +5 mm from the corresponding profile horizons.

Table 7.4 Measure of dispersion between the measured and predicted soil water content (mm mm^{-1}).

		Horizons		
Inflow rate	Distance (m)	A	B	C
20	5	0.98	3.90	0.75
	35	1.31	0.31	1.55
	55	1.22	0.00	2.60
40	5	0.91	0.64	1.95
	55	1.89	3.81	7.05
	85	8.80	1.48	25.15
80	5	2.67	6.17	36.28
	55	1.22	4.36	3.55
	85	1.03	4.72	24.41
160	5	0.85	0.61	0.49
	55	0.95	0.78	1.64
	85	1.49	0.19	16.67

In the 85 m furrow point, the measured and predicted volumetric SWC at the 455 hour of redistribution recorded changes amounting to -13, -0.13 and +0.1 mm, and -13, +0.6, and -3 mm, corresponding to the A, B and C-horizons, respectively. Measure of dispersion at the 5, 55 and 85 m furrow sections for the profile horizons ranged from 2.7 to 36.3, 1.2 to 4.4, and 1.0 to 24.4, respectively.

Noticeable changes in volumetric SWC after the 455 hours of redistribution from the 160 L min^{-1} inflow rate furrow were 14, +7, +2 mm, and 12, +5 and 1 mm from the measured and predicted at the 5 m furrow section. At 47 hours the measured volumetric SWC recorded -6, +5 and +2 while the predicted -10, +4 and -1 mm, for the respective A, B and C-horizons. At the 55 m distance, by the end of the redistribution period the measured volumetric SWC recorded changes of -15 mm in the A-horizon and +2 mm from the B and C-horizons. Changes from the predicted values were -14, -2 and +3 mm from the respective A, B and C-horizons. After 47 hours the measured volumetric SWC recorded -5, +0.3 and +3.4 mm from the corresponding A, B and C horizons. At the 85 m furrow section, the measured volumetric SWC had changed by -14, -5 and +1 mm from the respective A, B and C- horizons after the 455 hours of redistribution. The predicted had changed by -21, -1 and -17 mm from the corresponding horizons. Dispersion between the measured and predicted SWC ranged from 0.5 to 0.9, 0.8 to 1.6 and 0.2 to 16.7 for the 5, 55 and 85 m furrow sections among the soil profiles horizons.

7.3.3 Estimated effective K-coefficient during redistribution

Figures 7.5 to 7.8 illustrates the variation in the estimated K-coefficient from the measured and predicted SWC for the 20, 40, 80 and 160 $Lmin^{-1}$ inflow rate treated furrows. Redistribution at soil profile depths ranging from 0-600 and 0-850 mm were characterised using average K-coefficient (K_{eff}). Homogeneity test calculated from measured and predicted SWC were illustrated in Table 7.5.

The calculated K_{eff} from the measured and model prediction values showed considerable variations along the 20 L min^{-1} inflow rate furrow. At the 5 m furrow section it varied from 0.7 to 0.023 mm $hour^{-1}$ and 25 to 4.4 mm $hour^{-1}$ from the respective measured and predicted values for the 0-600 mm depth. At 0-850 mm depth estimates from the measured values ranged from 0.6 to 0.006 while from model predictions the K_{eff} ranged from 6 to 0.6 mm $hour^{-1}$. At the 35 m furrow section from the 0-600 mm depth, the K_{eff} values ranges from 0.2 to 0.009 mm mm^{-1} and 0.6 to 0.06 mm $hour^{-1}$ were observed from the measured and model predictions, respectively. Variations at the 0-850 mm depth ranged from 0.05 to 0.02 mm $hour^{-1}$ from the measured and 2.4 to 0.06 mm $hour^{-1}$ form models predictions. At the 0-600 and 0-850 mm depths from the 55 m point the estimated K_{eff} ranged from 0.15 to 0.005 mm $hour^{-1}$ and 0.04 to 0.001 mm $hour^{-1}$ from the measured and from 0.31 to 0.002 mm $hour^{-1}$ and 0.02 to 0.0002 mm $hour^{-1}$, consecutively. The K_{eff} estimated from measured and model predictions was found to homogeneous for the 0-850 mm profile domain at 35 and 55 m furrow sections.

Estimated K_{eff} from the 40 L min^{-1} inflow rate furrow varied between 0.13 to 0.01 mm $hour^{-1}$ and 0.63 to 8.3E-07 mm $hour^{-1}$ at the 5 m section from the measured and predicted values within the 0-600 mm depth. At the 0-850 mm depth it ranged from 0.33 to 0.007 mm $hour^{-1}$ from the measured and 1.41 to 0.0004 mm $hour^{-1}$ from the model predictions. At the 55 and 85 m furrow sections, the estimated K_{eff} from measured values within the 0-600 mm depth ranged from 1.4 to 0.004 mm $hour^{-1}$ and 0.002 to 0.00004 mm $hour^{-1}$, respectively while in the 0-850 mm depth from 1.4 to 0.004 mm $hour^{-1}$ and 0.001 to 0.00003 mm $hour^{-1}$. Corresponding to the consecutive furrow sections from model predictions was the K_{eff} ranging from 1.31 to 0.004 mm $hour^{-1}$ and 0.9 to 0.04 mm $hour^{-1}$ at 0-600 mm depth while at the 0-850 mm depth it ranged from and 3.5 to 0.0003 mm $hour^{-1}$ and 2.9 to 0.46 mm $hour^{-1}$, respectively.

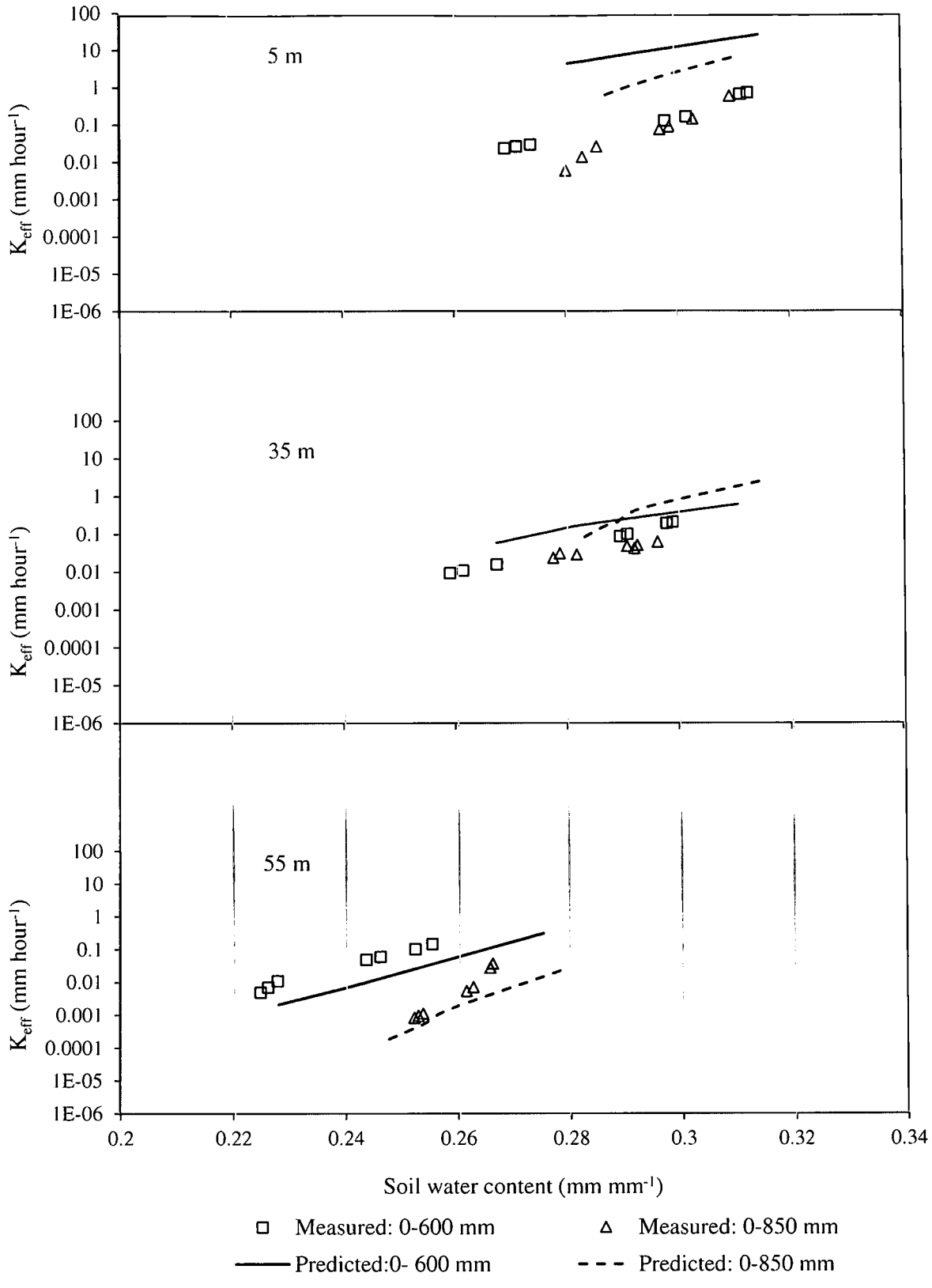

Figure 7.5 Effective K-coefficient from the furrow treated with 20L min^{-1} inflow rate for the 0-600 and 0-850 mm infiltrated depths at the 5 m, 35 m and 55 m distances

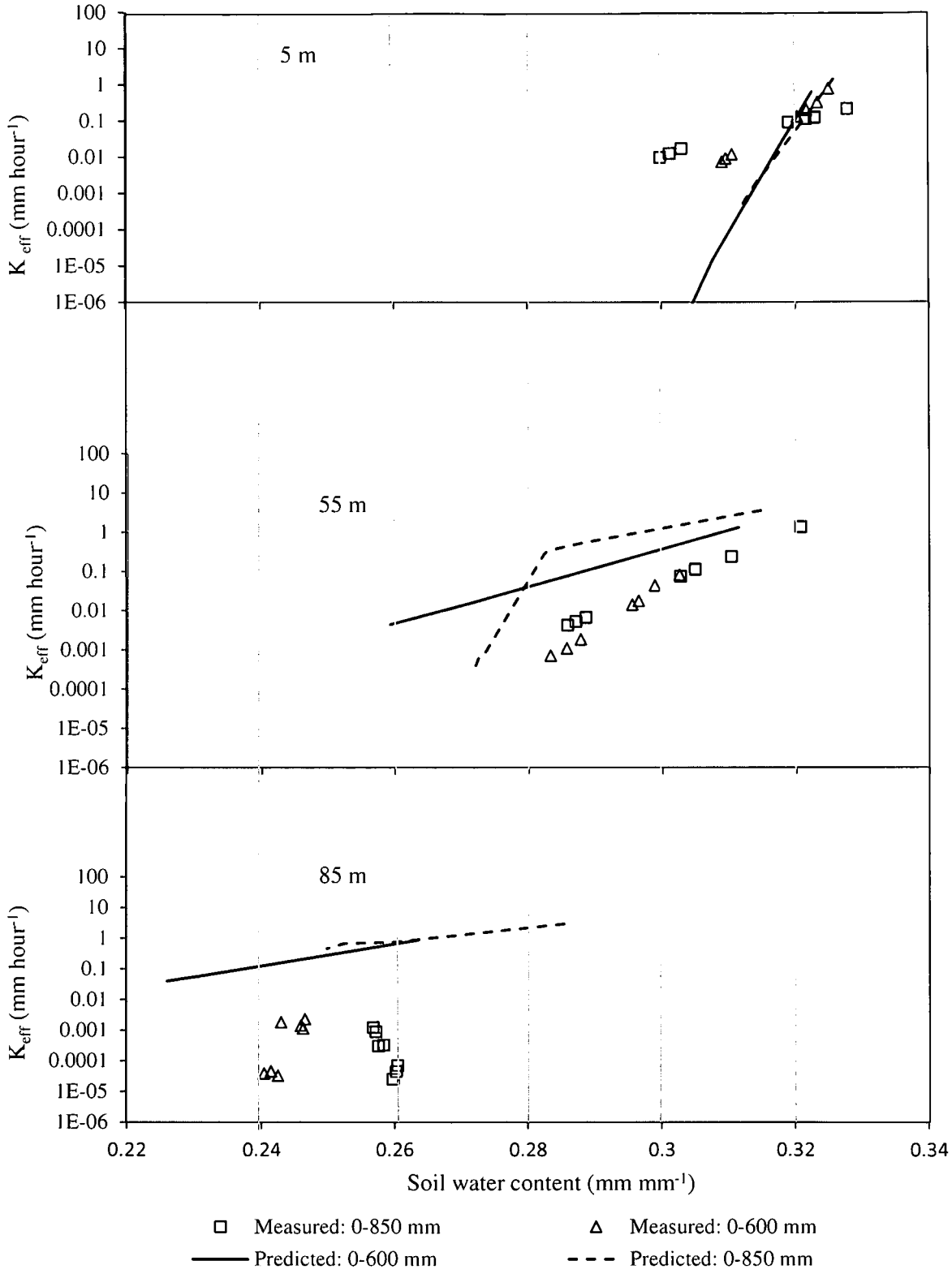

Figure 7.6 Effective K-coefficient from the 40 L min^{-1} inflow rate at 0-600 and 0-850 mm infiltrated depths of the 5 m, 55 m and 85 m furrow distances.

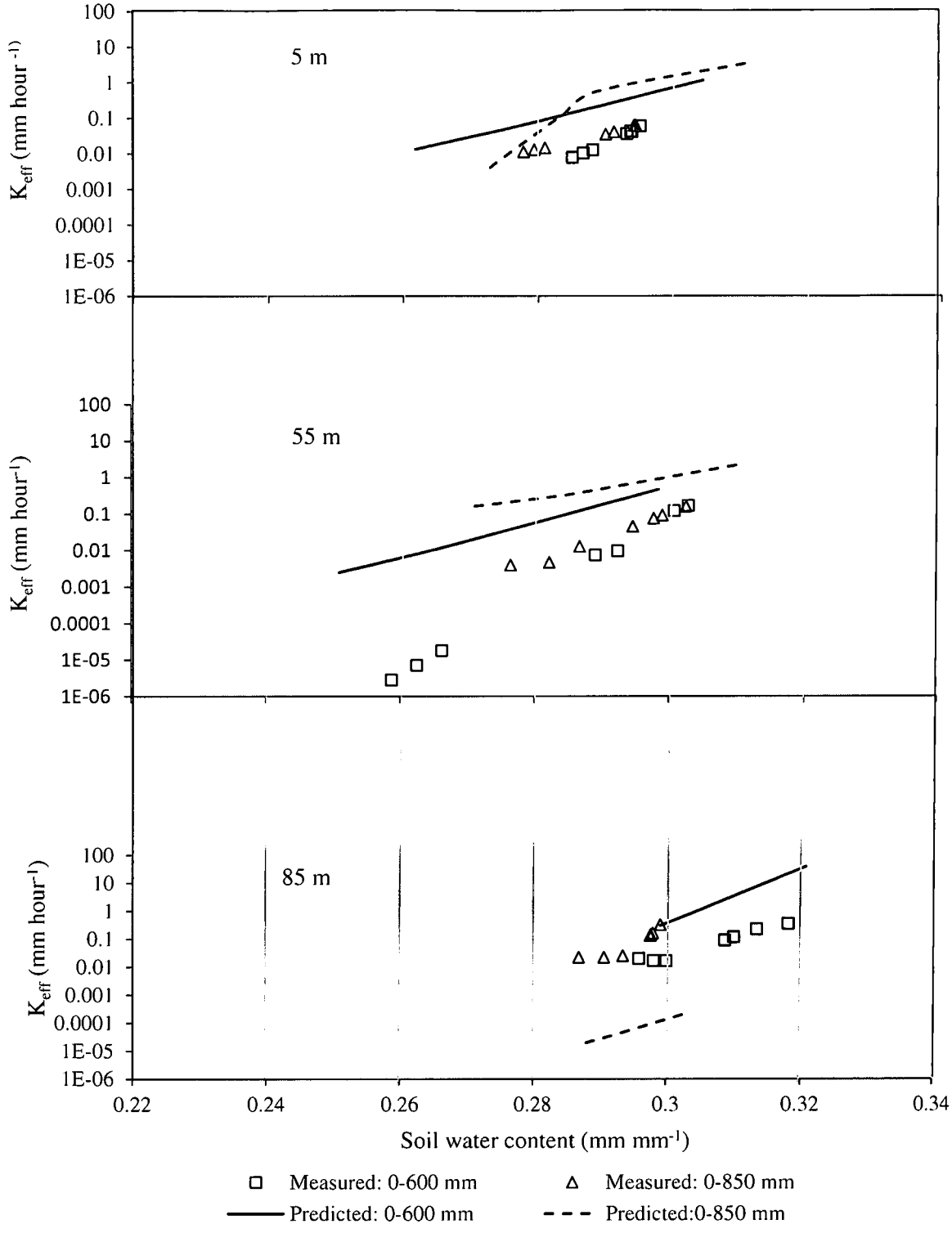

Figure 7.7 Effective K-coefficient from the 80 L min^{-1} inflow rate at 0-600 and 0-850 mm infiltrated depths of the 5 m, 55 m and 85 m furrow distances.

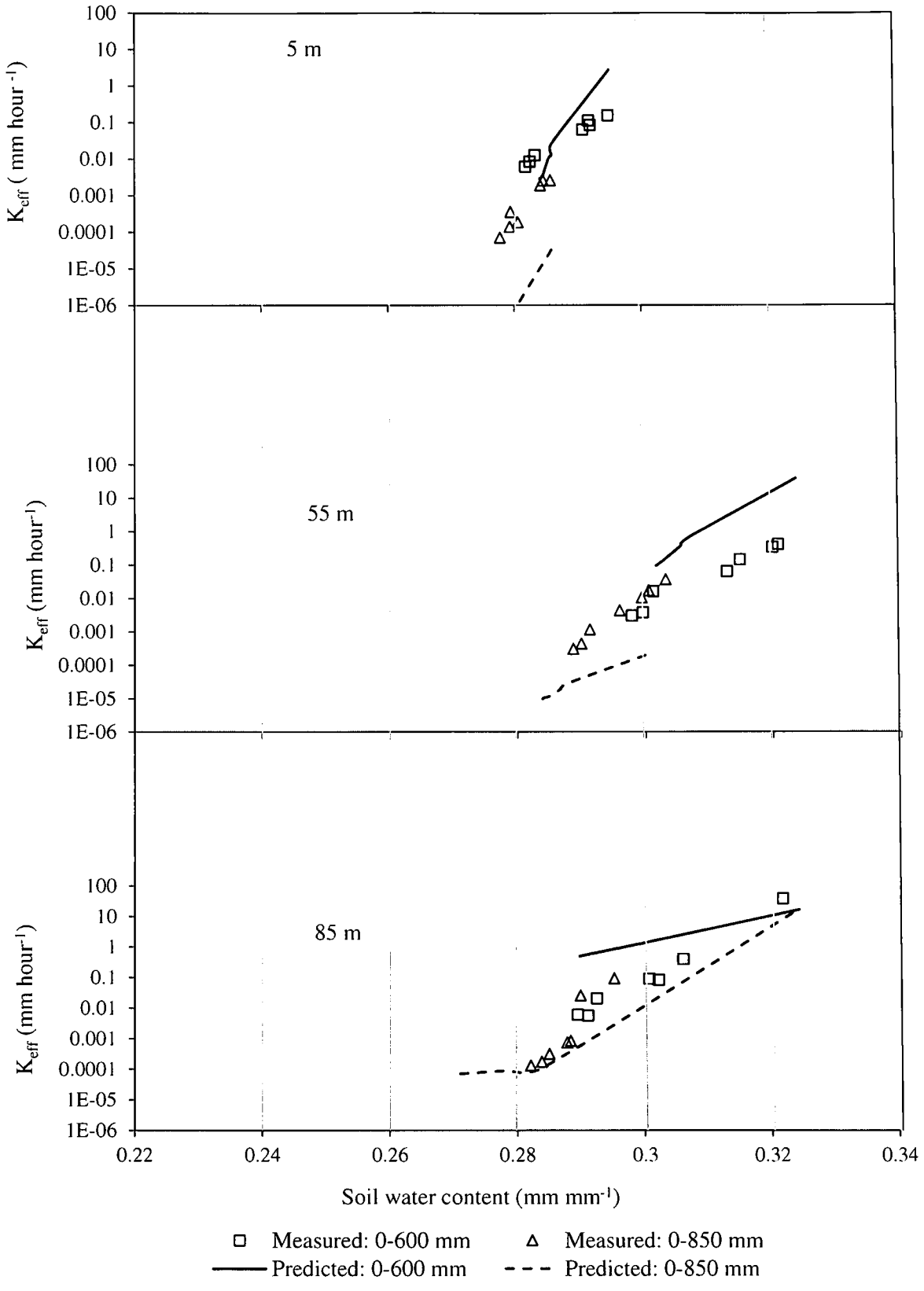

Figure 7.8 Effective K-coefficient from the 160 L min^{-1} inflow rate at 0-600 and 0-850 mm infiltrated depths of the 5 m, 55 m and 85 m furrow distances

Table 7.5 Homogeneity test for the effective K-coefficient calculated from measured and predicted soil water contents.

Inflow rate (L min^{-1})	Distance (m)	Bartlett's test analysis: Profile depth (M)	Computed $\chi 2$	Tabular $\chi 2_{(0.05,2)}$
20	5	0-600	28.16	3.84
		0-850	21.07	3.84
	35	0-600	9.53	3.84
		0-850	**0.41**	3.84
	55	0-600	9.96	3.84
		0-850	**0.02**	3.84
40	5	0-600	**2.10**	3.84
		0-850	34.00	3.84
	55	0-600	46.70	3.84
		0-850	**3.44**	3.84
	85	0-600	**0.02**	3.84
		0-850	**2.37**	3.84
80	5	0-600	**0.59**	3.84
		0-850	**1.55**	3.84
	55	0-600	8.68	3.84
		0-850	**0.50**	3.84
	85	0-600	24.59	3.84
		0-850	5.83	3.84
160	5	0-600	10.31	3.84
		0-850	**0.0003**	3.84
	55	0-600	29.28	3.84
		0-850	**0.00004**	3.84
	85	0-600	106.34	3.84
		0-850	4.11	3.84

Bold = passed homogeneity test at 0.05 $\chi 2$ Test

At 5m and 55m furrow length sections the estimated K_{eff} passed the homogeneity test at the 0-600 mm and 0-850 mm soil profile flow domains, respectively. At the 85 m furrow length section the measured and estimated K_{eff} were found to be homogeneous at both 0-600 mm and 0-850 mm profile flow domains.

Substantial variations in estimated K_{eff} were also observed in the 80 L min^{-1} inflow rate furrow. At the 5 m furrow section at depths of 0-600 mm and 0-850 mm the measured values ranged from 0.06 to 0.01 mm hour^{-1} and 0.04 to 0.008 mm hour^{-1}, respectively. Estimates from the models predictions ranged from 1.1 to 0.013 and 3.25 to 0.004 mm hour^{-1} for the respective consecutive depths. The K_{eff} at the 55 m furrow section from the 0-600 and 0-850

mm depths varied from 0.17 to 2.9 x 10^{-6} mm hour^{-1} and 0.05 to 0.004 mm hour^{-1} from the measured values while from the model predictions it ranged from 0.46 to 0.002 mm hour^{-1} and 2.1 to 0.15 mm hour^{-1}, respectively. In the 85 m furrow section the K_{eff} within 0-600 mm depth fell in the range of 0.35 to 0.02 mm hour^{-1} and 38 and 0.3 mm hour^{-1} for the measured and models predictions at 0-850 mm depth was in the range of 0.3 to 0.02 and 0.0002 to 1.73E-05 for the consecutive soil profiles depths. The estimated K_{eff} for measured and model predictions passed the homogeneity test at 0-600 mm and 0-850 mm profiles flow domains at the 5 m furrow section and at the 0-850 mm profile domain for the 55 m section.

Variable spatiality was also noticeable at the 160 L min^{-1} inflow rate furrow. The K_{eff} at the 5 m section was in the range of 0.11 to 0.01 mm hour^{-1} and 0.004 to 0.0001 mm hour^{-1} for the measured values from the respective 0-600 mm and 0-850 mm depths. Corresponding values from model predictions for the respective consecutive depths ranged from 2.73 to 0.003 and 0.00003 to 1.7E-07 mm hour^{-1}. At the 55 m and 85 m sections the estimated K_{eff} from the measured values varied from 0.4 to 0.0003 mm hour^{-1} and 38 to 0.006 mm hour^{-1} for the 0-600 mm depth while for the 0-850 mm it ranged from 0.004 to 0.0003 and 0.09 to 0.0001 mm hour^{-1}, respectively. The predictions of K_{eff} for the respective consecutive furrow sections ranged from 38 to 0.09 mm hour^{-1} and 16.4 to 0.5 mm hour^{-1} at the 0-600 mm depth and 0.0002 to 9.6E-06 mm hour^{-1} and 12.5 to 7.02E-05 mm hour^{-1} at the 0-850 mm depth. However, the estimated K_{eff} from measured and predicted values passed the homogeneity test at depths of 0-850 mm from the 5 m and 55 m furrow sections.

7.3.4 The rate of soil water redistribution

In this paper the rate of redistribution is represented by the ratio of $\frac{dK_{eff}}{d\theta}$ in relation to infiltrated depth (mm) as illustrated in Figure 8.9. For simplicity only the K-coefficient calculated from the measured SWC were used, and the semi log linear regression functions for vertical redistribution (Vz) and the corresponding coefficient of determinations (R^2) were summarized in Table 7.6.

A small linear variation between the rate of redistribution and infiltrated could be observed. Infiltrated depths of 82 to 46 mm and 90 to 60 mm in the 20 L min^{-1} inflow rate furrow produced Vz that varied from 0.03 to 0.008 and 0.02 to 0.003 mm hour^{-1} hours, respectively. From the 40 L min^{-1} inflow rate furrow, infiltrated depths of 93 to 36 mm and 102 to 37 mm

respectively, produced Vz that ranged between 0.07 to 0.001 and 0.06 to 0.004 mm hour^{-1}, respectively.

Table 7.6 Rate of vertical redistribution (Vz) expressed as a function of infiltrated depth (θz).

Inflow rate(L mm^{-1})	Depth (mm)	Regression	R^2
20	0-600	Log Vz = 0.015 (θz)- 2.866	0.91
	0-850	Log Vz = 0.028 (θz)- 4.368	0.77
40	0-600	Log Vz = 0.031(θz)- 4.375	0.95
	0-850	Log Vz = 0.027(θz)- 4.484	0.80
80	0-600	Log Vz = 0.032(θz) - 4.208	0.84
	0-850	Log Vz = 0.011(θz) - 2.827	0.99
160	0-600	Log Vz = 0.061(θz) - 5.626	0.65
	0-850	Log Vz = 0.048(θz) - 6.682	0.80

In the 80 L min^{-1} inflow rate furrow, infiltrated depths of 78 to 57 and 81 to 57 mm were attained with corresponding Vz of 0.03 to 0.005 and 0.01 to 0.007 mm hour $^{-1}$, respectively. The 160 L min^{-1} inflow rate furrow recorded infiltrated depths of 87 to 59 mm and 88 to 59 mm with respective Vz with range of 2 to 0.02 and 0.01 to 0.0002 mm hour^{-1}. The R^2 of the Vz regression functions was within the range of 0.99 to 0.65 from the furrow sections observed.

7.4 Discussion

Characterising soil water movement during redistribution in soils could be a difficult exercise because of the interactions of gravity and matrix suction gradients across a flow domain that could exhibit different physical properties. Monitoring changes in subsurface SWC and the use of the HYDRUS-2D model to predict changes in SWC along short furrows provided insight on how the layering of the horizons in the Tukulu soil affected redistribution.

Critical to the improvement of the model's prediction was parameter optimisation under field scale conditions. Although no strict format was followed in selecting the hydraulic parameters for optimization other than being cautious of not exceeding three at a time for concerns of uniqueness (Hopmans et al., 2002; Simunek et al., 2009). The θ_s and θ_r were among the most frequently optimised parameters irrespective of depth and inflow rate furrow regime.

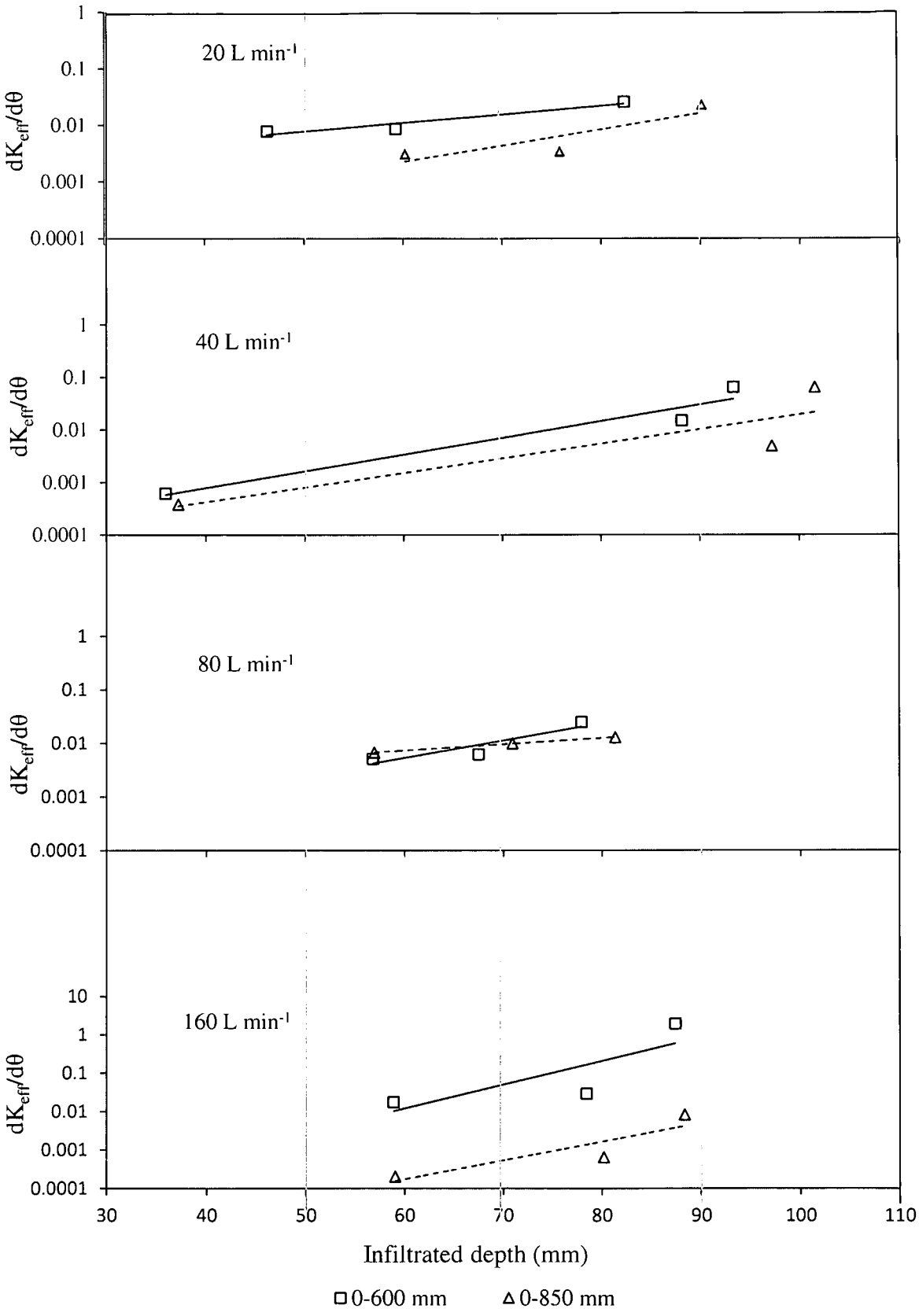

Figure 7.9 Relationship between the rate of redistribution and infiltrated depth at 0-600 and 0-850 mm profile depth for the 20, 40, 80 and 160 L min^{-1} inflow rates.

Although the θ_s were fairly comparable with field and laboratory measured porosity of this soil (Chimungu, 2009), the θ_r exhibited remarkable inconsistencies that could be partly be due soil mixing of the upper horizons with the C-horizons clay-rich soil during deep ploughing or ripping operations. The general differences among parameters within the profile and along the furrows were to be expected given the considerable spatial variability in this soil. An explanation could be given for this but it was interesting to notice that the optimization of α and n parameters at the same time either reduced the models prediction or led to failure of the inverse solution to converge.

Agreement between the measured and predicted SWC was fairly satisfactory with the R^2 varying from 0.88 to 0.52 of the regression of the measured versus the predicted. In most cases the model's predictions overestimated the SWC, especially from the upper horizons. This was to be expected because model's predictions do not consider entrapped or dissolved air which lowers θ_s under *in situ* conditions. Pronounced dispersion between observed and predicted SWC at near the soil surface could be due to evaporation that was not accounted for by the model's prediction while dispersion at deeper layers could be attributed to the model's redistribution diffusive flux (Wohling and Mailhol. 2007).

Despite some noticeable discrepancies between the measured and predicted SWC, the changes in SWC, which are an integral part of field experiments, on the XY line were reflective of the redistribution process. The upper layers demonstrated a remarkable soil water release to the lower horizons even though substantial levels of SWC were retained far above the θ_r as a result of hysteresis. However, the recorded gains from the lower layers were less than the losses from the upper layers suggesting that SWC measurements from the single neutron access tube could not capture the complete redistribution pattern across the furrow section domain (Barger et al., 1999). Despite calibration of the neutron water meter at 150 mm depth from the soil surface the general lack of precision of this instrument near the soil surface could have also contributed to the discrepancies in SWC measurements. Nevertheless, the change in the volumetric SWC with time and space within the flow domain was able show the variations in soil water storage in a meaningful and similar manner to that of the zeroth moment described by Yeh et al. (2005) and Lazarovitch et al. (2009). Changes in soil water storage were greatest in the orthic A-horizon and least in the underlying C-horizon, irrespective of the inflow rate. Although spatial differences in physical and hydraulic properties were a contributing factor, the infiltrated depth from this horizons and subsequent hysteresis were the primary reasons. Noticeable changes in SWC at the C-horizons were

observed where deep infiltration was realised especially at the furrow inlet of the 20 and 40 L min^{-1} inflow rates and at the furrow end of the 80 and 160 L min^{-1} furrows. Under these circumstances it is reasonable to suggest that deep infiltration augmented gravity driven redistribution a phenomenon that was also noted by Hillel (2004).

The actual permeability of the infiltrated domain during soil water redistribution was illustrated by the variability of the K_{eff}. Overestimations of K_{eff} were to be expected given the initial overestimates of SWC from model predictions, especially at the furrow inlets and ends. For the upper 0-600 mm soil profile flow domain K_{eff} were generally higher from both measured and predicted values indicating that this section of the profile was generally deeply wetted compared to the 0-850 mm domain. The loose structure and the smooth transition between of the A and B horizons supported the higher permeability is this domain. At the 0-850 mm the K_{eff} exhibited a steeper gradient in most furrow sections suggesting that the prismacutanic C-horizon at 600 to 850 mm depth could have played a major role in augmenting strong matrix suction against gravity driven redistribution. Although spatial variability was the reason for the inconsistencies in K_{eff} slope between the 0-600 and 0-850 mm profiles flow domains, a general linear relationship could be drawn between K_{eff} and the respective average SWC. Such linearity was also demonstrated by the K_{eff} values between 0-600 and 0-850 mm profile domain at each furrow section. In the former the K_{eff} fell in the range of 10 to 0.001 mm $hour^{-1}$ while in the latter it was between the ranges of 1 to 0.0001 mm $hour^{-1}$. This was not surprising since the permeability of the infiltrated depth decreased with increasing profile because of the increase in water gradient and matrix suction at the lower horizons of this soil. Inferences to the linearity between K_{eff} and infiltrated depth were also made in other others including the work of Rubin (1967) and Yeh et al. (2004).

In this work the linear relationship between K_{eff} and infiltrated depth was extended to determine the rate of redistribution (Vz) within a specified profile flow domain (0-600 or 0-850 mm depth). This analogy found its validity on the convective term representing the rate of change of the first spatial moments in the downward (z) direction as described by Yeh et al. (2005). In this soil an infiltrated depth of 100 mm would be expected to augment a redistribution rate of 0.1 to 0.01 mm $hour^{-1}$. An infiltrated depth of 50 mm of SWC would fall in range 0.01 to 0.001 mm $hour^{-1}$ within the profile depth of 600 mm and 0.01 to 0.0001 mm $hour^{-1}$ for the 850 mm depth. For a soil with a restrictive underlying horizon, these rates of redistribution indicated minimum drainage activity that is consistent with findings of and Fraenkel (2008) and Chimungu (2009). Therefore, the low rates of gravity augmented

redistribution could be said to offer greater flexibility not only to control the frequency of irrigation but also the desired infiltrated depth.

7.5 Conclusion

Soil water redistribution on the South African Tukulu, also referred as Cutanic Luvisols of the World Reference Group, was characterised along 90 m distant furrows. A single-run of flood irrigation was used for the subsurface soil water redistribution trial under different inflow rate treatments. The predicted soil water content distribution predicted from the parameter optimization of HYDRUS-2D matched fairly well with measured values. The results provide support to use the HYDRUS-2D as a tool for designing and evaluating the efficiency of furrow irrigation management systems. Despite discrepancies resulting from field spatial variability the use of the geometric mean scheme to calculate the K_{eff} provided reasonable estimates of the average permeability of the different furrow profile sections during redistribution. Vertical redistribution was estimated using the relationship between the ratio $\frac{dK_{eff}}{d\theta}$ and infiltrated depth and the results were able to discriminate redistribution at 0-600 mm from that of 0-850 mm profile depths. The rate of redistribution in a deeply infiltrated profile at depth up to 850 mm was found to be less than one order of magnitude when compared to partially infiltrated profiles up to depths of 500 mm. This result is consistent with the physical properties of the soil horizons layers of the Tukulu. The upper strata is course structured that encourages deep vertical redistribution while the underlying prismatic C-horizon is of low permeability and restricts percolation below the soil profile. Thus furrow irrigation practices can be developed in the Tukulu soil type and Cambisols, with similar layering composition, with confidence that deep subsurface redistribution shall support soil water storage and minimum deep drainage losses.

Acknowledgements

Acknowledgements to the staff and management of Paradys experiment station of the technical and hospitality they provided during this experiment. Special thanks to the Strategic Academic Cluster for the water management in water-scarce areas of the University of the Free State for the financial assistance in carrying out this experiment.

7.6 References

Abbasi, F., Jacques, D., Simunek, J. and van Genuchten, M. Th., 2003. Inverse estimation of soil hydraulic and solute transport parameters from transient field experiments: Heterogeneous soil. *Am. Soc. Of Agric. Eng.*, 46: 1097-1111.

Aris, R., 1956. On the dispersion of a solute in a fluid flowing through a tube. *Proc. R. Soc. London, Ser.*, 235: 67-78.

Austin, C., 2003. Micro flood, a new way of applying water. http://waterright.com., 22/09/2011, 10.00 am (LT).

Baker, D. L., Arnold, M. E. and Scott, H. D., 1999. Some analytical and approximate Darcian means. *Ground Water*, 37: 532-538.

Bargar, B., Swan, J. B. and Jaynes, D., 1999. Soil water recharge under un-cropped ridges and furrows. *Soil Sci. Soc. Am. J.*, 63:1290-1299.

Barry, D. A, and Sposito, G., 1990. Three-dimensional statistical moment analysis of Stanford/Waterloo Borden tracer data. *Water Resour. Res.*, 26:1735-1747.

Brooks, R. H. and Corey, A. T., 1964. Hydraulic properties of porous media, Hydrology paper no. 3. Civil Engineering Dep., Colarado State University, Fort Collins, USA.

Chimungu, J. G., 2009. Comparison of field and laboratory measured hydraulic properties of selected diagnostic soil horizons. M.Sc. (Agric) Dissertation, University of the Free State, Bloemfontein, South Africa.

Clemmens, A. J., Eisenhauer, D. E. and Maheshwari, B. L., 2001. Infiltration and Roughness equations for surface irrigation: How form influences estimation, An ASAE Meeting Presentation, Paper no. 01-2255, hq@asae.org: 08/08/ 2011, 15.30 pm (LT).

Fraenkel, C. H., 2008. Spatial variability of selected soil properties in and between map Units. Msc (Agric) Dissertation, University of the Free State, Bloemfontein.

Gasto, J. M., Grifoll, J. and Cohen, Y., 2002. Estimation of internodal permeabilities for numerical simulation of unsaturated flows. *Water Resour. Res.*, 38:1326-1340.

Gee, G. W., and Ward, A. L., 2001. Vadose zone transport field study: Status report, PNNL-13679, Pac., Northwest National Library, Richland, Washington DC, USA.

Gomez, K. A., and Gomez, A.A., 1984. Statistical procedures for agricultural research, 2 ed. John Wiley and Sons, New York, USA.

Hensley, M., Botha, J. J., Anderson, J.J ., van Staden, P. P. and du Toit, A., 2000. Optimising rainfall use efficiency for developing farmers with limited access to irrigation water, Water Research Commission report, 878, Pretoria, South Africa.

Hillel, D.H., 2004. Environmental soil physics, New York: Academic Press, USA.

Hopmans, J. W., Simunek, J., Romano, N. and Durner, W., 2002. Simultaneous determination of water transmission and retention properties, Inverse Methods. IN: Methods of Soil Analysis.Part 4.Physical Methods (J.H. Dane and G.C. Topp, Eds.), *Soil Science Society of America Book Series* No. 5: 963-1008.

Kool, J. B., and Parker, J. C., 1988. Analysis of the inverse problem for transient unsaturated flow, *Water Resour. Res.*, 24: 817–830.

Kosugi, K., 1996. Lognormal distribution model for unsaturated soil hydraulic properties, *Water Resour. Res.,* 32: 2697-2703.

Lazarovitch, N., Warrick, A.W., Furman, A. and Simunek, J., 2009. Water content distribution in drip irrigation described by moment analysis. *Vadose Zone J.*, 6: 116-123.

Lazarovitch, N., Warrick, A.W., Furman, A. and Zerihum, D., 2009. Subsurface water distribution from furrows described by moments analyses. *J. of Irrig. and Drain. Eng.*, 135: 7-12.

Leconte, R., and Brissette, F. P., 2001. Soil moisture profile model for two-layered soil based on sharp wetting front approach. *J. of Hydrologic Eng.*, 6: 141-149.

Mathews, C. J., Knight, F. J. and Braddock, R. D., 2004. Using analytic solutions for homogeneous soils to assess numerical solutions for layered soils. ARC Discovery Indigenous Research Development Program, C.mathews@griffith.edu.au, 31/04/2011, 17.00 pm (LT).

Rubin, J., 1967. Numerical method for analyzing hysteresis-affected, post-infiltration redistribution of soil moisture, *Soil Sci. Soc. Am. Proc.,* 31:13-20.

Schaap, M. G, Leij, F. J. and van Genuchten, M.Th., 2001. Rosetta: A computer program for estimating soil hydraulic parameters with hierarchical pedotransfer functions. *J. Hydrol.*, 25: 1163-1176.

Scotter, D. R., Clothier, B. E. and Harper, E. R., 1982. Measuring saturated hydraulic conductivity and sorptivity using twin rings. *Australian Journal of Soil Research*, 20: 295-304.

Simunek, J, Sejna, M. and van Genuchten, M. Th., 2009. The HYDRUS-2D software package for simulating two-dimensional movement of water, heat and multiple solutes in variably saturated media, Version 2.0. Rep. IGCWMC-TPS-53, p. 251, Int. Ground Water Model, Cent., Colo. Sch. of Mines, Golden, CO.

Soil Classification Working Group, 1991. Soil Classification - A taxonomic system for SouthAfrica, Memoirs on the Agricultural Natural Resources of South Africa No. 15. Department of Agricultural Development, Pretoria.

Srivastava, R., and Yeh, T.C.J., 1991. Analytical solutions for one-dimensional transient infiltration toward the water table in homogenous and layered soils. *Water Resour. Research,* 27: 753-762.

Sudicky, E. A., 1986. A natural gradient experiment on solute transport in a sand aquifer: Spatial variability of hydraulic conductivity and its role in the dispersion process, *Water Resour. Res.*, 22: 2069-2082.

van Genuchten, M.Th., 1980. A closed-form equation for predicting the hydraulic conductivity of unsaturated soils. *Soil Sci. Soc. Am. J.*, 44: 892-898.

Warrick, A. W., 1991. Numerical approximations of Darcian flow through unsaturated soil. *Water Resour. Res.,* 27: 1215-1222.

Wildenschild, D., and Jensen, K. H., 1999. Numerical modelling of observed effective flow behaviour in unsaturated heterogeneous sands. *Water Resour. Res.*, 35: 29-42.

Willmotti, C. J., Ackleson, S. G., Davis, R. E., Feddema, J. J., Klink, K. M., Legates, D. R., Dennel, O. J. and Rowe, C. M., 1985. Statistics for the Evaluation and Comparison of Models. *J. of Geophysical Research*, 90:8995-9005.

Wohling, T. H., and Maihol, J. C., 2007. A physically based coupled model for simulating 1D and surface -2D subsurface flow and plant water uptake in irrigation furrows, II: model test and evaluation. *J. of Irrig. and Drain. Eng.,* 133: 543-553.

Wohling, T. H., Schmitz, G. H. and Maihol, J. C., 2004. Modelling two-dimensional infiltration from irrigation furrows. *J. Irrig. Drain. Eng.,* 130: 296–303.

World Reference Base for Soil Resources (1998). World soil resources report, 84, ISSS / ISRIC FAO, Rome, Italy.

Yeh, T. C. J., Ye, M. and Khaleel, R., 2005. Estimation of effective unsaturated hydraulic conductivity tensor using spatial moments of observed moisture plume. *Water Resour. Res.*, 41: WO3014.

CHAPTER 8

INTEGRATING MICRO-FLOOD WITH IN-FIELD RAINWATER HARVESTING :(i) SOIL WATER BALANCE PROCEDURE AND APPLICATION

Abstract

A procedure for estimating soil water balance (SWB) components for the newly integrated micro-flood irrigation (MFI) with in-field rainwater harvesting (IRWH) was developed and validated. Gains and losses from the dryland (DL), supplemental (SPI) and full irrigation (FI) water regimes (WR) under IRWH with three (1 m, 2 m and 3 m) runoff strip widths (RSW) were accounted for. Site specific data was used to estimate rainfall-runoff relationships and deep drainage (DD). Plant canopy cover was considered during the estimation of evapo-transpiration (ET), evaporation (Ev) and transpiration (T). Full, partial and no-shaded were used describe certain sections of the experimental plots depending on the surface area under canopy cover. Consistency of the procedure with soil hydrological and agronomic principles led to its acceptance. It was then applied to determine the effect of the RSW and WR on the soil water balance components over the production season. Net gains from rainfall were comparably higher from the 2 m and 3 m RSW. The 1 m RSW had the least net gains from rainfall but had consistently higher ET and T for all WR. Greater surface area covered by crop canopy and accessible to plants roots from both twin and alternative rows was the possible explanation. Irrigation increased ET, Ev and T irrespective of the regime. Evaporation also increased with RSW irrespective of the WR. Deep drainage was only affected by RSW and WR following major rainfalls (>24 mm) and irrigation especially late in the season. Interactions were limited to change in soil water content, DD and T mainly after the occurrence of rainfalls at short intervals or after an irrigation event. It was therefore concluded that RSW and WR affected the SWB components and that the 1 m RSW offered an optimum surface area for substituting evaporation losses by transpiration.

Key word: soil water regime, runoff strip width, dryland, irrigation, rain water harvesting,

8.1 Introduction

Although the concept of integrating rainwater harvesting and irrigation is rather ancient, the integration of micro-flood (MFI) with in-field rainwater harvesting (IRWH) carries the prospects of transforming runoff farming in the Free State Province of South Africa. Common to runoff farming technologies is the harvesting of rainwater in the form of runoff from a larger area and concentrating it to a smaller area for immediate or later productive use (Owes et al., 1999; Hensley et al., 2000: Prinz and Malik, 2002: Anschutz et al., 2003). Micro-flood and IRWH use different forms of runoff and their integrated effect on the soil water balance (SWB) is yet to be established.

Improving soil water storage and availability for crop plants is the common goal of MFI and IRWH. Micro-flood irrigation makes use of available irrigation water to supplement rainfall through the application of small inflow rates to relatively short furrows (Austin, 2003). On the other hand IRWH, designate some relatively larger section of the field to serve as mini-catchments (runoff area) for the harvesting of in-field runoff that get stored in the soil profile of the cropped area (Hensley et al., 2000). The two practices appear to be compatible and well adapted to improve rainfall effectiveness and productive potential of difficult soils, especially those with a dry soil water regime.

Despite the fact that improving soil water regime by in-situ or in-field rainwater harvesting and supplemental irrigation is a well established practice in runoff farming, the necessary risk management procedures needs to be developed. One area of concern with integrated soil water management practices is the transformation of the soil water balance that if not well monitored could increase the risk of high evaporation, water logging, flooding that could result soil erosion and overtopping of the runoff storage structures, and rising of the water table. Traditionally, IRWH has guided against soil erosion and flooding risk related factors by earmarking specific soil types for in-field runoff harvesting. Although, ex-field runoff has been reduced to almost zero but high evaporation losses continues to be a challenge. Given that irrigation also increases evaporation especially flood methods, this condition would be expected to be made worse by the introduction of MFI. The use of organic mulches on IRWH alone has suppressed evaporation by 15 % on clay soils and 31 % on sandy soils (Botha, 2006) compared to bare soils. Nevertheless, a total of 79 % of annual rainfall is reported to have been lost to evaporation from IRWH fields (Botha, 2006).

One of the agronomic aspects that have become popular in recent times is the role of plant canopy cover in suppressing evaporation. Given that the size of the canopy increases with of annual crops, growth, various agronomic practices have been shown to encourage early canopy cover and hence, reduce evaporation as well as runoff losses. This included higher plant density (Maqbool et al., 2006), fertiliser application (Stroonijder, 2009) and narrow row spacing (Eberbatch and Pala, 2005), and irrigation (Zhang et al., 1998). The last two are implicated to the IRWH and MFI through the respective strip width of the basin and runoff area and provision of micro-flood supplemental irrigation. On the traditional IRWH design the basin and runoff area constitutes of a respective standard strip width of 1 m and 2 m (Figure 8.1). These strip widths were selected on the basis of mechanical convenience and optimising in-field runoff under the semi-arid conditions of the province. However optimising the surface area under canopy cover may require changes on the standard dimensions but without violating the acceptable runoff to basin area surface area ratio (Oweis et al., 1999). Aware of this predicament, Mzezewa et al. (2011) opted to encourage canopy cover in the basin area by including a legume crop as an intercrop.

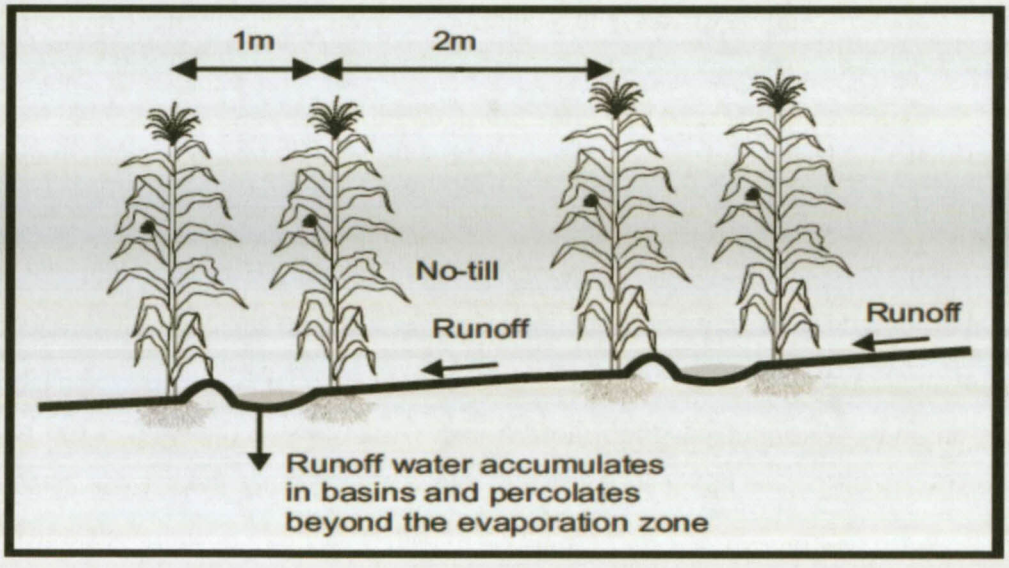

Figure 8.1 A diagrammatic representation of the in-field rainwater harvesting technique (Hensley et al., 2000).

Developing a mass conservation procedure of soil water gained and lost for the newly integrated MFI-IRWH management practice was the primary contribution of this to study. Previously, the soil water balance (SWB) components for IRWH was estimated without considering the role of canopy cover on crop water use. This could be understood given that

most early studies focused in getting the in-field rainfall-runoff relationships and seasonal crop water use and efficiency parameters correct. Given the growing pressure on efficient use of agricultural water resources in semi-arid areas (Stroosnijder, 1987), integrating MFI with IRWH make it necessary to account for every aspect that influences the soil water net gains and losses, including that of the crop canopy cover. On this regard the specific objectives of this study was firstly; to develop a procedure for quantifying SWB components for the integrated MFI-IRWH management practice and secondly, to determine the effect of runoff strip width (RSW) and water regime (WR) on the SWB components over the production season.

8.2 Procedures for solving IRWH soil water balance

8.2.1 Soil water storage

Soil water storage was defined by the drainage upper limit (DUL) and lower limit (DLL) boundary conditions. The DUL in our field studies was defined as the volumetric SWC when drainage flux approaches 0.001 mm hour^{-1} while the DLL was the regarded to be the lowest volumetric SWC recorded from each soil profile horizon during field trials. The difference between the average profiles DUL and DLL depicts the profiles available water capacity (PAWC). Under field conditions SWC normally fluctuates between this range illustrating different levels of soil water deficit. Characterising the experimental site were DUL and DLL values of 0.299 and 0.177 mm mm^{-1} in the areas where the underlying horizon was of a prismatic clay structure and the profile of 850 mm depth. On areas with dolorite C-horizon at 400 to 650 mm depth, the applicable average profiles DUL and DLL values were 0.28 to 0.12 mm mm^{-1}, respectively. Differences between initial and final SWC during the production is a function of soil water recharging and withdrawal processes. The latter is represented by deep drainage, runoff (R), and evapo-transpiration (ET) and the former in profiles without water table contribution by rainfall (P) and irrigation (I). Since runoff is converted from losses to gains by IRWH, the soil water balance components influencing soil water storage could be expressed as

$$\Delta SWC = (I + P) - ET - DD \qquad (8.1)$$

Where ΔSWC is change in soil water storage and DD being deep drainage.

8.2.2 Harvested runoff

Rainwater harvested as in-field runoff or run-on for the different runoff strip widths were estimated using linear regression equations summarized in Table 8.1, developed on site according to the procedure described by Hensley et al. (2000). Runoff coefficient from rainfall-runoff functional relationships was almost equal to zero at rainfalls amounting to 9.2, 22.1 and 24.5 mm from the respective 1, 2 and 3 m RSW.

Table 8.1 Regression functions of rainfall (P) and runoff (R_{in}) relationships from different runoff strip widths.

Runoff strip width (m)	Linear regression	R^2
1	$R_{in} = 0.373P - 7.13$	0.98
2	$R_{in} = 0.405P - 8.959$	0.94
3	$R_{in} = 0.513P - 12.549$	0.99

Although rainfall received over the experimental area was assumed to be the same, the infiltrated depth varied between the runoff and basin strips. The run-off generated over the runoff strip and collected in the basin strip was accounted for by partitioning rainfall events according to the runoff-basin area ratio.

8.2.3 Irrigation

According to the BEWAB$^+$ (van Rensburg and Zerizqhu, 2008) irrigation scheduling model an amount of 625 mm of water would be required for a 120 day maturing maize cultivar to attain a maize yield of 10000 kg ha^{-1}. Given that more than 50% of the long term average rainfall is received between the months of November to March, a seasonal rainfall of around 300 mm was expected.Therefore, the balance was provided by means of the micro-flood irrigation following a fixed schedule for FI and SPI produced by the BEWAB+ irrigation software. For the 30 m furrow run the 40 L min^{-1} inflow rate from previous test showed that advance times between 20 to 30 minutes could attain infiltrated depths of 30 mm. The designated 40 L min^{-1} inflow rate at 100 % efficiencies could supply 0.9 m^3 or 900 litres of water on the 30 m furrow run at a cut-off time of 23 minutes.

8.2.4 Deep drainage

Soil water (θ) lost to deep drainage (D_D) was estimated using the internal drainage curves determined from earlier field studies on the same site. Due to spatial variation, the prismatic and dolorite rock were the two predominant C-horizons across the experimental area. The soil water content-drainage relationship from the prismatic and dolorite horizons assumed exponential functions, respectively written as:

$$D_D = 4\,x10^{-63}\exp^{440.5.\theta} \quad (8.2)$$

$$D_D = 2\,x10^{-8}\exp^{67.21.\theta} \quad (8.3)$$

Accumulative drainage over the production season from each plot was presented as the total drainage component of the soil water balance.

8.2.5 Evapo-transpiration

Evapo-transpiration is the component of the soil water balance that is generally unknown and constitutes of evaporation and transpiration. The soil water balance expression (8.1) could be re-arranged to become:

$$ET = (I + P) - DD - \Delta SWC \quad (8.4)$$

Because the IRWH involves different tillage and row systems for the runoff and basin strips, the calculations of ET treated these areas as separate subsystems. The contributions of evaporation and transpiration to ET from the runoff (ET_r) and basin strips (ET_b) were considered important in assessing the effects of different runoff strips on IRWH under different soil water regimes. In the basin area ET_b was mainly a function of crop water use and canopy cover. During seed germination and seedling establishment that lasted about 2 weeks after planting, canopy cover or crop water use was considered to be zero, hence evaporation constituted 100 % of ET_b. At full canopy cover contributions from evaporation were assumed to be 10 % and after cob filling was completed increased to 50 %. Canopy cover as a function of crop height was observed to reach maximum at 7 and 8 weeks for the irrigated and rain-fed plots, respectively. Transpiration (T_b) and evaporation (Ev_b) from the basin area was related to ET_b using the expression:

$$T_b = \beta ET_b \quad (8.5)$$

$$Ev_b = (1 - \beta)\, ET_b \quad (8.6)$$

Where β is the parameter that ranged from 0 to 0.9 (Figure 8.2), was considered to be zero at the initial stage and 0.9 at full canopy cover. Partial canopy cover as for the 2 and 3 m RSW; β ranged from 0 to 0.5 from establishment to the mid-vegetative stage. In the runoff area ET_r was the function of the runoff strip width and the effect of crop canopy. When the crop was fully grown three classes of canopy cover were used to describe three runoff strip widths used in this study. A full canopy was used for the 1 m runoff strip width and thus it was treated in a similar manner with the basin strip. In the 2 m runoff strip and the 1 m strips of the 3 m runoff area that were adjacent to the basin crop rows were considered to be under partial canopy cover. The central strip in the 3 m runoff area was not affected by canopy cover and therefore represented the total evaporation ($Ev_{100\%}$). An average of the $Ev_{100\%}$ from the same block treatment provided reference evaporation (Ev_{ref}) for the experimental site. Calculation of the ET_r from the 2 and 3 m runoff strips assumed the same soil water balance expression in Eq. 8.4. At the plot scale the ET_p was calculated using the weighted average of the basin and runoff ET written as:

$$ET_p = \frac{ET_b + (ET_r . N)}{Wp} \tag{8.7}$$

Where N is number of 1 m width runoff strips and W_p is the plot total width (m). To characterise the contributions of evaporation and transpiration at plot scale also required that ET_r be partitioned. At the initial crop stage $ET_r = Ev_r$ for all the N strip units. The β parameter ranging from 1 to 0.5 (Figure 8.2) was used to relate the decreasing contribution of evaporation from the partially shaded strips (Ev_{rp}) to ET_r. At mid and late season Ev_{rp} was estimated from the average Ev_{ref} using the expression

$$Ev_{rp} = \beta . Ev_{ref} \tag{8.8}$$

Where, β assumed a constant coefficient of 0.5. Subtracting from ET_r yielded the transpiration component (T_{rp}) from the partially shaded strips. Integrating Ev_{rp} and T_{rp} on the ET_p for a 2 m runoff strip the expression in Eq. 8.7 could be re-written as:

$$ET_p = T_p + Ev_p \tag{8.9}$$

$$Ev_p = \frac{Ev_b + (Ev_{rp} . 2)}{3} \tag{8.10}$$

For the 3 m runoff strip Eq. 8.10 becomes:

$$Ev_p = \frac{Ev_b + (Ev_{rp}.2) + Ev_{100\%}}{4} \quad (8.11)$$

8.2.6 Statistics

A split plot analysis of variance was used to establish the effect of RSW and WR and its interaction on SWB components under IRWH. The SAS 9 software was used in this endeavour in combination with the procedures for least significant different (LSD) test described by Gomez and Gomez (1984).

8.3 Results and discussions

8.3.1 Illustrations of the soil water balance procedure

Figure 8.2 and Table 8.2 show results that illustrates the soil water balance procedure over the one production season from a 2 m RSW plot under supplemental irrigation. Integrating MFI with IRWH presented the basin area (BA) with two water management functions; first, to store rainfall plus run-on (Rn) produced in the runoff area (RA) and secondly, to distribute uniformly the advance stream from supplemental micro-flood irrigation. Because of the presence of a crop in the BA the procedure was able to discriminate between the gains and losses from the BA, RA and the plot area (PA) during the major rainfalls and irrigation to mitigate the dry spells.

Over the production period a total rainfall of 281 mm was received with major rainfall occurring on the 7, 39, 60 and 99 DAP. The corresponding rainfall amounts were respectively, 49 mm, 30 mm, 36 and 49 mm. The BA had a relatively steeper rise in PSWC with the first two rainfalls recording an increase of 54 mm compared to the 42 mm from RA. The 3rd and 4th rainfalls brought increases for profile soil water content (PSWC) of 37 and 51 mm from the BA and 16 and 24 mm from the RA, respectively. The additional contribution from in-field runoff harvested from the RA as run-on into the BA over and above the rainfall it received explains the differences in PSWC between the BA and RA. This was consistent with the principle of *in situ* rainwater harvesting that runoff collected from a larger area gets concentrated in a smaller area where crops grow to complement the short falls brought by low rainfalls (Oweis et al., 1999; Hensley et al., 2000). At plot scale the corresponding increases in PSWC for the same rainfall events were 46, 19 and 31 mm reflecting a weighted average of the BA and RA. These gains were lower than those from the BA since in the 2 m RSW the BA constituted only 33 % of the total plot area with the balance assigned to the RA.

Previous studies preferred to use the arithmetic mean to determine the plot water balance components even though the proportional surface area from the BA and RA were different (Botha, 2006; Joseph, 2007; Mzezewa et al., 2011). Overestimation in soil water studies as a result of using the arithmetic mean due to its mathematical structure is well acknowledged in literature (Yeh et al., 1985; Yeh and Harvey, 1990).

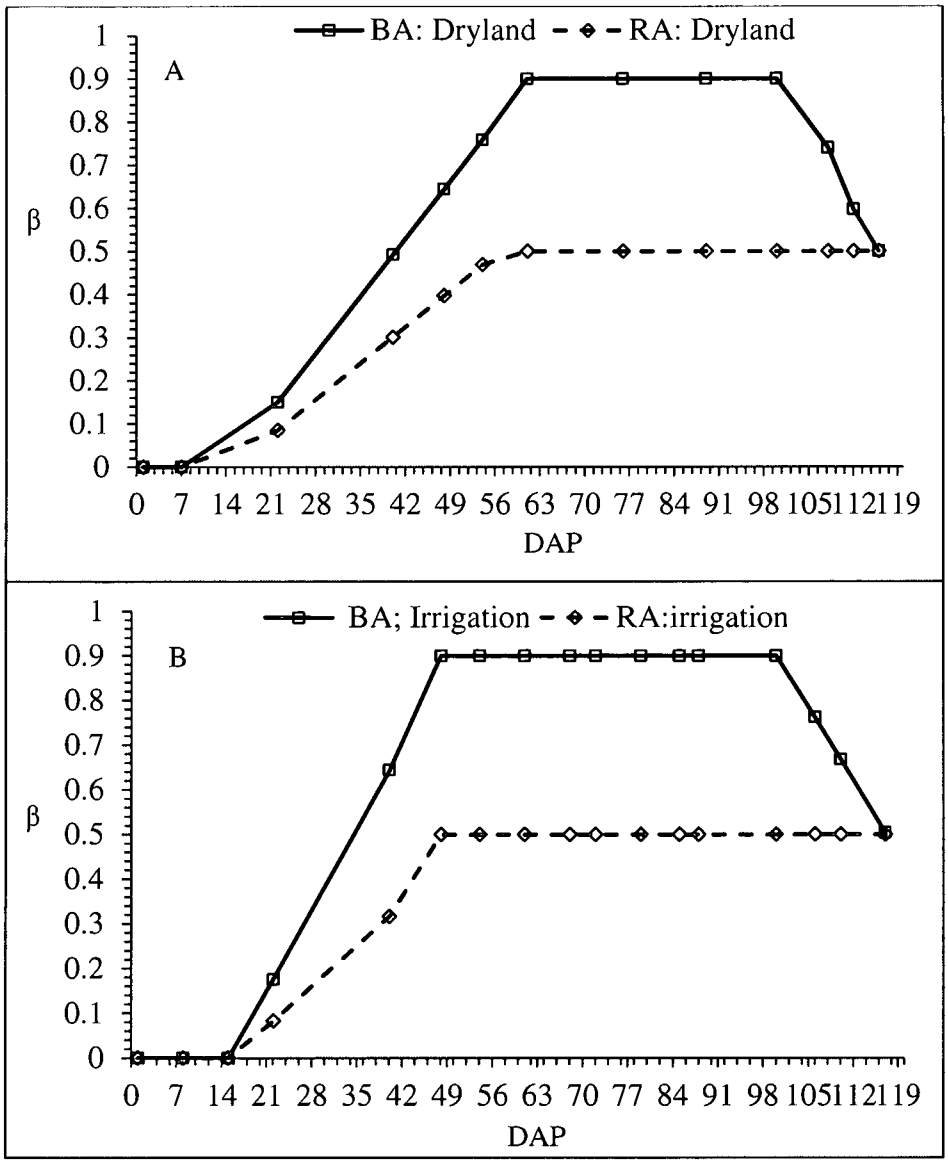

Figure 8.2 Approximated β parameter representing the fraction of canopy cover during the production season for the basin area (BA) and runoff area (RA) of the dryland (A) and irrigation (B) plots.

Table 8.2 Illustration of the soil water balance procedure using estimated water processes over the production season from the basin, runoff and plot area of in-field rainwater harvesting with a 2 m runoff strip under micro-flood supplemental irrigation.

Designated		Days after planting															
Area	SWB (mm)	7	14	21	39	47	53	60	67	71	78	84	87	99	105	109	116
	PSWC	179.5	185.2	177.0	122.9	128.1	141.1	152.1	151.2	132.9	133.3	121.5	148.2	173.2	142.8	168.9	177.1
	Δ SWC	-48.1	-5.6	-8.1	-54.1	5.2	13.0	11.0	-0.9	-18.3	0.5	-11.8	26.7	25.0	-30.4	26.1	8.3
Basin	DD	0.02	0.01	0.03	0.00	0.00	0.00	0.00	0.00	0.00	0.00	0.00	0.00	0.01	0.00	0.12	0.18
	ET	22.1	25.3	54.9	89.8	56.9	42.9	36.3	48.1	18.3	47.9	23.9	28.6	53.9	24.3	27.3	16.5
	E	22.1	25.3	45.2	32.0	5.7	4.3	3.6	4.8	1.8	4.8	2.4	2.9	5.4	5.8	9.1	8.2
	T	0.0	0.0	9.7	57.8	51.2	38.6	32.6	43.3	16.5	43.1	21.5	25.7	48.5	18.5	18.3	8.3
	PSWC	161.6	173.2	159.3	152.0	140.3	147.1	156.2	141.0	129.8	123.0	126.8	129.3	147.9	133.7	139.1	154.3
	Δ SWC	-30.4	-11.6	-13.9	-7.3	-11.7	6.7	9.1	-15.2	-11.2	-6.8	3.8	2.5	18.6	-14.2	5.5	15.2
Runoff	DD	0.0	0.0	0.0	0.0	0.0	0.0	0.0	0.0	0.0	0.0	0.0	0.0	0.0	0.0	0.0	0.0
	ET	15.1	26.9	31.5	67.7	57.6	8.4	42.5	34.8	22.5	20.3	16.6	15.6	46.2	24.3	6.0	15.8
	E	15.1	26.9	28.8	46.2	28.8	4.2	21.2	17.4	11.2	10.2	8.3	7.8	23.1	12.2	3.0	7.9
	T	0.0	0.0	2.6	21.4	28.8	4.2	21.2	17.4	11.2	10.2	8.3	7.8	23.1	12.2	3.0	7.9
	PSWC	167.6	177.2	165.2	142.3	136.3	145.1	154.8	144.4	130.8	126.4	125.0	135.6	156.3	136.7	149.0	161.9
	Δ SWC	-36.3	-9.6	-12.0	-22.9	-6.1	8.8	9.8	-10.5	-13.6	-4.3	-1.4	10.6	20.7	-19.6	12.3	12.9
Plot	DD	0.0	0.0	0.0	0.0	0.0	0.0	0.0	0.0	0.0	0.0	0.0	0.0	0.0	0.0	0.0	0.1
	ET	12.4	17.4	28.8	52.5	38.2	17.1	26.2	27.7	13.6	22.7	13.5	14.7	33.4	16.2	11.1	10.8
	E	12.4	17.4	24.7	26.1	14.3	5.1	11.0	10.3	5.8	7.7	4.9	4.7	13.4	8.0	5.1	7.3
	T	0.0	0.0	4.1	26.4	23.9	12.0	15.2	17.3	7.8	15.1	8.6	10.1	20.0	8.2	6.0	3.5

PSWC= profile soil water content, ΔSWC= change in soil water content, DD= deep drainage, ET= evapotranspiration, E= evaporation, and T= transpiration

Stabilising soil water storage and crop water use is one of the primary goals for integrating supplemental irrigation with *in situ* rainwater harvesting (World Bank, 2005; Rockstrom et al., 2007). Supplemental irrigation was used to bridge the persistent dry spells of 25, 21, 39, and 17 days that occurred during the periods of 14 to 39 DAP, 39 to 60 DAP, 60 to 99 DAP and 99 to 116 DAP, respectively. The rain that occurred during these periods was too low to adequately recharge the soil water and this was not strange given the low and erratic rainfalls of the area (Botha, 2006). Supplemental irrigation maintained the PSWC at relatively higher levels in the BA than that from the RA that only relied on rainfall, typical of IRWH under dryland conditions. Increased soil water availability in the BA area was of paramount importance given that crop water demand had increased over the production period reaching critical levels between 47 to 105 DAP, a time corresponding to the vegetative growth and reproductive crop growth phase (FAO, 2011).

Concentrating in-field runoff and introducing supplemental irrigation in BA was illustrated in the procedure by increased water availability not only for total crop water use (ET) but also for DD. In the first 21 DAP, ET was predominately in the form of Ev and recorded an increase from 22 to 55 mm while DD ranged from 0.01 to 0.03 mm. For the same period DD remained practically zero while ET increased from 15 to 32 mm in the RA. Given that the soil was primarily bare and crop water demand at a very infant stage, the high Ev and low DD captured by the procedure was reasonable. Rockstrom et al. (2007) recommended dry planting and delaying water application early in the season to minimize high Ev and DD. Throughout the season ET from BA remained higher than that from the RA irrespective of rainfalls events with the exception of the 71, 105 and 116 DAP. The low ET for the BA corresponding to these DAP can be attributed the short time interval of 4 days for 71 DAP SWC measurement, and the general slow down in crop growth at the onset of the reproductive stage (FAO, 2005). Decline in growth rate towards the end of the season could be attributed to ET being lower than in the RA. Interestingly, the procedure was able to capture the small amounts of DD at the later stages of the growing period while during the mi-season it was nearly zero. This was an indication of that transpiration during the high crop water demand kept the PSWC low enough to prevent significant DD losses. Similar findings were found by Gobeze (2012) who recognised that DD during the growing season despite regular irrigation DD was kept at negligible levels by maize transpiration in a well rooted soil profile. The function of root water uptake on reducing DD was complemented by the

selection of soils suitable for IRWH with a restrictive layer in the B or C horizon (Hensley et al., 2000).

Over and above the noticeable differences in ET between the BA and RA was the inverse relationship between Ev and T during the production season. While Ev dominated ET in the early stages of plant growth, the proportion of T increased remarkably from 39 to 99 DAP. With an approximated average reference evapo-transpiration (ET_o) of 6.5 mm per day for the same period, the corresponding daily average increase in T that could be deduced from the SWB table (Table 8.2) was an increase from 3 mm to 6 mm in the BA and 1 to 2.1 mm in RA. On the other hand Ev decreased from a daily average of 6 to 1.3 mm in the BA and from 4 to 2.4 mm in the RA for the same period. The increase in T was consistent with crop growth and crop water demand that is widely described using the crop coefficient (K_c); depicted as the ratio of crop water use to ET_o (FAO, 2011). In this study a β parameter was used to represent the crop growth with respect to canopy cover; a primary factor in the approximation of K_c.

The benefit of concentrating harvested runoff and supplemental irrigation water to where crop plants grow was well illustrated in the overall water balance. Although at plot scale Ev and shared an equal proportion of 46 % of the total available water, Ev from the BA was 50 % less than that of the BA indicating that much of the water concentrated in the BA was channelled to T than Ev. In addition, ET from the BA was approximately 40 % greater than that of the RA with corresponding T values of 254 mm more than the RA. This was consistent with the 315 mm of water applied in the BA through supplemental irrigation. Despite these increases in water storage DD was within negligible levels in agreement with previous studies that soils with a restrictive layer were effective in reducing DD losses (Hensely et al., 2000; Hensley et al., 2007). However prospects of lateral drainage occurring from the BA to the RA could be supported by the ET in the RA that was 170 mm higher than the seasonal rainfall. Given the restrictive DD conditions, this was not surprising because water was concentrated only to a 1 m RSW and the remaining 2 m RSW constituting of the the RA was virtually dry in most cases.

8.3.2 Effect of runoff strip width and water regime on the soil water balance components

Table 8.3 summarizes the gains from rainfall and irrigation under supplemental and full irrigation during the production period. Statistical summary pertaining to the effect of main

and sub treatment on soil water storage and losses at different stage of crop growth was presented in Table 8.4, Table 8.5 (plant establishment), Table 8.6 (vegetative stage), Table 8.7 (reproductive) and Table 8.8 (ripening) stages. Although the RSW (1 m, 2 m and 3 m) and WR (DL, SPI and FI) had variable effect on the SWB components over the production season, some comparisons could be drawn.

Plant establishment stage:

The plant establishment phase lasted for 21 DAP and this was within the time frame of 15 to 25 days reported by Smith (2006). Early during this period water components started to be affected by the RSW and WR main treatments while their interaction had an effect towards the end of this stage. Predominately affected was the soil water storage and water use related components. This was attributed to the 48.7 mm and 27 mm rainfalls received after the respective 7 and 14 DAP and were of sizable amounts to recharge the soil profile. Affected by RSW throughout this period was the PSWC and ΔSWC. The PSWC on the 7, 14 and 21 DAP recorded a respective range of 0.20 to 0.25 mm mm^{-1}, 0.23 to 0.26 mm mm^{-1} and 0.23 to 0.24 mm mm^{-1}. The 1 m and 2 m RSW had comparably higher PSWC than the 3 RSW. Improvement in PSWC among the RSW was expected to favour the 3 m RSW because of the large surface area of its runoff or catchment area to harvest in-field runoff (Oweis et al., 1999). But this was not the case because of the high roughness of the field surface especially at this early stage when mechanical activities from basin preparation and fertiliser application are still new.

Change in SWC was also affected by RSW with the 1 m and 2 m RSW recording equally high net gains of 33 mm on the 7 DAP and equally low net gains of -10 mm on the 21 DAP. The 3 m RSW had a high net gain of 23 mm on the 14 DAP; a period that was also characterised by a relative increase in DD and Ev from all RSW. Water application from the FI on the 14 DAP could have exacerbated this situation; hence FI had the highest net gain of 22 mm. Despite the increases in DD following the rainfall and subsequent irrigation there were no significant differences suggesting that the soil profile was initially dry at planting, a common phenomenon in semi-arid areas (Stroosnijder, 1987). Rockstrom et al. (2007) described dry planting as a conservative strategy to minimise Ev and DD, given that the soil is predominately bare and crop water demand is still at infant stage. This was supported by the fact that ET was predominately in the form of Ev and increased with water availability an observation that was well established in literature (FAO, 2011).

Table 8.3 Summary of the analysis of variance depicting the effect of runoff strip width (RSW) and water regime (WR) on selected soil water balance SWB components.

SWB components (mm)	Factors	Days after planting: Establishment 7	14	21	Vegetative 39	47	53	60	67	Reproductive 71	78	84	87	99	105	Ripening 109	116
Profile SWC	RSW	*	*	*	ns	ns	ns	*	ns	ns	*	ns	ns	*	ns	ns	ns
	WR	ns	ns	ns	ns	ns	ns	ns	ns	ns	ns	ns	ns	ns	ns	ns	ns
	RSW x WR	ns	ns	ns	ns	ns	ns	ns	ns	ns	ns	ns	ns	ns	ns	ns	ns
ΔSWC	RSW	*	*	*	ns	ns	ns	*	ns	ns	ns	*	ns	ns	ns	*	ns
	WR	ns	*	*	*	*	*	*	*	*	*	*	*	*	*	*	*
	RSW x WR	ns	ns	*	ns	ns	ns	ns	ns	ns	ns	ns	ns	ns	ns	*	ns
Deep drainage	RSW	ns	ns	ns	ns	ns	ns	ns	ns	ns	ns	ns	ns	*	*	ns	*
	WR	ns	ns	ns	*	ns	ns	ns	*	*	*	ns	ns	*	ns	ns	*
	RSW x WR	ns	ns	ns	ns	ns	ns	ns	ns	ns	ns	ns	ns	*	ns	ns	ns
Evapo-transpiration	RSW	ns	ns	ns	ns	*	*	*	*	*	ns	*	ns	*	*	ns	ns
	WR	ns	ns	*	*	ns	ns	ns	ns	*	ns	*	*	ns	ns	*	ns
	RSW x WR	ns	ns	ns	ns	ns	ns	ns	ns	ns	ns	ns	ns	ns	ns	ns	ns
Evaporation	RSW	ns	ns	ns	ns	*	*	*	*	*	*	*	*	*	*	*	ns
	WR	ns	*	*	ns	ns	*	ns	ns	ns	ns	ns	ns	ns	ns	ns	ns
	RSW x WR	ns	ns	ns	ns	ns	ns	ns	ns	ns	ns	ns	ns	ns	ns	ns	ns
Transpiration	RSW	.	.	*	*	*	*	*	*	*	*	*	*	*	*	*	*
	WR	.	.	ns	*	*	*	*	ns	*	*	*	*	*	ns	*	ns
	RSW x WR	.	.	*	ns	ns	ns	*	ns	ns	ns	ns	ns	ns	ns	ns	ns

*= Significant at 0.05% probability level, ns= not significant, -=data not available.
SWC: soil water content.

The plant establishment stage was concluded with RSW and WR interactions on ΔSWC and T. From the 14 to the 21 DAP is relatively a period of a dry spell and for that reason supplemental and full irrigation were applied. At this period plant canopy cover was approximated at 18 % compared to the 10 % approximated by FAO (2011). Interaction effect on ΔSWC shows that the 2 m and 3 m RSW were affected by irrigation in the same manner while net losses from the 1 m RSW were comparable for all WR. Dryland had the highest net gain of 16 mm coming from the 3 m RSW, although it could be too early to attribute this strong interaction to the in-field runoff potential of this RSW, but it could be taken as an indication that net gain from in-field runoff could exceed that from irrigation provided sufficient rainfall is available. Interaction on T ranged from 6.7 mm to 1.2 mm with the highest and lowest coming from the DL with the 2 m and 3 m RSW. The strong involvement of the DL especially from both interactions could be attributed to the substantial amount of rainfall received at the onset of this growth stage. Although irrigation was introduced towards the end of this period, the strong interaction of 5.8 and 5.1 mm from the respective SPI and FI confirmed the potential contribution of supplemental irrigation could have on transpiration (World Bank, 2005).

Vegetative growth stage:

Soil water components were widely affected by the RSW and WR main effects and interaction effect coming late during this growth stage that lasted about 46 days. Rainfalls of 29.1 mm, 17.1 mm, 10.9 mm and 36 mm received the respective 39, 47, 53 and 60 DAP were the major gains for the DL. Water applied at plot scale from the FI was a depth of 45 mm, 15 mm, and 30 mm on the 39, 53 and 67 DAP, respectively. On the other hand, 15 mm SPI was applied on the 47, 53 and 67 DAP. Despite the fairly even rainfall distribution, the first significant rainfall occurred after 25 days of dry spell, a reminder of the erratic nature of rainfall in the area (Botha, 2006).

Changes in soil water content were the most frequently affected component by the RSW and WR main effects. On the 39 DAP ΔSWC was affected by WR factors recording the highest net loss of -21 mm followed by DL with -12 mm.The higher losses from SPI reflect the nature of deficit irrigation (Bennie et al. 1998) mainly because the crop establishment phase has just passed. Deep drainage was affected by WR on the 39 and 67 DAP and both cases the FI recording highest drainage of 4.1 and 2.6 mm, respectively with the lowest coming from the DL although it was comparable with SPI. The relatively low activity in DD despite the

frequent rainfall and irrigation could be suggesting that water uptake for T increased with water availability throughout this growth phase.

This stage was concluded with RSW and WR interactions on ΔSWC and T. From the 14 to the 21 DAP is relatively a period of a dry spell and for that reason supplemental and full irrigation were applied. At this period plant canopy cover was approximated at 18 % compared to the 10 % approximated by FAO (2011). Interaction effect on ΔSWC shows that the 2 m and 3 m RSW were affected by irrigation in the same manner while net losses from the 1 m RSW were comparable for all WR. Dryland had the highest net gain of 16 mm coming from the 3 m RSW, although it could be too early to attribute this strong interaction to the in-field runoff potential of this RSW, but it could be taken as an indication that net gain from in-field runoff could exceed that from irrigation provided sufficient rainfalls are available. Interaction on T ranged from 6.7 mm to 1.2 mm with the highest and lowest coming from the DL with the 2 m and 3 m RSW. The strong involvement of the DL especially from both interactions could be attributed to the substantial amount of rainfall received at the onset of this growth stage. Although irrigation was introduced towards the end of this period, the strong interaction of 5.8 and 5.1 mm from the respective SPI and FI confirmed the potential contribution supplemental irrigation could have on transpiration (World Bank, 2005).

Evapo-transpiration, Ev and T were also affected by RSW for the greater part of this phase with only T affected as early as on 39 DAP. Transpiration was constantly higher at all times from the 1 m RSW while it was comparably similar from the 2 and 3 m RSW. In contrast Ev ranged from 23 to 3 mm, 29 to 9.4 and 30 to 11 mm from the respective 1 m, 2 m and 3 m RSW. The increase in Ev with increasing RSW could be explained by the surface area available for direct radiation and that which is covered by the plant canopy (Eberbach and Pala, 2005). Most plants from twin rows interlock leaves during the vegetative stage (FAO, 2011) and this is more pronounced on narrow rows of 0.5 to 1 m wide (Onyango, 2009). In this study this was illustrated by a linear relationship between plant height and canopy cover and it was estimated to reach full canopy cover after the 47 DAP. To this effect the proportional contribution of Ev on ET was rapidly reduced to 10 % while that of T was increased up to 90 % depending on the surface area under full canopy cover. The 1 m RSW had 90 % of its surface area under full canopy cover while 2 and 3 m RSW had 50 and 33% under partial canopy cover. This explains why Ev from the wider RSW was comparably higher than from the 1 m RSW.

Table 8.4 Effect of runoff strip width (RSW) and water regime (WR) on soil water balance (SWB) during plant establishment growth stage.

		Factors						RSW x WR									LSD(t ≤ 0.05)			CV (%)	
		RSW (m)			WR			1 m			2 m			3 m							
DAP	SWB	1	2	3	DL	SP	FI	DL	SP	FI	DL	SP	FI	DL	SP	FI	RSW	WR	RSW x WR	RSW	WR
	PSWC	0.25^{a}	0.24^{a}	0.20^{b}	0.24	0.23	0.22	0.26	0.24	0.24	0.24	0.26	0.23	0.22	0.19	0.20	0.02	ns	ns	6.72	30.38
	Δ SWC	32.7^{a}	33.0^{a}	19.0^{b}	26.2	29.2	29.3	30.1	33.1	34.8	31.7	33.5	33.7	16.7	21.0	19.3	4.3	ns	ns	12.5	23.8
7	Dr	0.8	0.9	1.1	1.3	0.7	0.9	0.6	0.6	1.2	1.5	0.5	0.7	1.8	0.9	0.6	ns	ns	ns	92.8	123.1
	ET	15.0	14.3	15.5	15.4	14.9	14.5	16.8	14.9	13.3	13.8	14.8	14.3	15.6	15.0	16.0	ns	ns	ns	15.2	39.7
	E	15.0	14.3	15.5	15.4	14.9	14.5	16.8	14.9	13.3	13.8	14.8	14.3	15.6	15.0	16.0	ns	ns	ns	15.2	39.7
	T	-	-	-	-	-	-	-	-	-	-	-	-	-	-	-	-	-	-	-	-
	PSWC	0.26^{a}	0.26^{a}	0.23^{b}	0.24	0.25	0.26	0.26	0.24	0.27	0.25	0.27	0.26	0.23	0.23	0.25	0.02	ns	ns	5.28	32.77
	Δ SWC	11.2^{b}	12.7^{b}	23.1^{a}	13.3^{b}	11.7^{b}	22.0^{a}	9.8	4.0	19.9	14.1	8.1	16.1	16.1	23.2	30.0	3.8	6.1	ns	19.6	63.7
	Dr	3.0	1.9	2.3	1.4	2.5	3.3	0.8	4.0	4.1	2.2	1.1	2.5	1.3	2.4	3.2	ns	ns	ns	88.6	118.0
14	ET	18.7	19.1	17.4	16.1	16.9	22.3	17.6	19.5	19.0	16.0	17.9	23.5	14.6	13.2	24.3	ns	4.4	ns	14.4	39.5
	E	18.7	19.1	17.4	16.1^{b}	16.9^{b}	22.3^{a}	16.2	19.5	19.0	11.8	17.9	23.5	14.1	13.2	24.3	ns	4.4	ns	14.4	39.5
	T	-	-	-	-	-	-	-	-	-	-	-	-	-	-	-	-	-	-	-	-
	PSWC	0.24^{a}	0.24^{a}	0.23^{b}	0.24	0.23	0.24	0.25	0.23	0.25	0.25	0.25	0.23	0.24	0.21	0.23	0.03	ns	ns	6.14	32.39
21	Δ SWC	-10^{a}	-10^{a}	-3^{b}	1^{a}	-12^{b}	-12^{b}	-10^{bc}	-9^{bc}	-9^{bc}	-4^{b}	-12^{c}	-15^{c}	16^{a}	-12^{c}	-13^{c}	4.3	3.3	7.4	-45.2	-69.4
	Dr	1.8	2.3	1.5	1.5	1.5	2.5	1.0	1.6	2.9	2.8	1.1	2.8	0.8	1.7	1.9	ns	ns	ns	36.8	87.6
	ET	23.5	24.9	22.9	16.8	27.2	27.3	18.5	25.9	26.1	18.2	28.1	28.6	13.7	27.7	27.3	ns	ns	ns	20.7	40.2
	E	18.9	17.0	16.1	12.9	19.4	19.7	15.7	20.1	20.9	10.4	20.1	20.4	12.5	18.1	17.7	ns	ns	ns	22.8	42.8
	T	4.6^{a}	4.9^{a}	2.7^{b}	3.6	4.4	4.2	2.8^{c}	5.8^{ab}	5.1^{b}	6.7^{a}	3.9^{c}	4.0^{c}	1.2^{d}	2.1^{cd}	3.4^{cd}	1	ns	1.8	19.7	32.3

Dl = dry-land; SP= supplemental irrigation; FI= full irrigation; ns = not significant

Table 8.5 Effect of runoff strip width (RSW) and water regime (WR) on soil water balance (SWB) during plant establishment growth stage.

		Factors						RSW x WR													
		RSW (m)			WR			1 m			2 m			3 m			LSD(t ≤ 0.05)			CV (%)	
DAP	SWB	1	2	3	DL	SP	FI	DL	SP	FI	DL	SP	FI	DL	SP	FI	RSW	WR	RSW x WR	RSW	WR
	PSWC	0.25[a]	0.24[a]	0.20[b]	0.24	0.23	0.22	0.26	0.24	0.24	0.24	0.26	0.23	0.22	0.19	0.20	0.02	ns	ns	6.72	30.38
	Δ SWC	32.7[a]	33.0[a]	19.0[b]	26.2	29.2	29.3	30.1	33.1	34.8	31.7	33.5	33.7	16.7	21.0	19.3	4.3	ns	ns	12.5	23.8
7	Dr	0.8	0.9	1.1	1.3	0.7	0.9	0.6	0.6	1.2	1.5	0.5	0.7	1.8	0.9	0.6	ns	ns	ns	92.8	123.1
	ET	15.0	14.3	15.5	15.4	14.9	14.5	16.8	14.9	13.3	13.8	14.8	14.3	15.6	15.0	16.0	ns	ns	ns	15.2	39.7
	E	15.0	14.3	15.5	15.4	14.9	14.5	16.8	14.9	13.3	13.8	14.8	14.3	15.6	15.0	16.0	ns	ns	ns	15.2	39.7
	T	-	-	-	-	-	-	-	-	-	-	-	-	-	-	-	-	-	-	-	-
	PSWC	0.26[a]	0.26[a]	0.23[b]	0.24	0.25	0.26	0.26	0.24	0.27	0.25	0.27	0.26	0.23	0.23	0.25	0.02	ns	ns	5.28	32.77
	Δ SWC	11.2[b]	12.7[b]	23.1[a]	13.3[b]	11.7[b]	22.0[a]	9.8	4.0	19.9	14.1	8.1	16.1	16.1	23.2	30.0	3.8	6.1	ns	19.6	63.7
	Dr	3.0	1.9	2.3	1.4	2.5	3.3	0.8	4.0	4.1	2.2	1.1	2.5	1.3	2.4	3.2	ns	ns	ns	88.6	118.0
14	ET	18.7	19.1	17.4	16.1	16.9	22.3	17.6	19.5	19.0	16.0	17.9	23.5	14.6	13.2	24.3	ns	4.4	ns	14.4	39.5
	E	18.7	19.1	17.4	16.1[b]	16.9[b]	22.3[a]	16.2	19.5	19.0	11.8	17.9	23.5	14.1	13.2	24.3	ns	4.4	ns	14.4	39.5
	T	-	-	-	-	-	-	-	-	-	-	-	-	-	-	-	-	-	-	-	-
	PSWC	0.24[a]	0.24[a]	0.23[b]	0.24	0.23	0.24	0.25	0.23	0.25	0.25	0.25	0.23	0.24	0.21	0.23	0.03	ns	ns	6.14	32.39
21	Δ SWC	-10[a]	-10[a]	-3[b]	1[a]	-12[b]	-12[b]	-10[bc]	-9[bc]	-9[bc]	-4[b]	-12[c]	-15[c]	16[a]	-12[c]	-13[c]	4.3	3.3	7.4	-45.2	-69.4
	Dr	1.8	2.3	1.5	1.5	1.5	2.5	1.0	1.6	2.9	2.8	1.1	2.8	0.8	1.7	1.9	ns	ns	ns	36.8	87.6
	ET	23.5	24.9	22.9	16.8	27.2	27.3	18.5	25.9	26.1	18.2	28.1	28.6	13.7	27.7	27.3	ns	ns	ns	20.7	40.2
	E	18.9	17.0	16.1	12.9	19.4	19.7	15.7	20.1	20.9	10.4	20.1	20.4	12.5	18.1	17.7	ns	ns	ns	22.8	42.8
	T	4.6[a]	4.9[a]	2.7[b]	3.6	4.4	4.2	2.8[c]	5.8[ab]	5.1[b]	6.7[a]	3.9[c]	4.0[c]	1.2[d]	2.1[cd]	3.4[cd]	1	ns	1.8	19.7	32.3

Dl = dry-land; SP= supplemental irrigation; FI= full irrigation; ns = not significant

Table 8.6 Effect of runoff strip width (RSW) and water regime (WR) on soil water balance in the vegetative growth stage.

		Factors						RSW x WR													
		RSW			WR			1 m			2 m			3 m			LSD(t ≤ 0.05)			CV (%)	
DAP	SWB	1	2	3	D	SP	FI	D	SP	FI	D	SP	FI	D	SP	FI	RSW	WR	RSW.WR	RSW	WR
	PSWC	0.22	0.22	0.22	0.23	0.20	0.24	0.22	0.20	0.26	0.22	0.21	0.23	0.23	0.19	0.24	ns	ns	ns	7.9	33.4
	Δ SWC	-13.0	-14.3	-4.9	-11.9^{b}	-21.3^{c}	1.0^{a}	-19.7	-21.2	2.0	-11.4	-28.5	-3.1	-4.6	-14.1	4.0	ns	3.8	ns	-81.3	-59.0
39	Dr	2.2	2.3	2.0	1.1^{b}	1.4^{b}	4.1^{a}	0.9	2.1	3.6	1.5	1.5	3.8	0.8	0.6	4.8	ns	1.3	ns	51.0	79.0
	ET	61.1	57.2	51.1	44.7	52.3	72.4	48.4	57.3	77.7	41.0	56.6	73.9	44.7	43.1	65.5	ns	12.4	ns	19.7	36.2
	E	22.8	29.1	29.8	27.4	23.9	30.4	24.6	16.8	27.0	24.1	29.5	33.7	33.6	25.4	30.5	ns	ns	ns	25.7	38.7
	T	38.3^{a}	28.1^{b}	21.3^{c}	17.2^{b}	28.4^{a}	42.0^{a}	23.8	40.4	50.7	16.8	27.1	40.2	11.1	17.8	35.0	7.0	6.4	ns	19.6	36.1
	PSWC	0.21	0.21	0.21	0.21	0.20	0.22	0.20	0.20	0.23	0.22	0.21	0.22	0.22	0.19	0.22	ns	ns	ns	9.2	34.1
	Δ SWC	-8.7	-5.6	-5.4	-7.0^{b}	0.3^{a}	-13.0^{c}	-10.4	2.6	-18.3	-5.2	-2.4	-9.3	-5.5	0.7	-11.4	ns	2.9	ns	-49.3	-73.8
	Dr	1.2	0.7	0.3	0.6	1.4	0.2	1.4	2.0	0.2	0.1	1.7	0.2	0.4	0.4	0.2	2.2	2.8	3.7	53.1	68.9
47	ET	34.9^{a}	25.1^{b}	26.6^{ab}	24.3	29.5	32.9	26.2	37.1	41.4	21.4	27.8	26.2	25.3	23.5	31.0	9.6	ns	ns	27.1	37.1
	E	5.6^{b}	10.6^{ab}	15.6^{a}	12.9	8.6	10.4	9.3	2.8	4.8	11.2	10.8	9.9	18.1	12.2	16.5	6	ns	ns	45.8	57.2
	T	29.3^{a}	16.2^{b}	13.5^{b}	11.4^{b}	25.0^{a}	22.5^{a}	16.9	34.3	36.6	10.3	22.0	16.4	7.2	18.7	14.5	6.2	4.1	ns	25.8	34.8
	PSWC	0.22	0.23	0.23	0.21	0.22	0.25	0.19	0.22	0.24	0.21	0.22	0.25	0.22	0.21	0.26	ns	ns	ns	8.0	37.1
53	Δ SWC	2.7	4.3	4.3	-6.6^{b}	9.9^{a}	8.0^{a}	-10.0	9.2	8.9	-4.1	9.6	7.4	-5.8	10.8	7.8	ns	3.2	ns	46.9	64.3
	Dr	1.7	1.7	1.5	0.0	2.4	2.4	0.02	3.1	1.9	0.03	2.0	3.0	0.1	2.1	2.2	ns	ns	ns	65.1	83.9
	ET	25.6^{a}	20.0^{b}	24.6^{b}	20.1	24.9	25.2	20.9	28.8	27.0	14.9	21.0	24.2	24.5	24.8	24.4	3.2	ns	ns	11.3	39.4
	E	21.9^{b}	12.8^{b}	12.6^{a}	10.3	18.7	18.4	15.8	26.6	23.3	7.1	14.7	16.6	7.9	14.8	15.2	2.8	3.5	ns	14.6	36.3
	T	26.1^{a}	16.5^{b}	11.6^{b}	14.9^{b}	19.2^{a}	20.2^{a}	22.9	26.3	29.1	12.7	15.8	20.9	9.0	15.5	10.5	4.7	3.6	ns	21.4	32.9
	PSWC	0.21^{b}	0.23^{a}	0.22^{a}	0.2	0.23	0.24	0.17	0.22	0.25	0.20	0.25	0.23	0.22	0.21	0.24	0.01	ns	ns	5.0	34.7
	Δ SWC	10.3^{b}	12.2^{b}	16.9^{a}	19.7^{a}	9.6^{b}	10.1^{b}	16.6	4.8	9.5	18.1	9.1	9.3	24.4	14.9	11.5	3.8	2.7	ns	23.6	34.4
	Dr	0.7	0.8	0.8	0.5	0.7	1.2	0.01	0.6	1.5	0.7	0.2	1.4	0.7	1.1	0.6	ns	ns	ns	71.4	84.0
60	ET	32.4^{a}	24.7^{b}	21.7^{b}	23.1	29.2	26.5	25.3	41.0	30.8	22.2	26.6	25.3	21.7	20.0	23.4	3.6	ns	ns	11.1	34.5
	E	3.2^{b}	10.3^{a}	12.0^{a}	8.5	8.2	8.8	2.5	3.0	4.0	10.5	10.5	9.9	12.4	11.0	12.5	2.8	ns	ns	26.9	62.1
	T	29.2^{a}	14.4^{b}	9.7^{b}	14.6^{b}	21.0^{a}	17.7^{ab}	22.8^{b}	38.0^{a}	26.9^{b}	11.7^{cd}	16.1^{c}	15.4^{c}	9.3^{cd}	8.9^{d}	10.9^{cd}	4.9	2.8	6.5	22.7	26.2
	PSWC	0.21	0.22	0.21	0.20	0.20	0.23	0.17	0.20	0.25	0.21	0.21	0.22	0.21	0.19	0.22	ns	ns	ns	6.4	35.0
	Δ SWC	-2.6	-5.3	-7.9	-2.1^{a}	-8.8^{c}	-4.9^{b}	-3.2	-6.7	2.2	-1.6	-7.7	-6.6	-1.4	-12	-10	ns	2.8	ns	-91.9	-86.6
67	Dr	1.0	1.6	1.3	0.3^{b}	1.1^{b}	2.6^{a}	0.1	1.1	1.9	0.5	0.8	3.4	0.4	1.3	2.3	ns	1	ns	42.9	56.3
	ET	28.7^{a}	25.9^{b}	22.2^{b}	21.4	26.9	28.5	24.3	28.6	33.3	23.1	24.2	30.4	16.8	27.9	21.8	5.1	ns	ns	18.9	32.6
	E	2.6^{b}	9.4^{a}	10.5^{a}	6.6	7.7	8.4	1.4	2.3	4.2	10.4	8.4	9.5	7.8	12.4	11.4	3.2	ns	ns	35.3	47.8
	T	26.1^{a}	16.5^{b}	11.6^{b}	14.9	19.2	20.2	22.9	26.3	29.1	12.7	15.8	20.9	9.0	15.5	10.5	4.7	ns	ns	21.4	32.9

D = dry-land; SP = supplemental irrigation; FI = full irrigation; ns = not significant

Table 8.7 Effect of runoff strip width (RSW) and water regime (WR) on soil water balance in the reproductive growth stage.

		Factors						RSW x WR									LSD(t ≤ 0.05)			CV (%)	
		RSW			WR			1 m			2 m			3 m							
DAP	SWB	1	2	3	DL	SP	FI	DL	SP	FI	DL	SP	FI	DL	SP	FI	RSW	WR	RSW.WR	RSW	WR
	PSWC	0.21	0.22	0.20	0.20	0.20	0.23	0.17	0.2	0.25	0.21	0.21	0.22	0.21	0.19	0.22	ns	ns	ns	6.4	35.0
	Δ SWC	-10.5	-9.7	-9.8	-12.8^{b}	-12.6^{b}	-4.5^{a}	-14.2	-14.6	-2.5	-12.5	-12.2	-4.6	-11.8	-11.0	-6.4	ns	2.5	ns	-38.5	-41.1
71	Dr	0.3	1.0	0.4	0.2^{a}	0.1^{b}	1.4^{b}	0.1	0.1	0.8	0.4	0.05	2.5	0.2	0.1	1.0	ns	5.9	ns	45.6	66.6
	ET	17.3^{a}	12.0^{b}	10.9^{b}	11.2	13.9	15.1	12.9	18.8	20.2	11.7	12.1	12.0	8.8	10.9	12.9	3.8	ns	ns	23.5	39.0
	E	1.6^{b}	4.7^{a}	5.4^{a}	3.4	4.0	4.4	0.7	1.4	2.7	5.3	4.7	4.2	4.1	5.8	6.4	1.9	ns	ns	38.9	76.8
	T	15.7^{a}	7.2^{b}	5.5^{b}	7.8	10.0	10.6	12.2	17.3	17.5	6.5	7.4	7.8	4.7	5.2	6.5	3.1	ns	ns	26.4	31.0
	PSWC	0.18^{a}	0.20^{b}	0.19^{b}	0.18	0.17	0.21	0.16	0.17	0.23	0.21	0.19	0.20	0.19	0.16	0.20	0.01	ns	ns	4.9	32.9
	Δ SWC	-14.4	-14.1	-16.4	-31.0^{b}	-5.5^{a}	-8.4^{a}	-32.6	-3.2	-7.4	-30.7	-3.6	-8.0	-29.9	-9.7	-9.7	3.9	ns	ns	-36.1	-42.6
	Dr	0.59	0.76	0.31	0.12^{b}	0.22^{b}	1.32^{a}	0.14	0.32	1.30	0.20	0.02	2.05	0.01	0.32	0.60	ns	0.6	ns	54.1	69.5
78	ET	23.2^{a}	17.4^{ab}	17.0^{b}	15.9	20.5	21.1	16.6	24.3	28.6	15.7	17.0	19.4	15.4	20.3	15.4	6.1	ns	ns	26.6	48.0
	E	2.1^{b}	6.9^{a}	8.9^{a}	6.2	6.4	5.3	1.7	2.0	2.5	7.8	6.4	6.5	9.1	10.9	6.8	2.4	ns	ns	32.4	82.1
	T	21.1^{a}	10.5^{b}	8.1^{b}	9.7^{b}	14.1^{a}	15.9^{a}	15.0	22.3	26.1	7.9	10.6	12.9	6.3	9.4	8.6	5.3	3	ns	32.5	36.9
	PSWC	0.18	0.20	0.19	0.18	0.17	0.21	0.16	0.17	0.23	0.21	0.19	0.20	0.19	0.16	0.20	ns	ns	ns	7.0	33.6
84	Δ SWC	-8.9^{b}	-5.9^{ab}	-4.3^{a}	-15.7^{b}	-2.1^{a}	-1.3^{a}	-16.6	-4.3	-5.8	-14.0	-2.2	-1.6	-16.6	0.3	3.4	2.8	2.3	ns	-48.6	-58.3
	Dr	0.06	0.14	0.13	0.14	0.04	0.15	0.12	0.05	0.01	0.27	0.02	0.13	0.02	0.06	0.3	ns	ns	ns	67.8	75.0
	ET	18.4^{a}	12.7^{b}	11.7^{b}	10.8^{b}	15.7^{a}	16.3^{a}	11.1	21.2	22.7	10.5	14.2	13.6	10.8	11.7	12.6	4.2	3.1	ns	24.0	36.2
	E	1.7^{b}	5.5^{a}	6.6^{a}	5.1	4.2	4.5	1.3	1.6	2.1	6.1	5.4	5.2	8.0	5.7	6.2	1.7	ns	ns	29.2	52.7
	T	17.2^{a}	7.5^{b}	5.8^{b}	7.3^{b}	11.5^{a}	11.8^{a}	11.5	19.6	20.6	5.5	8.8	8.4	4.9	6.0	6.4	3.5	2	ns	28.1	32.0
	PSWC	0.20	0.20	0.19	0.18	0.19	0.22	0.16	0.19	0.24	0.19	0.20	0.21	0.19	0.18	0.21	ns	ns	ns	7.4	34.4
	Δ SWC	6.7	6.1	3.1	-0.4^{c}	10.9^{a}	5.4^{b}	-0.6	13.2	7.5	2.7	10.4	5.4	-3.3	9.3	3.3	ns	2.2	ns	71.7	67.7
	Dr	0.2	0.2	0.1	0.2	0.3	0.1	0.1	0.4	0.1	0.3	0.3	0.02	0.04	0.2	0.1	ns	ns	ns	50.7	62.2
87	ET	11.0^{a}	8.3^{b}	7.6^{b}	5.7^{b}	10.8^{a}	10.3^{a}	5.6	14.3	13.0	5.3	9.7	9.9	6.3	8.4	8.1	2.4	1.8	ns	22.1	33.1
	E	1.1^{b}	3.7^{a}	4.2^{a}	2.6	3.2	3.2	0.6	1.1	1.8	3.2	3.9	3.8	4.1	4.5	3.9	1.7	ns	ns	47.8	51.2
	T	9.8^{a}	4.6^{b}	3.4^{b}	3.1^{b}	7.6^{a}	7.2^{a}	5.1^{b}	13.3^{a}	11.2^{a}	2.1^{c}	5.7^{b}	6.1^{b}	2.2^{c}	3.9^{bc}	4.2^{bc}	1.3	1.2	2.7	17.6	33.1
	PSWC	0.20^{b}	0.23^{a}	0.22^{a}	0.22	0.21	0.22	0.21	0.18	0.21	0.24	0.23	0.23	0.23	0.21	0.23	0.01	ns	ns	5.3	33.6
	Δ SWC	19.5	21.0	20.3	31.2^{a}	17.5^{b}	12.1^{c}	32.3	15.2	11.0	30.4	18.7	13.9	30.9	18.6	11.5	ns	3.7	ns	21.5	29.8
99	Dr	0.9^{b}	1.4^{b}	3.6^{a}	0.4^{c}	1.8^{b}	3.7^{a}	0.01^{cd}	1.7^{bcd}	0.9^{bcd}	0.8^{cd}	0.2^{cd}	3.2^{bc}	0.5^{cd}	3.4^{b}	7.0^{a}	1.2	1.2	2.7	51.9	67.4
	ET	42.7^{a}	35.3^{ab}	33.6^{b}	32.3	37.9	41.5	31.1	46.5	50.6	32.7	35.5	37.7	33.1	31.7	36.1	8.0	ns	ns	17.7	35.8
	E	5.1^{b}	14.5^{a}	17.8^{a}	12.1	10.9	14.3	3.1	3.7	8.4	15.2	13.1	15.4	18.1	15.9	19.3	5.7	ns	ns	37.6	66.3
	T	37.7^{a}	20.8^{b}	15.9^{b}	20.2^{b}	27.0^{a}	27.1^{a}	28.0	42.8	42.2	17.5	22.4	22.4	15.0	15.8	16.8	6.6	4.2	ns	21.7	28.1
	PSWC	0.21	0.21	0.21	0.22	0.19	0.22	0.19	0.19	0.24	0.22	0.20	0.21	0.23	0.18	0.21	ns	ns	ns	6.1	31.8
105	Δ SWC	-6.7	-9.4	-12.3	-0.9^{a}	-18.2^{c}	-9.3^{b}	6.9	-17.7	-9.2	.7	-19.1	-10.0	-10.2	-17.7	-8.8	ns	4.9	ns	-66.2	-86.1

Continued

	Dr	0.1[b]	0.5[a]	0.6[a]	0.3	0.2	0.6	0.02	0.2	0.1	0.5	0.2	1.0	0.5	0.4	0.8	0.4	ns	ns	66.2	77.8
	ET	20.4[a]	17.3[b]	16.4[b]	20.5	16.5	17.2	19.9	19.1	22.1	20.6	15.7	15.7	21.0	14.5	13.8	2.8	ns	ns	12.8	31.2
	E	4.5[b]	7.4[a]	8.5[a]	7.0	6.7	6.8	3.4	3.7	6.4	8.3	7.4	6.6	9.2	9.0	7.4	2.8	ns	ns	33.3	50.5
	T	14.0[a]	8.1[b]	5.9[b]	7.8	9.8	10.4	10.9	15.4	15.6	6.8	8.4	9.1	5.7	5.5	6.4	2.3	ns	ns	20.5	28.1

D = dry-land; SP= supplemental irrigation; FI= full irrigation; ns=not significant

Table 8.8 Effect of runoff strip width (RSW) and water regime (WR) on soil water balance in the ripening growth stage.

		Factors						RSW x WR									LSD(t ≤ 0.05)			CV (%)	
		RSW (m)			WR			1 m			2 m			3 m							
DAP	SWB	1	2	3	DL	SP	FI	DL	SP	FI	DL	SP	FI	DL	SP	FI	RSW	WR	RSW.WR	RSW	WR
	PSWC	0.21	0.21	0.21	0.21	0.20	0.22	0.18	0.20	0.24	0.21	0.22	0.21	0.23	0.19	0.21	ns	ns	ns	7.3	33.0
	Δ SWC	-2.6[b]	-2.6[b]	4.4[a]	-10.5[c]	10.4[a]	-0.6[b]	-18.6[c]	12.0[a]	-1.2[d]	-18.1[c]	11.6[a]	-1.2[d]	5.2[bc]	7.5[ab]	0.5[cd]	3.3	2.3	5.3	-50.5	-69.3
109	Dr	0.4	0.3	0.6	0.2	0.8	0.3	0.03	1.2	0.1	0.2	0.3	0.4	0.5	0.8	0.5	ns	ns	ns	50.9	71.2
	ET	11.2[a]	8.5[b]	8.7[b]	8.7	9.3	10.4	8.8	13.7	11.2	8.4	6.6	10.5	8.9	7.7	9.6	2.2	ns	ns	19.0	32.5
	E	3.6[a]	4.8ab	5.9a	5.0	4.1	5.3	3.5	3.8	3.5	5.2	3.6	5.7	6.3	5.0	6.5	1.4	ns	ns	24.1	37.1
	T	7.6[a]	3.7[b]	2.8[b]	3.7	5.2	5.2	5.2	9.9	7.6	3.2	3.1	4.9	2.6	2.7	3.1	1.3	2.7	ns	22.7	38.6
	PSWC	0.22	0.32	0.22	0.22	0.22	0.23	0.20	0.22	0.25	0.23	0.23	0.22	0.23	0.20	0.22	ns	ns	ns	6.3	32.8
	Δ SWC	11.1	9.9	10.2	15.4[a]	9.0[b]	6.8[b]	16.7	8.5	8.2	13.9	9.5	6.3	15.7	9.1	5.9	ns	2.4	ns	30.5	38.0
	Dr	0.15[b]	0.69[a]	0.74[a]	0.25[b]	0.44[b]	0.90[a]	0.0	0.3	0.1	0.5	0.2	1.4	0.2	0.9	1.1	0.5	0.35	ns	57.4	68.8
116	ET	16.6	15.6	13.1	13.8	15.4	16.1	14.2	18.5	17.2	16.8	14.0	16.0	10.5	13.7	15.1	ns	ns	ns	30.5	37.6
	E	7.8	9.4	10.6	9.5	8.6	9.7	7.1	7.7	8.7	10.2	8.4	9.6	11.3	9.7	10.8	ns	ns	ns	28.8	42.0
	T	8.8[a]	6.2[b]	4.2[b]	6.0	6.8	6.4	7.1	10.8	8.6	6.6	5.6	6.4	4.2	4.1	4.3	2.4	ns	ns	22.3	33.3

D = dry-land; SP= supplemental irrigation; FI= full irrigation; ns=not significant

The surface area from the 1 m RSW appears to have not only increased the area shaded by plant canopy but also the accessibility of plant roots to soil water storage (Onyango, 2009). Given the high surface area under full canopy cover from the 1 m RSW, the corresponding high net losses from the soil water storage could only be attributed to the higher ET. This appears to favour the introduction of irrigation on IRWH because the increased water availability gets directed towards photosynthesis rather than unproductive losses (DD and Ev). Dryland had the lowest ET and T among the WR a reflection of the water stress environment confronting IRWH (Botha, 2006). Interaction was on the 60 DAP for the T component with an interaction ranging from 38 to 8.9 mm. The SPI had the strongest and lowest interaction from the respective 1 m RSW and 3 m RSW, illustrating the potential of the SPI in stabilising the plant growth when integrated with IRWH.

Reproductive growth stage:

Soil water components were variably affected by the RSW and WR main effects. Effect from the RSW and WR interaction on T and DD was seen on the 87 and 99 DAP. This stage lasted about 45 days with flowering occurring as early as the 60 DAP falling under the vegetative stage. Despite the high crop water demand required for grain development, there were three rainfalls with corresponding amount of 12.1 mm, 10.3 mm and 48.5 mm on the 84, 87 and 99 DAP, respectively. Apparently a 24 day dry spell occurred during the flowering period and a net loss of -31 mm from the soil water storage was reflected from the DL water regime. This was undesirable given that water stress conditions at flowering could directly reduce grain yield approximately up to 40% (Westgate et al., 2004).

Mitigation of dry spell included SPI with two applications of 15 mm on the 78 and 87 DAP and FI with 15 mm water application for the 71, 78 and 105 DAP as well as 7.5 mm on the 87 DAP. Showing more consistency with the irrigation events were improved changes on ΔSWC and ET as the result of the main effect from WR. The FI continued to record highest net gains and ET, while DL had the least and improvements were consistent with rainfall events.

Affected by RSW throughout this stage were ET and its constituents. The 1 m RSW had ET ranging from 43 to 11 mm, the 2 m RSW ranging from 8 to 35 mm and the 3 m RSW ranging from 8 to 34 mm. The nearly similar ET range between the 2 and 3 m RSW is not surprising given that both these RSW experienced partial shading from the spatially arranged runoff area. The evidence of spatiality was shown Ev that ranged from 1 to 5 mm, 4 to 15 mm, and 4.2 to 18 mm from the 1 m, 2 m, and 3 m RSW, respectively. Although ET decreased with

increasing RSW the opposite is shown by the Ev range suggesting that T was higher at narrow RSW. This was confirming earlier observations in this study that the 1 m RSW suppressed Ev and enhanced T. Increasing canopy cover and concentration of crop roots within the accessible near the basin area are the possible reasons (Magbool et al., 2006; Grena and Hess, 1994).

Rare to these observations was a RSW and WR interaction on DD captured on the 99 DAP just after the 49 mm rainfall. The DD losses from the interaction ranged from 7 to 0.01 mm with the strongest interaction obtained from the FI of the 3 m RSW and the lowest from the DL of the 1 m RSW. This was consistent with the constant recharge of soil water storage from the FI and the capacity of the 3 m RSW to harvest sizeable in-field runoff. On the other hand the 1 m RSW had the lowest DD losses and the reason could be twofold. Firstly, the high abstraction of soil water from the plants roots concentrated over a small area (Eberbatch and Pala, 2005) and secondly the low capacity of the RSW surface area to harvest adequate in-field runoff could be the reason (Rockstrom et al., 2007). The SPI had DD interaction ranging from 3 to 0.2 mm confirming the conservative advantage of recharging the soil profile while reserving adequate rainfall storage space (Bennie and Hensley, 2001)

Ripening stage:

Runoff strip width and WR affected soil water components including an interaction on the ΔSWC. Although this stage persisted beyond the 120 DAP, soil water measurements were discontinued on the 116 DAP following a rainstorm with strong winds that lodged the crop. Gains at this stage were from rainfalls of 8.5 mm and 24 mm from the respective 109 and 116 DAP. The first rain occurred just after the SPI and risk of DD was well taken care off given the low and infrequent applications from SPI. This stage is characterised by grain development including grain filling and dry matter accumulation that requires sustainable supply of water (Westgate et al., 2004).

Apart from the RSW and WR interaction affecting ΔSWC, ET and its constituents were affected by RSW on the 109 DAP. Because of the interaction, the ΔSWC ranged from 12 to -19 mm with the highest net gain and losses coming from SPI of the 1 m RSW and DL of the 1 m RSW. The high net losses from DL were expected given the water stress conditions encountered by dryland crop production. The strong interaction on SPI could be attributed to the fact that 8.5 mm rainfall had just occurred after the SPI was applied and inadequate to offset the abstraction that occurs in the 1 m RSW. Corresponding to the same period was the

highest Ev recorded from the 3 m RSW of 6.8 mm and lowest from 1 m RSW of 3.6 mm. Transpiration was 7.6, 4.8 and 4.5 mm from the respective 1 m, 2 m and 3 m RSW. Transpiration was also affected by RSW having a range of 3.7 to 8 mm with the highest from the 1 m RSW. Corresponding ET followed the same trend with a range from 11 to 8.8 mm. Following a 2 consecutive month period being affected by the main effects of RSW and WR, the change in ET on the 116 DAP to become unaffected by any of the main factors could be considered to be a sign of slowing down by the crop plants and also of the atmospheric evaporative demand at this late stage of the season (Kaisi, 2000; FAO, 2011). However, T was affected until the 116 DAP with the highest T recorded from the 1 m RSW suggesting that even though the crop could be approaching maturing water was still required for the kernels to achieve physiological maturity (Westgate et al. 2004). Deep drainage was also affected by RSW and WR following the last rainfall of 24 mm suggesting that at this stage of plant growth the soil profile water was no longer abstracted as it was during the vegetative and reproductive stage. Although the amounts were relatively small with 1 mm being the highest from the FI, suggesting that the soil profile from the FI was still having adequate soil water reserves.

8.5 Conclusion

In this study a soil water balance was developed and applied to quantify the effect of the integrated management practices of IRWH and MFI on the gains and losses over the production season. The procedure considered the surface area available for in-field runoff harvesting for the 1 m, 2 m and 3 m RSW. Also the surface area under canopy cover at various crop growth stages was considered for the basin and runoff area. Available surface area for in-field runoff was estimated to be 50, 67 and 75 % for the respective 1 m, 2 m and 3 m RSW with a corresponding canopy cover of 90, 50 and 33 % at mid season. The procedure was consistent with the basic runoff farming and agronomic principles and therefore it was regarded to be reasonable and fit for adoption.

The developed procedure was then applied to determine the effect of the runoff strip width (1 m, 2 m and 3 m) and water regimes (dryland, supplemental and full irrigation) on the soil water gains and losses over the production season. At the plant establishment phase the soil was initially dry, bare and with a high surface roughness. Therefore the influence of the RSW surface area and canopy cover on soil water storage and evapo-transpiration was negligible; hence evapo-transpiration was mainly in the form of evaporation. During the vegetative,

reproductive and ripening phases, net gain from the 2 and 3 m RSW were comparably higher than from the 1 m RSW especially after the main rainfall not less than 24 mm. A net loss of about -12 mm and more were associated with the dryland especially after dry spells of more than 14 days.

Water application from either supplemental or full irrigation improved PSWC and net gain in the same manner and that translated to higher evapo-transpiration, evaporation and transpiration irrespective of the RSW. The 1 m RSW had superior evapo-transpiration and transpiration despite the relatively low net gains. This phenomenon was attributed to the high surface area fully shaded by the plant canopy and densely rooted as well. Rainfalls of not less than 24 mm just after irrigation or at short intervals resulted on RSW x WR interaction. While deep drainage was affected in a comparably similar manner between dryland and supplemental irrigation, net water gain from the 2 m and 3 m RSW (dryland) was consistently higher than that from irrigation.

Acknowledgements

We acknowledge the technical support rendered by the management and staff of Paradys experiment station. Gratitude's to Mike Fair for his assistance regarding the use the SAS 9 software during the statistical analysis in this work.

8.6 References

Al-Kaisi, M., 2000. Crop water use or evapo-transpiration: Integrated crop management. http://www.ipm.ipm.oastate.edu , 19/11/2011. 10.30 am (LT).

Anschutz, J., Kome, A., Nederlof, M., de Neef, R., and van de Van T., 2003. Water harvesting and Soil water retention. Sec ed. *Agromisa Foundation*. Wageningen, Netherlands.

Araya, A. and Stroosnijder, L., 2010. Effects of tied ridges and mulch on barley (Hordeum vulgare) rainwater use efficiency and production in Northern Ethiopia. *Agricultural Water Management*, 97: 841-847.

Austin, C., 2003. Micro flood, a new way of applying waters. http://waterright.com. 22/09/2011, 10.00 a.m (LT).

Bennie, A.T.P. and Hensley, M., 2001. Maximising precipitation utilization in dryland agriculture in South Africa- a review. *J. Hydrol.*, 241: 124-139.

Bennie, A. T. P., Strydom, M. G. and Vrey, H. S., 1998. The use of computermodels or agricultural water management on ecotope level. Water Research Commission report, TT 102/98, Pretoria, South Africa.

Botha, J. J., 2006. Evaluation of maize and sunflower production in a semi-arid area using In-field rainwater harvesting. Ph.D. (Agric) Dissertation, University of the Free State, Bloemfontein.

Eberbatch, P. and Pala M., 2005. Crop row spacing and its influence on the partitioning of evapo-transpiration by winter-grown wheat in Northern Syria. *Plant and soil*, 268: 195-208.

FAO, 2011. Chapter 5; Introduction to crop evapo-transpiration.http://www.fao.org. 20/11/2011, 10.30 am (LT);

Gobeze, L., 2012. Establishing optimum plant populations and water use of an ultra fast maize hybrid (*Zea Mays L*) under irrigation. Ph.D. (Agric) Dissertation, University of the Free State, Bloemfontein.

Gomez, K. A. and Gomez, A.A., 1984.Statistical procedures for agricultural research. 2nd ed. John Wiley and Sons, New York, USA.

Hensley, M., Botha, J. J., Anderson, J. J., van Staden, P. P. and DuToit, A., 2000. Optimising rainfall use efficiency for developing farmers with limited access to irrigation water. Water Research Commission Report no. 878/1/00, Pretoria, South Africa.

Hensley, M., Le Roux, P. A. L., Du Preez, C. C., Van Huyssteen, C., Kotze, E. and Van Rensburg, L. D., 2007. Soils; the Free State agricultural base. *South African Geographical Journal.* 88: 11-21.

Iptas S. and Acar, A. A., 2006. Effects of hybrid and row spacing on maize forage yield and quality. *Plant and Soil Environment*, 52: 515-522.

Joseph, F., 2007. Maize response to in-field rainwater harvesting on the Fort Hare/Oakleaf Ecotope. MSc (Agric) Dissertation, University of the Free State, Bloemfontein, South Africa.

Lascano, R. J., 1991. Review of models for predicting soil water balance. Soil water balance in the Sudano-Sahelian Zone (proceedings of the Niamey Work shop) No. 199.

Maqbool, M. M., Tanveer, A., Ata, Z. and Ahmad, R., 2006. Growth and yield of maize (Zea Mays L.) as affected by row spacing and weed competition durations. *Pak. J. Bot.*, 38:1227-1236.

Mzezewa, J. and van Rensburg, L. D., 2011. Effects of tillage on runoff from a bare clayey soil on a semi-arid ecotope in the Limpopo Province of South Africa. *Water SA* 37: 1-8.

Mzezewa, J., Gwata, E. T. and van Rensburg, L. D., 2011. Yield and seasonal water productivity of sunflower as affected by tillage and cropping systems under dryland conditions in the Limpopo Province of South Africa. *Agricultural water Management*, 98: 1641-1648.

Onyango, O. C., 2009. Decreased row spacing as an option for decreasing maize (Zea may L.) yield in Trans Nzoi district, *Kenya. J. of Plant Breeding and Crop Science*, 1: 281-283.

Oweis, T., Hachum, A. and Kijne. J., 1999. Water harvesting and supplementary irrigation for improved water use efficiency in dry areas. IWMI Contribution (No. 7), System Wide Initiative on Water Management (SWIM). Colombo, Sri Lanka.

Prinz, D., and Malik, A. H., 2002. Runoff farming. Institute of Water Resources Management, Hydraulic and Rural Engineering. Department of Rural Engineering, University of Karlsruhe. Germany.

Stroosnijder, L., 1987. Soil evaporation; test of a practical approach under semi-arid conditions. *Netherlands Jour. of Agricultural Science*, 35: 417-426.

Stroosnijder, L., 2009. Modifying land management in order to improve efficiency of rainwater use in the African highlands. *Soil and Tillage Research*, 103: 247–256

Teh, C. B. S., Simmonds, L. P. and Wheeler, T. R., 2006. Modelling the partitioning of evapotranspiration in a maize-sunflower intercrop. *Malaysian Journal of Soil Science*, 6. http://www.msss.com. 20/12/2011, 9.00 am (LT).

The World Bank, 2005. Shaping the future of water for agriculture; A source book for investment in agricultural water management. Rural and Agricultural Development, Washington D.C. USA.

van Rensburg, L. D. and Zerizghy, M,.G., 2008. The BEWAB+ computer program for irrigation scheduling. Department of Soil, Crop and Climate Science, University of the Free State, Bloemfontein, South Africa.

Westgate, M. E., Otegui, M. E. and Andrade, F. H., 2004. Physiology of corn plant. In: W. Smith, C. Betrain, C. and J. Runge (eds). Corn; Origin, history, technology and production. John Wiley and Sons, Inc., Hoboken, New Jersey.

Yeh, T. C. J., Gelhar, L.W. and Gutjahr, A. L., 1985. Stochastic analysis of unsaturated flow in heterogeneous soils, 2. Statistically anisotropic media with variable xa. *Water Resources Research*, 21: 457-464.

Yeh, T. and Harvey, D., 1990. Effective unsaturated hydraulic conductivity of layered sands. *Water Resources Research*, 26:1271-1279.

Zhang, H., Oweis, T. Y., Garabet, S. and Pala, M., 1998. Water use efficiency and transpiration efficiency of wheat under rain-fed conditions ad supplemental irrigation in a Mediterranean-type environment.*Plant and Soil*, 201: 295-305.

CHAPTER 9

INTEGRATING MICRO-FLOOD WITH IN-FIELD RAINWATER HARVESTING: (ii) MAIZE YIELD AND WATER USE EFFICIENCY

Abstract

In this study micro-flood irrigation (MFI) and in-field rainwater harvesting (IRWH) management practices were integrated for the first time. Its effect on maize yield and water use efficiency (WUE) was tested using the dryland (DL), supplemental (SPI) and full irrigation (FI) water regime (WR) treatments on the 1 m, 2 m and 3 m runoff strip width (RSW) for IRWH. Four blocks with nine subplots were prepared to suit the complete block 3x 3 split plot factorial experiment. Each plot constituted of a standard 1 m basin strip and a runoff strip that varied according to the RSW assignment. The basin and runoff strip were 30 m long and prepared using the respective basin and no till as required by the IRWH. Irrigated plots received water from a 40 mm low pressured pipe calibrated to deliver 40L min $^{-1}$. In addition to the 281 mm seasonal rainfall a total depth of 105 and 173 mm irrigation was applied per plot for the respective SPI and FI treatments. Seasonal changes in soil water storage (ΔSWC), deep drainage (DD) and evapo-transpiration (ET) were determined. Partitioning of ET into evaporation (Ev) and transpiration (T) was done using a simple algorithm that relied on a β parameter for approximated crop canopy cover of the different RSW. Results revealed that the 1 m RSW had the highest biomass and grain yields that were respectively 19% and 32% above average. Correspondingly, seasonal ET and T were 10 % and 44% above average. Total biomass and grain yield WUE based on T confirmed the 1 m RSW as an optimum RSW although the 2 m RSW a comparable biomass WUE to become an alternative. Shading from plant canopy aided in suppressing Ev and enhanced light interception for photosynthesis as well as increased surface area that is well rooted for optimum water and nutrient uptake were the main reasons. Introduction of irrigation through MFI also improved crop yields and WUE with the FI producing biomass and grain increases of about 200 % higher than DL. It was therefore concluded that the 1 m RSW and FI would produce optimum maize yields and WUE for the newly integrated MFI-IRWH soil water management system under the climate and soil conditions that prevails at Parady's Experiment Farm of the University of the Free State, South Africa.

Key words: Dryland, irrigation, runoff strip width, in-field runoff, evapo-transpiration

9.1 Introduction

Increased innovation of conservational soil water management practices has made sustainable food production possible especially under difficult climate and soil conditions. Among these attractive technologies is the micro-flood irrigation (MFI) (Austin, 2003) and in-field rainwater harvesting (IRWH) (Hensley et al., 2000). To exploit the water productivity of the former and conservational potential of the latter, the two management practices have been newly integrated in this study.

Micro-flood irrigation is a typical short furrow irrigation method developed to optimise water productivity on soils with dry soil water regimes. Benefits of irrigation especially under supplemental regime in stabilizing crop growth and yields under prolonged dry spells are well covered in literature (Oweis et al., 1999; Rockstrom, 2000; Walker, 2003; Rodriguez et al., 2004; World bank, 2005; Moult et al., 2009). However, the efficiency of flood and furrow irrigation methods has always come under scrutiny given its poor distribution uniformity and unproductive losses through deep drainage and furrow end runoff. To improve application and distribution efficiencies developers of MFI (Austin, 2003) used small inflow rates to match soil water basic intake with advance time. On conventional furrow systems this was normally achieved by using very large inflow rates with cyclical or surge flows and automated cutback systems (Walker, 2003; Rodriguez et al., 2004). Attainment of distribution uniformity that were competitive to pressured systems as high as 95% by MFI were recorded when a 40 L min^{-1} inflow rate was used on a 20 m furrow run prepared on sandy loam soils (Austin, 2003). High application and water use efficiencies from other forms of micro-flood systems especially those integrated with rainwater harvesting were reported in various East African and South Asian countries (Awulachew et al., 2005; World Bank, 2005; Rockstrom et al., 2007).

Developed for soils that produce appreciable surface runoff and evaporation losses under conventional tillage system, IRWH has become popular in soil water conservation especially in South Africa (Botha, 2006; Manona and Baiphethi, 2008; Hensley et al., 2011; Mzezewa et al., 2011). The soils that have impermeable surface crust formed by raindrop impact (Hensley et al. 2007), low organic matter (Stroosnijder, 2009) and swelling clay either in the B or C-horizons (Hensley et al., 2000) have a persistent dry soil water regime (Hensley et al., 2007). However, IRWH was able to turnaround the negative influences of these soil characteristics into high in-field runoff, deep infiltration and improved soil water regime for crop growth

and natural nutrient cycling as well. Crop yields and water use efficiency were respectively up to 50 % and 106 % higher to conventional tillage (Botha, 2006; Mzezewa and van Rensburg, 2011).

Despite the improvement in efficient water use by the MFI and IRWH, high evaporation losses associated with irrigation (Annandale et al., 2011) and *in situ* rainwater harvesting (Both et al., 2006) remains a challenge. Developers of MFI claims that the use of unconventionally short furrows and small inflow rates as small as 20 L min^{-1} reduce above surface stream flow volumes but encourage sub-surface flow which minimise evaporation losses. On IRWH fields evaporation losses as high as 75 % of annual rainfall has been reported even though in-field runoff was encouraged to infiltrate deep into the profile below the evaporation sensitive zone (Bennie et al., 1994; Hensley et al., 2000; Mzezewa et al., 2011). Evaporation competes directly with transpiration that is related to crop growth and yields. Therefore, soil water management practices that reduce the former would simultaneously increase the latter (Stroosnijder, 1987). Even though this could be the case most of the transpired water is used for cooling purposes and a negligible amount is retained by the crop for crop growth (Schneekloth and Andales, 2009). Therefore, the amount of water used to produce a kilogram of yield (food) becomes critical for evaluating soil water management practices designated for semi-arid environments.

Different approaches of suppressing evaporation especially on IRWH have been attempted. One ground breaking work was the testing of different mulching materials on the basin and runoff area (Botha, 2006). Organic mulches had the most promising results with evaporation suppressed by 15% on clay soils and 31% on fine sandy loam soils compared to bare soils. In the absence of supplemental irrigation the conservational benefits of mulches were eroded by dry spells that exceeded 14 days (Botha, 2006). Intercropping with a legume on IRWH was also found to suppress evaporation and this was attributed to increased plant density (Mzezewa et al., 2011). Application of mulches and increasing plant density are among the cultural and agronomic practices that encourage ground cover (Magbool et al., 2006) and thus substitute evaporation for transpiration (Grena and Hess, 1994).

Other well established agronomic practices includes narrow row spacing (Eberbatch and Pala, 2005), irrigation (Zhang et al., 1998) and fertiliser application (Stroonijder, 2009). Despite their equal significance in encouraging early crop growth and canopy cover the first two have an important bearing in the integration of MFI and IRWH. Irrigation increases water

availability for crop water use, but if not properly applied evaporation could be exacerbated. Pilbeam et al. (1995) reported a scenario where irrigation on a bean crop increased evaporation by more than 55 %, while only 10 to 19 % of the applied water was transpired. Transpiration and evaporation are expected to vary with row spacing because of the variation in surface area shaded by the crop canopy cover (Kumar et al., 1988). This is more pertinent to the IRWH with two row spacing; the 1 m for basin strip and 2 m for runoff strip width (RSW). The latter could be varied with change in seasonal rainfall and field runoff coefficient. For dryland conditions the 2 m RSW was considered as standard for most soils earmarked for IRWH especially from the areas receiving annual rainfall of 550 mm (Hensley et al., 2000). Given the erratic nature of semi-arid rainfalls varying the 2 m RSW to optimise crop water use would subject the surface storage structures into more risk than the use of alternative methods such as mulches and intercropping. However the integrating of MFI with IRWH may necessitate the establishment of optimum RSW for certain irrigation regimes. It is against this background that the study specific objective was to determine the effect of RSW and water regime (WR) on maize production.

9.2 Material and methods

9.2.1 Description of experimental site

The field experiment was carried out at Parady's Experiment Farm (29°13'24, 69"S, 26°12'40, 93" E, altitude 1422 m) of the University of the Free State, South Africa. The area has an average annual rainfall of 550 mm, mainly from October to April. December and January are the hottest months of the production season with respective average maximum and minimum air temperatures of 30 and 14 °C and 31 and 15 °C. The selected site had two predominant soil forms, the Tukulu and Swartland (Soil Classification Working Group, 1991) that are similar to the respective Cutanic Luvisols and Cutanic Cambisols of the World Reference Base for Soil Resources (1998). The corresponding soil profile description is summarized in Table 9.1. The site has been used for maize cultivation under conventional tillage for the past decade.

9.2.2 Experimental design and layout

A complete block 3 x 3 split plot factorial experimental design was used. The two main treatments were the runoff strip width (RSW) a special form of row spacing adapted for IRWH plots and water regime (WR) management factors. The RSW had the 1 m, 2 m and 3

m as sub treatments while the WR constituted of the dryland (DL), and micro-flood irrigation in the form of supplemental (SPI) and full irrigation (FI).

Table 9.1 Summary of the physical and chemical characteristics of the Tukulu and Swartland soil types found in the experimental area.

	Soil physical properties					
Soil forms	Tukulu			Swartland		
Master Horizons	A	B1	C	A	B1	C
Coarse sand (%)	5.3	9.2	2.1	4.7	3.2	54.3
Medium sand (%)	9.3	8.8	3.8	7.6	5.3	4.6
Fine sand (%)	41.2	31	28.3	42	37.6	17.2
Very fine sand (%)	25.3	21	8.4	31.7	26.6	2.5
Coarse silt (%)	2.1	2	3	2	3	3
Fine silt (%)	4.6	2.5	6.5	1	2	3
Clay (%)	11.3	26.4	47.9	11.3	21.9	15
Bulk density (kg m^{-3})	1670	1597	1602	1670	1530	1450
Porosity (%)	34	33	32.4	35	39.9	41.6
Ks (mm $hour^{-1}$)	36.1	40	9.6	23.5	42.8	76.5
	Chemical properties					
pH (water)	5.8	6.1	6.5	5.5	5.8	6.8
Ca (c $mol_c.kg^{-1}$)	35.3	40.8	62.7	23	25.78	45
Mg (c $mol_c.kg^{-1}$)	18.8	20.8	54.7	12.1	13.1	25.4
K (c $mol_c.kg^{-1}$)	12.8	6.8	12.9	5.5	7.45	7.7
Na (c $mol_c.kg^{-1}$)	2.4	2.5	3.4	0.7	1.52	2.3

Four blocks with nine subplots were prepared to suit the 3x3 split plot factorial. Basin tillage was used to prepare the basin area (BA) of about 0.5 m width and 30 m long running on a zero degree slope. Runoff strip width between alternative rows also referred as the runoff area (RA) in this study was treated with no till to serve as mini-catchments for rainwater harvesting. Each plot had five basins with the peripheral basins serving as plot boarders. A 15 m buffer zone was maintained between blocks with a 5 m strip between unit subplots. On plots that received irrigation treatment the basins were levelled using a furrow ridger to ensure a smooth advance flow. The basins to serve as furrows were also close ended to detain runoff within plots and to comply with the zero ex-field runoff of IRWH.

9.2.3 Planting and agronomic practices

A 120 day yellow maize cultivar (PAN 6236 B) was used for the experiment. Plant density and intra row spacing was determined by soil water regime and runoff strip width as outlined in Table 9.2 To ensure accurate intra row spacing, planting on straight lines was carried by hand using a calibrated string. Basal and top dressing fertilizers were applied as required for maize production under varying soil water regimes.

Table 9.2 Intra-row plant spacing at planting time (mm).

Water regime	Plant density	Runoff strip width (m)		
		1	2	3
Dryland	25000	363	266	200
Supplemental	40000	227	67	125
Full	70000	130	95	71

A non selective herbicide was used to control weeds before planting on the RA and BA. Thereafter it was applied following a new growth of weeds appeared on the experimental plot. The field trial was conducted only for one season.

9.2.4 Irrigation design and application

The short furrow irrigation used for the supplement and full irrigation water regimes was designed and tested on previous chapters. Low pressure pipes of 40 mm diameter were used to deliver 80 mm of water per minute to individual 30 m length furrows at a distribution efficiency of 85-91 %. A 333 and 190 mm seasonal water depth was applied using a seven day cycle for the full and supplemental water regime. Individual furrows were wetted for an average time of 15 minutes for 16 weeks from the day of planting (25 November 2007).

According to the BEWAB^{+} (van Rensburg and Zerizghy, 2008) irrigation scheduling model an amount of about 625 mm of water would be required for a 120 day maturing maize cultivar to attain a maize yield of 10000 kg ha^{-1}. Given that more than 50% of the long term average rainfall is received between the months of November to March, a seasonal rainfall of around 300 mm was expected. Therefore, the balance was provided by means of the micro-flood irrigation using a fixed schedule for the FI and SPI produced by the BEWAB+ irrigation software. For the 30 m furrow run the 40 L min^{-1} inflow rate from previous test showed that advance times between 20 to 30 minutes could attain infiltrated depths of 30 mm. For FI the depth applied per plot was 173 mm and SPI was fixed at 60 % of FI. The

designated 40 L min^{-1} inflow at 100 % application efficiency could supply 0.9 m^3 or 900 litres of water on the 30 m furrow run at a cut-off time of 23 minutes.

9.2.5 Field measurements

Soil water content and climatic parameters were measured on site during the experiment. Individual subplots were installed with two neutron access tubes. Each was installed in the central position of the RA and BA at 15 m distance of plot length. Access tubes were installed to depths corresponding to the effective root depth of individual subplot soil profile. The neutron water meter (NWM) was used to measure the soil water content (SWC). Initial intentions to measure SWC before and after rainfall and irrigation events proved not to be practical and measurements were then taken after rainfall once drainage and the rapid phase of Ev has occurred. Rainfall, temperature, and relative humidity as well as potential evaporation data was obtained from the local automated weather station. Distribution of seasonal rainfall or precipitation (P) including the accumulative (Acc.) depth of P, SPI+P, and FI+P is illustrated in Figure 9.1. Soil water content and climatic data was used to develop the soil water balance (SWB) functions.

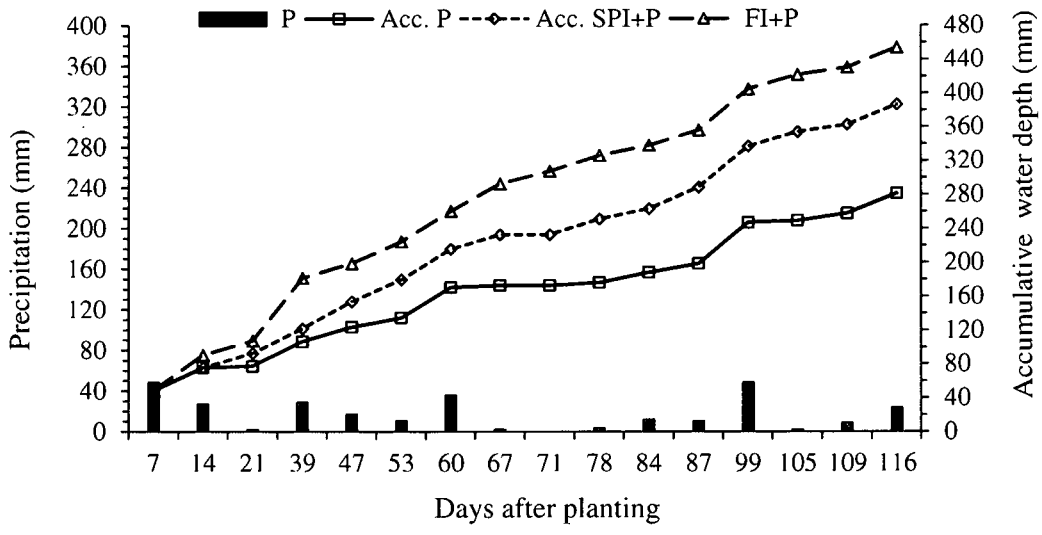

Figure 9.1 Seasonal precipitation distribution and its accumulative totals with supplemental (SPI) and full irrigation (FI).

9.2.6 Estimation of soil water balance components

The change in SWC (ΔSWC) of the profile for a given period during the production season was mathematically described as;

$$\Delta SWC = (P + I) - DD - ET \quad (9.1)$$

Where, P is rainfall amount (mm), I is irrigation amount (mm), DD is deep drainage (mm) and ET is evapo-transpiration (mm). Due to spatial variation of the soil profile layers DD from the Tukulu prismatic and Swartland saprolite C-horizons were respectively estimated using the exponential expressions, respectively written as:

$$DD = 4\,x10^{-63}\exp^{440.5.\theta} \quad (9.2)$$

$$DD = 2\,x10^{-8}\exp^{67.21.\theta} \quad (9.3)$$

Evapo-transpiration was determined from the re-arranging the expression (1) to become:

$$ET = (I + P) - D_d - \Delta SWC \quad (9.4)$$

Where, ΔSWC is difference in profile average SWC between two consecutive measurements.

Partitioning of ET into Ev and T components was carried using the extent of canopy cover during the four growth stages (plant establishment, vegetative, reproductive and ripening) proposed by the FAO (2011). Plant height measured at the end of plant establishment and when plants has interlock leaves between neighbouring rows and was linearly translated to the extent of canopy cover. A β-parameter was used ranging from 0 to 0.9 for the BA and 0 to 0.5 for the RA especially from the 2 and 3 m RSW. The 1 m RSW was treated the same way as the BA. Transpiration (T) and evaporation (Ev) was related to ET using the expressions:

$$T = \beta TE \quad (9.5)$$

$$Ev = (1 - \beta)ET \quad (9.6)$$

9.2.7 Crop yields and biomass

Above ground biomass and grain yield were the primary crop evaluative indicators to treatments responses. Given that the integrity of the crop stand was affected by a rainstorm during the ripening stage, a 9 m^2 was demarcated per sub plot and the number of plants and cobs were counted and sampled for yield and biomass analysis. Suckers and primary maize stalks were separated and weighed. A representative of five cobs from the sample was oven dried to 12% moisture content, shelled and seeds weighed. Grain yield was expressed as kg ha^{-1} by equating the seed mass from the sampled plants to the corresponding plant density per unit hectare. In the same manner the representative biomass weight was expressed in kg ha^{-1}.

9.2.8 Water use efficiency

Water use efficiency (WUE) was calculated for total biomass (WUE_b) and grain yield (WUE_g). To have a more meaningful on the productivity of the different management practices biomass or grain yield was expressed as a ratio to seasonal T.

9.2.9 Statistical analysis

A split plot analysis of variance was used to establish the effect of RSW and WR and its interaction on seasonal water components, maize yield and water use efficiency. The SAS 9 software was used in this endeavour in combination with the procedures for least significant different (LSD) test described by Gomez and Gomez (1984).

9.3 Results

A summary of analysis of variance depicting the effect of RSW and WR on seasonal SWB components, biomass and grain yield and WUE of biomass and grain yield are presented in Table 9.3 and 9.4. Variable was the effect of RSW and WR on the water, yield and WUE parameters. The profile SWC was not affected by the RSW and WR factors, while ΔSWC was the only component affected by these factors interaction.

Water components:

Runoff strip width (RSW) and its interaction with WR affected the ΔSWC. Seasonal net gain ranged from 17 to 37 mm with the amount gained decreasing with the RSW. Net gain differed among the WR factors ranging from 7 to 40 mm, decreasing with water unavailability. The effect of interaction on ΔSWC had the highest net gain of 51 mm from the 1 m RSW of the FI. The same RSW had a net loss of -24 mm but from the DL. The 2 and 3 m RSW for the different WR had a ΔSWC that ranged from 11 to 38 mm with net gain decreasing from FI to DL. Seasonal deep drainage was only affected by WR with the highest amount of 26 mm recorded from FI and followed by the SPI and DL that had comparable values of 15 and 9 mm, respectively. Evapo-transpiration had a significant respond to RSW with the highest value of 399 mm from the 1 m RSW. The 2 and 3 m RSW had comparable respective ET values of 348 and 338 mm. Evaporation was affected by RSW recording a range of 118 to 203 mm, increasing with widening of the RSW. On the contrary, T decreased with increasing RSW having a range of 135 to 281 mm. Effect of FI and SPI on T was comparable higher with respective values of 230 and 219 mm while DL had 138 mm.

Table 9.3 Summary of analysis of variance depicting the effect of runoff strip width (RSW) and water regime (WR) on seasonal soil water components, crop yield and water use efficiency (WUE).

Seasonal parameters	Factors	End of season
Water components		
Profile SWC ($mm\ mm^{-1}$)	RSW	ns
	WR	ns
	RSW x WR	ns
Δ SWC (mm)	RSW	*
	WR	*
	RSW x WR	*
Deep Drainage (mm)	RSW	ns
	WR	*
	RSW x WR	ns
Evapo-transpiration (mm)	RSW	*
	WR	ns
	RSW x WR	ns
Evaporation (mm)	RSW	*
	WR	ns
	RSW x WR	ns
Transpiration (mm)	RSW	*
	WR	*
	RSW x WR	ns
Crop yield		
Total Biomass ($Kg\ ha^{-1}$)	RSW	*
	WR	*
	RSW x WR	ns
Grain yield ($Kg\ ha^{-1}$)	RSW	*
	WR	*
	RSW x WR	ns
Water use efficiency		
Total biomass ($Kg\ ha^{-1}\ mm^{-1}$)	RSW	*
	WR	*
	RSW x WR	ns
Grain yield ($Kg\ ha^{-1}\ mm^{-1}$)	RSW	*
	WR	*
	RSW x WR	ns

* = significant at 5% probability level, ns= not significant

Table 9.4 Effect of runoff strip width and water regime on seasonal water components and crop yield.

Treatments		ΔSWC (mm)	DD (mm)	ET (mm)	Ev (mm)	T (mm)	Biomass (Kg ha^{-1})	Grain yield (Kg ha^{-1})	Biomass WUE (Kg ha^{-1} mm^{-1})	Grain yield WUE (Kg ha^{-1} mm
A. Runoff strip width (m)										
	1	17.3^{b}	15.2	398.9^{a}	117.6^{c}	281.3^{a}	15665^{a}	7535^{a}	38.2^{a}	18.4^{a}
	2	21.9^{b}	17.0	347.7^{b}	177.6^{b}	170.1^{b}	12892^{b}	5577^{b}	35.8^{ab}	15.4^{b}
	3	37.2^{a}	17.4	338.4^{b}	203.1^{a}	135.3^{b}	10791^{c}	3986^{c}	30.9^{b}	11.4^{c}
	LSD(T≤0.05)	15.5	ns	24.0	24.5	38.2	1779	730	5.7	2.6
CV(%)		49.8	48.0	5.4	12.1	16.0	11.1	10.5	13.3	14.3
B. Water regime										
	DL	7.4^{c}	8.7^{b}	296.5	158.9	137.6^{b}	7124^{c}	3011^{c}	24.0^{b}	10.1^{c}
	SPI	28.6^{b}	15.4^{b}	378.5	159.5	219.0^{a}	12413^{b}	5333^{b}	32.7^{b}	13.9^{b}
	FI	40.4^{a}	25.5^{a}	410.0	179.8	230.2^{a}	19812^{a}	8754^{a}	48.2^{a}	21.2^{a}
	LSD(T≤0.05)	10.3	8.4	ns	ns	36.5	3465	1332	9.3	3.6
	CV(%)	66.4	84.1	34.8	43.2	30.8	43.6	38.5	43.9	39
C. Interaction										
	DL	-24.0^{c}	5.4	312.9	113.0	199.9	8650	4146	27.7	13.3
1m	SPI	25.4^{ab}	19.3	429.6	106.6	323.0	14377	6762	33.5	15.7
	FI	50.6^{a}	20.9	454.3	133.1	321.1	23967	11697	53.3	26.1
	DL	10.5^{b}	12.4	284.5	163.0	121.5	6895	2792	24.3	9.8
2m	SPI	22.3^{ab}	10.1	361.7	177.8	183.9	12366	5496	34.2	15.2
	FI	33.0^{ab}	28.5	396.9	191.9	205.0	19416	8442	49.0	21.3
	DL	35.5^{ab}	8.4	292.2	200.8	91.3	5826	2095	19.9	7.2
3m	SPI	38.3^{ab}	16.7	344.1	194.0	150.1	10495	3741	30.5	10.9
	FI	37.6^{ab}	27.2	378.9	214.5	164.4	16052	6124	42.3	16.1
LSD (T≤0.05)		33.2	ns	ns	ns	ns	ns	ns	ns	ns

ΔSWC = change in soil water content, DD= deep drainage, ET= evapo-transpiration, Ev=evaporation, T=transpiration, DL= dryland, SPI =supplemental irrigation, FI= full irrigation, WUE= water use efficiency, ns= not significant

Maize yield:

Seasonal biomass and grain yield were affected differently by the RSW and WR factors even though the resulting interaction was insignificant. Biomass yield ranged from 15665 to 10791 kg ha^{-1}, increasing with decreasing RSW. Water regime resulted in biomass that was high as 19812 kg ha^{-1} from the FI, followed by 12413 and 7124 kg ha^{-1} for the respective SPI and DL. Grain yield ranged from 7535 to 3986 kg ha^{-1} for the RSW with the highest from the 1 m RSW. The WR had grain yield of 8754 kg ha^{-1} from the FI, 5333 kg ha^{-1} from the SPI and 3011 kg ha^{-1} from the DL.

Water use efficiency:

Seasonal WUE for biomass and grain yield were affected by RSW and WR differently. The 1 and 2 m RSW had comparably higher WUE_b with respective mean values of 38 and 36 kg ha^{-1} mm^{-1}. The 3 m RSW recorded the lowest value of 31 kg ha^{-1} mm^{-1}, although it was not different from that of the 2 m RSW. The WUE_b from the WR ranged from 48 to 24 kg ha^{-1} mm^{-1} with the FI having a significantly higher mean value. The 1 and 2 m RSW affected the WUE_g in a comparable way with respective mean values of 38 and 36 kg ha^{-1} mm^{-1}. The 3 m RSW had a value of 31 kg ha^{-1} mm^{-1} different from the 1 m RSW but comparable with the 2 m RSW. The WUE_g were all significantly different with FI, SPI and DL recording 21, 14 and 10 kg ha^{-1} mm^{-1}, respectively.

9.4 Discussion

Improving crop yields under limited water supplies is a desirable attribute for semi-arid soil water management practices. The newly integrated MFI with IRWH had three WR (Dryland, supplemental and full irrigation) and RSW (1 m, 2 m and 3 m) investigated for their effect on maize production. Carried out on a single season of 2007/2008, total biomass and grain yield were affected differently by the WR and RSW.

Traditionally the IRWH was developed to improve crop yields and water use efficiencies under dryland conditions using the 2 m RSW as a standard row spacing (Hensley et al., 2000). The DL maize yields including total biomass and grain yields fell below the range of those reported by Hensley et al. (2000) under IRWH. Despite the differences in local climates and soil types, the below average (51%) seasonal rainfall was attributed to the low yields obtained from this study. However, the results from Hensley et al. (2000) were reflective of the high productive potential of IRWH especially when compared to conventional systems under optimum rainfalls.

Among the RSW the 2 m RSW recorded a total biomass that was 19% higher than from the 3 m RSW and 18% lower than from the 1 m RSW. It also had a grain yield that was 40% higher and 26 % lower than from the respective 3 m and 1 m RSW. The crop yields showed a decrease with an increase in RSW and the 2 m RSW being an intermediate RSW fell within the average. This result reflects that the initial selection of the 2 m RSW for IRWH was reasonable. Under the conditions that seasonal DD and runoff was insignificant, the total water use (ET) loss from the soil plant system could give an insight on the differences on

yields among the RSW. Seasonal ET followed same trend as crop yields with the 2 m RSW being 3% higher and 12% lower than the respective 3 and 1 m RSW. When ET was partitioned into Ev and T, the proportion of Ev to ET was 29%, 51% and 60% for the 1 m, 2 m and 3 m RSW, respectively. In comparison with results reported by Hensley et al. (2000) for three consecutive seasons, the total Ev mainly from the 2 m RSW constituted a proportion ranging from 67 to 84% of seasonal ET that was also within the same range with those reported by Botha (2006). Given that Ev is defined as soil water loss from the surface directly to the atmosphere, suggest that increasing RSW encouraged Ev by increasing the surface area exposed to direct radiation; a sentiment that is well supported in literature (Sangoi et al., 2001; Onyango, 2009; Acciaresi and Zulunga, 2006).

On the contrary, reducing the RSW implied that much of the surface area becomes shaded by the crop canopy and hence more light get intercepted to promote photosynthesis rather than evaporation (Eberbach and Pala, 2005). Maize plants are appreciated for their tendency to interlock leaves much earlier during the vegetative growth phase (FAO, 2011). In this regard, the direct relationship between photosynthesis and T was translated to higher crop yields especially from the 1 m RSW. Seasonal T from the 1 m RSW increased by 65% and 100% over and above that from the respective 2 and 3 m RSW. Reducing row spacing for the same plant density was also acknowledged for improving water and nutrient uptake through increased surface area accessible to crop plants roots (Onyango, 2009) a phenomenon that is considered to have led to the higher yields from the 1 m RSW despite the low seasonal net gains.

Introducing irrigation either by supplemental or full irrigation through the integration of MFI with IRWH resulted to improved yields and water use efficiencies. This was expected given that maize yields generally increase linearly with water application (Schneekloth and Andales, 2009; Annandale et al. 2011). Total biomass from the SPI and FI was respectively higher than DL by 74% and 200% and the corresponding grain yield that was 77% and 200% higher. Similar yield trends on maize (Bello, 2008), wheat (Zhang et al., 1998) and Tomatoes (Agele et al., 2011) have been reported. More insight could be shared by the seasonal ET and its constituents whereby SPI and FI had an increase of about 28% and 38% respectively higher than DL. In another study irrigated maize had a higher seasonal ET than rain-fed maize by of 12% while for irrigated wheat it was 5% higher than rain-fed (Suyker and Verma, 2009). But the question of how much of seasonal ET was translated to crop growth was inversely shown by the proportion of Ev that was about 42% and 44% of seasonal ET

from the respective SPI and FI. This was not strange in irrigation given that water is usually applied during dry spells when atmospheric evaporative demand was fairly high.

The question of water-use efficiency (WUE) then becomes important if water availability in IRWH has to support plant growth and yields rather than unproductive losses (Ev and DD). Given that plant growth and yield is directly a function of T, therefore a more meaningful judgement of WUE is obtained in reference to T as a measure of crop performance (Stroosnijder, 1987; Zhang et al., 1998; Eberbach and Pala, 2005). Increasing RSW decreased WUE_b while increasing water availability had the opposite effect. The 2 m RSW compared with both the 1 and 3 m RSW suggesting its ability to exploit the benefits of in-field runoff and partial crop canopy cover to sustain a reasonable crop growth. This productive potential of the 2 m RSW was also appreciated by Hensley et al. (2000). Full irrigation had the highest WUE_b despite significant DD losses that was approximately 10.1 mm and 17 mm higher than that from the respective SPI and DL. Interestingly, the DL and SPI had comparable WUE_b and could be attributed to the similarities in DD losses (Table 9.4). Hensley et al. (2000) noted that management practices that result to same DD usually have homogeneous WUE. The World Bank (2005) pointed out that management practices that encourage some level of water stress maximise the benefits of water applied. This could be realised through increasing soil water storage capacity and rainfall capture by in-field runoff from DL and deficit irrigation with SPI.

Regarding WUE_g, significant differences between RSW and WR were observed that were consistent with the variations in grain yield and corresponding net gains. The 1 m and 2 m RSW had WUE_g that was higher than the 3 m RSW by respectively 64% and 35% suggesting that the amount of water required to produce a kilogram of dry matter was higher with increasing RSW. This was justified by the high claims Ev from the RSW with greater surface area exposed to direct radiation (Aberbach and Pala, 2005; Onyango, 2009). In comparison the WUE_g from all the RSW were fairly lower than those recorded from Hensley et al., (2000). Different climatic conditions and the application of a different method (Tanner and Sinclair (1983) method to partition Ev and T could be the reason. Despite being developed under different climatic conditions it also rely on the transpiration efficiency that is generally an insensitive to water stress and water availability (Morgan et al., 2003) which could lead to overestimates when used in semi-arid areas. However the Ev/T ratio which is a critical indicator of WUE (Zhang et al., 1998) was 42%, 105% and 150% for the 1 m, 2 m and 3 m, reflecting an increase with RSW, justifying the decline in WUE_g with widening of the RSW.

The same ratio (Ev/T) decreased with water availability confirming the 100% and 40% rise in WUE_g from the respective FI and SPI over and above that from the DL. Syker and Verma (2009) also recoded similar results whereby the WUE_g for DL lagged behind that from irrigation by 25%.

However, prospects of achieving reasonably high yields and WUE from the DL and SPI could be inferred from the RSW and WR interaction that affected the change in soil water storage (ΔSWC). From this interaction the net gains were apparently similar for all SPI irrespective of RSW and these were comparable with the FI of the 2 and 3 m RSW and DL from the 3 m RSW. The highest net gain from the 1 m RSW under FI was reflective of the potential of this RSW of substituting Ev for T under full plant canopy cover that could shade up to 90% of the surface area that is also concentrated with plants roots.

9.5 Conclusion

Integration of MFI with IRWH was tested for its effects on maize yield and WUE using different RSW (1 m, 2 m and 3 m) and WR (DL, SPI and FI). The effect of the RSW and WR on seasonal water and yield components and biomass and grain yield WUE that was based on T was reflective of the productive potential of the newly integrated management practices.

The 1 m RSW had optimum total biomass and grain yields that were higher than the 2m and 3m RSW by 21 % and 45 % and 35 and 89 %, respectively. This was supported by the seasonal high ET with an Ev/T ratio that increased with RSW with that from the 1 m RSW being 31 % lower than the 3 m RSW. This was because the 1 m RSW had plant canopy shading the ground much earlier to suppress Ev and had much of its surface area concentrated with plants roots that enhanced water and nutrient uptake. Confirming the 1 m RSW as the optimum RSW was the WUE from the biomass and grain yield that were respectively above average by 9% and 22%. However, the 2 m RSW presented itself as viable alternative with a competitive biomass WUE that was 2.3 % above average.

Introducing irrigation through MFI also improved yield and WUE by increasing soil water storage net gains. Full irrigation had the highest biomass and grain yields that were about 200% higher than the DL while SPI had an average increase of 76 % for both yield components. The benefits of FI were supported by the high biomass and grain WUE even though the SPI also competed fairly with the T component falling in the range with the FI.

Nevertheless, the application of FI with the 1 m RSW could be said to produce optimum yields and WUE for the newly integrated MFI-IRWH soil water management system.

Acknowledgements

Acknowledgements directed to the technical team at Kenilworth Experimental Station of the University of the Free State for their assistant in drying sampled maize plants for dry matter determination.

9.6 References

Acciaresi, H. A. and Zulunga, M. S., 2006. Effect of plant row spacing and herbicide use on weed above ground biomass and corn grain yield. *Planta Daninha Vicosa-MG*, 24: 287-293.

Agele, S. O., Iremiren, G. O. and Ojeniyi, S. O., 2011. Evapo-transpiration, water use efficiency and yield of rain-fedand irrigated tomato. *Inter. J. of Agric. and Bio.*, 13: 469-476.

Annandale, J. G., Stirzaker, R. J. Singles, A., van der Laan, M. and Laker, M. C., 2011. Irrigation scheduling research: South African experiences and future prospects. *Water SA*, 37: 751-762.

Austin, C., 2003. Micro flood, a new way of applying waters. http://waterright.com. 22/09/211, 10.00 am (LT).

Awulachew, S. B., Merrey, D. J., Kamara, A. B., Koppen Van, B., de Vries, P. and Boelee E., 2005. Experiences and opportunities for promoting small scale/micro irrigation and rainwater harvesting for food security in Ethiopia. International Water Management Institute, Working Paper 98, Addis Ababa, Ethiopia.

Bello, W. B., 2008. The effect of rain-fed and supplemetal irrigation on the yield and yield components of maize in Mekelle, Ethopia. *Ethopian J. of Env. Studies and management,* 2: 1- 7.

Botha, J. J., 2006. Evaluation of maize and sunflower production in a semi-arid area using In-field rainwater harvesting. Ph.D. (Agric) Dissertation, University of the Free State, Bloemfontein, South Africa.

Eberbatch, P. and Pala M., 2005. Crop row spacing and its influence on the partitioning of evapo-transpiration by winter- grown wheat in Northern Syria. *Plant and Soil*, 268:195-208.

FAO, 2011.Chapter 5; Introduction to crop evapo-transpiration. http://www.fao.org. 20/11/2011,10.30 am (LT).

Gomez, K. A. and Gomez, A. A., 1984.Statistical procedures for agricultural research. 2nd ed. John Wiley and Sons, New York, USA.

Grena, A. K, and Hess, T.M., 1994. Water balance and water use of pearl millet-cow pea intercrops in north east Nigeria, *Agricultural Water Management*, 26: 169-185.

Hensley, M., Bennie, A. T. P., van Rensburg, L. D. and Botha, J. J., 2011. Review of plant available water aspects of water use efficiency under irrigated and dryland conditions. *Water SA*, 37: 771-779.

Hensley, M., Botha, J. J., Anderson, J. J., van Staden, P. P. and DuToit, A., 2000. Optimising rainfall use efficiency for developing farmers with limited access to irrigation water. Water Research Commission Report no. 878/1/00, Pretoria, South Africa.

Hensley, M., Le Roux, P., Gutter, J. and Zerizghy, M. G., 2007. A procedure for an improved soil survey technique for delineating land suitable for rainwater harvesting. WRC Report No. TT 311/07.Water Research Commission, Pretoria, South Africa.

Kumar, K. K ., Dantas, R. C. D. and Bezerra, V. F. 1988. The effect of row spacing on Evapo-transpiration patterns in a crop field. Department of Atmospheric Sciences, Federal University of Paraiba, Campida Grande-PB.

Manona, S. and Baiphethi, M. N., 2008. Developing a land register and a set of rules from application of in-field rainwater harvesting in three villages in Thaba Nchu. WRC Report No.TT367/08. Water Research Commission, Pretoria, South Africa.

Maqbool, M. M., Tanveer, A., Ata, Z. and Ahmad, R., 2006. Growth and yield of maize (Zea Mays L.) as affected by row spacing and weed competition durations. *Pak. J. Bot.*, 38: 1227-1236.

Morgan, C. L. S., Norman, J. M. and Lowery, B., 2003. Estimating plant available water across a field with an inverse yield model. Division S-6; Soil and Water Management and Conservation, *Soil Sci. Soc. Am. J.*, 67: 620-629.

Moult N.C., Lecler N. I., and Smithers J. C., 2009. A catchment-scale irrigation systems model for sugarcane; Model application. *Water SA*, 35: 29-36.

Mzezewa, J., Gwata, E. T. and van Rensburg, L. D., 2011. Yield and seasonal water productivity of sunflower as affected by tillage and cropping systems under dryland conditions in the Limpopo Province of South Africa. *Agricultural water Management*, 98: 1641-1648.

Onyango, O. C., 2009. Decreased row spacing as an option for decreasing maize (Zea may L.) yield in Trans Nzoi district, *Kenya. J. of Plant Breeding and Crop Science*, 1: 281-283.

Oweis, T., Hachum, A. and Kijne. J., 1999. Water harvesting and supplementary irrigation for improved water use efficiency in dry areas. IWMI Contribution (No. 7), System Wide Initiative on Water Management (SWIM). Colombo, Sri Lanka.

Pilbeam, C. J., Simmonds, L.P., Kavilu, A.W., 1995. Transpiration efficiencies of maize and beans in semi-arid Kenya. *Field Crops Research,* 41:179-188.

Rockstrom, J., 2000. Water resources management in smallholder farms in Eastern and Southern Africa: An overview. *Phys. Chem. Earth*, 25: 275- 283.

Rockstrom, J., Hatibu, N., Oweis, T. Y. and Wani, S., 2007. Managing water in rain-fed agriculture, Part 4 In: Unlocking the potential of rain-fed agriculture, IWMI, Colombo, Sri Lanka.

Rodríguez, J. A, Díaz, A., Reyes J. A. and Pujols R., 2004.Comparison between surge irrigation and conventional furrow irrigation for covered black tobacco cultivation in a Ferralsol soil. *Span J. Agric. Res.,* 2: 445-458.

Sangoi, L., Ender, M., Guidolin, A. F., de Almeida, M. L. and Heberle, P. C., 2001. Influence of row spacing reduction on maize grain yieldin regions with a short summer. *Pesq.agropes bras.*, 36:861-869.

Schneekloth, J. and Andales, A., 2009. Irrigation: seasonal water needs and opportunities for limited irrigation for Colorado crops. Department of Agriculture, Colorado State University. Colorado, USA.

Soil Classification Working Group, 1991. Soil Classification - A taxonomic system for South Africa. Memoirs on the Agricultural Natural Resources of South Africa Nr. 15. Pretoria: Department of Agricultural Development.

Stroosnijder, L., 2009. Modifying land management in order to improve efficiency of rainwater use in theAfrican highlands. *Soil and Tillage Research*, 103: 247–256.

Suyker, A. E. and Verma, S., 2009. Evapo-transpiration of irrigated and rain-fed maize–soybean cropping systems. Agricultural and Forest Meteorology 149: 443-452.

Tanner, C. B. and Sinclair, T. R., 1983. Efficient water use in crop production: Research or re-search? In: H.M Taylor et al., (ed.) Limitations to efficient water use in crop production. ASA, CSSA, and SSSA, Madison, WI.

The World Bank, 2005. Shaping the future of water for agriculture; A source book for investment in agricultural water management. Rural and Agricultural Development, Washington D.C. USA.

van Rensburg, L.D. and Zerizghy, M. G., 2008. The BEWAB+ computer program for irrigation scheduling. Department of Soil, Crop and Climate Science, University of the Free State, Bloemfontein, South Africa.

Walker W.R., 2003. SIRMOD III; Surface Irrigation Simulation, Evaluation and Designs.Guide and technical document. Department of Biological and irrigation Engineering, Utah State University

World Reference Base for Soil Resources (1998). World soil resources report, 84, ISSS / ISRIC FAO, Rome, Italy.

Zhang, H., Oweis, T. Y., Garabet, S. and Pala M., 1998. Water use efficiency and transpiration efficiency of wheat under rain-fed conditions and supplemental irrigation in a Mediterranean-type environment. *Plant and Soil*, 201: 295-305.

CHAPTER 10

PERSPECTIVE ON RESEARCH

10.1 Introduction

Sustainable soil water storage is a major challenge of cultivated fields in the semi-arid areas. A number of soil water management practices have been developed by local and international studies to improve soil water regimes especially for small scale farmers. Rainfall capture and supplemental irrigation are among the common water management options. Intensively researched in the Free State Province of South Africa is the in-field rainwater harvesting (IRWH) that partition the field into basin and runoff area. Although clay soils have been earmarked for IRWH on the basis of their high water holding capacity, erratic rainfall distribution and high evaporation prevailing in the region undermines water storage potential of these soils, especially when dry spells persist longer than 14 days. In search for solutions this thesis integrated micro-flood irrigation (MFI) system with IRWH. In this endeavour three fields of study were researched including soil hydraulic properties of three soil types (Tukulu and Sepane also known as Cutanic Luvisols, and Swartland as Cutanic Cambisols), short furrow irrigation and integration of MFI with IRWH of which soil water balance (SWB) management was of primary importance.

10.2 Soil hydraulic properties

Soil hydraulic properties are physical functions and parameters that describe the soil water systems. These include soil water content (SWC), flux rates, and soil water characteristic curve (SWCC or θ-h) as well as hydraulic conductivity (K-θ). Soil morphological attributes such as depth, texture and structure has profound influence on water flow patterns especially on layered soil profiles. In this thesis morphological and hydraulic properties were investigated concurrently using laboratory and *in situ* procedures. In Chapter 3 pedological aspect of three representative layered soil forms were characterised in relation to internal drainage and it was shown that horizons with clay content ranging from 26 to 48% contributed less than 5 mm to total drainage. This observation was supported by the θ-h relationship with a very small slope and K-θ relationship dropping by several orders of magnitudes at near the saturated soil water content.

For optimal description of θ-h and K-θ relationships especially for structured soils, appreciated for the many challenges in measuring hydraulic properties either in either *in situ*

or laboratory conditions, application of hydraulic models is widely practiced. In Chapter 4 three parametric models predictions were tested by fitting to laboratory measured SWCC and *in situ* determined K-θ curves. Model predictions showed high accuracy for the former compared to the latter. Predictions on the K-θ relationship were showed to improve more than one order of magnitude when simulations were performed with HYDRUS-1D software based on soil profile layers initial and boundary conditions and optimization of model parameters. Model performance were also showed to vary with soil profile layers an observation that was consistent with observations in Chapter 3 and later in Chapter 5 that soil layers affected water flow and soil water storage differently. The effect of layered soils on evaporation is dealt with in Chapter 5 and clayey horizons were shown to augment a steep soil water gradient against drying front progression. This phenomenon restricted evaporation losses an observation that corresponds to the findings about deep drainages losses in Chapter 3 especially in soil profiles where the restrictive layer occupied the underlying position.

10.3 Micro-flood irrigation designs and evaluation

Conservational concepts and principles advocated by the developers of MFI in designing and management of short furrow irrigation were tested in Chapters 6 and 7. Having been shown in Chapters 3 to 5 to have higher soil water storage capacity the Tukulu soil form was selected for this exercise. In Chapter 3 four inflow rates (20, 40, 80 and 160 L min^{-1}) were compared with respect to irrigation and opportunity time, advance stream distance-time and infiltrated depth for a single-run irrigation in a 90 furrow length. Description of surface characteristics of furrow irrigation was based on *in situ* observations only. From the smallest to the largest inflow rate the advance and recession times ranged from 2.7 to 0.4 hours and 7 minutes to an hour respectively, with the 20 L min^{-1} failing to reach the furrow end at a 60 m distance.

Infiltration in furrows is basically two dimensional and this phenomenon was successfully described using HYDRUS-2D software simulations. Remarkable agreement between measured and predicted SWC was shown at all furrow distances and profile depths. Infiltrated depths were observed to be a function of opportunity time, and this was confirmed by the high distribution uniformity (DU) from all inflow rates at shorter furrow distances. Deep percolation ratio (DPR) was showed to be insignificantly low for all inflow rates. This observation corresponds with findings in Chapter 3 for deep drainage. Vertical redistribution (Vz) of infiltrated SWC was dealt with in Chapter 7. The rate of Vz for small (20 and 40 L

min^{-1}) and large (80 and 160 L min^{-1}) inflow rates was showed to be high at soil profile depths of 0 to 600 mm and 0 to 850 mm, respectively. Simulated SWC during the 455 hour redistribution was also showed to be accurate on drier soils compared to near saturated soils.

10.4 Integrating MFI with IRWH

The merging of MFI with IRWH was based on their handling of runoff, though in different forms, at field or plot scale with the aim of improving soil water storage and crop water use. The merged MFI-IRWH water management system was tested in a maize crop grown for a single season described in Chapter 8 and Chapter 9. Runoff strip width (RSW) and water regime (WR) were the two main treatments with each having three sub treatments combined on a 3 x 3 split plot factorial with four replications in a complete randomised design experiment. One of the three sub-treatments combinations represented the traditional design for IRWH of 2 m RSW and dryland (DL). The other two sub treatments were the 1 m and 2 m for RSW and full irrigation (FI) and supplemental irrigation (SPI) for WR. Experimental plots were conceptualised into two components, the basin area (BA) and runoff area (RA).

In chapter 9 a SWB procedure was developed to take into account the gains and losses in soil water storage effected in the BA and RA. Site specific empirical functions including rainfall-runoff relationships and soil water content-time relationship were used to estimate total harvested rainfall and deep drainage (DD) losses for the BA and RA. A fixed irrigation schedule for the FI and SPI was followed produced by the BEWAB+ irrigation software for semi-arid areas. For optimal rainfall capture at plot scale IRWH uses basin tillage and closed ended furrows for MFI. Consequently, the SWB procedure disregarded runoff (ex-field) losses and considered evapo-transpiration (ET) and DD as the major losses against the gains from rainfall and irrigation. Though DD increased with increased RSW and water availability it was shown in Chapter 10 to be significantly small over the production season. This result corresponded to the observations made in Chapters 3, 6 and 7 for the Tukulu soil form. Evapo-transpiration was partitioned into evaporation (Ev) and Transpiration (T). The BA was distinguished as the area where crops grow by considering the area covered by plant canopy to be proportional to the T contribution to ET by a β-parameter ranging from 0 to 0.9, while in the RA it ranged from 0 to 0.5 over the production season. Tests of the SWB procedure showed consistency with the water gains and losses during the different maize growth stages as affected by the RSW and WR main treatments. In evaluating the productive potential of the merged MFI-IRWH system the SWB procedure showed optimum net gains for the 2 m

and 3 m RSW, especially from rainfalls not less than 24 mm. It was also showed that because of the large surface area not shaded from direct radiation from these RSW most of the net gain from rainfall were directed to Ev. This observation was illustrated by the Ev/T ratio that was 30% larger for the 3 m RSW compared to the 1 m RSW. Dry spells more than 14 days corresponded to net losses of about -12 mm, irrespective of RSW. Irrigation increased ET with FI and SPI corresponding to higher seasonal ET compared to DL by 113 mm and 82 mm, respectively. Though the increase in ET with water availability was expected it was shown that this increase was translated into production differently by the RSW. Total biomass and grain yields for the 1 m RSW were shown to be higher compared to the 2 m and 3 m RSW by 21% and 45% and 35 and 89%, respectively. The DL had a total biomass of 7124 kg ha^{-1} and grain yield of 3011 kg ha^{-1}. Total biomass and grain yields for FI and SPI were higher compared to DL by 200% and 76%. Correspondingly, the 1m RSW had the highest WUE based on T for both grain (18.4 kg $ha^{-1}mm^{-1}$) and total biomass (38.2 kg ha^{-1} mm^{-1}) yield compared to the 2 m and 3 RSW. Among water regimes the highest WUE for total biomass (48.2 kg $ha^{-1}mm^{-1}$) and grain yield (21 kg $ha^{-1}mm^{-1}$) corresponded to FI.

10.5 Thesis contributions and conclusions

Reflection on the procedures and findings from the series of studies including soil hydraulic characteristics, MFI designs and evaluation and merging the MFI system with IRWH, important contributions can be highlighted and conclusions made.

In Chapter 3 to Chapter 5 the functional role of clay soils in soil water storage for a draining and evaporating profile was demonstrated and quantified using pertinent hydraulic parameters such as SWC, flux rates, hydraulic conductivity and θ-h relationships. Matric suction range of 0 to -10 kPa was shown to be appropriate for describing matric suction gradients on draining layered profiles compared to the 0 to -33 kPa proposed by Ratliff et al. (1983). Inspection of drainage curves of other similar studies on layered profiles indicated that drainage upper limit was approached at near -10 kPa even though they have initially employed matric suction range of Ratliff et al. (1983). To this effect it can be concluded that the 0 to -10 kPa matric suction range provided accurate description of matric suction gradients during internal drainage and thus recommended for applications in matters pertaining to estimation of drainage upper limit (DUL). In addition, re-defining DUL in terms of drainage flux (0.001 mm $hour^{-1}$) that amounts to DD losses proportional to 1% of annual

rainfall (Chapter 3) over a 7 month fallow period provided an alternative approach of evaluating water storage potential of clay soils.

The MFI concept of selecting inflow rate according to soil's basic infiltration rate was tested and evaluated in Chapters 6 and Chapter 7 using 20, 40, 80 and 160 L min^{-1} inflow rates. Though all inflow rates produced higher distribution uniformity (DU) at short compared to long furrow distances, and the 20 and 40 L min^{-1} treatments were much easier to handle especially for a 30 m furrow run. In comparison, the 40 L min^{-1} treatment had a higher DU and smaller advance times. Therefore the 40 L min^{-1} and 30 m furrow length were considered appropriate for designing the merged MFI system with IRWH.

In Chapters 8 and Chapter 9 the merged MFI-IRWH water management system was successfully tested on a maize crop for a single season. A soil water balance procedure was developed that articulated the dynamic aspects of the soil-plant-atmosphere continuum for the merged system and showed reasonable sensitivity to changes in water availability and RSW. Application of the SWB procedure in evaluating the merged MFI and IRWH indicated higher crop yields and water use efficiencies for the 1 m RSW and full irrigation. Therefore it can be concluded that the 1 m RSW and full irrigation is appropriate for the newly merged MFI with IRWH water management system. Though tested only for a single season this technique is ready to be used by small scale farmers located on clay soils and who have access to irrigation water to improve food security at household levels in Africa.

Appendices

Appendix A Profile description of the Tukulu soil form.

Map/photo:	2926 Bloemfontein	Soil form and Family:	Tukulu Dikeni
Latitude +Longitude:	29^0 13' 24.69'' S/ 26 ^{0} 12.40.93'' E	Surface rockiness:	None
Altitude:	1421.9 m	Occurrence of flooding:	None
Terrain unit:	Midslope	Wind erosion:	Slight wind
Slope:	1%	Water erosion:	None
Slope shape:	Straight	Vegetation/land use:	Agronomic field crops
Aspect:	South	Water Table:	None
Micro relief:	None	Described by:	M. Hensley/ S. Mavimbela
Parent material Solum:	Origin binary,aeolin, solid rock	Date Described:	1/11/2006
Underlying Material:	Sandstone (Feldspathic)	Weathering of underlying material:	Moderate physical, moderate chemical
		Alternation of underlying material:	Ferrugised

Horizon	Depth (mm)	Description	Diagnostic horizon
A	0-300	Moist state; dry colour: reddish brown (5YR4/8); moist colour; reddish brown (5YR4/8); texture: fine sandy loam; structure: apedal massive: consistence: friable; few fine pores; common roots; gradual transition	Orthic
B1	300-600	Moist state; dry colour: reddish brown (5YR3/6); reddish brown (5YR3/6);texture: fine sandy clay loam; Neoucutanic Structure: apedal massive becoming weak subangular blocky towards transition: consistence: friable; few fine pores;few clay cutans; very few fine pores; common roots; clear, tonguing transition	Neocutanic
C1	600-850	Moists state; dry colour. Dark grey, olive and yellow mottles; moist colour: olive grey with yellow mottles; texture: clay; common distinct grey material, and yellow reduced iron oxide mottles; few prominent black oxidised iron oxide mottles; structure: prismatic; consistence firm; few slickensides; common clay cutans; very few roots; gradual transition	Unconsolidated with signs of wetness
C2	850- $\pm$ 1350	Allows water to enter, hence the presence roots. It chops out the profile relatively easily up to £$\pm$1350 m, getting harder towards the bottom and probably very impermeable slightly deeper. Unconsolidated:	soft rock

Appendix B Profile description of the Sepane soil form.

Map/photo:	2926 Bloemfontein	Soil form and Family:	Sepane Rambles
Latitude +Longitude:	29^0 13'41.47" S/26^0 12'37.86 E	Surface rockiness:	None
Altitude:	1414.3 m	Occurrence of flooding:	None
Terrain unit:	Midslope	Wind erosion:	Slight wind
Slope:	1%	Water erosion:	None
Slope shape:	Straight	Vegetation/land use:	Agronomic field crops
Aspect:	South	Water Table:	None
Micro relief:	None	Described by:	M. Hensley/ S. Mavimbela
Parent material Solum:	Origin binary,aeolin, solid rock	Date Described:	1/11/2006
Underlying Material:	Sandstone (Feldspathic)	Weathering of underlying material:	Moderate physical, moderate chemical
		Alternation of underlying material:	Ferrugised

Horizon	Depth (mm)	Description	Diagnostic horizon
A	0-300	Moist state; dry colour: reddish brown (5YR4/8); moist colour; reddish brown (5YR4/8); texture: fine sandy loam; structure: apedal massive: consistence: friable; few fine pores; common roots; abrupt transition	Orthic
B1	300-700	Moist state; dry colour: dark grey (5YR3/4); reddish brown (2.5YR3/4);texture: fine sandy clay loam; Pedocutanic Structure: moderate to medium sub-angular blocky: consistence: slightly firm; few normal fine pores; many clay cutans; clay Skins; common roots; abrupt transition	Pedocunatic
C1	700-800	Moists state; dry colour. Dark greyish brown (2.5YR4/2); moist colour: grey (2.5T5/0); texture: sandy clay; common distinct grey and yellow reduced iron oxide mottles; abundance of red, grey and black mottles; structure: prismatic; consistence: slightly firm; few slickenside's; common clay cutans; very few roots; abrupt transition.	Prismacunatic,
C2	800- ± 1000	Undisturbed, signs of calcium deposits. It chops out the profile relatively easily up to £±1350 m, getting harder towards the bottom and probably very impermeable slightly deeper. Unconsolidated:	Soft rock

Appendix C Profile description of the Swartland soil form.

Map/photo:	2926 Bloemfontein	Soil form and Family:	Swartland /Rouxville
Latitude +Longitude:	29^0 13'23.98"S/ 26^0 12'44.29" E	Surface rockiness:	None
Altitude:	1421.9 m	Occurrence of flooding:	None
Terrain unit:	Midslope	Wind erosion:	Slight wind
Slope:	1%	Water erosion:	None
Slope shape:	Straight	Vegetation/land use:	Agronomic field crops
Aspect:	South	Water Table:	None
Micro relief:	None	Described by:	M. Hensley/ S. Mavimbela
Parent material Solum:	Origin binary,aeolin, local colluvium	Date Described:	1/11/2006
Underlying Material:	Sandstone (Feldspathic)	Weathering of underlying material:	Moderate physical, moderate chemical
		Alternation of underlying material:	Ferrugised

Horizon	Depth (mm)	Description	Diagnostic horizon
A	0-200	Moist state; dry colour: reddish brown (5YR5/8); moist colour; reddish brown (5YR/8); texture: fine sandy loam; structure: apedal massive: consistence: friable; few fine pores; common roots; clear smooth transition	Orthic
B1	200-400	Moist state; dry colour: dark reddish brown (5YR3/6); reddish brown (5YR3/6);texture: fine sandy clay; Pedocutanic Structure: moderate coarse sub-angular blocky: consistence: friable ; very few fine sesquioxide concretions; few roots; smooth transition	Pedocunatic
C1	400 ± 700	Moist state; undisturbed; dolorite rock; black concretions; many reddish-yellow geogenic mottles, very few fine sesquioxides concretions; Non hardened free lime; strong effervescence, very few roots; not observed transition.	Saprolite